SYSTEMATICS AND SIGNALLING OF MADAGASCAN CHAMELEONS OF THE *CALUMMA NASUTUM* GROUP

DISSERTATION ZUR ERLANGUNG DES DOKTORGRADES DER NATURWISSENSCHAFTEN AN DER FAKULTÄT FÜR BIOLOGIE DER LUDWIG-MAXIMILIANS-UNIVERSITÄT MÜNCHEN

DISSERTATION PRESENTED TO OBTAIN THE DEGREE OF DOCTOR RERUM NATURALIUM AT THE FACULTY OF BIOLOGY, LUDWIG-MAXIMILIANS-UNIVERSITÄT MUNICH, GERMANY

VORGELEGT VON
PRESENTED BY

DAVID PRÖTZEL

Erstgutachter: Prof. Dr. Gerhard HASZPRUNAR

Zweitgutachter: Prof. Dr. Joachim HAUG

Væĕ Åå^¦ÁŒ̃ă*æà^K̃ÁGFĔFĖ̈Ǝ∈FÌ

Væĕ Åå^¦Á(>}å|æ&@̃}ÁÚ¦>˘}*K̃ÁGÍ ĔÊ ĖƎ∈FJ

Eidesstattliche Erklärung

Ich versichere hiermit an Eides statt, dass die vorgelegte Dissertation von mir selbständig und ohne unerlaubte Hilfe angefertigt wurde.

München, den 08.07.2019

_____

(David Prötzel)

Erklärung

Hiermit erkläre ich, dass die Dissertation nicht ganz oder in wesentlichen Teilen einer anderen Prüfungskommission vorgelegt worden ist und dass ich mich nicht anderweitig einer Doktorprüfung ohne Erfolg unterzogen habe.

München, den 08.07.2019

_____

(David Prötzel)

Table of Contents

1 Background of this work

1.1 Abbreviations

ATP   Adenosine triphosphate

BC   before Christ

BEAST   Bayesian evolutionary analysis sampling trees

COI   mitochondrial cytochrome C oxidase subunit I gene

CMOS   nuclear oocyte maturation factor gene

CT   computed tomography

FF   frontoparietal fenestra

FT   fluorescent tubercle

diceCT   diffusible Iodine contrast enhanced CT

DNA   deoxyribonucleic acid

IUCN   International Union for Conservation of Nature

LSID   life science identifier

mtDNA   mitochondrial DNA

ND(1, 2, 4)   NADH Dehydrogenase subunit (1, 2, 4)

nDNA   nuclear DNA

OTU   operational taxonomic unit

PCA   principal component analysis

RAG-1   recombination-activating gene 1

rRNA   ribosomal ribonucleic acid

UV   ultraviolet

ZSM   Zoologische Staatssammlung München (Bavarian State Collection of Zoology, Munich)

1.2 Curriculum Vitae

DAVID PRÖTZEL

CURRICULUM VITAE

RESEARCH AND WORK EXPERIENCE

2014 – to date	PhD position at Zoologische Staatssammlung München (LMU): *Systematics and signalling of Madagascan chameleons of the* Calumma nasutum *group* (Prof. Dr. Haszprunar, Dr. Glaw)
2014 – to date	Gymnasium Bad Aibling, Teacher, biology and chemistry
2014	**2nd state examination** in biology and chemistry for teaching secondary school

EDUCATION

2012	**1th state examination** in biology and chemistry for teaching secondary school
2011	"Zulassungsarbeit", *Tree-bark beetle diversity along climate-driven altitudinal and structural gradients in* Podocarpus *NP, Ecuador* (Prof. Dr. Klingler, Dr. Schmidl)
2007–2012	work as research assistant in practical courses: • systematic diversity • zoological cytology and anatomy • biology of organisms • zoological excursion to Pula, Croatia
2007–2011	excursions: • Banyuls-sur-Mer, France (marine biology) • Helgoland, Germany (botany) • Beka, Slovenia (entomology) • Neusiedler See, Austria (botany) • Pula, Croatia (zoology)
2006	*Work and Travel* in Australia
2005–2006	civil service at Environmental Agency Passau
2005	„Abitur", Gymnasium Leopoldinum, Passau

PUBLICATIONS

Prötzel, D., Scherz, M.D., Ratsoavina, F., Vences, M. & Glaw, F. (in prep.). Revision of the *Calumma nasutum* complex. – *Vertebrate Zoology.*

Prötzel, D., Lambert, S.M., Andrianasolo, G.T., Hutter, C.R., Cobb, K.A., Scherz, M.D., Glaw, F. (2018). The smallest 'true chameleon' from Madagascar: a new, distinctly colored species of the *Calumma boettgeri* complex (Squamata: Chamaeleonidae). – *Zoosystematics and Evolution*. (94), 409–423.

Prötzel, D., Forster, J., Krautz, T. & Glaw, F. (2018). Predator versus predator: Four-lined Snake (*Elaphe quatuorlineata*) feeding on a Least Weasel (*Mustela nivalis*) in Istria, Croatia. – *Spixiana* (41), 157–159.

Sentis, M., Chang, Y., Scherz, M.D., Prötzel, D., Glaw, F. (2018). Rising from the ashes: resurrection of the Malagasy chameleons *Furcifer monoceras* and *F. voeltzkowi* (Squamata: Chamaeleonidae), based on micro-CT scans and external morphology. – *Zootaxa* (3), 549–566.

Glaw, F., Scherz, M.D., Prötzel, D., Vences, M. (2018). Eye and webbing colouration as predictors of specific distinctness: a genetically isolated new treefrog species of the *Boophis albilabris* group from the Masoala peninsula, northeastern Madagascar. – *Salamandra* (54), 163–177.

Altmetric Score

Prötzel, D., Vences, M., Scherz, M.D., Hawlitschek, O., Ratsoavina, F. & Glaw, F. (2018). Endangered beauties: micro-CT osteology, molecular genetics and external morphology reveal three new species of chameleons in the *Calumma boettgeri* complex (Squamata: Chamaeleonidae). – *Zoological Journal of the Linnean Society* (184), 471–498.

121

Prötzel, D., Heß, M., Scherz, M.D., Schwager, M., van't Padje, A. & Glaw, F. (2018). Widespread bone-based fluorescence in chameleons. – *Scientific Reports* (8), 698.

644

Prötzel, D., Vences, M., Scherz, M.D., Vieites, D.R. & Glaw, F. (2017). Splitting and lumping: an integrative taxonomic assessment of Malagasy chameleons in the *Calumma guibei* complex results in the new species *C. gehringi* sp. nov. –*Vertebrate Zoology* (67), 231–249.

Prötzel, D., Glaw K., Forster, J. & Glaw, F. (2016). Hibernation in tropical Madagascar? Unusual roosting sites of chameleons of the genus *Calumma.* – *Spixiana* (39), 272.

Prötzel, D., Ruthensteiner, B. & Glaw, F. (2016). No longer single! Description of female *Calumma vatosoa* (Squamata, Chamaeleonidae) including a review of the species and its systematic position. – *Zoosystematics and Evolution* (92), 13–21.

Prötzel, D., Ruthensteiner, B., Scherz, M.D., Glaw, F. (2015). Systematic revision of the Malagasy chameleons *Calumma boettgeri* and *Calumma linotum* (Squamata: Chamaeleonidae). *Zootaxa* (4048), 211–231.

TALKS and POSTERS

Prötzel, D. (2018). Entdeckung der Fluoreszenz bei Chamäleons und Kurzvorstellung neuer Chamäleonarten von Madagaskar. Talk at meeting of AG Chamäleons, Boppard.

Sentis, M., Chang, Y., Scherz, M.D., Prötzel, D., Glaw, F. (2017). Rising from the ashes: resurrection of the Malagasy chameleons *Furcifer monoceras* and *F. voeltzkowi* (Squamata: Chamaeleonidae), based on micro-CT scans and external morphology. Poster at SEH (Societas Europaea Herpetologica), annual conference, Salzburg, Austria.

Prötzel, D., Heß, M., Scherz, M.D., Schwager, M., van't Padje, A. & Glaw, F. (2017). Fluoreszenz bei Chamäleons. Talk at DGHT (Deutsche Gesellschaft für Herpetologie und Terrarienkunde), annual conference, Ulm.

Prötzel, D. (2017). Ungeahnte Vielfalt in der *Calumma nasutum*-Gruppe. ÖGH (Österreichische Gesellschaft für Herpetologie), annual conference, Vienna.

Prötzel, D. (2017). Kommunikation bei Chamäleons – sie lassen Farbe sprechen. Talk at Freunde der ZSM, Munich.

Schmidl, J., Prötzel, D., Pfeifer, T. (2012). Monitoring tree-bark arthropod diverstity along altitudinal and structural gradients in tropical forests. Talk and Poster on GFOe-Conference, Lüneburg.

PEER REVIEW: Current Zoology

IUCN ASSESSMENTS

Glaw, F., Prötzel, D. & Jenkins, R.K.B. 2015. *Calumma linotum*. The IUCN Red List of Threatened Species 2015, e.T75976541A75976544.

Glaw, F., Jenkins, R.K.B., Prötzel, D. & Tolley, K. 2015. *Calumma boettgeri*. The IUCN Red List of Threatened Species 2015, e.T176301A82125738.

POPULAR SCIENCE ARTICLES

Prötzel, D. 2018. Unter Forschern – auf der Suche nach neuen Chamäleonarten in Ost-Madagaskar. – *Elaphe/Terraria* (72), 66–69.

Prötzel, D. & Forster, J. 2017. Masoala – ein herpetologischer Reisebericht von den letzten Tieflandregenwäldern Madagaskars. – *Reptilia* (127), 72–79.

Prötzel, D. 2014. Der Palmatogecko – ein sozialer Gecko? – *Reptilia* (107), 4–5.

Prötzel, D. & Forster J. 2014: Eine herpetologische Reise nach Sumatra. – *Reptilia* (109), 80–85.

Prötzel, D. 2011. USA – Auf Reptiliensuche in den Nationalparks des Westens. – *Terraria* (32), 71–76.

Prötzel, D. 2009. Backpacking in down under – der Reptilien wegen. – *Terraria* (16), 73–84.

Prötzel, D. 2007. Haltung von Echsen im Gewächshaus. – *Reptilia* (63), 64–70.

PARTICIPATION in FILMING PROJECTS/TELEVISION (hyperlinks)

Animals Decoded, episode 3: Invisible Signals. *Documentary*, Smithsonian Channel USA, in prep.

Leuchtende Chamäleons, *nano*, 3sat, 6th September 2018.

Die Welt ist bunt - aber ist mein Blau auch dein Blau?, *W Wie Wissen*, ARD, 18th August 2018.

Glowing Chameleons, *Daily Planet*, Discovery Channel Canada, 21st February 2018.

LMU snippets, Ludwig-Maximilians-Universität München, 24th January 2018.

PRESS COVERAGE

Printed issues:

Nature, Spektrum, VBIO – Biologie in unserer Zeit, Scholastic – Science World (USA), How it works (USA), Science & Vie (France), Reptilia, Chamaeleo, GfBS newsletter (Cover), several newspapers (via dpa)

Online (hyperlinks of selected samples, accessed in July 2018):

- Spiegel Online: Disco-Effekt: UV-Licht lässt Chamäleons blau strahlen
- National Geographic: Chameleon Bones Glow in the Dark, Even Through Skin
- BBC Wildlife Magazine: Madagascar's reptile list grows following discoveries
- Spektrum: EVOLUTION: Wenn das Chamäleon blau leuchtet
- Spektrum: Fauna in Madagaskar: Neue, bunte und bizarre Chamäleonspezies
- Süddeutsche Zeitung: UV-Licht lässt Chamäleons in blauen Mustern strahlen
- Handelsblatt: Chamäleons im Disco-Look
- BR: Chamäleons – Leuchten und faszinieren
- Neue Züricher Zeitung: Chamäleons leuchten unter UV-Licht um die Wette
- ORF: Chamäleon: Disco-Effekt entdeckt
- Fox News: Chameleons' secret glow comes from their bones
- El País: Los nuevos camaleones de colores de Madagascar
- The Hindu: The secret to the chameleon's glow
- Discover Magazine: Fun fact: chameleon bones glow in the dark
- Daily Mail: The invisible language of chameleons revealed
- ScienceDaily: Biodiversity: 3 new rainbow chameleon species discovered
- Phys.org: Researchers discover three new, highly threatened chameleon species in Madagascar
- Eurekalert: Biodiversity: All the colors of the rainbow
- LaborJournal: Expedition ins Unbekannte

FIELD WORK

Field work experience on beetles (Ecuador) and reptiles/amphibians (Madagascar)

- April 2018: Mahajanga, Madagascar
- August – September 2017: Andasibe and Masoala, Madagascar
- December 2016 – January 2017: Andasibe and East Coast, Madagascar
- July – September 2009: Podocarpus NP, Ecuador

FELLOWSHIPS

- German Association for Herpetology (DGHT): Wilhelm-Peters-Fonds (2016)
- German Academic Exchange Service (DAAD): fellowship for field work in Podocarpus NP, Ecuador (2009)
- DAAD: fellowship for field work in Madagascar (2015)

1.3 Declaration of contributions as a co-author

I hereby declare that I have provided the following own contribution to the work on the scientific articles contained in my cumulative dissertation:

I have carried out independently for all articles under the guidance of my supervisor Frank Glaw the conceptual design and planning, the collection of data and samples, the processing of samples, the preparation and analysis of data, as well as the preparation of manuscripts, their submission to publication, their revision after the review process, and all other work.

In doing so, I mark the exceptions (authors are indicated with initials) for following works:

Prötzel, D, Scherz, MD, Ratsoavina, F, Vences, M & Glaw, F (in prep.): Revision of the *Calumma nasutum* group. *Vertebrate Zoology*.

About 80% of the specimens were sampled by MDS, FR, MV, FG, and others; genetic data were generated and processed by MV.

Prötzel, D, Lambert, SM, Andrianasolo, GT, Hutter, CR, Cobb, KA, Scherz, MD, Glaw, F 2018): The smallest 'true chameleon' from Madagascar: a new, distinctly colored species of the *Calumma boettgeri* complex (Squamata: Chamaeleonidae). *Zoosystematics and Evolution (94),* 409–423.

Specimens were sampled by SML, GTA, and GTH; DNA-sequences were generated by SML, GTA, and KAC; genetic data were processed by SML, GTA, and MDS.

Prötzel, D, Vences, M, Scherz, MD, Hawlitschek, O, Ratsoavina, F & Glaw, F (2018): Endangered beauties: Micro-CT cranial osteology, molecular genetics and external morphology reveal three new species of chameleons in the *Calumma boettgeri* complex (Squamata: Chamaeleonidae). *Zoological Journal of the Linnean Society 184,* 471–498.

About 60% of the specimens were sampled by OH, FR, and FG; genetic data were generated and processed by MV; the distribution map was designed by MDS.

Prötzel, D, Heß, M, Scherz, MD, Schwager, M, van't Padje, A & Glaw, F (2018): Widespread bone-based fluorescence in chameleons. *Scientific Reports 8*, 698.

Histology, Volume rendering, and Transmission Electron microscopy was initiated and performed by MH; Fluorescence spectroscopy and Quantum yield calculation were made by MS; statistical analyses were made to a large extent by MDS; about 40% of the micro-CT scans were provided by AvP.

Prötzel, D, Vences, M, Scherz, MD, Vieites, DR & Glaw, F (2017): Splitting and lumping: An integrative taxonomic assessment of Malagasy chameleons in the *Calumma guibei* complex results in the new species *C. gehringi* sp. nov. *Vertebrate Zoology*, *67*, 231–249.

Specimens were sampled by MV, MDS, DRV, and FG; genetic data were generated and processed by MV; the distribution map was designed by MDS.

Prötzel, D, Ruthensteiner, B & Glaw, F (2016): No longer single! Description of female *Calumma vatosoa* (Squamata, Chamaeleonidae) including a review of the species and its systematic position. *Zoosystematics and Evolution 92*, 13–21.

Micro-CT scans were made under the supervision of BR.

Prötzel, D, Ruthensteiner, B, Scherz, MD, Glaw, F (2015): Systematic revision of the Malagasy chameleons *Calumma boettgeri* and *Calumma linotum* (Squamata: Chamaeleonidae). *Zootaxa 4048*, 211–231.

Micro-CT scans were made with great support and guidance of BR; specimens were collected by FG and others.

Further, all published articles have been modified following the suggestions of the peer-reviewers. All authors contributed to the revision of the respective manuscripts. Most articles were linguistically and stylistically improved by MDS. Photographs were taken by the author or one of the co-authors, unless otherwise stated.

1.4 Summary

1.4.1 Summary (English)

Background

Madagascar is famous for its biodiversity and exceptional degree of endemism, especially in chameleons, hosting almost half of the world's species. The exploration of its species diversity started with the famous Georges Cuvier who described the first Madagascan chameleons in 1829. Since then, the quality of species descriptions and, subsequently, the species concepts have substantially changed. While the first descriptions were based on a few characters of the external morphology only, today the collected specimens are usually DNA barcoded and their taxonomic status is evaluated based on genetic distances as a first step. In doing so, a previous molecular study of the *Calumma nasutum* group, which are small chameleons with a rostral appendage on the snout tip in most species, resulted in an impressive 33 deep mitochondrial lineages. Only seven of these corresponded to named species leaving 26 lineages as operational taxonomic units (OTUs). In times of DNA based taxonomy and species delimitation algorithms taxonomists face new challenges of how to describe a species and to avoid oversplitting.

In this dissertation I evaluate, based on a taxonomic revision of *Calumma nasutum* group, the significance of mitochondrial lineages for species delimitation and promote micro-computed tomography (micro-CT) as an additional tool for integrative taxonomy. The second part deals with the discovery of the phenomenon of widespread fluorescence in chameleons. Biofluorescence is only rarely found in land vertebrates, so far, but has been reported for several marine organisms where it is used, inter alia, for intraspecific communication. As chameleons also communicate visually, the fluorescent pattern might work as an additional signal for species recognition.

Methods and Procedure

To describe (or redescribe) species of the *Calumma nasutum* group, I followed an integrative taxonomic approach incorporating five lines of evidence (for details, see below): External Morphology, micro-CT-scans of the skulls, dice-CT scans of the hemipenes, mitochondrial gene sequences (ND2), and nuclear gene sequences (CMOS).

In the *Calumma nasutum* group a number of species have remained poorly characterized, because their original descriptions date to over a century ago and lack precise locality data, or because the holotype is a juvenile specimen. These species were redescribed here using a combination of micro-CT scans and detailed study of external morphology. With the help of diagnostic characters of the skull, the old type specimens were matched to recently collected and sequenced specimens.

Additionally, micro-CT scanning was used for the first time to produce 3-dimensional models of chameleon hemipenes. In preparation for scanning, each hemipenis was removed from the specimen and immersed in iodine solution for several days to enhance the contrast when X-raying this soft tissue. This method is called dice-CT, and the resulting scans provide a more objective and detailed illustration of the hemipenes than the conventional 2-dimensional drawings. Further, sequences of mitochondrial (ND2) and nuclear (CMOS) genes were analysed for most of the new species described here. To provide comparability, access, and fast taxonomic progress, all new species were registered at ZooBank with an LSID number, their sequences were uploaded to GenBank, and all taxonomic acts were published in open access journals.

To study fluorescence in chameleons, we used a fluorimeter to measure the excitation and emission spectra and to calculate the quantum yield for the intensity of fluorescence. The distribution of the fluorescent tubercles was recorded with photographs under UV light illumination, and the bony origins of fluorescence were studied using micro-CT and Transmission Electron microscopy of histological sections.

Conclusions

The taxonomic part or this dissertation resulted in the description of eight new chameleon species, "*Calumma emelinae*", *C. gehringi*, *C. juliae*, *C. lefona*, "*C. ratnasariae*", *C. roaloko*, "*C. tjiasmantoi*", and *C. uetzi* (see chapter 3.1.2, 3.1.3, 3.1.4, 3.1.5), contributing nearly 4% of all known species of the family Chamaeleonidae. Furthermore, one species, *C. radamanus* (Mertens, 1933) was revalidated, five species, *C. boettgeri* (Boulenger, 1888)*, C. fallax* (Mocquard, 1900)*, C. guibei* (Hillenius, 1959), *C. linotum* (Müller, 1924), and *C. nasutum* (Duméril & Bibron, 1836) were redescribed, and the females of *C. vatosoa* Andreone, Mattioli, Jesu & Randrianirina, 2001 were described for the first time.

Using an integrative taxonomic approach, I showed that current species delimitation algorithms based on mitochondrial gene sequences alone greatly overestimate the actual number of species. Micro-CT proved essential for analysing skull morphology, which resulted more appropriate for species delimitation than some highly variable external characters. Further, this tool enabled to find frontoparietal fenestrae, which are cranial openings of potential adaptive importance found only in chameleon species living at high elevations. Using novel dice-CT imaging, I also analysed hemipenial morphology in minute detail and described a new ornament, the "cornucula gemina".

Finally, the phenomenon of fluorescence in chameleons was discovered in species belonging to eight of the twelve chameleon genera. The optimal excitation wavelength is in the UV-A spectrum at 353 nm, emitting light with wavelengths from 360 nm to 500 nm, with a maximum at 433 nm (blue spectrum). We showed that the fluorescent patterns result from bony tubercles on the skull are species specific, sexually dimorphic, and occur especially in

forest living species. Based on these findings, and also because the colour blue is a conspicuous signal in forest habitats, I hypothesize that chameleons use fluorescence as a constant signal for intraspecific communication supplementing their vibrant body-colour language. Further, as-of-yet unpublished examples suggest that fluorescence is more common in squamates and might be an interesting field for further studies.

1.4.2 Zusammenfassung (Deutsch)

Hintergrund

Madagaskar ist bekannt für seine Biodiversität und seine außergewöhnlich hohe Endemismusrate. Dies gilt vor allem für Chamäleons, da auf der Insel beinahe die Hälfte aller Arten weltweit vorkommt. Die Erforschung dieser Artenvielfalt begann mit dem berühmten Georges Cuvier, der die ersten madagassischen Chamäleons im Jahre 1829 beschrieb. Seit damals haben sich die Qualität der Artbeschreibungen und folglich auch das Artkonzept substanziell verändert. Beruhten die ersten Beschreibungen noch auf wenigen Merkmalen der äußeren Morphologie, so werden heutzutage die gesammelten Exemplare gewöhnlich erst sequenziert und ihre Artzugehörigkeit anhand von genetischen Abständen bewertet. Auf diese Weise stellte eine vorangegangene Studie fest, dass die *Calumma-nasutum*-Gruppe, die aus kleinen Chamäleons mit gewöhnlich einem Nasenfortsatz auf der Schnauze besteht, insgesamt 33 tiefe mitochondriale Linien enthält. Nur sieben davon gehörten zu bereits beschriebenen Arten, wodurch noch 26 Linien als *operational taxonomic units (OTUs)* übrig blieben. In Zeiten der DNA-geleiteten Taxonomie und der Verwendung von Algorithmen zur Artabgrenzung stehen Taxonomen neuen Herausforderungen gegenüber, eine Art zu beschreiben und ein sogenanntes „oversplitting" zu vermeiden.

In dieser Dissertation bewerte ich am Beispiel der Revision der *Calumma-nasutum*-Gruppe die Bedeutung von mitochondrialen Linien zur Artabgrenzung und stelle Mikrocomputertomografie (Mikro-CT) als zusätzliches Werkzeug der integrativen Taxonomie vor. Der zweite Teil handelt von der Entdeckung des Phänomens der weitverbreiteten Fluoreszenz bei Chamäleons. Biofluoreszenz wurde bisher nur selten bei Landvertebraten nachgewiesen, ist jedoch bei einigen Meeresorganismen gut bekannt, welche die Fluoreszenz unter anderem zur intraspezifischen Kommunikation nutzen. Da Chamäleons ebenfalls optisch kommunizieren, könnten die Fluoreszenzmuster als zusätzliches Signal zur Arterkennung dienen.

Methoden und Vorgehensweise

Um Arten der *Calumma-nasutum*-Gruppe (wieder) zu beschreiben, nutzte ich einen integrativen taxonomischen Ansatz mit fünf Beweislinien (siehe unten im Detail): Äußere Morphologie, Mikro-CT-Scans der Schädel, *dice*-CT-Scans der Hemipenisse, Sequenzen der mitochondrialen Gene und Sequenzen der Kerngene.

Einige Arten der *Calumma-nasutum*-Gruppe waren bisher wenig charakterisiert, da ihre Originalbeschreibung über einhundert Jahre zurücklag und genaue Typuslokalitäten fehlten oder weil der Holotypus ein Jungtier ist. Diese Arten wurden unter Verwendung von mikro-CT-Scans und genauer Untersuchung der äußeren Morphologie wiederbeschrieben.

Mit Hilfe diagnostischer Merkmale des Schädels wurden die alten Holotypen kürzlich gesammelten und sequenzierten Individuen zugeordnet.

Zusätzlich wurden zum ersten Mal Mikro-CT-Scans genutzt, um dreidimensionale Modelle von Chamäleonhemipenissen zu entwerfen. Zur Vorbereitung des Scans wurde jeder Hemipenis vom Tier abgetrennt und in Lugolscher Lösung für mehrere Tage eingelegt, um den Kontrast dieses weichen Gewebes beim Röntgen zu erhöhen. Diese Methode nennt sich *dice*-CT und die resultierenden Scans bieten eine objektivere und detailliertere Darstellung des Hemipenis als die herkömmlichen zweidimensionalen Zeichnungen. Weiterhin wurden Sequenzen von mitochondrialen Genen (ND2) und Kerngenen (CMOS) für die meisten der hier neu beschriebenen Arten analysiert. Um Vergleichbarkeit, weltweiten Zugang und schnellen taxonomischen Fortschritt zu garantieren, wurden alle neuen Arten bei ZooBank unter einer LSID-Nummer registriert, ihre Sequenzen bei GenBank hochgeladen und alle taxonomischen Arbeiten in *open-access*-Journalen veröffentlicht.

Zur Untersuchung der Fluoreszenz bei Chamäleons benutzten wir ein Fluorimeter, um die Anregungs- und Emissionsspektren zu messen und die Quantenausbeute zu berechnen. Die Verteilung der fluoreszierenden Tuberkel wurde mit Fotos unter UV-Beleuchtung dokumentiert und ihr knöcherner Ursprung mit Mikro-CT und Transmissionselektronenmikroskopie der histologischen Schnitten untersucht.

Schlussfolgerungen

Im taxonomischen Teil dieser Dissertation wurden acht Chamäleonarten neu beschrieben, die beinahe 4% aller bisher bekannten Arten der Familie Chamaeleonidae ausmachen: "*Calumma emelinae*", *C. gehringi*, *C. juliae*, *C. lefona*, "*C. ratnasariae*", *C. roaloko*, "*C. tjiasmantoi*", und *C. uetzi* (siehe Kapitel 3.1.2, 3.1.3, 3.1.4, 3.1.5). Weiterhin wurde eine Art, *C. radamanus* (Mertens, 1933), revalidiert. Es wurden fünf Arten wiederbeschrieben: *C. boettgeri* (Boulenger, 1888)*, C. fallax* (Mocquard, 1900)*, C. guibei* (Hillenius, 1959), *C. linotum* (Müller, 1924), und *C. nasutum* (Duméril & Bibron, 1836), und die Weibchen von *C. vatosoa* Andreone, Mattioli, Jesu & Randrianirina, 2001 wurden erstmals beschrieben.

Mit Verwendung eines integrativ taxonomischen Ansatzes konnte ich zeigen, dass Algorithmen zur Artabgrenzung, die allein auf mitochondrialen Gensequenzen basieren, die eigentliche Anzahl an Arten deutlich überschätzen. Mikro-CT bewährte sich um die Schädelmorphologie zu untersuchen, welche sich besser zur Artabgrenzung eignete als die sehr variablen äußeren Merkmale. Außerdem konnten mit Hilfe dieses Werkzeugs auch Frontoparietalfenster gefunden werden. Diese Schädelöffnungen wurden nur bei Chamäleons aus Montangebieten nachgewiesen und könnten eine besondere Anpassung an den Lebensraum darstellen. Das neuartige *Dice*-CT-Verfahren ermöglichte die

Hemipenismorphologie im kleinsten Detail zu untersuchen und auch ein neues Ornament, die "cornucula gemina", zu beschreiben.

Schließlich wurde bei Arten aus acht der zwölf Chamäleongattungen das Phänomen der Fluoreszenz entdeckt. Die optimale Anregungswellenlänge liegt im UV-A-Spektrum bei 353 nm und Licht mit Wellenlängen von 360 bis 500 nm, mit einem Maximum bei 433 nm im blauen Spektrum, wird emittiert. Wir konnten zeigen, dass die Fluoreszenzmuster von knöchernen Tuberkeln des Schädels stammen, artspezifisch und sexualdimorph sind und vor allem bei waldbewohnenden Arten vorkommen. Darauf aufbauend und auch, da die Farbe Blau im Wald ein auffallendes Signal darstellt, formuliere ich die Hypothese, dass Chamäleons die Fluoreszenz als konstantes Signal zur intraspezifischen Kommunikation nutzen und damit ihre Farbensprache ergänzen. Nicht-publizierte Beispiele lassen außerdem vermuten, dass Fluoreszenz bei Squamaten weiter verbreitet ist und ein interessantes Gebiet für nachfolgende Studien darstellen könnte.

1.5 Aims and overview

My dissertation, entitled 'Systematics and Signalling of Madagascan Chameleons of the *Calumma nasutum* group', was prepared at the Zoologische Staatssammlung (Bavarian State Collection of Zoology) in collaboration with the Ludwig-Maximilians-Universität, Munich, between 2014 and 2018. The work was supervised by Prof. Dr. Gerhard Haszprunar, and Dr. Frank Glaw.

One part of this work was the revision of this group of rather cryptic chameleon species including the (re)description of several species. Based on the detailed morphological and genetic data, my aims were to evaluate the significance of mitochondrial lineages for species delimitation and to establish micro-CT as an additional tool in taxonomy. Thanks to a fortuitous discovery, I could also add the description of fluorescence in chameleons as a second part to my dissertation. Here, the questions arose of the mechanism of this fluorescence and whether there were species specific and sexual dimorphic fluorescent pattern in the whole family Chamaeleonidae.

My thesis is structured beginning with chapter 2 providing a broad introduction to the state of the art in chameleon research, integrative taxonomy with a focus on the methodology in taxonomic papers on chameleons, and a general overview of the occurrence of biofluorescence. In chapter 3 I present the results of taxonomic research, describing, revalidating and redescribing the different species of the *Calumma nasutum* group, and describe fluorescence in chameleons. Chapter 4 ties the previous chapters together with a discussion of species diversity of the chameleons and its implications for conservation, micro-CT as a tool for taxonomy, and the possibility of a new field of research on fluorescence in squamates.

I admit that the revision of the *Calumma nasutum* group is not completed yet. Additional sampling is necessary to untangle the *C. gallus* complex, and more detailed analyses are required to evaluate the deep mitochondrial linages within the *C. radamanus* complex. Further, fluorescence might just be an incidental property of the underlying bone, or may turn out to serve a different biological function than hypothesized here.

2 Introduction

2.1 Chameleons – an exceptional group of lizards

"The chameleon may be slow, but it always reaches its target"

Ghanaian Proverb

Chameleons are a unique group of lizards and have held a strong fascination for people for a long time. Their remarkable biology inspired many myths and legends in their home countries and they were first mentioned in a scientific context by Aristotle in the year 350 BC (Tolley & Herrel, 2014). The laterally compressed body, prehensile feet and tail and a specialized sensory system make chameleons highly adapted arboreal predators. The Malagasy proverb "walk like a chameleon – look forward but watch your back," refers to the ability of chameleons to move their eyes independently. The chameleon eye is its most developed sensory organ (Anderson & Higham, 2014) and both eyes scan the environment constantly in saccadic movements with uncoupled accommodation from each other (Ott, 2001). Nearly bulging out of the orbit, each eye covers an oculomotor range of more than 180° horizontally and about 90° vertically (Sándor *et al.*, 2001). Additionally, the chameleon eye has a higher image resolution than any other vertebrate eye of a similar size (Ott & Schaeffel, 1995). This results from a negative powered lens which allows more precise focussing due to an increased retinal image size (Ott & Schaeffel, 1995). The retina contains four types of cones, one of which has maximum absorbance in the UV-A spectrum. This results in a visual spectrum from about 350–750 nm for the investigated species (Bowmaker *et al.*, 2005). Although usually both eyes are used to focus on prey (Ott *et al.*, 1998), chameleons are also able to focus monocularly, using corneal accommodation for depth perception (Srinivasan, 1999).

Once within reach, chameleons capture their prey with a projectile tongue. Projection distances of up to 2.5 body lengths can be achieved and the tongue is projected with peak accelerations of 264 *g*, which is the highest acceleration ever measured for any amniote movement (Anderson, 2016). Especially the smaller species reach the highest acceleration rates and the furthest projectile distances relative to their body lengths (Anderson, 2016). The ballistic tongue projection works according to a "bow and arrow" mechanism: the elastic collagen tissue is first slowly contracted by the tongue accelerator muscle and then rapidly recoiled. Thanks to this elastically powered movement the velocity of the tongue projection declines only slightly at lower temperatures (Anderson & Deban, 2010). The ability to feed at relatively low temperature (Hebrard *et al.*, 1982; Reilly, 1982) and the energy-efficiency of prey acquisition in combination with other adaptations might explain why many chameleon species are able to live at high elevation, even up to 5000 m above sea level in eastern Africa (Tilbury, 2018; Tolley & Menegon, 2014).

The anatomy of chameleons is specialized for an arboreal lifestyle. Their feet are forceps-like (the term "zygodactylus" is used by some authors but originally refers to birds only, Tolley, pers. comm.) with grouped toes in opposing bundles (Anderson & Higham, 2014). The skin is fused between the digits and covered with specialized scales that allow for effective grasping. Most species, except for the ground dwelling genera *Brookesia*, *Rieppeleon, Palleon,* and *Rhampholeon*, have a prehensile tail that functions like a fifth limb when climbing.

Most of the myths about chameleons, however, refer to their ability to change colour, as for example is reflected in the African proverb: "A chameleon can only change its colour but never change its skin". Contrary to the common meaning, chameleons are intrinsically well camouflaged and use colour change primarily for communication and thermoregulation, and only to a lesser degree for camouflage (Keren-Rotem *et al.*, 2016; Stuart-Fox, 2014; Stuart-Fox & Moussalli, 2009). For social signalling even colours are used that contrast most against the environmental background as shown for males of the South African genus *Bradypodion* Gray, 1865 (Stuart-Fox & Moussalli, 2008; Stuart-Fox *et al.*, 2007). Moreover, not all chameleons are able to change between a wide variety of colours; for example, species of the ground dwelling genus *Brookesia* can usually only switch between different shades of brown. Males of the 'true chameleons' (the subfamily Chamaeleoninae) show the most conspicuous colours in interactions with conspecifics—during male-male contests or when displaying to a female. The females may react and signal that they are receptive, for example with yellow spots (Cuadrado, 1998), or may use specific colour patterns to indicate that that they are already gravid (Nečas, 2004). Physiological colour change in chameleons is produced by specialized types of chromatophores (melanophores, xanthophores, and guanophores), which are dermal cells that can translocate their pigments in dendritic structures. The prominent role of guanine nanocrystals in colour change was only recently described (Teyssier *et al.*, 2015).

Their dorsoventrally flattened body enables chameleons to hide behind small branches or, on the contrary, to enlarge their body surface from a lateral view for signalling. For an even more impressive body shape, males of several species (especially in *Kinyongia, Trioceros*) have developed elaborate ornaments including cranial casques, keratinized or dermal rostral appendages, gular spines or lobes, occipital lobes, or dorsal crests (Tilbury, 2018). The degree of sexual dimorphism is variable among species; in some species only the males are ornamented, in others, both sexes or neither of them are ornamented and sexes are difficult to distinguish externally. Also the body size varies from "male-biased to female-biased" (Stuart-Fox, 2014). Much is still unknown about the ornamentation of chameleons, such as the function of the lateral or temporal crests, which are formed by bony tubercles and occur in many species. Comparable to anole lizards, whose ecology and morphological diversity has been extensively studied (Losos, 2009), chameleons are interesting model organisms to investigate the variation of natural and sexual selection,

especially in the context of visual signalling (Karsten *et al.*, 2009; Stuart-Fox *et al.*, 2006; Stuart-Fox *et al.*, 2007).

2.2 Integrative Taxonomy

2.2.1 The species concepts

"What are the characteristics that permit the assignment of individuals to species? This question is easily answered, when the difference between two species is as clear-cut as that between the lion and the tiger."

Ernst Mayr, 1982

Species are one of the fundamental units in biology. They represent the lowest level of genuine discontinuity above the level of the individual and express the "elementary urges of man" (Mayr, 1982) to name and classify the elements of his environment. The existence of species, connected with the belief in eternally fixed forms, was already proposed by ancient philosophers such as Aristotle; however, early thinkers did not recognise the biological integrity of this term (Flashar, 2015). Aristotle and Theophrastus, for example, accepted the folk wisdom that seeds of one species of plant could germinate into plants of another species (Mayr, 1982). However, the Greek philosophers differentiated already between "genus" and "species" though this distinction was not always consistent and did not follow a logical division (Balme, 1975). In his seminal work *Systema Naturae*, Linnaeus (1758) was the first to formally begin codifying the science of taxonomy, the systematic description and classification of species based on his own appraisal or on the expert knowledge of other taxonomists.

Darwin (1859) struggled with the species concept in his book *On the Origin of Species* and did not provide a clear definition of a species: "No one definition has satisfied all naturalists; yet every naturalist knows vaguely what he means when he speaks of a species". Darwin (1859) held that "the amount of difference is one very important criterion in settling whether two forms should be ranked as species or varieties", following the experience and judgment of a naturalist.

In the decades that followed, taxonomists continued to describe species on basis of external characters only. The degree of morphological difference was used as the delimiting criterion, known as the "morphological species concept" (Mayr, 1982). It took several years until Dobzhansky made the connection between the theory of evolution and genetics in his *Genetics and the Origin of Species* (Dobzhansky, 1937) and finally Mayr (1942) stated the biological species concept: "Species are groups of actually or potentially interbreeding natural populations which are reproductively isolated from other such groups". This concept was later revised: "A species is a reproductive community of populations (reproductively

isolated from others) that occupies a specific niche in nature," (Mayr, 1982). Although Mayr's species concept is widely used and has strongly influenced systematics and evolutionary biology, it still does not solve the problem concerning the nature of species (De Queiroz, 2005). Organisms that reproduce parthenogenetically or the several cases of hybridisation between species or even genera did not fit into this concept; for taxonomists, reproductive barriers are usually not verifiable when evaluating the species status of one or a few (preserved) specimens. Discussion of the species problem intensified over the next decades and more than 24 different concepts have been proposed as of today (De Queiroz, 2007; Mayden, 1997).

Molecular analyses revolutionised taxonomy and greatly influenced our conception of species. With the advent of molecular data, it became possible to produce phylogenies on the basis of one or several gene sequences which resulted in a tree comprised of different clades. The term "clade" goes back to Hennig (1950, 1965) who proposed in his cladistics that a taxon should consist of specimens which have descended from a common ancestor and, therefore, form a monophyletic group. Based on gene sequences, species delimitation can be carried out mathematically using different algorithms, for example net p-distances in Bayesian analysis (BEAST; Drummond & Rambaut, 2007) or the SpeciesIdentifier "Cluster" algorithm (Meier *et al.*, 2006). The easy comparability of sequences has even led to a push for DNA-based taxonomy (Tautz *et al.*, 2003).

However, the genetic distances between populations or species vary widely: in chameleon taxonomy, for example, species have been described on the basis of as much as 30% or even less than 5% difference in mitochondrial gene sequence from their closest relative (see chapter 2.2.2). Consequently, the question of species delimitation has only been raised to the next level. Thus, several authors propose the "integrative future of taxonomy" (Padial *et al.*, 2010) using a multiscore approach of different methods to discover and classify biodiversity (Dayrat, 2005; Padial *et al.*, 2009; Schlick-Steiner *et al.*, 2010). In herpetology, this approach was implemented by Miralles *et al.* (2011) and Vasconcelos *et al.* (2012) who each used three lines of evidence (mtDNA, nDNA, and external morphology) and described lineages as separate species if at least two of these lines showed clear differences.

2.2.2 Methodology and history of chameleon taxonomy

In his *Systema Naturae* Linnaeus (1758) mentioned the chameleon species *Lacerta chamaeleon*, referring to the European chameleon (*Chamaeleo chamaeleon*). The early species descriptions were usually short and based on qualitative differences in external morphology only, as were the first descriptions of chameleons from Madagascar, *Calumma parsonii*, *Furcifer pardalis*, and *F. verrucosus* (Cuvier, 1824, 1829). Species were described on the basis of preserved specimens in the museum by taxonomists who had never seen their study organism in its natural habitat. With the increasing number of species, however, the need for more detailed diagnoses and more diagnostic characters arose. Hillenius (1959)

divided the "true chameleons", the former genus *Chamaeleo*, Laurenti, 1768, into groups based on external characteristics only. Cope (1896) provided the first (short and verbal) descriptions of chameleon hemipenes and showed that their morphology differs between species. Decades later, drawings of hemipenes were sometimes included in species descriptions and diagnoses (Brygoo *et al.*, 1970, 1973; Brygoo & Domergue, 1971). Along with lung morphology and karyological data, hemipenial morphology was also used to construct a preliminary phylogeny of the family Chamaeleonidae Gray, 1825 (Klaver & Böhme, 1986).

Osteology, especially of the skull, served as the early basis for a cladistics interpretation resolving relationships within the Chamaeleonidae (Rieppel, 1981). Modern methods such as micro-Computed Tomography (micro-CT) have since made osteology more easily accessible and illustratable. This method was first used to analyse a fragment of a chameleon fossil (Dollion *et al.*, 2015) and to study skull morphology in an ecological context (Dollion *et al.*, 2017). Until recently, micro-CT has not been used in chameleon taxonomy.

With the improvement of scientific photography and increased access to chameleon habitats, documentation of the colouration in life of these optically communicating lizards became possible. Colour photographs have also served as a basis for a phylogeographic study on *Furcifer pardalis* (Cuvier, 1829) and were matched with different mitochondrial lineages within this species (Grbic *et al.*, 2015).

Molecular analyses were first used for chameleons by Pook and Wild (1997) who investigated the relationships within the African *Trioceros cristatus* (Stutchbury, 1837) group using a sequence of the 12S rRNA gene. Sequence data from other genes or molecular markers (for example mitochondrial genes ND1, ND2, ND4, and COI and nuclear genes RAG-1 and CMOS) were later used to construct phylogenies of *Brookesia* Gray, 1865 (Townsend *et al.*, 2009) and the whole Chamaeleonidae (Raxworthy *et al.,* 2002, Tolley *et al.*, 2013, Townsend & Larsen, 2002). Modern species descriptions now often include sequences of mitochondrial genes. However, there are great differences in the genetic distances that are used to delimit species. In some cases, species of the genera *Brookesia* or *Calumma* Gray, 1865, differ by 10% to more than 30% pairwise distance in ND2 (Gehring *et al.*, 2011; Glaw *et al.*, 2012) and species of *Bradypodion* or *Kinyongia* Tilbury, Tolley & Branch, 2006, are described with 5% distance or even less (Branch *et al.*, 2006; Hughes *et al.*, 2017; Tilbury & Tolley, 2009).

Some chameleon species exhibit strong ontogenetic, sexually dimorphic, sexually dichromatic, and intraspecific variation (Tilbury, 2014). Thus, modern species descriptions follow an integrative taxonomical approach (see chapter 2.2.1) and combine genetic data with biogeography, external and hemipenial morphology, and further lines of evidence to evaluate the species status of different populations. In this way, cryptic diversity can also be uncovered, as was recently found in some chameleon taxa (Gehring *et al.*, 2012; Hughes *et al.*, 2017).

Currently 210 species of chameleons are scientifically described (Uetz *et al.*, 2018). They are distributed primarily across Africa, with a few species occurring in Southern Europe and the Arabian Peninsula. A single species occurs in Sri Lanka, Pakistan and India (Tilbury, 2018). Although comprising only a fraction of their total range, Madagascar harbours 89 species, more than a third of the species worldwide (Uetz *et al.*, 2018). The Malagasy chameleons are divided into four genera; the ground living genera *Brookesia* and *Palleon* Glaw, Hawlitschek & Ruthensteiner, 2013, are sister to the "true chameleons" (subfamily Chamaeleoninae Gray, 1825) including *Calumma* and *Furcifer* Fitzinger, 1843 (Tolley *et al.*, 2013). *Calumma* is the most diverse genus found in Madagascar, with 37 species to date, having increased by seven species (19%) over the last decade (Glaw, 2015; Prötzel *et al.*, 2017, 2018a, b) with three additional species currently being described (see manuscripts in chapter 3.1.3 and 3.1.5).

2.2.3 The *Calumma nasutum* group – a taxonomic challenge

The taxonomic part of this dissertation deals with the revision of the phenetic *Calumma nasutum* species group that consists of small chameleon species usually characterised by a soft dermal appendage on the snout tip. The following seven (valid) species had been described before the revision started: *C. boettgeri* (Boulenger, 1888)*, C. fallax* (Mocquard, 1900)*, C. gallus* (Günther, 1877)*, C. guibei* (Hillenius, 1959)*, C. linotum* (Müller, 1924)*, C. nasutum* (Duméril & Bibron, 1836), and *C. vohibola* Gehring, Ratsoavina, Vences & Glaw, 2011. Within the phenetic *C. nasutum* group, three species (*C. boettgeri, C. guibei,* and *C. linotum*) are distinguished by the possession of well-defined occipital lobes (Brygoo, 1971) and will hereafter be referred to as the *C. boettgeri* complex.

According to the most comprehensive chameleon phylogeny (Tolley *et al.*, 2013) the *C. nasutum* group is not monophyletic. A phylogeny of the whole family Chamaeleonidae based on next-generation sequencing methods is currently in preparation and the phylogeny of the *C. nasutum* group will be treated in this future work (Scherz *et al.* unpublished).

The comprehensive molecular study of Gehring *et al.* (2012) initiated the revision of the *Calumma nasutum* species group. This study distinguished 33 deep mitochondrial lineages within this group, and considered each an operational taxonomic unit (OTU). Seven of these apparently corresponded to existing species (see above), leaving 26 mitochondrial lineages in need of taxonomic assessment. One goal of the present work was to evaluate the species status of these genetic lineages and to assign them to the already described species. *Calumma nasutum* was one of the first chameleon species described from Madagascar by Duméril and Bibron (1836) on the basis of four syntypes, which were collected by Bernier with type location "Madagascar". Similarly, *Calumma linotum* was originally described with the imprecise type locality "Madagascar" on the basis of a single holotype (Müller, 1924) and *C. guibei* was described based on a type series of juvenile specimens (Hillenius, 1959). Without any genetic data from these old type specimens, the

identity of all three species has been unclear so far and needed to be revised (Glaw & Vences, 2007). Only with a clear definition of the already existing species can new species be described. In this work, the taxonomic status of the *C. nasutum* group is revised including the new-description and revalidation of species, following an integrative taxonomic approach. The *C. gallus* complex was not revised in this work due to lack of a sufficient number of specimens.

Taxonomic Act Disclaimer: This thesis makes reference to names of several new species of chameleons from taxonomic studies in the process of publication. For the ease of understanding, throughout the thesis I use the names in this paper and they appear in quotation marks. However, I hereby disclaim all taxonomic names published in this thesis for nomenclatural purposes (except for the already published names), and state that these are not to be considered available in the sense of the International Code of Zoological Nomenclature (ICZN), following Article 8.3 of the Code (ICZN, 1999).

2.3 Biofluorescence

"The world is full of magic things, patiently waiting for our senses to grow sharper."

William Butler Yeats

Biofluorescence is a fascinating phenomenon in itself, but is also in the focus of researchers looking for further fluorescent proteins that can be used in genetic engineering, for example as reporter genes (Arun *et al.*, 2005). Recently, fluorescence was discovered in the South American tree frog *Boana punctata* (Schneider, 1799) and in the closely related *B. atlantica* (Caramaschi and Velosa, 1996), produced by compounds in lymph and skin glands (Taboada*, et al.*, 2017a; Taboada, *et al.*, 2017b). Shortly afterwards followed the discovery of another fluorescent frog in Costa Rica (Deschepper *et al.*, 2018). These were the first reports of fluorescence in amphibians. Up to that time, the phenomenon of biofluorescence was mostly known from marine organisms, including more than 180 marine fish species (Sparks *et al.*, 2014), catsharks (Gruber *et al.*, 2016), and invertebrates including corals (Salih *et al.*, 2000), deep-sea siphonophores (Haddock *et al.*, 2005), hydromedusa (Haddock & Dunn, 2015), and mantis shrimp (Mazel *et al.*, 2004). The most well-known example of fluorescent organisms on land might be scorpions (Fasel *et al.*, 1997; Kloock, 2008; Kloock *et al.*, 2010), along with several species of spiders (Andrews *et al.*, 2007; Lim *et al.*, 2007) and butterflies (Vukusic & Hooper, 2005) as well as a species of parrot (K. Arnold *et al.*, 2002). Fluorescent reptile species have been reported as well, including hawksbill sea turtles, *Eretmochelys*

imbricata (Linnaeus, 1766) by Gruber & Sparks (2015) and the Iberian Worm-lizard *Blanus cinereus* (Vandelli, 1797) by Maitland & Hart (2008).

Little is known about the function or evolution of biofluorescence (Andrews *et al.*, 2007), but hypotheses as to its biological significance include photo protection (Salih *et al.*, 2000), UV-light detection (Kloock *et al.*, 2010), prey (Haddock & Dunn, 2015) or pollinator attraction (Gandía-Herrero *et al.*, 2005), and signalling for species recognition (Gruber *et al.*, 2016; Kloock, 2008; Lim *et al.*, 2007; Mazel *et al.*, 2004; Michiels *et al.*, 2008; Wucherer & Michiels, 2012), or male-male interactions (Gerlach *et al.*, 2014).

To demonstrate the fluorescent ability of an organism, three properties need to be investigated: the excitation spectrum, the emission spectrum, and the efficiency (Johnsen, 2012). While comparing the excitation and emission maxima a simple reflection of light can be ruled out. The efficiency of a fluorophore (the fluorescent molecule) is given with the "quantum yield" which is calculated by dividing the photons emitted by the photons absorbed:

$$\Phi = \frac{N_{emission}}{N_{absorption}}$$

Fluorescence does not produce light and is not a form of bioluminescence. This is often confused in popular thinking or even by biologists (Johnsen, 2012) and needs to be clarified. Bioluminescent organisms usually produce light by the oxidation of a light-emitting molecule, called "luciferin", and is catalysed by an enzyme—either a luciferase or photoprotein (Haddock *et al.*, 2010). This reaction requires energy, provided by ATP (Johnsen, 2012). Fluorescent molecules, however, are pigments that absorb light and emit a part of the absorbed energy as a photon (Figure 1). Usually this photon has a lower energy, and, therefore, a longer wavelength, than the incident photon (Figure 2). The extra energy is converted to vibrational states of the electron in the excited state (Johnsen, 2012).
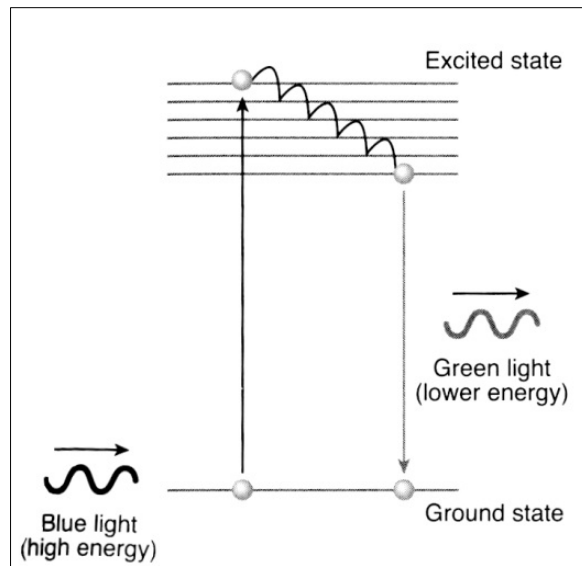
Figure 1. Simplified Jablonski diagram showing the excitation of an electron after the absorption of a photon. During the relaxation process fluorescence occurs at a longer wavelength. Modified from (Johnsen, 2012), used with permission.
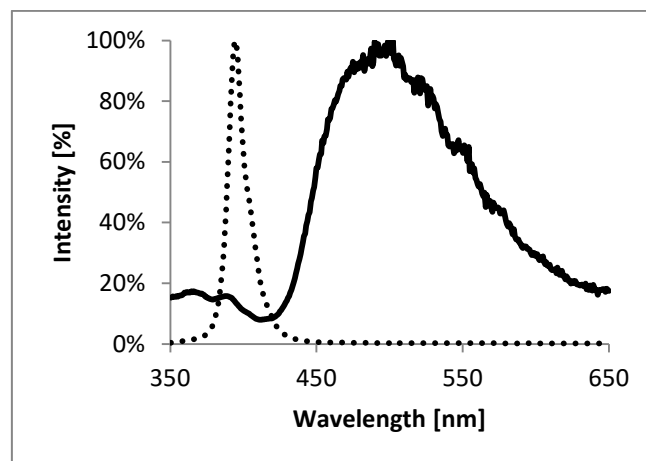
Figure 2. Excitation (dotted line) and emission spectra (solid line) of fluorescence in chameleons. As UV-source a 21 UV LED flashlight (Lighting EVER GmbH) was used illuminating florescent tubercles of the left temporal region of a large Madagascan chameleon (*Calumma globifer*, ZSM 221/2002). The maximum intensity value was set at 100%.

Although fluorescence cannot produce light, it can make parts of the organism appear brighter by converting incoming light to wavelengths that are better perceivable by the receiver's visual system. For example, green light at 550 nm appears much brighter to humans than the same intensity/number of photons of blue light at 440 nm (Johnsen, 2012). Therefore, a shift of blue to green photons by a fluorophore would enhance the total brightness.

Moreover, fluorophores can emit wavelengths that are rare in the surrounding environment. At a depth of ten meters below the ocean surface, red light (600–700 nm) is totally absorbed. If a fish converts the remaining blue light into red light, then a conspicuous

signal is created (Michiels *et al.*, 2008) that might be even invisible to predators whose visual systems have not been adapted to these wavelengths. Fluorescence also holds the advantage of scattering equally in all directions regardless of the irradiation angle (Figure 3). Johnsen notes that, "therefore, even a relatively inefficient fluorophore can appear quite bright when viewed horizontally, because it has taken a fraction of the much brighter down-dwelling light and converted it to light that is emitted in all directions. Even this fraction can be brighter than the horizontal background light" (Johnsen, 2012).
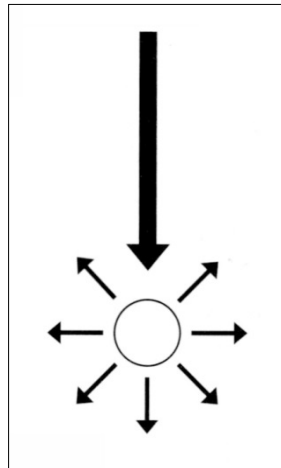

Figure 3. A fluorescent object with excitation light from above emits light in all directions. Although only a fraction of the light is converted to fluorescence, the emitted light can still be brighter than the background when viewed horizontally. Modified from (Johnsen, 2012), used with permission.

Only a few studies have empirically investigated the biological function of fluorescence. In the parrot species *Melopsittacus undulates* (Shaw, 1805) mate choice experiments showed that individuals of both sexes prefer partners with fluorescent plumage that naturally occurs on the crown and cheeks (K. Arnold *et al.*, 2002). In the cryptically coloured pygmy coral reef goby *Eviota pellucida* Larson, 1976, fluorescent chromatophores are used as a "private communication mechanism" (Michiels *et al.*, 2008) and the distribution of fluorescent pigments in the skin can even be regulated (Wucherer & Michiels, 2012). Gruber *et al.* (2016) built a shark-eye camera and proposed that the fluorescence occurring in their catshark species *Cephaloscyllium ventriosum* (Garman, 1880) and *Scyliorhinus rotifer* (Garman, 1881) makes them more conspicuous in their visual spectrum. In the first report on a fluorescent frog the authors found that fluorescence contributes 18–29% of the total emerging light at night (Taboada *et al.*, 2017b). The authors avoid a statement about a possible biological function but the recent discovery of nocturnal colour discrimination in amphibians (Yovanovich *et al.*, 2017) makes a signalling role probable. Given these few studies in contrast to the high number of reports on biofluorescence, Johnson argues that "the ecology of fluorescence is still very much a scientific frontier" (Johnsen, 2012). In chapter 3.2.1 the widespread fluorescence in chameleons is described as a previously unknown potential signalling mechanism.

3 Results

3.1 Taxonomy of the *Calumma nasutum* group

3.1.1 PAPER: Systematic revision of the Malagasy chameleons *Calumma boettgeri* and *C. linotum* (Squamata: Chamaeleonidae)

The taxonomic revision of the *Calumma nasutum* group began with species that have occipital lobes (=dermal flaps in the neck region) and are considered as the *C. boettgeri* complex. Here, the status of valid species recognized up to that date needed to be clarified. *Calumma linotum* (Müller 1924) was described based on a single male holotype with locality "Madagascar" (Müller, 1924) and had been considered either a synonym of *C. boettgeri* by some authors (e.g. Gehring *et al.,* 2011) or as a mysterious, poorly defined taxon (Raxworthy *et al.,* 2008). Using pholidosis, morphological measurements and micro-CT scans of the skull, both taxa were clearly delimited and redescribed. For the first time, micro-CT scans of the skeleton and hemipenes were used as a taxonomic tool. In preparation for scanning, the hemipenes were immersed in iodine solution, a method later named dice-CT (Gignac *et al.*, 2016). For an easy accessibility and exchange the large scan data was converted to a 3D PDF model and may be found in the supplementary materials.

Prötzel, D, Ruthensteiner, B, Scherz, MD, Glaw, F (2015): Systematic revision of the Malagasy chameleons *Calumma boettgeri* and *Calumma linotum* (Squamata: Chamaeleonidae). *Zootaxa 4048*, 211–231.

Post-publication comments and errata:

- Specific ornaments of the hemipenes of the *Calumma nasutum* group that are here called "pair of papillae" were later defined as the new character "cornucula gemina" (see chapter 3.1.2).
- Coordinates for *Calumma boettgeri* from Maromiandra are corrected from 13°99'65''S, 48°21'77''E to 13.9965°S, 48.2177°E. The correction was already published in Prötzel *et al.* (2017), see chapter 3.1.2.

Article

Systematic revision of the Malagasy chameleons *Calumma boettgeri* and *C. linotum* (Squamata: Chamaeleonidae)

DAVID PRÖTZEL[1,2], BERNHARD RUTHENSTEINER[1], MARK D. SCHERZ[1] & FRANK GLAW[1]

[1]*Zoologische Staatssammlung München (ZSM-SNSB), Münchhausenstr. 21, 81247 München, Germany*
[2]*Corresponding author. E-mail: david.proetzel@mail.de*

Abstract

We revise the taxonomic status of two species of Madagascan chameleons in light of a recent molecular phylogenetic study on the *Calumma nasutum* group. The investigation of morphological and osteological characters led to a clear delineation between two species within the *C. boettgeri* complex, *C. boettgeri* and *C. linotum*. *Calumma linotum* has been considered either a synonym of *C. boettgeri* or a dubious, poorly defined taxon. So far it has only been known from the male holotype with the imprecise locality 'Madagascar'. Based on pholidosis, morphological measurements and characters of the skull that were analyzed using micro-X-ray computed tomography (micro-CT) scans, we ascribe the population of chameleons from Montagne d'Ambre, formerly assigned to *C. boettgeri,* to *C. linotum*. *Calumma linotum* differs from *C. boettgeri* in the larger size of tubercle scales on the extremities and rostral appendage, the larger diameter of the extremities relative to the body size, the presence of a parietal crest as well as the form of the nasal bones and the anterior tip of the frontal. The life colouration of the males is also characteristic, with a blue rostral appendage and greenish turquoise extremities. The body and rostral appendage of *C. boettgeri* in contrast are inconspicuously yellowish brown coloured. All confirmed distribution records of *C. boettgeri* are confined to the biogeographic Sambirano region whereas *C. linotum* is only known from Montagne d'Ambre and a locality at the base of the Tsaratanana massif. Additional literature records of *C. boettgeri* and *C. linotum* from northeastern Madagascar are in need of confirmation. We also confirm the synonymy of *Chamaeleo macrorhinus* (described from a female holotype with an unknown locality) with *Calumma boettgeri*. The use of micro-CT exposed further characteristics for species delimitation in an integrative taxonomic approach. In addition to the skull, we also micro-CT scanned the hemipenes of *C. boettgeri* and *C. linotum*, using an iodine-based tissue stain, and provide 3D PDF models of these organs. This method enables detailed illustration and the detection of variation in particular characters, and might be an important tool in further taxonomic studies on the *C. nasutum* group and other squamate reptiles.

Key words: *Calumma boettgeri, Calumma linotum*, Chamaeleonidae, micro-computed tomography, hemipenis morphology, skull structure, Madagascar

Introduction

The island of Madagascar is one of the most valuable natural resources on the planet. In addition to an impressive number of animal and plant species, endemism reaches 85% for vascular plants, 84% for land vertebrates (Goodman & Benstead 2005), 92% for non-marine reptiles (Glaw & Vences 2007), and 100% for species in the chameleon genus *Calumma* (Townsend *et al.* 2011). Description of the island's species level diversity is far from complete, and modern molecular methods have contributed to an increase of species descriptions in recent years. Molecular analyses enable the discovery of cryptic species that show few or no external morphological differences (Bickford *et al.* 2007). Among Malagasy reptiles, cryptic diversity and microendemism is presumed to be widespread, but the level of these phenomena has not been rigorously explored (Gehring *et al.* 2012; Glaw *et al.* 2012).

The chameleon genus *Calumma* currently comprises 33 species, many of them described in the last 10 to 15 years (Tilbury 2014; Glaw 2015). Small *Calumma* species with a soft dermal appendage on the snout tip are clustered into the *Calumma nasutum* group, which includes the seven described species *C. boettgeri, C. fallax, C.*

gallus, C. guibei, C. linotum, C. nasutum and *C. vohibola* (Gehring *et al*. 2012). Within the *C. nasutum* group, three species (*C. boettgeri, C. guibei* and *C. linotum*) differ from the other species by the possession of well-defined occipital lobes, and this character has provided support for the phenetic *C. boettgeri* complex (Gehring *et al.* 2012). In contrast, molecular phylogenetic evidence suggests that neither the *C. nasutum* group nor the *C. boettgeri* complex are monophyletic (Gehring *et al*. 2012; Nagy *et al.* 2012; Tolley *et al.* 2013). Therefore, a comprehensive assessment within a phylogenetic framework is needed to fully resolve the taxonomy of this species complex.

The first species of the *C. nasutum* group with occipital lobes was described by Boulenger (1888) as 'Chamaeleon Boettgeri', based on two males and one female from Nosy Be. Fifteen years later Barbour (1903) described 'Chamaeleo macrorhinus' on the basis of an adult female from the imprecise type locality 'Madagascar' without naming any delimiting characters from *Ch. boettgeri. Chamaeleo macrorhinus* was synonymized with *Ch. boettgeri* by Mocquard (1909). In 1924, Müller described 'Chamaeleo linotus' based on one adult male from the collection of the Zoologische Staatssammlung München (ZSM), again with the vague type locality 'Madagascar'. According to the ZSM catalogue, this specimen was received in an exchanged with the Natural History Museum in Stuttgart (SMNS) in 1923, but no additional data is available on this specimen, and the catalogue of the SMNS collection was destroyed during WWII (A. Kupfer, pers. comm., 2014). Müller (1924) distinguished this species from *Ch. boettgeri* by the absence of a dorsal crest, the broader scales on the extremities, which also stand closer together, and the less distinct and less regular gular folds. Mertens (1933) assigned four female chameleons from northeast Madagascar to *Ch. linotus*, though these females lack rostral appendages. According to Angel (1942) *Ch. linotus* differs from *Ch. boettgeri* in the absence of a dorsal crest, larger scales on the legs and absence of a rostral appendage in females. Hillenius (1959) claimed the only important distinguishing characters of *Ch. linotus* compared to *Ch. boettgeri* are the lack of a dorsal crest and the lack of a rostral appendage in females. Brygoo (1971) characterised *Ch. linotus* as having a total length between 124 mm (males) and 109 mm (females), and a rostral appendage length of more than 3 mm (males), with un-notched occipital lobes and without a dorsal crest, claiming the latter to be the only difference between it and *Ch. boettgeri*. Based on their phylogenetic analysis, Klaver & Böhme (1986) transferred numerous Malagasy chameleons, including all species of the *Ch. nasutus* group, into the genus *Calumma*. Since these authors assumed that *Calumma* would be of feminine gender, they changed names accordingly; *Chamaeleo linotus* became *Calumma linota*. Lutzmann & Lutzmann (2004) and Walbröl & Walbröl (2004) argued *Calumma* to be of neutral gender and changed the species epithet to *C. linotum*.

The identity of *Calumma linotum,* which has only been reliably known from the holotype, is disputed and considered as poorly defined, and is sometimes considered a synonym of *C. boettgeri* (Gehring *et al.* 2011). Photographs shown in Nečas (2004), titled as an undescribed species of the *C. nasutum* complex, correspond well with *C. linotum* as it is herein re-defined. Raxworthy *et al*. (2008) applied the name "Calumma cf. linota" to a population from the Tsaratanana massif but without description or justification for this assignment. Gehring *et al*. (2012) tentatively adopted this assignment, emphasizing that this definition requires confirmation. Since the holotype of *C. linotum* is too old for successful DNA extraction and was probably fixed in formalin, it was not included in their phylogenetic analyses.

Species identification within the *Calumma nasutum* group is difficult due to high morphological variation, e.g. absence or presence of dorsal crests, heterogeneity in scalation or colour and shape of the rostral appendage. Similar to the *Calumma brevicorne* complex (Raxworthy & Nussbaum 2006), the broad distribution of *C. nasutum* along Madagascar's eastern rainforest chain raises expectations that it actually consists of a complex of cryptic species (Glaw & Vences 2007). The molecular phylogenetic study of Gehring *et al*. (2012) for the *C. nastutum* group based on the mitochondrial gene *ND2* suggested there may be as many as 33 operational taxonomical units (OTUs), despite only seven species being currently recognized (see above). That study included 215 individuals from 60 localities, of which 82 individuals were from the *C. boettgeri* complex (*C. boettgeri, C. guibei* and *C. linotum*). Eleven clades (A–K) were recovered, with at least 8% sequence divergence between them. Based on morphological features, clade D corresponded to *C. boettgeri*, clade E to *C. linotum*, and clade F to *C. guibei.* The classification of *C. linotum* by Gehring *et al*. (2012) remained uncertain because the holotype was not studied. In addition, clade D (*C. boettgeri*) showed geographic variation, with populations from Nosy Be and Manongarivo (D I), Montagne d'Ambre (D III), and Tsaratanana (D II). To define OTUs, Gehring *et al*. (2012) chose an uncorrected pairwise distance of > 6% as threshold, supported by additional Bayesian species delimitation algorithms. According to this threshold, genital morphology and pholidosis, *C. boettgeri* from Montagne d'Ambre forms a confirmed candidate species (CCS).

Although the information to date suggests that the *C. nasutum* group is in need of revision, molecular phylogenetics or barcoding approaches based on single markers alone are insufficient for taxonomic decisions and the choice of an inappropriate gene can result in incorrect tree topologies, making additional lines of evidence important for validation. With modern methods of imaging and three-dimensional computed tomography, the anatomical features of chameleons can be much better appreciated than with traditional methods, and this may potentially provide a wealth of new structural apomorphies (Tilbury 2014). In this work, the taxonomy of *Calumma boettgeri* and *C. linotum* is revised with an integrative taxonomic approach. In addition to the widely used morphological measurements and pholidosis, we investigated internal morphology using the example of sutures of the skull and, for the first time, fine details of the hemipenes, with the aid of X-ray micro-Computed Tomography (micro-CT).

Material and methods

Thirty-eight specimens of *C. boettgeri* sensu lato were obtained from the collections of the Museum of Comparative Zoology of Harvard University, Cambridge, Massachusetts (MCZ), the Senckenberg Museum, Frankfurt am Main (SMF), the Zoologisches Forschungsmuseum Alexander Koenig, Bonn (ZFMK) and the Zoologische Staatssammlung München (ZSM).

Terms of morphological measurements taken on these specimens were adapted from previous studies (Gehring *et al*. 2011; Eckhardt *et al*. 2012). Measurements (Fig. 1) were taken with a digital caliper to the nearest 0.1 mm through a binocular dissecting microscope: Snout-vent length (SVL) from the snout tip (not including the rostral appendage) to the cloaca; tail length (TaL) from the cloaca to tail tip; total length (TL) as a sum of SVL + TaL; the ratio of TaL to snout-vent length (RST); length of the rostral appendage (LRA) from the upper snout tip; ratio of length of rostral appendage and snout-vent length (RRS); number of peripheral scales on the rostral appendage (RAPSC); RAPSC divided by the length of the rostral appendage (NPSCM); rostral crest (RC) present (+) or absent (-); number of supralabials (NSL); number of infralabials (NIL); lateral diameter of the occipital lobes (OLD); depth of the dorsal notch in the occipital lobes (OLN); parietal crest (PC) absent (-) or represented by a number of scales; likewise the dorsal crest (DC), dorsal cones counted when visible with the naked eye without the use of a binocular microscope according to Eckhardt *et al*. (2012); axillary pits (AP) of the upper extremities present (+) or absent (-); diameter of the broadest scale (DSC) of the upper arm (defined as the area from the armpits to the elbow in lateral view, Fig. 1); relation of DSC to the snout-vent length (RSB); number of large scales (diameter ≥ 0.2 mm) of the heterogeneous scalation of the upper arm (NSC); upper arm diameter at the level of the armpit (UAD); and the ratio of UAD to snout-vent length (RAS). Figures 1–3 were taken with digital and analogous cameras.

For internal morphology micro-CT scans of the head were prepared for ten specimens *C. boettgeri* sensu lato representing both major localities (5 of each sex): ZSM 440/2000 and ZSM 444/2000, males from Nosy Be; ZSM 441/2000 and ZSM 227/2002, females from Nosy Be; ZSM 2072/2007 and ZSM 2073/2007, males from Montagne d'Ambre; ZSM 551/2001, female from Andampy; ZSM 873/1920/2, female with unknown locality, but morphologically identical with the Montagne d'Ambre form; ZSM 21/1923, male holotype of *C. linotum*, type locality 'Madagascar'; MCZ 5988, female holotype of *C. macrorhinus*, type locality 'Madagascar'. For micro-CT scanning, specimens were placed in a closed plastic vessel slightly larger than the specimen with the head oriented upwards, and stabilized with ethanol soaked paper. To avoid disturbances during scanning, it was ensured that the paper did not cover the head region. Micro-CT scanning was performed with a phoenix nanotom m (GE Measurement & Control, phoenix|x-ray, Wunstorf, Germany) at a voltage of 130 kV and a current of 80 µA for 29 minutes (1800 projections). 3D data sets were processed with VG Studio Max 2.2 software (Visual Graphics GmbH, Heidelberg, Germany); the data were visualized using the Phong volume renderer to show the surface of the skull. Osteological terminology follows Rieppel & Crumly (1997). Measurements were taken with VG Studio Max 2.2 using the following abbreviations (Fig. 4): NL, nasal length; NW, nasal width; PS, parietal at the smallest diameter; PL, parietal at the largest diameter; PC, parietal crest absent (-) or number of tubercles.

Hemipenes of three male specimens from Montagne d'Ambre (ZSM 1683/2012, ZSM 2072/2007 and ZSM 2073/2007) and two males from Nosy Be (ZSM 440/2000 and ZSM 444/2000) were micro-CT scanned (Fig. 5). One hemipenis was clipped off from each specimen and immersed in iodine solution (I$_2$ in 1% ethanol) for two days to increase X-ray absorbance. For scanning, the hemipenes were placed with their apices oriented upwards in a plastic tube immersed in 70% ethanol. Scanning was performed for 30 or 60 min at a voltage of 60 kV and a current of 300 or 240 µA (2400/3600 projections), respectively. 3D data were processed with VG Studio Max 2.2 as described above. 3D models were prepared with the software Amira (version 5.4.5, VSG, Hillsboro, OR)

essentially following Ruthensteiner & Heß (2008). Hemipenial terminology follows Klaver & Böhme (1986). The distribution map was modified from vegmad.org (Fig. 6).
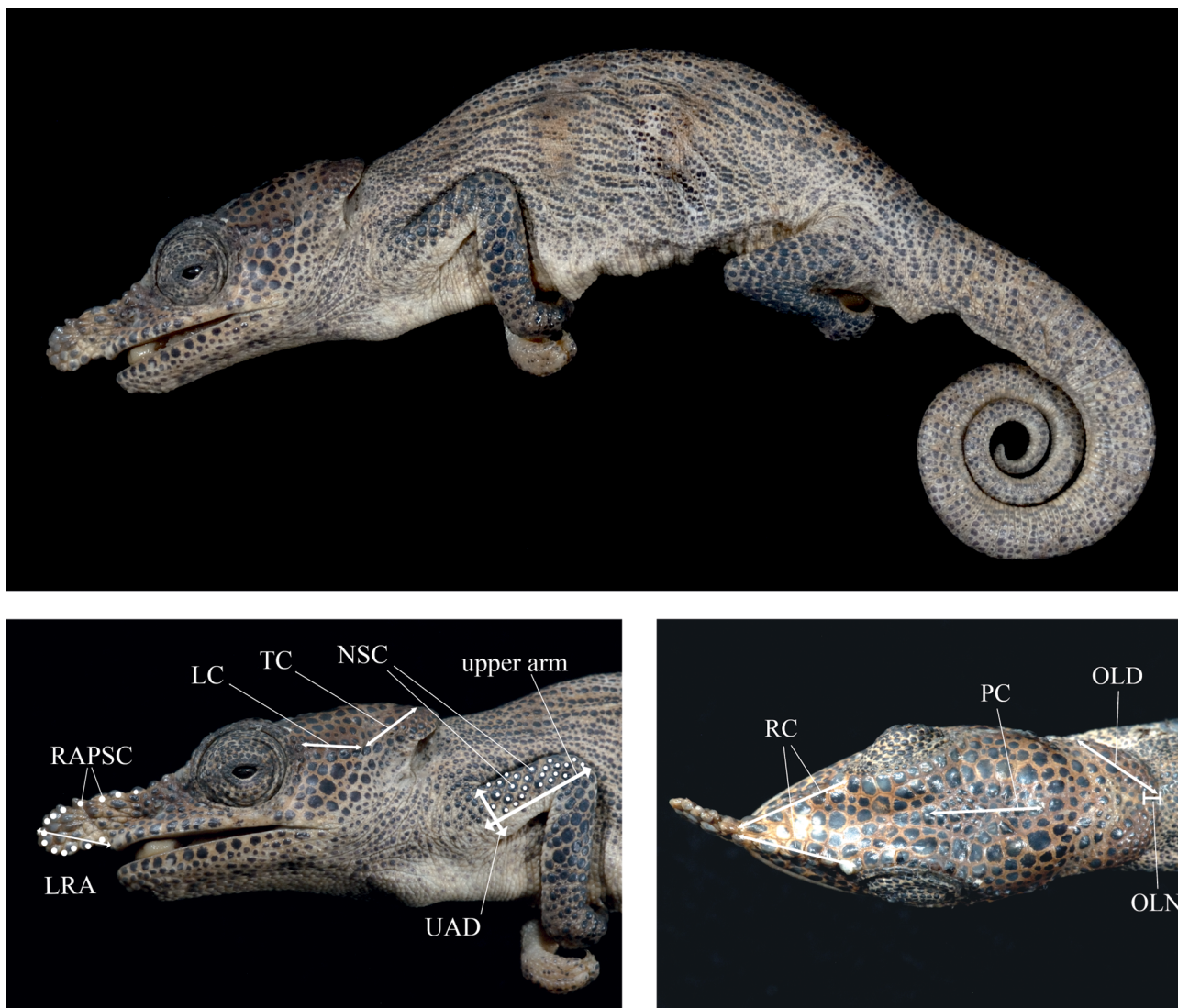
FIGURE 1. Landmarks for morphometric measurements and pholidosis, shown in lateral and dorsal view of a male *C. linotum* (ZSM 873/1920/3) with unknown locality. Notes: LRA, length of rostral appendage from snout tip; RAPSC, number of peripheral scales on rostral appendage; RC, rostral crest; PC, parietal crest; LC, lateral crest; TC, temporal crest; OLD, lateral diameter of the occipital lobe; OLN, occipital lobe dorsally notched; UAD, upper arm diameter; NSC, number of big scales on upper arm from lateral view.

Results

Morphology of *Calumma boettgeri* sensu lato

External morphology. Measurements of important morphological parameters were taken from 23 specimens (11 males, 12 females) from Nosy Be, six specimens (five males, one female) from Montagne d'Ambre, and another nine specimens without exact locality data (Table 1). Because there was only one female from Montagne d'Ambre available, only males from both species were considered for comparison of body size, extremities and appendages. The specimens without localities were not included in mean value calculations but could be assigned according to their morphology to the Nosy Be morphotype (four specimens) and the Montagne d'Ambre morphotype (five specimens), respectively.

TABLE 1. Morphological measurements of *Calumma boettgeri* and *C. linotum*. Abbreviations: m, male; f, female; SVL, snout-vent length; TaL, tail length; TL, total length; RST, ratio of tail to snout-vent length; LRA, length of rostral appendage; RRS, ratio of length of rostral appendage from snout tip; RAPSC, number of peripheral scales on rostral appendage; NPSCM, number of peripheral scales per mm on rostral appendage; RC, rostral crest present (+) or absent (-); NSL, number of supralabials; NIL, number of infralabials; OLD, lateral diameter of the occipital lobe; OLN, depth of the dorsal notch in occipital lobe; PC, parietal crest absent (-) or number of parietal cones; DC, dorsal crest absent (-) or number of dorsal cones; AP, axillary pits present (+) or absent (-); DSC, diameter of broadest scale on upper arm; RSB, ratio of broadest scale to snout-vent length; NSC, number of big scales on upper arm from lateral view; UAD, upper arm diameter; RAS, ratio of arm diameter to snout-vent length; all measurements in mm.

collection no.	species	locality	sex	SVL	TaL	TL	RST	LRA	RRS	RAPSC	NPSCM	RC	NSL
ZFMK 51389	C. boettgeri	Nosy Be	m	51.5	51.8	103.4	0.99	4.0	0.077	26	6.5	+	12
ZFMK 51520	C. boettgeri	Nosy Be	m	50.7	54.2	104.9	0.94	3.0	0.060	21	7.0	+	13
ZFMK 45987	C. boettgeri	Nosy Be	m	51.6	52.8	104.4	0.98	2.6	0.051	13	4.9	+	11
ZFMK 45988	C. boettgeri	Nosy Be	m	49.9	54.4	104.3	0.92	3.1	0.062	18	5.8	+	12
ZFMK 51518	C. boettgeri	Nosy Be	m	46.0	45.5	91.4	1.01	2.6	0.057	17	6.5	+	12
ZFMK 51519	C. boettgeri	Nosy Be	m	50.7	50.2	100.9	1.01	3.2	0.062	26	8.3	+	12
ZFMK 51521	C. boettgeri	Nosy Be	m	41.1	45.8	86.9	0.90	4.1	0.100	22	5.4	+	12
ZSM 36/1913	C. boettgeri	Nosy Be	m	41.4	44.0	85.4	0.94	2.5	0.059	15	6.1	+	12
ZSM 440/2000	C. boettgeri	Nosy Be	m	50.1	54.1	104.2	0.93	3.0	0.060	14	4.6	+	12
ZSM 444/2000	C. boettgeri	Nosy Be	m	51.9	55.0	106.9	0.94	2.9	0.057	17	5.8	+	12
SMF 16471	C. boettgeri	Nosy Be	m	50.3	54.3	104.6	0.93	3.6	0.072	15	3.6	+	13
ZFMK 51514	C. boettgeri	-	m	49.4	51.2	100.6	0.96	3.5	0.072	17	4.8	+	13
ZSM 866/1920	C. boettgeri	-	m	54.6	55.7	110.3	0.98	3.6	0.065	17	4.8	+	16
ZFMK 45985	C. boettgeri	Nosy Be	f	48.9	46.7	95.6	1.05	3.8	0.077	20	5.3	+	12
ZFMK 51516	C. boettgeri	Nosy Be	f	51.4	51.2	102.6	1.00	2.2	0.042	20	9.2	+	11
ZFMK 51517	C. boettgeri	Nosy Be	f	50.5	47.6	98.1	1.06	3.1	0.062	18	5.8	+	11
ZFMK 50615	C. boettgeri	Nosy Be	f	42.0	41.8	83.8	1.00	3.0	0.072	18	5.9	+	11
ZFMK 45983	C. boettgeri	Nosy Be	f	50.8	48.6	99.4	1.05	4.1	0.081	-	-	+	12
ZFMK 45986	C. boettgeri	Nosy Be	f	45.0	45.2	90.3	1.00	-	-	-	-	+	12
ZFMK 48226	C. boettgeri	Nosy Be	f	47.6	47.3	94.9	1.01	2.5	0.052	14	5.7	+	15

TABLE 1. (Continued)

collection no.	species	locality	sex	SVL	TaL	TL	RST	LRA	RRS	RAPSC	NPSCM	RC	NSL
ZFMK 45984	C. boettgeri	Nosy Be	f	55.5	52.5	108.0	1.06	1.2	0.022	10	8.1	+	12
ZSM 227/2002	C. boettgeri	Nosy Be	f	48.8	52.8	101.6	0.92	3.2	0.065	15	4.7	+	12
ZSM 441/2000	C. boettgeri	Nosy Be	f	45.5	43.4	88.9	1.05	2.7	0.060	16	5.9	+	12
SMF 16471	C. boettgeri	Nosy Be	f	50.0	46.7	96.7	1.07	2.8	0.056	14	5.0	+	13
SMF 16472	C. boettgeri	Nosy Be	f	46.0	45.7	91.7	1.01	3.0	0.065	14	4.7	+	12
ZSM 865/1920	C. boettgeri	-	f	49.4	46.7	96.1	1.06	3.5	0.070	20	5.8	+	15
ZFMK 51515	C. boettgeri	-	f	51.3	48.2	99.5	1.06	2.9	0.057	17	5.8	+	13
MCZ 5988	Ch. macrorhinus	'Madagascar'	f	48.1	44.9	93.1	1.07	2.8	0.058	17	6.1	+	17
ZSM 236/2004	C. linotum	M. d'Ambre	m	55.4	63.0	118.4	0.88	4.3	0.077	16	3.7	+	13
ZSM 1683/2012	C. linotum	M. d'Ambre	m	53.0	56.3	109.3	0.94	4.7	0.089	cut	-	+	13
ZSM 2073/2007	C. linotum	M. d'Ambre	m	59.6	64.8	124.4	0.92	4.5	0.075	18	4.0	+	-
ZSM 2072/2007	C. linotum	M. d'Ambre	m	53.7	59.2	112.8	0.91	4.3	0.080	13	3.0	+	13
ZFMK 52308	C. linotum	Joffreville	m	36.2	37.9	74.1	0.96	2.5	0.068	15	6.1	+	-
ZSM 873/1920/3	C. linotum	-	m	54.6	58.1	112.6	0.94	4.4	0.081	14	3.2	+	12
ZSM 873/1920/1	C. linotum	-	m	52.4	cut	52.4	-	4.3	0.081	16	3.8	+	12
ZFMK 36630	C. linotum	-	m	55.6	61.9	117.5	-	4.7	0.085	15	3.2	+	12
ZSM 551/2001	C. linotum	Andampy	f	50.6	50.7	101.3	1.00	2.0	0.040	9	4.5	+	13
ZSM 622/1999	C. linotum	-	f	54.5	54.9	109.4	0.99	4.1	0.075	15	3.7	+	13
ZSM 873/1920/2	C. linotum	-	f	42.7	47.4	90.1	0.90	3.1	0.072	15	4.9	+	12
ZSM 21/1923	C. linotum	'Madagascar'	m	56.1	70.0	126.1	0.80	4.3	0.077	15	3.5	+	14

Continued.

collection no.	species	locality	sex	NIL	OLD	OLN	PC	DC	AP	DSC	RSB	NSC	UAD	RAS
ZFMK 51389	*C. boettgeri*	Nosy Be	m	12	3.7	0.3	-	19	-	0.4	0.008	7	2.0	0.038
ZFMK 51520	*C. boettgeri*	Nosy Be	m	13	3.1	0.3	-	2	-	0.4	0.007	10	2.2	0.044
ZFMK 45987	*C. boettgeri*	Nosy Be	m	11	4.7	0.4	-	0	-	0.5	0.010	9	2.1	0.040
ZFMK 45988	*C. boettgeri*	Nosy Be	m	11	3.0	0.4	-	12	-	0.2	0.004	10	2.0	0.041
ZFMK 51518	*C. boettgeri*	Nosy Be	m	13	3.4	0.3	-	0	-	0.4	0.008	8	2.2	0.048
ZFMK 51519	*C. boettgeri*	Nosy Be	m	11	4.3	0.6	-	18	-	0.3	0.006	9	2.0	0.039
ZFMK 51521	*C. boettgeri*	Nosy Be	m	11	3.8	0.6	-	5	-	0.3	0.007	9	1.5	0.036
ZSM 36/1913	*C. boettgeri*	Nosy Be	m	12	3.2	0.0	-	0	-	0.4	0.008	12	1.8	0.043
ZSM 440/2000	*C. boettgeri*	Nosy Be	m	12	4.8	0.3	-	28	-	0.4	0.008	14	2.5	0.050
ZSM 444/2000	*C. boettgeri*	Nosy Be	m	12	3.7	0.5	-	15	-	0.4	0.008	11	2.3	0.045
SMF 16471	*C. boettgeri*	Nosy Be	m	13	4.0	0.0	-	11	-	0.4	0.009	9	2.0	0.040
ZFMK 51514	*C. boettgeri*	-	m	13	3.7	0.3	-	14	-	0.5	0.009	11	2.2	0.044
ZSM 866/1920	*C. boettgeri*	-	m	15	3.7	0.3	-	20	-	0.4	0.008	8	2.0	0.036
ZFMK 45985	*C. boettgeri*	Nosy Be	f	13	4.6	0.5	-	0	-	0.4	0.007	10	1.8	0.036
ZFMK 51516	*C. boettgeri*	Nosy Be	f	11	3.8	0.5	-	0	-	0.3	0.007	12	2.2	0.042
ZFMK 51517	*C. boettgeri*	Nosy Be	f	11	2.7	0.5	-	0	-	0.4	0.007	14	2.2	0.044
ZFMK 50615	*C. boettgeri*	Nosy Be	f	12	3.4	0.4	-	0	-	0.4	0.008	8	1.5	0.036
ZFMK 45983	*C. boettgeri*	Nosy Be	f	12	3.5	0.0	-	0	-	0.3	0.006	11	2.1	0.040
ZFMK 45986	*C. boettgeri*	Nosy Be	f	11	3.0	0.5	-	3	-	0.3	0.007	9	2.0	0.044
ZFMK 48226	*C. boettgeri*	Nosy Be	f	14	2.7	0.3	-	0	-	0.2	0.004	-	1.9	0.039
ZFMK 45984	*C. boettgeri*	Nosy Be	f	11	2.8	0.4	-	0	-	0.3	0.005	11	2.0	0.036
ZSM 227/2002	*C. boettgeri*	Nosy Be	f	12	3.3	0.1	-	0	-	0.3	0.006	11	2.0	0.041
ZSM 441/2000	*C. boettgeri*	Nosy Be	f	12	3.9	0.5	-	0	-	0.4	0.008	9	2.2	0.048

TABLE 1. (Continued)

collection no.	species	locality	sex	NIL	OLD	OLN	PC	DC	AP	DSC	RSB	NSC	UAD	RAS
SMF 16471	C. boettgeri	Nosy Be	f	10	4.2	0.0	-	0	-	0.4	0.007	9	2.2	0.044
SMF 16472	C. boettgeri	Nosy Be	f	13	3.5	0.1	-	11	-	0.4	0.009	10	1.8	0.039
ZSM 865/1920	C. boettgeri	-	f	13	2.8	0.1	-	0	-	0.3	0.006	9	1.9	0.038
ZFMK 51515	C. boettgeri	-	f	13	3.3	0.7	-	0	-	0.3	0.006	12	2.1	0.041
MCZ 5988	Ch. macrorhinus	'Madagascar'	f	6.1	3.2	0.1	-	0	-	0.3	0.007	8	2.3	0.047
ZSM 236/2004	C. linotum	M. d'Ambre	m	13	4.5	0.0	4	10	-	0.7	0.012	18	2.9	0.052
ZSM 1683/2012	C. linotum	M. d'Ambre	m	13	4.7	0.1	3	8	-	0.7	0.014	20	2.9	0.055
ZSM 2073/2007	C. linotum	M. d'Ambre	m	12	4.2	0.0	3	13	-	0.6	0.010	22	3.1	0.052
ZSM 2072/2007	C. linotum	M. d'Ambre	m	12	3.8	0.2	4	12	-	0.8	0.015	21	3.1	0.058
ZFMK 52308	C. linotum	Joffreville	m	-	2.8	0.0	3	9	-	0.4	0.011	20	1.7	0.048
ZSM 873/1920/3	C. linotum	-	m	14	4.1	0.2	6	5	-	0.7	0.013	19	3.0	0.054
ZSM 873/1920/1	C. linotum	-	m	12	4.8	0.1	5	4	-	0.8	0.015	19	3.0	0.058
ZFMK 36630	C. linotum	-	m	12	3.7	0.3	4	0	-	0.7	0.012	23	3.0	0.054
ZSM 551/2001	C. linotum	Andampy	f	13	5.1	0.0	(5)	6	-	0.6	0.011	16	2.8	0.055
ZSM 622/1999	C. linotum	-	f	13	4.1	0.2	(4)	0	-	0.6	0.011	22	2.9	0.054
ZSM 873/1920/2	C. linotum	-	f	12	3.9	0.0	6	0	-	0.5	0.013	17	2.8	0.065
ZSM 21/1923	C. linotum	'Madagascar'	m	14	4.7	0.1	(5)	0	-	0.7	0.013	22	3.0	0.054

Individuals from Montagne d'Ambre show clear morphological differences from Nosy Be specimens (Fig. 7). The adult males examined from Montagne d'Ambre are larger than those from Nosy Be (mean values of TL 107.8 mm in Montagne d'Ambre vs. 99.3 mm in Nosy Be, Table 2), their rostral appendage is longer related to the snout-vent length (RRS 0.078 vs. 0.065) and the ratio of arm diameter to snout-vent length is larger (UAD/SVL 0.053 vs. 0.042).

TABLE 2. Mean values and standard deviations (SD) of morphological measurements of *Calumma boettgeri*, n (males) = 11, n (females) = 12 and *C. linotum* males (n =5); all measurements in mm. For abbreviations see Table 1.

species	*C. boettgeri*		*C. boettgeri*		*C. linotum*	
locality	Nosy Be		Nosy Be		M. d'Ambre	
sex	m		f		m	
	mean value	SD	mean value	SD	mean value	SD
SVL	48.5	4.2	48.6	3.8	51.6	9.0
TaL	50.8	4.2	47.7	3.7	56.2	10.8
TL	99.3	8.1	96.3	7.2	107.8	19.7
RST	0.96	0.04	1.02	0.04	0.92	0.03
LRA	3.1	0.5	2.9	0.9	4.1	0.9
RRS	0.065	0.014	0.059	0.018	0.078	0.008
RAPSC	18.9	4.7	16.4	3.4	15.5	2.1
NPSCM	6.1	1.0	6.3	1.5	4.2	1.3
NSL	12	0.5	12	1	13	0
NIL	11.8	0.8	11.9	0.9	12.5	0.6
OLD	3.8	0.6	3.7	0.4	4.0	0.7
DSC	0.36	0.08	0.32	0.05	0.64	0.15
RSB	0.0075	0.0015	0.0066	0.0012	0.0124	0.0019
NSC	9.9	2.0	10.6	1.8	20.2	1.5
UAD	2.1	0.3	2.0	0.2	2.7	0.6
RAS	0.042	0.005	0.041	0.004	0.053	0.004

Both populations show heterogeneous scalation, especially at the extremities and the rostral appendage. The enlarged rounded tubercles on the limbs are distinctly larger in animals from Montagne d'Ambre; the mean diameter of the largest tubercle of the upper arm is 0.64 mm compared to 0.36 mm (Nosy Be). Additionally the number of the enlarged tubercles on the upper arm of males from Montagne d'Ambre is approximately twice that of males from Nosy Be, with a mean of 20.2 compared to 9.9, respectively, and the tubercles are not bordering each other on Nosy Be individuals. This character is also confirmed from a juvenile of SVL 26.9 mm (ZFMK 48227, Nosy Be) and a juvenile of SVL 36.2 mm (ZFMK 52308, Joffreville). Another morphological difference between both populations can be found in the pholidosis of the rostral appendage. Although the rostral appendage is significantly smaller in males from Nosy Be (see above), they have more peripheral scales on it, with a mean of 18.9 compared to 15.5 in Montagne d'Ambre males. In relation to the size of the appendage, this means 6.1 scales per mm compared with 4.1 scales per mm in Montagne d'Ambre. In summary, specimens from Montagne d'Ambre show a more heterogeneous scalation with broader tubercles on extremities and the rostral appendage. This is true of females as well (note that only one female with locality data was examined). Montagne d'Ambre individuals differ also in both sexes from Nosy Be specimens in the presence of a parietal crest which is best visible in the micro-CT scan (see below).

The other morphological features either were highly variable or did not differ between the populations. For example, the number of dorsal cones was 0–28 in Nosy Be, and 9–13 in Montagne d'Ambre. Likewise the edges of the occipital lobes vary between the specimens. They range between un-notched and clearly notched (up to 0.7 mm) in Nosy Be, and are either not or only slightly notched (up to 0.3 mm) in Montagne d'Ambre. All specimens have a rostral crest and none have axillary pits.

Colouration. Males also show great differences between the populations in colouration (see Fig. 2A, B). Males from Montagne d'Ambre were more colourful, with a true blue rostral appendage and greenish turquoise extremities (Fig. 2A). The colour of the legs is induced only by the coloured tubercle scales. The body is pale green or light brown with two dark brown spots and (occasionally) a beige lateral stripe on each side that stops at the base of the tail. The tail is the same colour as the body and (in stress colouration) possesses black annulations. The head is also greenish or brown with a dark stripe from the snout crossing the eyes to the occipital lobes. The skin around the mouth and the throat can be white. The colour description is based on a total of seven pictures of the Montagne d'Ambre form, referred to as *C. boettgeri* in Schmidt *et al.* (2010), *C. boettgeri* (picture 1c) in Glaw & Vences (2007) *Calumma* sp. in Nečas (2004) and *C. boettgeri* in Garbutt *et al.* (2001). The body and head of females is brown; the rostral appendage can be coloured bright blue, see picture of *C. boettgeri* in Schmidt *et al.* (2010).
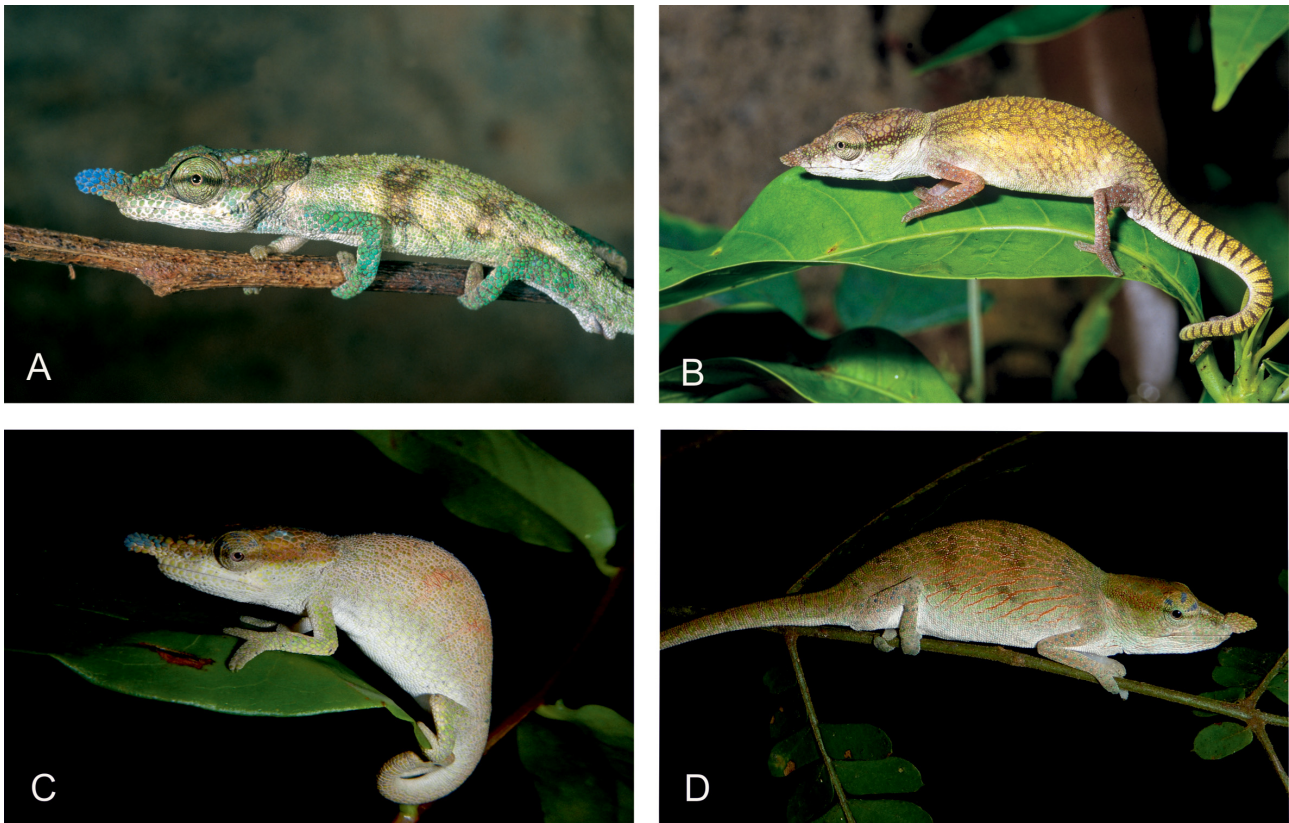

FIGURE 2. (A) Baseline colouration in life of male *Calumma linotum* from Montagne d'Ambre during day; (B) Baseline colouration in life of male *C. boettgeri* from Nosy Be during day; (C) female *C. linotum* from Montagne d'Ambre at night; (D) female *C. boettgeri* from Nosy Be at night. Photos taken by FG.

The body colouration of males from Nosy Be in contrast is yellowish or greenish brown with little dark brown rosettes, when stressed (Fig. 2B). The legs are brown with little blue or green spots resulting from the tubercles. The colouration of the head is similar to the body colouration. The rostral appendage differs clearly from Montagne d'Ambre with the absence of any striking colour and is the same brown colour as the casque. Females are uniformly light or greenish brown coloured. Compare also a total of seven pictures of *Calumma boettgeri* in Hyde Roberts & Daly (2014), in Glaw & Vences (2007: 191) picture 1a and 1b, in Nečas (2004) and in Henkel & Schmidt (1995).

Osteology of the skull based on micro-CT scans. Micro-CT scans of heads of two males and two females from Nosy Be and from Montagne d'Ambre exposed additional differences between the two forms. Specimens from Montagne d'Ambre (Fig. 4, D and E) bear tubercles on the parietal in both sexes. These form a little parietal crest in the middle with three to four tubercles, laterally followed by two tubercles on each side. The frontal is also irregularly spotted with tubercles. The parietal and frontal of animals from Nosy Be in contrast are smooth (Fig. 4, A and B).

As in all species of the genus *Calumma*, the nasal bones are paired (Rieppel & Crumly 1997). These are broader in our specimens from Montagne d'Ambre (mean NW 0.35 mm vs. 0.24 mm in Nosy Be; mean NW/NL

0.18 vs. 0.14, Table 3, Fig. 4) and the anterior tip of the frontal bone does not exceed more than a half of the naris. In skulls from Nosy Be it does exceed this point, and the frontal meets the premaxilla, as described for *C. nasutum* (Rieppel & Crumly 1997). The parietal also varies between the two localities. In Nosy Be samples, the parietal tapers more tightly. Its diameter is at the tightest area on average 0.61 mm (vs. 1.06 mm) and 11% of the largest diameter of the parietal (vs. 22%, Table 3, Fig. 4). The parietal in Montagne d'Ambre samples appears wider and more compact. However, the form of the parietal is variable within localities and cannot be used as a diagnostic character. Although chameleons are sexually dimorphic animals, differences between sexes in skull structure were not proven (Table 3).

TABLE 3. Osteological measurements of important characters of the skull for differentiation between *Calumma boettgeri* und *C. linotum*.
Notes: m, male; f, female; NL, nasal length; NW, nasal width; RNWL, ratio of nasal width to length; PL, largest diameter; PS, parietal smallest diameter; RPSL, ratio of parietal smallest to largest diameter; PC, parietal crest absent (-) or number of tubercles.

collection no.	species	locality	sex	NL	NW	RNWL	PL	PS	RPSL	PC
ZSM 440/2000	*C. boettgeri*	Nosy Be	m	2.1	0.3	0.14	4.7	0.5	0.11	-
ZSM 441/2000	*C. boettgeri*	Nosy Be	f	2.2	0.2	0.09	3.9	0.5	0.13	-
ZSM 444/2000	*C. boettgeri*	Nosy Be	m	1.8	0.3	0.17	4.7	0.3	0.07	-
ZSM 227/2002	*C. boettgeri*	Nosy Be	f	1.3	0.2	0.15	4.1	0.6	0.15	-
mean value				1.85	0.25	0.14	4.35	0.49	0.11	
SD				0.40	0.06	0.03	0.41	0.11	0.03	
MCZ 5988	*Ch. macrorhinus*	'Madagascar'	f	2.0	0.2	0.10	3.9	1.1	0.28	1
ZSM 2072/2007	*C. linotum*	M. d'Ambre	m	2.5	0.4	0.16	4.5	1.5	0.33	4
ZSM 2073/2007	*C. linotum*	M. d'Ambre	m	2.1	0.4	0.19	4.6	0.6	0.13	3
ZSM 873/1920/2	*C. linotum*	M. d'Ambre	f	2.3	0.3	0.15	4.2	0.9	0.21	4
ZSM 551/2001	*C. linotum*	Andampy	f	1.4	0.3	0.23	4.3	0.9	0.21	3
mean value				2.07	0.36	0.18	4.40	0.97	0.22	3.50
SD				0.49	0.04	0.04	0.18	0.38	0.08	0.58
ZSM 21/1923	*C. linotum*	'Madagascar'	m	2.7	0.3	0.11	4.6	1.4	0.30	4

Hemipenial morphology based on micro-CT scans. The scans of hemipenes of specimens from each population enable a detailed view of their structure. The hemipenes are illustrated in sulcal and asulcal view with the apex on top (Fig. 5). Both populations show large and deep calyces with smooth ridges on the asulcal side of the truncus. The apex is ornamented with two pairs of long pointed papillae and two pairs of rotulae. The papillae rise from the sulcal side of the apex and are curved to the asulcal side. They can be completely everted (Fig. 5, C) or retracted in the apex (Fig. 5, D). One pair of rotulae is placed on the asulcal side (the smaller one) and one pair on the sulcal side. Here some differences between the populations are recognizable; in Nosy Be (n = 2) the rotulae are slightly more denticulated, with 6–11 tips on asulcal side and 14–16 tips on sulcal side, compared to Montagne d'Ambre (n = 3) with 6–8 tips on the rotulae of the asulcal side and 11–14 tips on both rotulae on the sulcal side.

Re-description of the holotype of *Calumma linotum* (Müller, 1924)

Holotype. ZSM 21/1923, adult male, hemipenes not everted, location unknown ('Madagascar'), collected by an unknown individual on an unknown date; in a good state of preservation, except a slit on the ventral side of the body; mouth open with tip of the tongue between the jaws.

FIGURE 3. Preserved specimens with detail view on the different scalation of the upper arm; (A) male holotype of *Calumma linotum* (ZSM 21/1923, Madagascar), note the bluish colour of the limb scales and the two large grey markings on back and flanks; (B) female holotype of *Chamaeleo macrorhinus* (MCZ 5988, Madagascar). Scale bar = 10 mm.

Morphology. SVL 56.1 mm; tail length 70.0 mm; distinct rostral ridges that fuse on the anterior snout in a soft, laterally compressed dermal rostral appendage that projects 4.3 mm beyond the upper snout tip, rounded distally; supra-orbital crest rounded in lateral view and formed by a single, rather smooth row of tubercles; lateral crest poorly developed and pointing straight posteriorly, fusing to form the poorly developed temporal crest that curves upwards to the highest point of the casque; distinct parietal crest; occipital lobes clearly developed and slightly notched (0.1 mm); no traces of gular and ventral crest; dorsal crest in the form of enlarged tubercles present,

starting 2.7 mm behind the occipital lobes without a defined ending, consisting of seven tubercles that are each separated by ~2.5 mm.

Body laterally compressed with fine homogeneous scalation, with the exception of the extremities and head region; legs with enlarged rounded tubercle scales bordering each other; heterogeneous scalation on the head and more strongly raised tuberclular scales on the rostral crest and rostral appendage; no axillary pits. Full morphological measurements are provided in Table 1.

Skull osteology of the holotype (Fig. 4F; Table 3). Broad nasal bones (NW: 0.3 mm, NL: 2.7 mm) are paired and meet anteriorly; the anterior tip of the frontal bone does not exceed more than half of the naris; the frontal is irregularly spotted with tubercles; four tubercles form a parietal crest in the middle of the parietal, laterally followed by two tubercles on each side. The parietal tapers posteriorly from 4.6 mm (largest diameter) to 1.4 mm (smallest diameter).
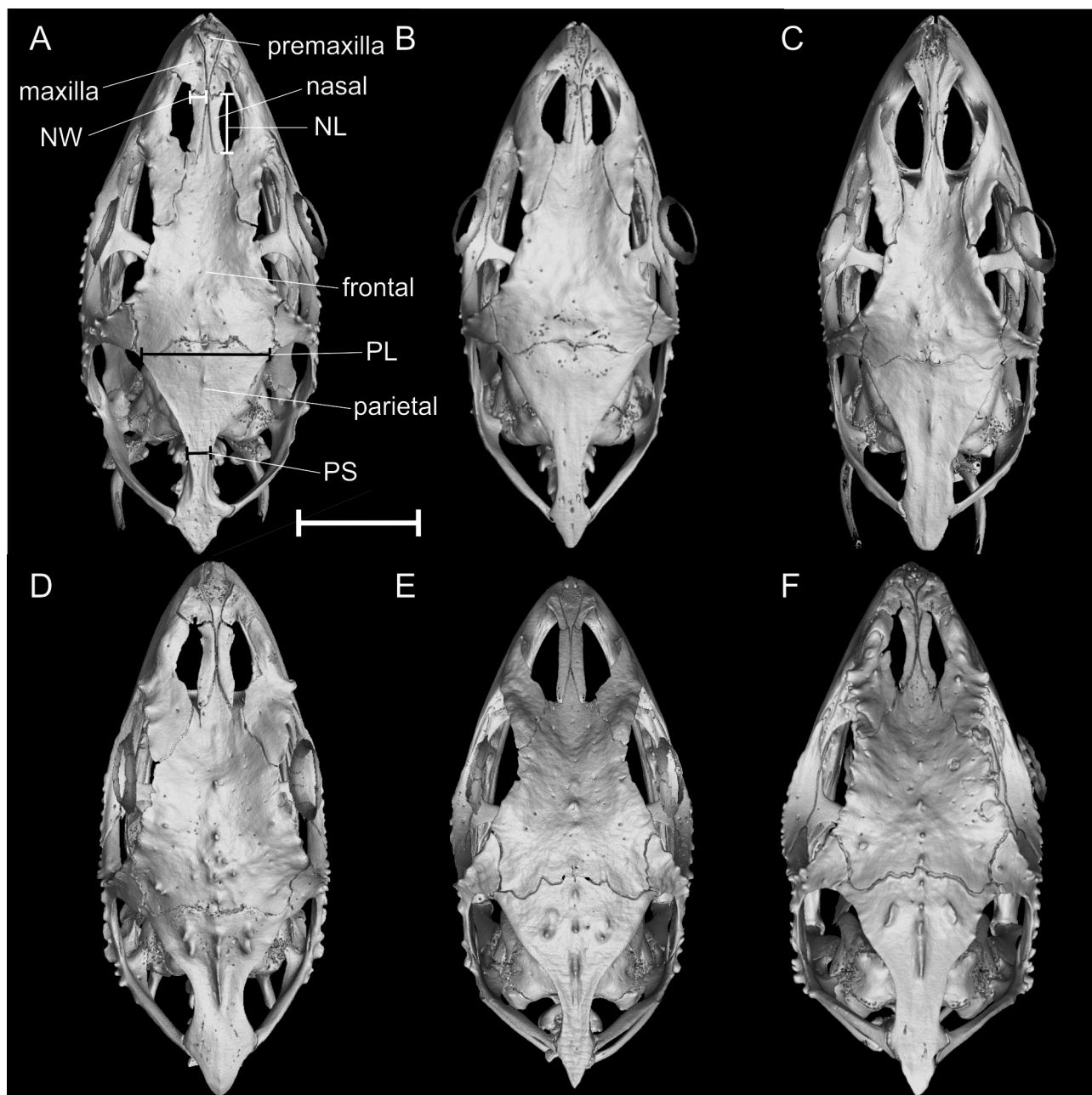

FIGURE 4. Micro-CT scans of skulls of *Calumma* in dorsal view; (A) male *C. boettgeri* (ZSM 440/2000, Nosy Be); (B) female *C. boettgeri* (ZSM 227/2002, Nosy Be); (C) female holotype of *Chamaeleo macrorhinus* (MCZ 5988, Madagascar); (D) male *Calumma linotum* (ZSM 2072/2007, Montagne d'Ambre); (E) female *C. linotum* (ZSM 873/1920/2, unknown locality); (F) male holotype of *C. linotum* (ZSM 21/1923, Madagascar). Scale bar = 5 mm. See Material & Methods for abbreviations.
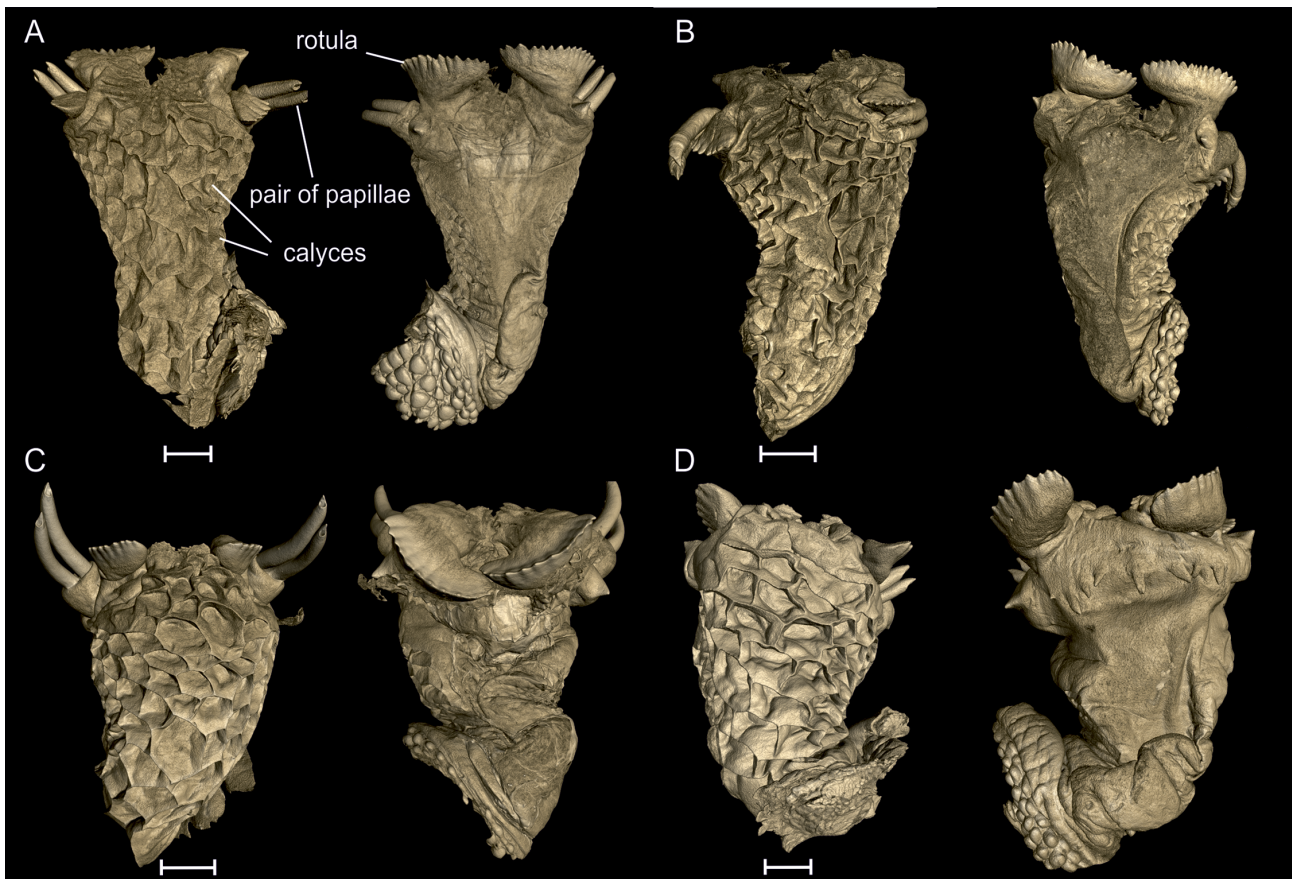
FIGURE 5. Micro-CT scans of hemipenes of *Calumma* species in asulcal and sulcal view. (A) *C. boettgeri* (ZSM 444/2000, Nosy Be); (B) *C. boettgeri* (ZSM 440/2000, Nosy Be); (C) *C. linotum* (ZSM 1683/2012, Montagne d'Ambre); (D) *C. linotum* (ZSM 2073/2007, Montagne d'Ambre). Scale bar = 1 mm.
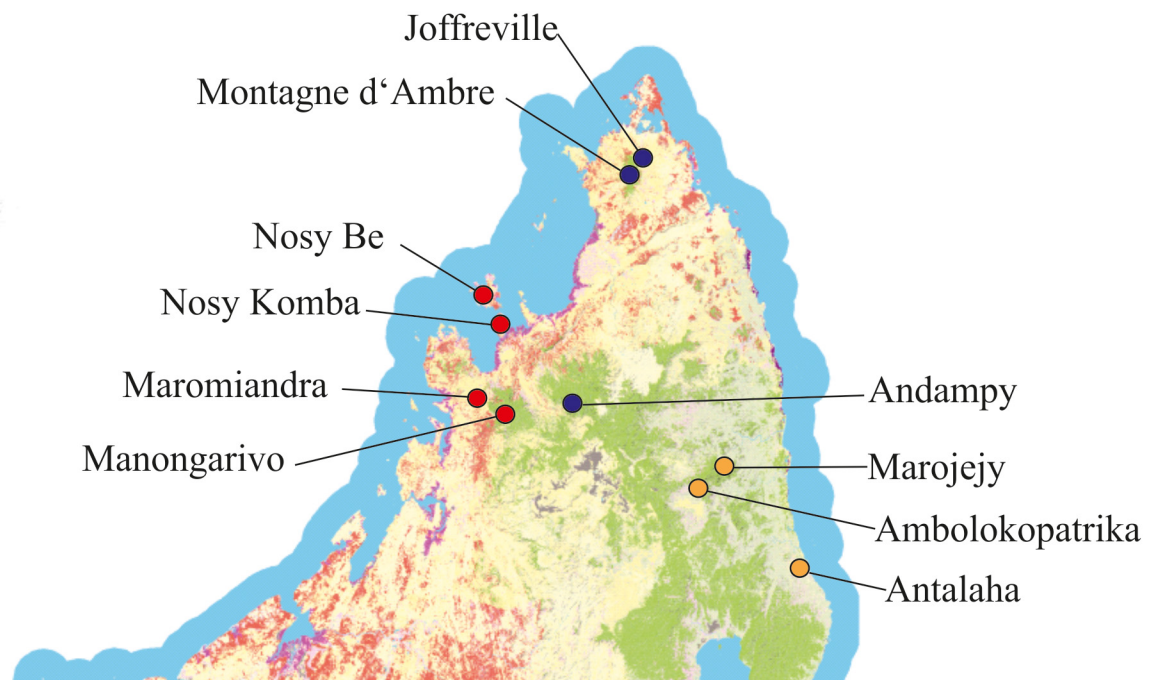

FIGURE 6. Map of Northern Madagascar with confirmed localities of *Calumma boettgeri* (red points) and *C. linotum* (purple points) and localities of *C. boettgeri* from the literature that are in need of confirmation (orange points). (www.vegmad.org)

Colouration of the holotype (Fig. 3A). The colour of the holotype is faded after storage in alcohol for almost one hundred years. Nonetheless, light blue colour of the extremities and the tip of the rostral appendage, as well as two dark spots on each side of the body and a slightly annulated tail are still recognizable.

Re-description of the holotype of *Chamaeleo macrorhinus* Barbour, 1903

Holotype. MCZ 5988, adult female, exact location unknown ('Madagascar'), collected by an unknown individual on an unknown date; in a good state of preservation, except body completely slit on the ventral side; mouth slightly opened.

Morphology. SVL 48.1 mm; tail length 44.9 mm; distinct rostral ridges that fuse on the anterior snout in a soft, laterally compressed dermal rostral appendage that projects 2.8 mm beyond the upper snout tip, rounded distally; no supra-orbital crest; lateral crest poorly developed and pointing straight posterior over a length of 3.0 mm; no temporal or parietal crests; occipital lobes clearly developed and slightly notched; no traces of gular, ventral or dorsal crest. Body laterally compressed with fine homogeneous scalation with the exception of the extremities and head region; legs with small rounded tubercle scales that are isolated from each other; heterogeneous scalation on the head and smooth tubercle scales on the rostral crest and rostral appendage; no axillary pits. Further morphological measurements are provided in Table 1.

Skull osteology of the holotype (Fig. 4C; Table 3). Narrow nasal bones (NW: 0.2 mm, NL: 2.0 mm) are paired and separated by the frontal and the premaxilla that meet between the nasal; the anterior tip of the frontal bone exceeds half of the naris; the frontal and parietal are smooth only with single tubercles. The parietal tapers strongly from 3.9 mm (largest diameter) to 1.1 mm (smallest diameter).

Colouration of the holotype (Fig. 3B). The colour of the holotype is almost completely faded after storage in alcohol for more than one hundred years. The light blue colour of tubercle scales on the extremities is still recognizable.

Identity and re-description of *Calumma linotum* (Müller, 1924)

Morphology, pholidosis, skull osteology, and colouration of the holotype of *Calumma linotum* allow us to assign it to the blue-nosed chameleons of Montagne d'Ambre, which were formerly considered *C. boettgeri* (Table 1–3, Figs. 2–4). The mean values of morphological measurements of male individuals from Montagne d'Ambre match those of the holotype (Table 1, 2): mean size of the broadest tubercle scale at the upper arm with 0.74 mm (vs. a mean of Montagne d'Ambre of 0.64); number of enlarged tubercles on the upper arm of 22 (vs. 20.20, SD 1.5); the diameter of the upper arm relative to the body size with 0.054 (vs. 0.053, SD 0.0038); the length of the rostral appendage, 4.3 mm (vs. 4.1 mm, SD 0.9) and the number of peripheral enlarged scales in relation to the length of the appendage, 3.5 per mm (vs. 4.1 per mm, SD 1.3).

Diagnosis. A small-sized chameleon (SVL 50.6–59.6 mm, TL 101.3–126.1 mm; TL up to 130 mm according to Mocquard 1895) that is characterised by a soft dermal, distally rounded, typically blue-coloured rostral appendage, slightly notched occipital lobes, a small parietal crest, a low casque, the absence of axillary pits, large rounded tubercles on the extremities bordering each other, presence or absence of a dorsal crest in males, low casque, and absence of gular and ventral crests. The three species *C. boettgeri, C. guibei,* and *C. linotum* differ from the other species of this group by the presence of occipital lobes. In *C. guibei* the occipital lobes are completely notched (vs. not or slightly notched in *C. linotum*). *Calumma linotum* differs from *C. boettgeri* in the larger rostral appendage of males related to the snout-vent length (RRS 0.078 vs. 0.065), the larger ratio of arm diameter to snout-vent length (UAD/SVL 0.053 vs. 0.042), the more heterogeneous scalation of the extremities (mean diameter of the largest tubercle of the upper arm 0.64 mm vs. 0.36 mm, mean number of enlarged tubercles on the upper arm 20.2 vs. 9.9), in skull structure (presence of parietal crest vs. absence, frontal bone not meeting premaxilla vs. meeting premaxilla, broad vs. narrow nasals), larger maximum total length, and in colouration (blue rostral appendage vs. brown; bright green extremities vs. brown). The karyotype of the species is described in Bourgat (1973) under the name of *C. boettgeri* from Montagne d'Ambre.

Colouration in life. The body of males in relaxed state is pale green or yellowish or light brown with two dark

brown spots and (occasionally) a beige lateral stripe on each side that stops at the base of the tail. Under certain conditions (e.g. during stress or conspecific encounters), dark colour patterns can become prominent and the tail becomes annulated. The head is also greenish or brown with a dark line running from the snout crossing the eyes to the occipital lobes. The skin around the mouth and the throat can be white. A noticeable characteristic of the species is the true blue rostral appendage and the greenish turquoise extremities (Fig. 2A). The colour of the legs is induced only by the coloured tubercle scales.

The colouration of the females can vary from beige to a reddish or greenish brown ground colouration without any obvious colour patterns in a relaxed state, except for two inconspicuous brown spots on each flank. The rostral appendage is bright blue and the extremities are less striking green than in the males. In a stressed state, three parallel bright blue spots appear on the upper half of the eyelids and one blue spot on each side of the casque and on the frontal (Fig. 2C).

Distribution. Most samples of *C. linotum* are from Montagne d'Ambre—a well protected area in the North of Madagascar. Further localities are Joffreville north of Montagne d'Ambre (ZFMK 52308, see table 1) and Andampy (Manarikoba forest) in the Tsaratanana massif (ZSM 551/2001, see table 1). We also consider the *C. boettgeri* records of Mocquard (1895) from the surroundings of Diégo-Suarez (today Antsiranana) and Montagne d'Ambre as belonging to *C. linotum*. All studied individuals were found at an altitude between 730 m and 1050 m a.s.l. (Fig. 6). However, Raxworthy & Nussbaum (1994) found this species (as *C. boettgeri*) at Montagne d'Ambre between 650–1250 m a.s.l., and the maximum altitudinal distribution was recorded at 1306 m a.s.l. (Gehring *et al.* 2012 suppl. Table 1). The females (SMF 26357–26359) from Col Pierre Radama (=Ambatond'Radama, 35–40 km northeast of Maroantsetra) mentioned in Mertens (1933) neither belong to *C. linotum* nor to *C. boettgeri*. Their identity will be discussed in a subsequent publication.

Identity of *Calumma boettgeri* (Boulenger, 1888)

Morphological measurements and pholidosis of the holotype require the assignment of *Chamaeleo macrorhinus* to the Nosy Be form of *Calumma boettgeri*. The measurements are similar to the mean values of the females from Nosy Be (Tables 1–2): diameter of the broadest tubercle on the upper arm 0.34 mm (vs. mean of Nosy Be females of 0.32 mm, SD 0.048), number of enlarged tubercles on the upper arm 8 (vs. 10.6, SD 1.8); ratio of the upper arm diameter to the body size, 0.046 (vs. 0.041, SD 0.0038), total length, 93.1 mm (vs. 96.3 mm, SD 8.1 mm) and length of the rostral appendage, 2.8 mm (vs. 2.7 mm, SD 0.5 mm).

Diagnosis. A small-sized chameleon (SVL 41.1–55.5 mm, TL 83.8–108.0 mm) that is characterised by a soft dermal, distally rounded, typically brown rostral appendage, slightly notched occipital lobes, the absence of a parietal crest, a low casque, the absence of axillary pits, small rounded tubercles not bordering each other on the extremities, presence or absence of a dorsal crest in males, low casque, and absence of gular and ventral crests. It differs from *C. guibei* by unnotched or only slightly (max. 0.7 mm) notched versus completely notched occipital lobes. For a distinction from *C. linotum*, see above.

Colouration in life. The body and head colouration of males in relaxed state ranges from light brown to yellow without any obvious colour patterns. When stressed, dark colour patterns become prominent and the tail becomes annulated. A dark line runs from the snout tip across the eyes to the occipital lobes. The skin around the mouth and the throat can be white. Remarkable is the inconspicuous brown colour of the rostral appendage. The extremities appear brown also, except for a few green or blue coloured tubercle scales (Fig. 2B).

The colouration of the females can vary from beige to a reddish or greenish brown ground colouration in a relaxed state. The rostral appendage and the extremities show the same colour as the body, except for a few green tubercle scales on the legs. In a stressed state, three parallel bright blue spots appear on the upper half of the eyelids.

Distribution. All confirmed distribution records of *C. boettgeri* are confined to the biogeographic Sambirano region in northwest Madagascar. It was found in both primary rainforest (Lokobe) and secondary forests (near Andoany) of Nosy Be (Andreone *et al.* 2003), in Manongarivo (Rakotomalala 2002; Gehring *et al.* 2012), and on Nosy Komba (Hyde Roberts & Daly 2014). Additionally Nagy *et al.* (2012, suppl. Fig. 2) identified a population with similar gene sequences to *C. boettgeri* from a forest fragment locally known as Maromiandra (13°99'65"S, 48°21'77"E, 283 m). According to molecular phylogenetic data, *C. boettgeri* from Nosy Be and one individual

from Manongarivo (FGMV 2002-813, 13°58'62"S, 48°25'32"E, 751 m a.s.l.) form their own clade (Gehring *et al.* 2012). The elevations of all these localities range from 0 to 751 m a.s.l. (Fig. 6).

We consider all additional records of *C. boettgeri*, all located in northeastern Madagascar, as in need of confirmation: Ambolokopatrika, 810–860 m a.s.l. (Andreone *et al.* 2000), Antalaha (Brygoo 1971), Andrakaraka forest station ca. 10 km from Antalaha (Ramanantsoa 1974), and Marojejy, 1100–1200 m a.s.l. (Raselimanana *et al.* 2000).
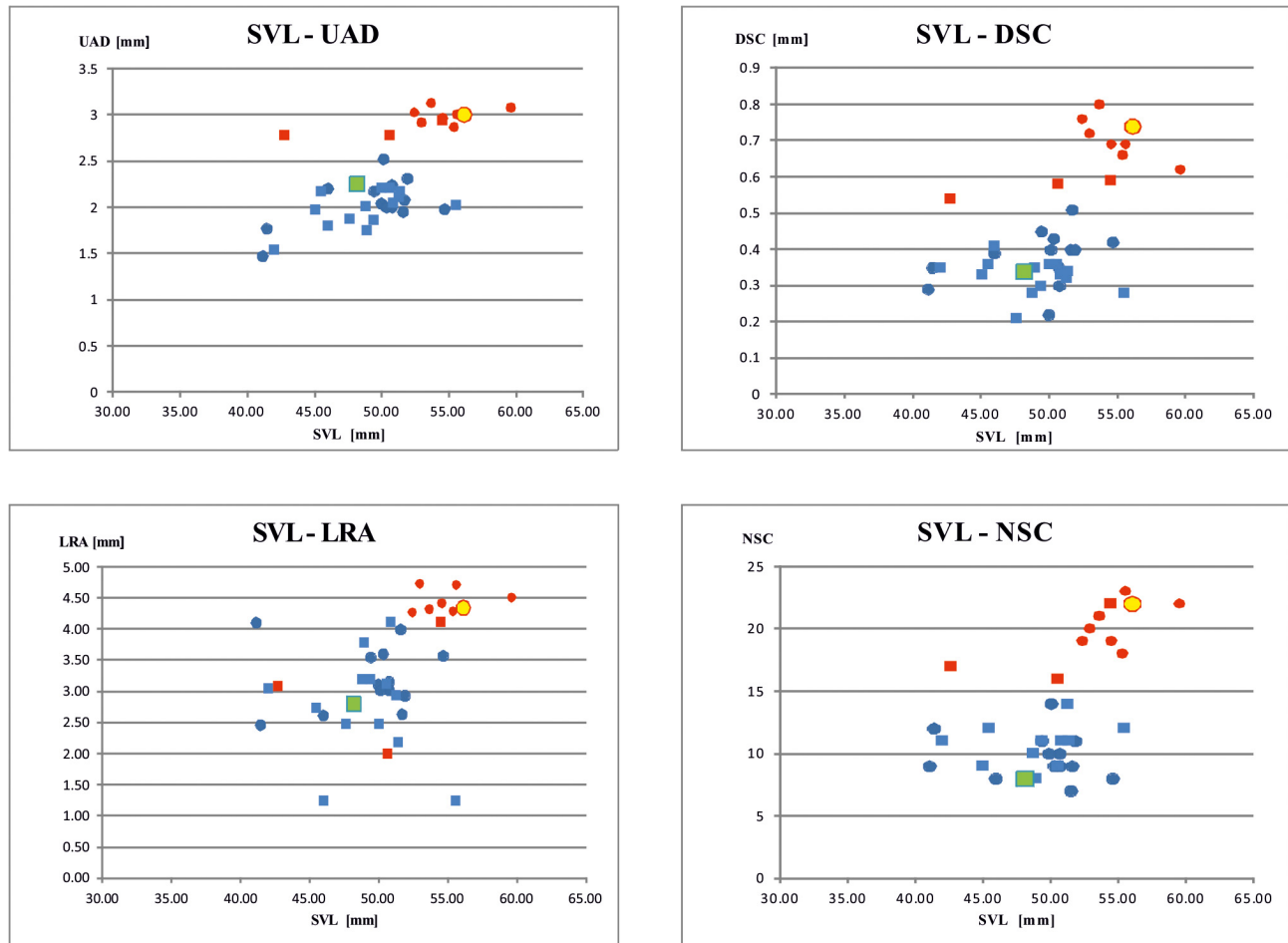

FIGURE 7. Important characters for the distinction of *C. boettgeri* (n = 27; blue symbols) and *C. linotum* (n = 11; red symbols) and the assignment of the holotypes of *C. linotum* (ZSM 21/1923; yellow symbol) and *Ch. macrorhinus* (MCZ 5988; green symbol) relative to the snout-vent length. Circles indicate males, while squares indicate females. Abbreviations: SVL, snout-vent length; UAD, upper arm diameter; DSC, diameter of broadest scale on upper arm; LRA, length of rostral appendage from snout tip; NSC, number of big scales on upper arm from lateral view.

Discussion

Using the approach of integrative taxonomy, the systematics of *C. linotum* is clarified in this work. Morphological characteristics could be assigned to two phylogenetic lineages of Gehring *et al.* (2012) within the *C. boettgeri* complex. The internal and external morphology of the holotype of *C. linotum* is in line with the individuals from Montagne d'Ambre and allows their assignment to *C. linotum*. Indeed, it is quite likely that the holotype was actually collected in Montagne d'Ambre, because the museum in Stuttgart harbours other reptile specimens without locality data which obviously originate from northern Madagascar, including the holotype of the typhlopid snake *Madatyphlops microcephalus*, a species which is mainly known from Montagne d'Ambre (Glaw & Vences 2007). Already Brygoo (1978) mentioned that a specimen from Montagne d'Ambre differs from specimens from Nosy Be.

Morphological measurements showed that *C. linotum* from Montagne d'Ambre is larger and more robustly built than *C. boettgeri*. The scalation of the extremities clearly differs between the species. In *C. linotum,* scales are heterogeneous with more tubercles, which are also larger. In contradiction of Brygoo (1971), the presence of a dorsal crest is not a characteristic for *C. linotum*, as it can be absent, present, or strongly developed in both species. Neither are the gular folds a distinctive character from *C. boettgeri* as mentioned in Müller (1924). According to Eckhardt *et al.* (2012), male *C. boettgeri* have significantly more dorsal spines than females; this is true for *C. linotum* as well, though in both sexes there are also specimens lacking a dorsal crest completely. Also variable is the shape of the notch between the occipital lobes. Both species possess rostral appendages in both sexes that are generally larger in males and possibly related to mate recognition and driven by sexual selection (Gehring *et al.* 2011). In *C. linotum* the rostral appendage is conspicuously blue coloured in both sexes and possibly reflecting in the ultraviolet spectrum. In the diffuse light of the rainforest in Montagne d'Ambre the coloured rostral appendage can play an important role in finding mates, as the experiments of Parcher (1974) have already shown in *C. nasutum*. The rostral appendage of *C. boettgeri* is of inconspicuous colour.

Calumma linotum also differs from *C. boettgeri* in the presence of a parietal crest. Micro-CT scans of the skull exposed this characteristic that is barely noticeable externally. Furthermore, differences in the form of the nasal, frontal, and parietal bone were identified. Some chameleons are known to show strong sexual dimorphism in terms of body size, colour or ornamentation (Stuart-Fox 2014). The micro-CT scans of several individuals of the same species showed remarkably little variation in characteristics like skull sutures between sexes within the *C. boettgeri* complex. Skeletal morphology has the potential to play an important role in future chameleon taxonomy. Unlike the method of clearing and staining (Rieppel & Crumly 1997), with micro-CT osteological data are more easily accessible and demonstrative to illustrate. This method is not invasive and the preserved samples are not destroyed, which is especially important when working with type specimens (Faulwetter *et al.* 2013).

The third species, *C. guibei*, which was not included in this study, differs morphologically from *C. boettgeri* and *C. linotum* in having largely separated occipital lobes (Hillenius 1959) and in the hemipenial structure, and represents its own phylogenetic lineage (clade F) as well, which contains two OTUs (Gehring *et al.* 2012). Further studies are necessary to refine the taxonomy of these OTUs as well as that of clade E (with two OTUs), which occur around the Tsaratanana massif at elevations from 1300–1550 m a.s.l (Gehring *et al.* 2012). For conservation issues clear species assignments with morphological characteristics are urgently needed. Due to its uncertain identity, *Calumma linotum* has not been assessed for the IUCN Red list of Threatened Species; it is commented within *C. boettgeri;* 'the identity of *C. linotum* is particularly unclear' (Jenkins *et al.* 2011a). *C. boettgeri* and *C. guibei* are listed as Least Concern and Near Threatened, respectively (Jenkins *et al.* 2011a, b). A new evaluation of the conservation status of *C. linotum* and *C. boettgeri* is in progress, in light of the revised taxonomy of this complex and our new understanding of their distributions. Species of the genus *Calumma* are also exported as pets, although the genus *Calumma* constitutes only a small part (1.7%) of chameleon exports (Jenkins *et al.* 2014). Clearly delimited species are the basis for correct export lists and also the protection of species with small distribution patterns.

In this study, micro-CT scans of hemipenes are presented for the first time for chameleons or even for squamate reptiles. Generally the hemipenis of *C. boettgeri* have rotulae that are slightly more denticulated than those of *C. linotum*, but no great differences are apparent. In cases of allopatric speciation, no pre-zygotic isolation is necessary to reinforce speciation. The hemipenis scans provide a comparatively objective and much more detailed view of the hemipenis structure than traditional illustrations; compare 3D PDF model (supplementary file) with illustrations of hemipenis from *C. boettgeri* in Gehring *et al.* (2012). By investigating more than one hemipenis per species, it became clear that there is intraspecific variation even in genital morphology. Furthermore, the ability to evert or retract the papillae can lead to an incorrect description. The risk of misinterpretation is much greater using classical techniques such as light microscopy and illustration than by 3D visualization and digitalization using X-ray micro-CT, and this technique should become the standard approach for the examination and description of this and similar important anatomical features. This further underlines the value and potential of micro-CT on its own and in combination with molecular analyses and classical morphological measurements in questions of taxonomy and systematics.

Acknowledgements

References

Andreone, F., Glaw, F., Nussbaum, R.A., Raxworthy, C.J., Vences, M., Randrianirina, J.E. (2003) The amphibians and reptiles of Nosy Be (NW Madagascar) and nearby islands: a case study of diversity and conservation of an insular fauna. *Journal of Natural History*, 37 (17), 2119–2149.
http://dx.doi.org/10.1080/00222930210130357

Andreone, F., Randrianirina, J.E., Jenkins, P.D. & Aprea, G. (2000) Species diversity of Amphibia, Reptilia and Lipotyphla (Mammalia) at Ambolokopatrika, a rainforest between the Anjanaharibe-Sud and Marojejy massifs, NE Madagascar. *Biodiversity and Conservation*, 9, 1587–1622.
http://dx.doi.org/10.1023/A:1026559728808

Angel, F. (1942) Les Lézards de Madagascar. *Mémoires de l'Académie Malgache*, 36, 1–193.

Barbour, T. (1903) Two new species of chamaeleon. *Proceedings of the Biological Society of Washington,* 16, 61–62.

Bickford, D., Lohman, D.J., Sodhi, N.S., Ng, P.K., Meier, R., Winker, K. & Das, I. (2007) Cryptic species as a window on diversity and conservation. *Trends in Ecology & Evolution*, 22 (3), 148–155.
http://dx.doi.org/10.1016/j.tree.2006.11.004

Boulenger, G.A. (1888) Descriptions of two new chamaeleons from Nossi-Bé, Madagascar. *Annales and Magazine of Natural History*, Series 6, 1 (1), 22–23.
http://dx.doi.org/10.1080/00222938809460666

Bourgat, R.M. (1973) Cytogénétique des caméléons de Madagascar. Incidences taxonomiques, biogéographiques et phylogénétiques. *Bulletin de la Societé zoologique de France*, 98 (1), 81–90.

Brygoo, E.R. (1971) Reptiles Sauriens Chamaeleonidae – genre *Chamaeleo. Faune de Madagascar*, 33, 1–318.

Brygoo, E.R. (1978) Reptiles Sauriens Chamaeleonidae – genre *Brookesia* et complément pour le genre *Chamaeleo. Faune de Madagascar,* 47, 1–173.

Eckhardt, F.S., Gehring, P.-S., Bartel, L., Bellmann, J., Beuker, J., Hahne D., Korte, J., Knittel, V., Mensch, M., Nagel, D., Pohl, M., Rostosky, C., Vierath, V., Wilms, V., Zenk, J. & Vences, M. (2012) Assessing sexual dimorphism in a species of Malagasy chameleon (*Calumma boettgeri*) with a newly defined set of morphometric and meristic measurements. *Herpetology Notes*, 5, 335–344.

Faulwetter, S., Vasileiadou, A., Kouratoras, M., Dailianis, T. & Arvanitidis, C. (2013). Micro-computed tomography: Introducing new dimensions to taxonomy. *ZooKeys*, 263, 1–45.
http://dx.doi.org/10.3897/zookeys.263.4261

Garbutt, N., Bradt, H. & Schuurman, D. (2001) *Madagascar wildlife – a visitor's guide.* Bradt Travel Guides, Bucks, 138 pp.

Gehring, P.-S., Ratsoavina, F.M. Vences, M. & Glaw, F. (2011) *Calumma vohibola*, a new chameleon species (Squamata: Chamaeleonidae) from the littoral forests of eastern Madagascar. *African Journal of Herpetology*, 60, 130–154.
http://dx.doi.org/10.1080/21564574.2011.628412

Gehring, P.-S., Tolley, K.A., Eckhardt, F.S., Townsend, T.M., Ziegler, T., Ratsoavina, F., Glaw, F. & Vences, M. (2012) Hiding deep in the trees: discovery of divergent mitochondrial lineages in Malagasy chameleons of the *Calumma nasutum* group. *Ecology and Evolution,* 2, 1468–1479.
http://dx.doi.org/10.1002/ece3.269

Glaw, F. (2015) Taxonomic checklist of chameleons (Squamata: Chamaeleonidae). *Vertebrate Zoology*, 65 (2), 167–246.

Glaw, F., Köhler, J., Townsend, T.M. & Vences, M. (2012) Rivaling the world's smallest reptiles: Discovery of miniaturized and microendemic new species of leaf chameleons (*Brookesia*) from northern Madagascar. *PLoS ONE*, 7 (2), e31314.
http://dx.doi.org/10.1371/journal.pone.0031314

Glaw, F. & Vences, M. (2007) *A field guide to the amphibians and reptiles of Madagascar*. Vences and Glaw Verlag, Cologne, 496 pp.

Goodman, S.M. & Benstead, J.P. (2005) Updated estimates of biotic diversity and endemism for Madagascar. *Oryx,* 39 (1), 73–

77.
http://dx.doi.org/10.1017/s0030605305000128

Henkel, F.W. & Schmidt, W. (1995) *Amphibien und Reptilien Madagaskars, der Maskarenen, Seychellen und Komoren*. Eugen Ulmer Verlag, Stuttgart, 311 pp.

Hillenius, D. (1959) The differentiation within the genus *Chamaeleo* Laurenti, 1768. *Beaufortia*, 89 (8), 1–92.

Hyde Roberts, S. & Daly, C. (2014) A rapid herpetofaunal assessment of Nosy Komba Island, northwestern Madagascar, with new locality records for seventeen species. *Salamandra*, 50, 18–26.

Jenkins, R., Measy, G.J. & Anderson, V. (2014) Chameleon Conservation. *In*: Tolley, K.A. & Herrel, A. (Eds.), *The Biology of Chameleons*. University of California Press, Berkeley, pp. 193–216.

Jenkins, R.K.B., Andreone, F., Andriamazava, A., Anjeriniaina, M., Brady, L., Glaw, F., Griffiths, R.A., Rabibisoa, N., Rakotomalala, D., Randrianantoandro, J.C., Randrianiriana, J., Randrianizahana, H., Ratsoavina, F., Raxworthy, C.J., Robsomanitrandrasana, E. & Carpenter, A. (2011a) *Calumma boettgeri*. *The IUCN Red List of Threatened Species*. Version 2014.3. Available from: www.iucnredlist.org (accessed 2 April 2015)

Jenkins, R.K.B., Andreone, F., Andriamazava, A., Anjeriniaina, M., Glaw, F., Rabibisoa, N., Rakotomalala, D., Randrianantoandro, J.C., Randrianiriana, J., Randrianizahana, H., Ratsoavina, F. & Robsomanitrandrasana, E. (2011b) *Calumma guibei*. *The IUCN Red List of Threatened Species*. Version 2014.3. Available from: http://www.iucnredlist.org (accessed 2 April 2015)

Klaver, C.J.J. & Böhme, W. (1986) Phylogeny and classification of the Chamaeleonidae (Sauria) with special reference to hemipenis morphology. *Bonner Zoologische Monographien*, 22, 1–64.

Lutzmann, N. & Lutzmann, H. (2004) Das grammatikalische Geschlecht der Gattung *Calumma* (Chamaeleonidae) und die nötigen Anpassungen einiger Art- und Unterartbezeichnungen. *Reptilia*, 9 (48), 4–5.

Mertens, R. (1933) Die Reptilien der Madagaskar-Expedition Prof. Dr. H. Bluntschli's. *Senckenbergiana biologica*, 15, 260–274.

Mocquard, M.F. (1895) Sur les reptiles recueillis a Madagascar par M. M. Alluaud et Belly. *Bulletin de la Société philomatique de Paris*, Series 8, 7, 112–136.

Mocquard, M.F. (1909) Synopsis des familles, genres et espèces des reptiles écailleux et batraciens de Madagascar. *Nouvelles Archives du Muséum d'Histoire Naturelle*, Series 5, 1, 1–100.

Müller, L. (1924) Ueber ein neues Chamaeleon aus Madagaskar. *Mitteilungen aus dem Zoologischen Museum in Berlin,* 11, 95–96.

Nagy, Z.T., Sonet, G., Glaw, F. & Vences, M. (2012) First large-scale DNA barcoding assessment of reptiles in the biodiversity hotspot of Madagascar, based on newly designed COI primers. *PLoS ONE*, 7 (3), e34506.
http://dx.doi.org/10.1371/journal.pone.0034506

Nečas, P. (2004) *Chamäleons – bunte Juwelen der Natur*. Edition Chimaira, Frankfurt am Main, 338 pp.

Parcher, S.R. (1974) Observations on the natural histories of six Malagasy Chamaeleontidae. *Zeitschrift für Tierpsychologie*, 34, 500–523.
http://dx.doi.org/10.1111/j.1439-0310.1974.tb01818.x

Rakotomalala, D. (2002) Diversité des reptiles et amphibiens de la Réserve Spéciale de Manongarivo, Madagascar. *Boissiera*, 59, 339–358.

Ramanantsoa, G.-A. (1974) Connaissance des caméléonidés commun de la province de Diégo Suarez par la population paysanne. *Bulletin de l'Académie Malgache*, 51, 147–149.

Raselimanana, A.P., Raxworthy, C.J. & Nussbaum, R.A. (2000) Herpetofaunal species diversity and elevational distribution within the Parc National de Marojejy, Madagascar. *Fieldiana Zoology*, 157–174.

Raxworthy, C.J. & Nussbaum, R.A. (1994) A rainforest survey of amphibians, reptiles and small mammals at Montagne d'Ambre, Madagascar. *Biological Conservation,* 69 (1), 65–73.
http://dx.doi.org/10.1016/0006-3207(94)90329-8

Raxworthy, C.J. & Nussbaum, R.A. (2006) Six new species of occipital-lobed *Calumma* chameleons (Squamata: Chamaeleonidae) from montane regions of Madagascar, with a new description and revision of *Calumma brevicorne*. *Copeia*, 2006 (4), 711–734.
http://dx.doi.org/10.1643/0045-8511(2006)6[711:snsooc]2.0.co;2

Raxworthy, C.J., Pearson, R.G., Rabibisoa, N., Rakotondrazafy, A.M., Ramanamanjato, J.B., Raselimanana, A.P., Wu, S., Nussbaum, R.A. & Stone, D.A. (2008) Extinction vulnerability of tropical montane endemism from warming and upslope displacement: a preliminary appraisal for the highest massif in Madagascar. *Global Change Biology*, 14 (8), 1703–1720.
http://dx.doi.org/10.1111/j.1365-2486.2008.01596.x

Rieppel, O. & Crumly, C. (1997) Paedomorphosis and skull structure in Malagasy chamaeleons (Reptilia: Chamaeleonidae). *Journal of Zoology*, 243 (2), 351–380.
http://dx.doi.org/10.1111/j.1469-7998.1997.tb02788.x

Ruthensteiner, B. & Heß, M. (2008) Embedding 3D models of biological specimens in PDF publications. *Microscopy Research Technique*, 71, 778–786.
http://dx.doi.org/10.1002/jemt.20618

Schmidt, W., Tamm, K. & Wallikewitz, E. (2010) *Chamäleons – Drachen unserer Zeit*. Natur- und Tier-Verlag, Münster, 333 pp.

Stuart-Fox, D. (2014) Chameleon behavior and color change. *In:* Tolley, K.A. & Herrel, A. (Eds.), *The Biology of Chameleons*. University of California Press, Berkeley, pp. 115–130.

Tilbury, C.T. (2014) Overview of the systematics of the Chamaeleonidae. *In*: Tolley, K.A. & Herrel, A. (Eds.), *The Biology of Chameleons*. University of California Press, Berkeley, pp. 151–174.

Tolley, K.A., Townsend, T.M. & Vences, M. (2013) Large-scale phylogeny of chameleons suggests African origins and Eocene diversification. *Proceedings of the Royal Society B*, 280, 1–8.
http://dx.doi.org/10.1098/rspb.2013.0184

Townsend, T.M., Tolley, K.A., Glaw, F., Böhme, W. & Vences, M. (2011) Eastward from Africa: palaeocurrent-mediated chameleon dispersal to the Seychelles islands. *Biology Letters*, 7 (2), 225–228.
http://dx.doi.org/10.1098/rsbl.2010.0701

Walbröl, U. & Walbröl, H.D. (2004) Bemerkungen zur Nomenklatur der Gattung *Calumma* (Gray, 1865) (Reptilia: Squamata: Chamaeleonidae). *Sauria*, 26 (3), 41–44.

Supporting information

Additional Supporting Information may be found online from:
http://www.mapress.com/zootaxa/2015/data/4048p211-231SupplementaryFile.pdf

Fig. S1. 3D model of hemipenis of *Calumma linotum* (ZSM 1683/2012).

3.1.2 PAPER: Splitting and lumping: An integrative taxonomic assessment of Malagasy chameleons in the *Calumma guibei* complex results in the new species *C. gehringi* sp. nov.

After the redescription of *Calumma boettgeri* and *C. linotum* (see chapter 3.1.1), the identity of *C. guibei* (Hillenius 1959), the third species of the *C. boettgeri* complex was addressed. *Calumma guibei* was originally described on the basis of a type series of juvenile specimens from the Tsaratanana massif in north Madagascar. Using external morphology and skull morphology, these specimens were assigned to a genetic clade from Tsaratanana at high altitude of Gehring *et al.* (2012) and *C. guibei* was redescribed. However, clades from Tsaratanana and the surrounding area at lower altitude differed morphologically. Using an integrative taxonomic approach including genetic data (mitochondrial ND2 gene and nuclear CMOS gene), as well as external, genital, and skull morphology, the new species *C. gehringi* was described. Although there were deep mitochondrial lineages with a maximal intraspecific genetic distance of 11.4 % in ND2, we could not find any morphological differences within *C. gehringi,* and the different deep mitochondrial clades also were not differentiated in the nuclear CMOS gene. Due to the lack of congruence among the different lines of evidence (strong differentiation in the mitochondrial gene versus no differentiation in the nuclear gene, the external and hemipenial morphology, as well as in the skull morphology) we decided not to describe these deep mitochondrial clades as different species and emphasize the importance of an integrative approach to taxonomy to avoid the oversplitting of species. Additionally, using dice-CT scans (see chapter 3.1.1) a new hemipenis ornament reminiscent of paired, small horns was described as the "cornucula gemina". This structure can be retracted, resulting in misleading descriptions and drawings in the past (e.g. Gehring *et al.* (2012). By changing the threshold of the scan images the retracted cornucula can be found inside the hemipenis.

Prötzel, D, Vences, M, Scherz, MD, Vieites, DR & Glaw, F (2017): Splitting and lumping: An integrative taxonomic assessment of Malagasy chameleons in the *Calumma guibei* complex results in the new species *C. gehringi* sp. nov. *Vertebrate Zoology*, 67, 231–249.

Splitting and lumping: An integrative taxonomic assessment of Malagasy chameleons in the *Calumma guibei* complex results in the new species *C. gehringi* sp. nov.

DAVID PRÖTZEL [1], *, MIGUEL VENCES [2], MARK D. SCHERZ [1, 2], DAVID R. VIEITES [3] & FRANK GLAW [1]

[1] Zoologische Staatssammlung München (ZSM-SNSB), Münchhausenstr. 21, 81247 München, Germany — [2] Zoological Institute, Technical University of Braunschweig, Mendelssohnstr. 4, 38106 Braunschweig, Germany — [3] Museo Nacional de Ciencias Naturales, Consejo Superior de Investigaciones Científicas, C/José Gutierrez Abascal 2, 28006 Madrid, Spain — *Corresponding author: david.proetzel@mail.de

Abstract

Calumma guibei (HILLENIUS, 1959) is a high-altitude chameleon species from the Tsaratanana massif in north Madagascar. Since its description was based on a juvenile holotype, its taxonomic identity is uncertain and little is known about its morphology. A recent molecular study discovered several deep mitochondrial clades in the Tsaratanana region assigned to *C. guibei* and *C. linotum* (MÜLLER, 1924). In this paper we study the taxonomy of these clades and clarify the identity of *C. guibei*. Using an integrative taxonomic approach including pholidosis, morphological measurements, osteology, and molecular genetics we redescribe *C. guibei* and describe the new species *C. gehringi* sp. nov. which comprises two deep mitochondrial lineages. In terms of external morphology the new species differs from *C. guibei* by an elevated rostral crest, the shape of the notch between the occipital lobes (slightly connected vs. completely separated), presence of a dorsal and caudal crest in males (vs. absence), and a longer rostral appendage in the females. Additionally, we analysed skull and hemipenis morphology using micro-X-ray computed tomography (micro-CT) scans and discovered further differences in skull osteology, including a large frontoparietal fenestra, and separated prefrontal fontanelle and naris in *C. guibei*. Furthermore, we provide a comparison of micro-CT scans with traditional radiographs of the skull. The hemipenes have ornaments of two pairs of long pointed cornucula gemina (new term), two pairs of dentulous rotulae, and a pair of three-lobed rotulae, and are similar in both species, but significantly different from other species in the *C. nasutum* group. Geographically, *C. guibei* has been recorded reliably from the higher elevations of the Tsaratanana Massif above 1580 m a.s.l., whereas *C. gehringi* sp. nov. is found at mid-altitude (730–1540 m a.s.l.) in Tsaratanana and the surrounding area.

Key words

Calumma guibei, *Calumma gehringi* sp. nov., Chamaeleonidae, micro-computed tomography, hemipenis morphology, skull structure, Madagascar, diceCT.

Introduction

Chameleons are a characteristic element of the herpetofauna of Madagascar, and show an impressive diversity (TOLLEY *et al*., 2013). Although the island is only a fraction of the size of the African continent, it hosts nearly the half (86) of the currently recognized 207 chameleon species (GLAW, 2015; MENEGON *et al*., 2015; HUGHES *et al*., 2017). Although they are charismatic and attractive animals, their species-level taxonomy remains poorly studied. The Madagascar-endemic genus *Calumma* in particular has increased by eight species (24%) over the last decade (GLAW, 2015). Despite this increase, several complexes within this genus remain to be satisfactorily addressed taxonomically (GEHRING *et al*., 2011, 2012).

A revision is particularly needed for small *Calumma* species characterised by a soft dermal appendage on the snout tip (in most species), assigned to the *Calumma nas-*

utum group. This group includes nine described species: *C. boettgeri* (BOULENGER, 1888)*, C. fallax* (MOCQUARD, 1900)*, C. gallus* (GÜNTHER, 1877)*, C. guibei* (HILLENIUS, 1959)*, C. linotum* (MÜLLER, 1924)*, C. nasutum* (DUMÉRIL & BIBRON, 1836), *C. vohibola* GEHRING, RATSOAVINA, VENCES & GLAW, 2011*, C. peyrierasi* (BRYGOO, BLANC & DOMERGUE, 1974), and *C. vatosoa* ANDREONE, MATTIOLI, JESU & RANDRIANIRINA, 2001 (GEHRING *et al.*, 2012; PRÖTZEL *et al.*, 2016). However, a recent molecular phylogeny and DNA barcoding data suggest that the *C. nasutum* group is not monophyletic (NAGY *et al.*, 2012; TOLLEY *et al.*, 2013). Within the phenetic *C. nasutum* group, three species (*C. boettgeri, C. guibei,* and *C. linotum*) differ from the others by the possession of well-defined occipital lobes, which are either well connected or separated by a distinct notch (BRYGOO, 1971).

It is clear from the comprehensive molecular study of GEHRING *et al.* (2012) that there are more than just these nine species in the *Calumma nasutum* group; these authors distinguished an impressive 33 deep mitochondrial lineages, considered as operational taxonomic units (OTUs). Seven of these corresponded to nominal species (*C. peyrierasi* and *C. vatosoa* were added to this group after 2012), leaving 26 mitochondrial lineages in need of taxonomic assessment. To investigate the significance of these lineages, an integrative correlation of morphological and genetic data is crucial (TILBURY, 2014). As a first step, we have recently clarified the identity of *Calumma boettgeri* and *C. linotum* (PRÖTZEL *et al.*, 2015). In the present work, we focus on the third species with occipital lobes within the *C. nasutum* group, *C. guibei.*

HILLENIUS (1959) described *Calumma guibei* based on a presumably female juvenile individual (snout-vent length 33 mm) and two juvenile paratypes. The type locality is stated as 'Mount Tsaratanana' at an altitude of 1800 m a.s.l. The species was distinguished from *C. boettgeri* and *C. linotum* by the total separation of the occipital lobes, the lack of a dorsal crest, and the very short rostral appendage (HILLENIUS, 1959). This author later placed *C. guibei* together with some Madagascan species and the African *Kinyongia tenuis* (MATSCHIE, 1892) and *Rhampholeon spinosus* (MATSCHIE, 1892) in a group of chameleons with flexible rostral appendages (HILLENIUS, 1963), but this was undone by BRYGOO (1971). In the last 20 years, this species has been recorded repeatedly, on the Tsaratanana Massif over an altitudinal range of 1600–2100 m a.s.l. (RAXWORTHY & NUSSBAUM, 1996) and on the Tsaratanana Mountain (Maromokotro) from 1975–2250 m a.s.l. (RAXWORTHY *et al.*, 2008). GLAW & VENCES (2007) presented a photograph of a male assigned to *C. guibei* with a distinct dorsal crest from Antsahamanara, Tsaratanana. RABEARIVONY *et al.* (2015, Suppl. Mat. S4) recorded *C. guibei* from the Tsaratanana Massif from 1000–1600 m a.s.l.. ANDREONE *et al.* (2009) found *C. boettgeri/guibei* in Andampy, Tsaratanana (1000 m a.s.l.), Antsahamanara, and Manongarivo, but they did not distinguish between the two species. However, most of these records cannot be proofed, because no voucher material was mentioned. At present, no records except

those of the type collections of this species can be confirmed as belonging to this species.

The identity of *Calumma guibei* may be further complicated by it being a species complex. According to a Bayesian inference analysis of a fragment of the mitochondrial ND2 gene, GEHRING *et al.* (2012) found the clade they assigned to *C. guibei* sensu lato to be split into two subclades ('E' and 'F'), containing four deep mitochondrial lineages (EI, EII, FI, FII). Their assignment of clade E to *C. linotum*, and clade F to *C. guibei*, largely followed RAXWORTHY *et al.* (2008) who used the name *C. linotum* for populations from mid-elevations in the Tsaratanana Massif, and *C. guibei* for populations from higher elevations in the same massif. However, this preliminary assignment was done without naming any morphological criteria or genetic data of the holotypes, which were probably fixed in formalin and have been stored in alcohol for more than 50 years. As the identity of *C. linotum* has been revised recently (assigned to part of clade D; PRÖTZEL *et al.*, 2015), the attribution of clade E must also be revised.

In this work, we investigate the identity of *Calumma guibei* based on morphological comparisons of new material with the type specimens, and we describe specimens of clade E (sensu GEHRING *et al.*, 2012) as new species *Calumma gehringi* sp. nov. on the basis of morphological and molecular datasets. Anticipating our taxonomic conclusions and to improve clarity, we will use the name '*C. gehringi*' within the manuscript already before its formal description.

Material and Methods

We studied 29 specimens of the *C. guibei* complex from the collections of the Muséum National d'Histoire Naturelle de Paris (MNHN) and the Zoologische Staatssammlung München (ZSM) and in addition tissue samples of specimens deposited in the Université d'Antananarivo, Département de Biologie Animale (UADBA). Specimens of *C. gehringi* sp. nov. were collected in the field by surveying at night. They were euthanized by injection of concentrated MS222 or chlorobutanol, fixed in 90% ethanol, and transferred to 70% ethanol for long-term storage. Field numbers refer to Mark D. Scherz (MSZC), Miguel Vences (ZCMV), David R. Vieites (DRV), and Angelica Crottini (ACZC).

Morphological investigation

Terms of morphological measurements taken on these specimens were adapted from previous studies (GEHRING *et al.*, 2011; ECKHARDT *et al.*, 2012; PRÖTZEL *et al.*, 2015). The following characters (Table 1) were measured with a digital caliper to the nearest of 0.1 mm, counted using a binocular dissecting microscope, evaluated by eye or cal-

Table 1. Morphological measurements (all in mm) and scale counts of *Calumma guibei* and *C. gehringi* sp. nov. Abbreviations: male (m), female (f), juvenile (j), holotype (HT), paratype (PT), further abbreviations see Material & Methods.

species	collection no.	field no.	clade	type status	altitude [m]	locality	sex	SVL	TaL	TL	RTaSV
C. guibei	MNHN 50.354	—		HT	1800	Mt. Tsaratanana	j(f)	33.4	31.8	65.2	0.95
C. guibei	MNHN 57.115	—		PT	1800	Mt. Tsaratanana	j	33.3	33.8	67.1	1.02
C. guibei	MNHN 57.116	—		PT	1800	Mt. Tsaratanana	j	26.9	30.9	57.8	1.15
C. guibei	ZSM 2855/2010	DRV 6140		—	2021	Tsaratanana	m	51.7	60.2	111.9	1.16
C. guibei	ZSM 2853/2010	DRV 6131		—	1589	Tsaratanana	m	53.0	62.8	115.8	1.18
C. guibei	ZSM 2854/2010	ZCMV 12325	FI	—	1589	Tsaratanana	m	53.7	62.1	115.8	1.16
C. guibei	ZSM 2857/2010	DRV 6168	FI	—	2021	Tsaratanana	f	49.1	49.6	98.7	1.01
C. guibei	ZSM 2856/2010	DRV 6167	FI	—	2021	Tsaratanana	f	48.1	45.5	93.6	0.95
C. gehringi	ZSM 2851/2010	ZCMV 12307	EII	HT	1207	Antsahan'i Ledy	m	52.6	63.2	115.8	1.20
C. gehringi	ZSM 1834/2010	ZCMV 12511	EI	PT	1466	Bemanevika	m	52.1	58.0	110.1	1.11
C. gehringi	ZSM 1835/2010	ZCMV 12512	EI	PT	1466	Bemanevika	m	52.1	57.0	109.1	1.09
C. gehringi	ZSM 2841/2010	DRV 6392	EII	PT	1466	Bemanevika	m	44.7	49.9	94.6	1.12
C. gehringi	ZSM 2842/2010	DRV 6393	EI	PT	1466	Bemanevika	m	51.6	61.3	112.9	1.19
C. gehringi	ZSM 2843/2010	DRV 6414		PT	1538	Bemanevika	m	53.7	60.0	113.7	1.12
C. gehringi	ZSM 42/2016	MSZC 0154	EI	PT	1434	Ampotsidy	m	50.1	55.4	105.5	1.11
C. gehringi	ZSM 39/2016	MSZC 0128	EI	PT	1320	Ampotsidy	m	53.3	68.2	121.5	1.28
C. gehringi	ZSM 2840/2010	DRV 6318	EII	PT	1411	Ambodikakazo	m	49.3	58.9	108.2	1.19
C. gehringi	ZSM 43/2016	MSZC 0211	EI	PT	1172	Andranonafindra	m	55.5	68.1	123.6	1.23
C. gehringi	ZSM 38/2016	MSZC 0041	EI	PT	1307	Ampotsidy	f	52.0	52.2	104.2	1.00
C. gehringi	ZSM 40/2016	MSZC 0084	EI	PT	1456	Ampotsidy	f	48.4	47.3	95.7	0.98
C. gehringi	ZSM 41/2016	MSZC 0139	EI	PT	1414	Ampotsidy	f	47.5	45.1	92.6	0.95
C. gehringi	ZSM 2844/2010	DRV 6415	EI	PT	1538	Bemanevika	f	48.3	51.4	99.7	1.06
C. gehringi	ZSM 2852/2010	ZCMV 12308		PT	1207	Antsahan'i Ledy	f	52.1	49.5	101.6	0.95
C. gehringi	ZSM 2847/2010	ZCMV 12244	EI	PT	1361	Analabe Forest	f	52.3	46.5	98.8	0.89
C. gehringi	ZSM 2848/2010	—		PT	1361	Analabe Forest	jf	44.5	45.4	89.9	1.02
C. gehringi	ZSM 2846/2010	—		PT	1361	Analabe Forest	j	32.9	35.0	67.9	1.06
C. gehringi	ZSM 2839/2010	DRV 6316	EII	PT	1411	Ambodikakazo	j	37.5	41.6	79.1	1.11
C. gehringi	ZSM 2850/2010	—		PT	1207	Antsahan'i Ledy	j	34.4	33.2	67.6	0.97
C. sp.	ZSM 2845/2010	DRV 6417	FI		1538	Bemanevika	f	51.8	51.9	103.7	1.00

Table 1 continued.

species	collection no.	LRA	RRASV	DRA	RDRSV	NDRA	RC	LC	TCL	TCR	PC	OL	OLND	RODSV	DSOL
C. guibei	MNHN 50.354	1.3	0.039	1.3	0.039	5	(+)	+	–	–	–	s	1.1	0.033	0.4
C. guibei	MNHN 57.115	1.0	0.030	1.1	0.033	6	(+)	+	–	–	–	s	1.0	0.030	0.5
C. guibei	MNHN 57.116	0.7	0.026	0.8	0.030	5	(+)	+	–	–	–	s	0.7	0.026	0.4
C. guibei	ZSM 2855/2010	4.0	0.077	2.3	0.044	6	(+)	+	–	1	(+)	s	1.5	0.029	0.8
C. guibei	ZSM 2853/2010	4.5	0.085	1.8	0.034	5	(+)	+	–	–	(+)	s	1.2	0.023	1.0
C. guibei	ZSM 2854/2010	4.0	0.074	2.3	0.043	6	(+)	+	–	–	(+)	s	1.5	0.028	0.9
C. guibei	ZSM 2857/2010	2.0	0.041	2.0	0.041	5	(+)	+	–	–	(+)	s	1.9	0.039	1.0
C. guibei	ZSM 2856/2010	1.7	0.035	1.5	0.031	4	(+)	+	**–**	**–**	**+**	s	1.5	0.031	0.9
C. gehringi	ZSM 2851/2010	5.1	0.097	3.2	0.061	6	+	+	1	1	+	c	0.5	0.010	0.9
C. gehringi	ZSM 1834/2010	3.6	0.069	2.5	0.048	6	+	+	–	–	–	c	1.3	0.025	1.0
C. gehringi	ZSM 1835/2010	3.6	0.069	2.5	0.048	5	+	+	–	–	–	c	1.3	0.025	1.3
C. gehringi	ZSM 2841/2010	3.4	0.076	2.1	0.047	5	+	+	–	–	–	c	1.0	0.022	1.0
C. gehringi	ZSM 2842/2010	3.1	0.060	2.3	0.045	5	+	+	1	1	–	c	1.2	0.023	1.0
C. gehringi	ZSM 2843/2010	4.4	0.082	2.8	0.052	5	+	+	1	1	+	c	1.3	0.024	0.8
C. gehringi	ZSM 42/2015	3.4	0.068	2.3	0.046	5	+	+	–	–	+	(c)	1.5	0.030	1
C. gehringi	ZSM 39/2016	3.1	0.058	2.2	0.041	6	+	+	1	1	–	s	1.4	0.026	0.8
C. gehringi	ZSM 2840/2010	5.4	0.110	3.5	0.071	8	+	+	2	1	+	c	0.7	0.014	1.0
C. gehringi	ZSM 43/2016	5.0	0.090	2.6	0.047	5	+	+	1	1	(+)	c	1.0	0.018	0.9
C. gehringi	ZSM 38/2016	3.4	0.065	2.0	0.038	5	+	+	1	1	(+)	s	1.3	0.025	0.8
C. gehringi	ZSM 40/2016	3.3	0.068	2.1	0.043	6	+	+	–	–	(+)	(c)	1.4	0.029	0.9
C. gehringi	ZSM 41/2016	3.2	0.067	2.0	0.042	5	+	+	1	–	(+)	s	1.2	0.025	1
C. gehringi	ZSM 2844/2010	3.3	0.068	2.0	0.041	6	+	+	0	0	(+)	s	1.3	0.027	0.6
C. gehringi	ZSM 2852/2010	3.9	0.075	2.6	0.050	6	+	+	–	–	+	c	0.5	0.010	1.1
C. gehringi	ZSM 2847/2010	4.4	0.084	2.1	0.040	5	+	+	–	1	–	c	0.7	0.013	0.7
C. gehringi	ZSM 2848/2010	4.0	0.090	2.2	0.049	6	+	+	–	–	–	c	1.5	0.034	0.8
C. gehringi	ZSM 2846/2010	2.7	0.082	2.0	0.061	6	+	+	–	–	–	c	0.8	0.024	0.6
C. gehringi	ZSM 2839/2010	3.2	0.085	2.0	0.053	6	+	+	1	–	+	c	1.0	0.027	0.7
C. gehringi	ZSM 2850/2010	3.0	0.087	2.3	0.067	5	+	+	–	–	+	c	0.7	0.020	0.8
C. sp.	ZSM 2845/2010	3.6	0.069	2.8	0.054	5	+	+	1	1	(+)	c	1.4	0.027	0.8

Table 1 continued.

species	collection no.	OLD	RODSV	OLW	ROWSV	DSCT	DC	CaC	DSA	NSA	SL	NSL	NIL	HNC	HNR
C. guibei	MNHN 50.354	3.6	0.108	1.5	0.045	0.5	—	—	0.4	22	het	14	13	—	—
C. guibei	MNHN 57.115	3.9	0.117	1.7	0.051	0.4	—	—	0.4	20	het	15	15	—	—
C. guibei	MNHN 57.116	2.8	0.104	1.2	0.045	0.6	—	—	0.3	18	het	14	12	—	—
C. guibei	ZSM 2855/2010	4.9	0.094	2.5	0.048	0.9	—	—	0.7	16	het	11	11	4	4+2
C. guibei	ZSM 2853/2010	4.1	0.077	2.0	0.038	1.1	—	—	0.6	22	het	12	13	4	4+2
C. guibei	ZSM 2854/2010	4.5	0.084	2.1	0.039	0.8	—	—	0.5	20	het	12	13	4	4+2
C. guibei	ZSM 2857/2010	5.4	0.110	2.6	0.053	1.0	—	—	0.5	17	het	11	12	—	—
C. guibei	ZSM 2856/2010	5.1	0.106	2.6	0.054	0.7	—	—	0.5	19	het	11	11	—	—
C. gehringi	ZSM 2851/2010	5.1	0.097	2.8	0.053	0.7	13	+	0.7	13	het	11	13	4	4 (nfe)
C. gehringi	ZSM 1834/2010	5.5	0.106	3.0	0.058	0.8	8	—	0.5	16	het	13	14	4	4 (nfe)
C. gehringi	ZSM 1835/2010	5.7	0.109	3.1	0.060	0.9	8	+	0.8	15	het	11	13	4	4+2
C. gehringi	ZSM 2841/2010	4.7	0.105	2.9	0.065	0.8	13	+	0.7	13	het	10	13	4	4 (nfe)
C. gehringi	ZSM 2842/2010	5.5	0.107	2.9	0.056	1.0	10	—	0.9	12	het	12	13	4	4+2
C. gehringi	ZSM 2843/2010	6.0	0.112	3.0	0.056	1.0	14	+	0.6	20	het	12	12		4+2
C. gehringi	ZSM 42/2015	5.8	0.116	3.5	0.070	0.9	9	+	0.5	16	het	12	14	4	4+2
C. gehringi	ZSM 39/2016	5.7	0.107	3.3	0.062	1.0	7	+	0.5	15	het	12	12	4	4+2
C. gehringi	ZSM 2840/2010	6.1	0.124	3.5	0.071	1.1	15	+	0.8	15	het	12	13	4	4 (nfe)
C. gehringi	ZSM 43/2016	6.4	0.115	3.0	0.054	1.0	15	+	0.6	21	het	13	12	4	4+2
C. gehringi	ZSM 38/2016	5.3	0.102	3.1	0.060	1.0	—	—	0.6	17	het	12	11	—	—
C. gehringi	ZSM 40/2016	4.8	0.099	2.7	0.056	0.9	—	—	0.6	17	het	12	11	—	—
C. gehringi	ZSM 41/2016	5.1	0.107	2.8	0.059	0.9	—	—	0.6	18	het	11	11	—	—
C. gehringi	ZSM 2844/2010	5.0	0.104	2.2	0.046	0.7	—	—	0.5	23	het	11	12	—	—
C. gehringi	ZSM 2852/2010	5.2	0.100	2.8	0.054	1.0	—	—	0.6	15	het	10	11	—	—
C. gehringi	ZSM 2847/2010	5.3	0.101	2.5	0.048	0.8	—	—	0.5	14	het	12	11	—	—
C. gehringi	ZSM 2848/2010	5.3	0.119	3.3	0.074	0.8	—	—	0.5	15	het	10	13	—	—
C. gehringi	ZSM 2846/2010	3.8	0.116	2.4	0.073	0.6	—	—	0.4	13	het	11	14	—	—
C. gehringi	ZSM 2839/2010	4.3	0.115	2.3	0.061	0.8	—	—	0.4	16	het	13	14	—	—
C. gehringi	ZSM 2850/2010	4.0	0.116	2.0	0.058	0.5	—	—	0.4	17	het	11	13	—	—
C. sp.	ZSM 2845/2010	5.5	0.106	2.8	0.054	0.8	—	—	0.6	17	het	13	14	—	—

Table 2. Osteological measurements (all in mm) and relations of important characters of the skull for differentiation between *Calumma guibei* und *C. gehringi* sp. nov., obtained from micro-CT scans. Abbreviations: snout-vent length (SVL; measured externally), width of frontal between the orbits (FW), length of frontal (FL), ratio of FL and SVL (RFL), lateral diameter of frontoparietal fenestra (FFD), ratio of FFD and SVL (RFD), parietal width (PW), ratio of PW and SVL (RPW), length of parietal (PL), ratio of PL and SVL (RPL), ratio of FW and SVL (RFW), prefrontal fontanelle and naris separated (PNS), squamosal meets parietal (SMP), anterior tip of the frontal exceeds more than the half of the naris (FEN).

species	collection number	clade	type status	SVL	FW	FL	RFW	RFL	FFD	RFD	PW	RPW	PL	RPL	PNS	SMP	FEN
C. guibei	MNHN 50.354		HT	33.4	1.7	3.7	0.051	0.111	2.8	0.085	1.6	0.047	3.1	0.094	–	–	–
C. guibei	MNHN 57.115		PT	33.3	1.3	3.6	0.040	0.107	2.2	0.066	1.2	0.035	3.2	0.097	–	–	–
C. guibei	ZSM 2855/2010	FI		51.7	2.8	4.6	0.054	0.089	2.6	0.050	1.6	0.030	4.8	0.092	–	–	–
C. gehringi	ZSM 2851/2010	EII	HT	52.6	2.5	6.2	0.048	0.118	0.8	0.015	1.4	0.027	6.4	0.122	+	+	+
C. gehringi	ZSM 2840/2010	EII	PT	49.3	3.9	5.5	0.080	0.112	1.1	0.022	1.3	0.026	5.9	0.119	+	+	–
C. gehringi	ZSM 2841/2010	EII	PT	44.7	2.4	5.8	0.054	0.130	0.9	0.020	0.9	0.020	5.3	0.119	+	+	+
C. gehringi	ZSM 2842/2010	EI	PT	51.6	2.9	6.6	0.056	0.128	0.7	0.014	1.0	0.019	6.0	0.115	+	+	+

culated: snout-vent length (SVL) from the snout tip (not including the rostral appendage) to the cloaca; tail length (TaL) from the cloaca to the tail tip; total length (TL) as a sum of SVL + TaL; ratio of TaL and SVL (RTaSV); length of the rostral appendage (LRA) from the upper snout tip; ratio of LRA and SVL (RRASV); diameter of rostral appendage (DRA), measured dorsoventrally at the widest point; ratio of DRA and SVL (RDRSV); number of scales across DRA (NDRA); distinct rostral crest (RC) presence (+) or absence (−); lateral crest (LC), running from the posterior of the eye horizontally, presence (+) or absence (−); temporal crest, running dorsally to the LC, curving toward the midline, absence (−) or number of tubercles on left side (TCL) or right side (TCR); parietal crest (PC) presence (+) or absence (−); occipital lobes (OL) completely separated (s) or at least slightly, connected (c); depth of the dorsal notch in the occipital lobes (OLND); ratio of OLND and SVL (RODSV); diameter of largest scale on OL (DSOL); lateral diameter of OL (OLD); ratio of OLD and SVL (RODSV); width of OL measured at the broadest point (OLW); ratio of OLW and SVL (ROWSV); diameter of largest scale on temporal region (DSCT), measured on the right side; dorsal crest (DC) absence (−) or number of dorsal cones visible to the naked eye without the use of a binocular microscope according to ECKHARDT *et al.* (2012); caudal crest (CaC) presence (+) or absence (−); diameter of broadest scale on the lower arm (DSA), defined as the area from the elbow to the manus in lateral view on the right side; number of scales on lower arm in a line from elbow to manus (NSA); scalation on lower arm (SL), heterogeneous (het) or homogeneous (hom); number of supralabial scales (NSL), counted from the first scale next to the rostral to the last scale that borders directly and entirely (with one complete side) to the mouth slit of the upper jaw on the right side; and number of infralabial scales (NIL), analogous to the definition of NSL above, on the right side. In male specimens additionally hemipenial morphology was investigated, concerning number of cornucula gemina (HNC; new term, see discussion) and number of rotulae (HNR). This was not possible in all specimens, since the hemipenes were not fully everted (nfe).

Micro-CT

For internal morphology, micro-Computed Tomography (micro-CT) scans of the head were prepared for seven specimens of the *Calumma guibei* complex representing three OTUs from the clades EI, EII, and FI in GEHRING *et al.* (2012): ZSM 2851/2010 (clade EII), male from Antsahan'i Ledy; ZSM 2840/2010 (clade EII), male from Ambodikakazo; ZSM 2841/2010 (clade EII) and ZSM 2842/2010 (clade EI), both males from Bemanevika; ZSM 2855/2010 (clade FI), male from Tsaratanana massif and the type material of *C. guibei*: holotype MNHN 50.354 and paratype MNHN 57.115, both from Mount Tsaratanana and presumably juvenile females. For micro-CT scanning, specimens were mounted vertically in a

closed plastic vessel slightly larger than the specimen with the head oriented upwards, and stabilized with ethanol soaked paper. To avoid artefacts, it was ensured that the paper did not cover the head region. Micro-CT scanning was performed with a phoenix|x nanotom m (GE Measurement & Control, Wunstorf, Germany) using a tungsten target at a voltage of 130 kV and a current of 80 µA for 29 minutes (1800 projections). 3D data sets were processed with VG Studio Max 2.2 software (Visual Graphics GmbH, Heidelberg, Germany); the data were visualized using the Phong volume renderer to show the surface of the skull and reflect a variety of different levels of x-ray absorption. Osteological terminology follows RIEPPEL & CRUMLY (1997). Skull measurements were taken in VG Studio Max 2.2 using the following abbreviations (Table 2): width of frontal between the orbitals (FW); ratio of FW and SVL (RFW); length of frontal (FL); ratio of FL and SVL (RFL); diameter of frontoparietal fenestra (FFD), measured laterally at the border of frontal and parietal; ratio of FFD and SVL (RFD); parietal width, measured at the midpoint (PW); ratio of PW and SVL (RPW); length of parietal along the midline (PL); ratio of PL and SVL (RPL); prefrontal fontanelle and naris separated (PNS) by contact of prefrontal with maxilla (+) or fused (−); presence (+) or absence (−) of squamosal-parietal contact (SMP); anterior tip of the frontal exceeding the midpoint of the naris (FEN), (+) or (−). The presence of the frontoparietal fenestra was also checked externally in preserved specimens by gently pushing the top of the head with forceps.

Hemipenes of one *Calumma guibei* (ZSM 2855/2010) and two *C. gehringi* sp. nov. (ZSM 2840/2010, ZSM 2842/2010) were diceCT (diffusible Iodine contrast enhanced micro-CT) scanned. One hemipenis was clipped off from each specimen and immersed in iodine solution (I$_2$ in 1% ethanol) for two days to increase X-ray absorbance. For scanning, the hemipenes were placed with their apices oriented upwards in a plastic tube immersed in 70% ethanol. Scanning was performed for 30 min at a voltage of 60 kV and a current of 200 µA (2400 projections). 3D data were processed in VG Studio Max 2.2 as described above. Hemipenial terminology follows largely KLAVER & BÖHME (1986). Due to their incomplete eversion the hemipenes of the holotype of *C. gehringi* sp. nov. (ZSM 2851/2010) were not scanned and investigated externally only. Hemipenes of the remaining males were investigated using a binocular dissecting microscope.

The skulls of all adult male specimens of both species were additionally radiographed using a Faxitron UltraFocus LLC x-ray unit. Morphological terminology and description structure largely follow PRÖTZEL *et al.* (2015).

Genetic analysis

We extracted total genomic DNA from tissue samples using proteinase K digestion (10 mg/mL concentration) followed by a salt extraction protocol (BRUFORD *et al.*,

1992). We amplified a segment of the mitochondrial gene for NADH dehydrogenase subunit 2 (ND2) using standard PCR protocols with the primers ND2F17 (5'-TGACAAAAAAT TGCNCC-3') (MACEY *et al.*, 2000) and ALAR2 (5'-AAAATRTCTGRGTTGCATTCAG-3') (MACEY *et al.*, 1997). PCR products were purified using ExoSAPIT (USB) and sequenced on an automated DNA sequencer (ABI 3130 XL; Applied Biosystems). The newly determined DNA sequences were checked for sequencing errors with the software CodonCode Aligner (CodonCode Corporation), and submitted to GenBank (accession numbers MF579737 – MF579749). ND2 sequences were combined with those of GEHRING *et al.* (2012) and aligned manually by amino-acid translation in MEGA 7 (KUMAR *et al.*, 2016). We used jModeltest 2 (DARRIBA *et al.*, 2012) to determine the most appropriate model of evolution under the Bayesian Information Criterion (a TNR + I + G model), and subsequently reconstructed the phylogeny under the maximum likelihood (ML) optimality criterion in MEGA 7, with 1000 bootstrap replicates to test the robustness of nodes. A sequence of *Calumma oshaughnessyi* was used as an outgroup. In our species delimitation rationale, we furthermore rely on concordance of the differentiation in mitochondrial DNA represented by the ND2 gene, with differentiation in the nuclear gene for oocyte maturation factor (CMOS) for which we exclusively used previously published sequences from GEHRING *et al.* (2012).

Results

Molecular differentiation of *Calumma nasutum* group species with occipital lobes

The maximum likelihood tree based on the mitochondrial ND2 gene (Fig. 1) agrees with the tree in GEHRING *et al.* (2012) in most aspects. At the basal-most nodes, specimens of clade FI (herein considered as *C. guibei)* and FII (a candidate species from Andrevorevo that will be treated elsewhere) split off the tree, whereas the remaining clades DI (*C. boettgeri*), DII/DIII (*C. linotum*), and EI/EII (*C. gehringi*) together form a monophyletic group but with negligible bootstrap support (52%). On the contrary, each of the main lineages receives strong support (94 – 97%): the sister species (1) *C. linotum* and (2) *C. boettgeri* as defined in PRÖTZEL *et al.* (2015); (3) *C. guibei*; and (4) the new species *C. gehringi* sp. nov. Our tree only contains a representative set of sequences of *C. boettgeri* and *C. linotum*, as the differentiation among and within these species has been discussed before (PRÖTZEL *et al.*, 2015). Uncorrected pairwise distances in the ND2 gene among the four included species of the *C. boettgeri* group ranged from 11.8% (*C. boettgeri* vs. *C. linotum*) to 20.8% (*C. boettgeri* vs. *C. guibei*). Important but consistently lower distances were also found within species: up to 11.4% within *C. gehringi* sp. nov.,
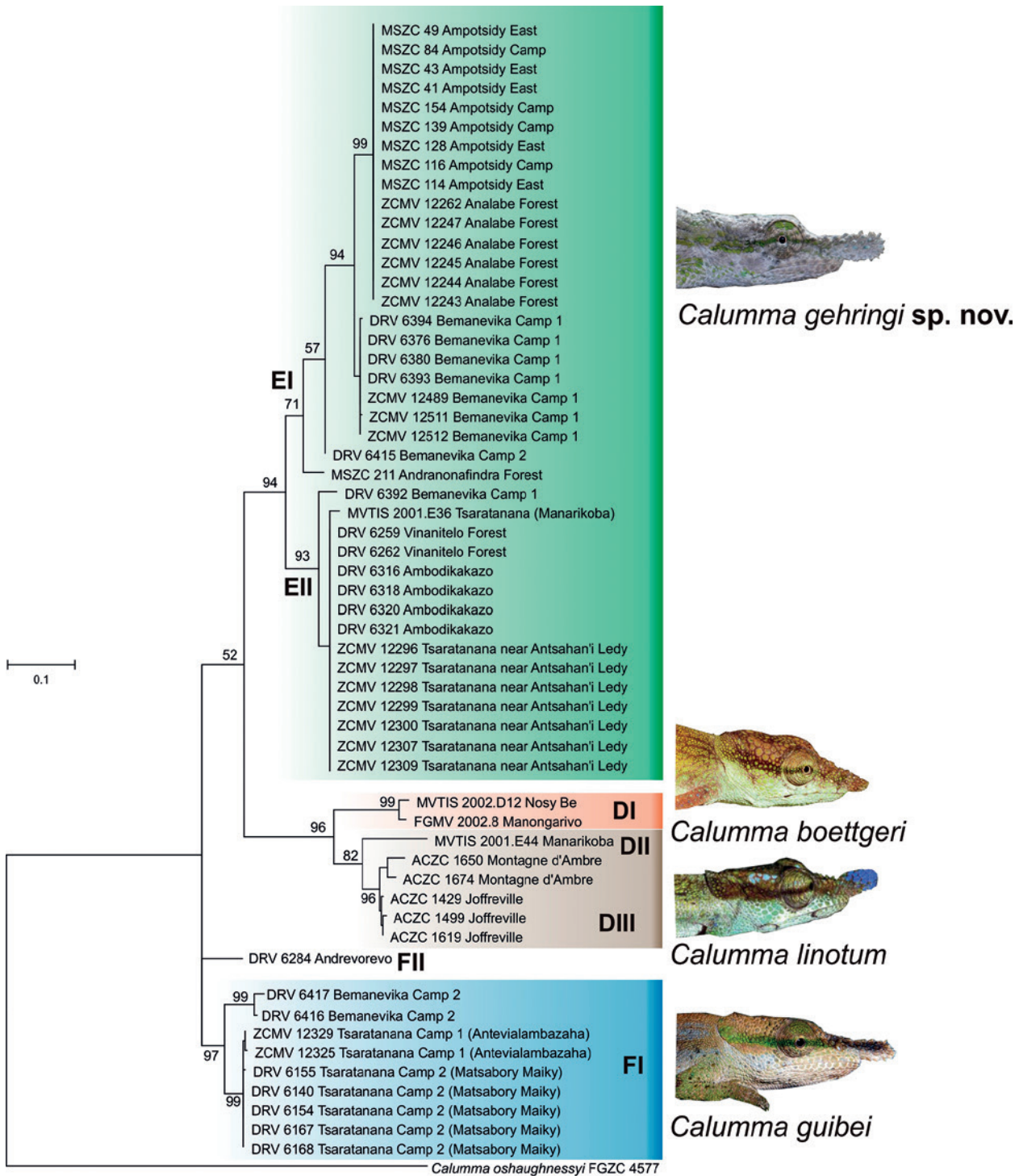
Fig. 1. Maximum likelihood tree based on an alignment of 508 bp DNA sequences of the mitochondrial ND2 gene, depicting phylogenetic relationships among species of the *Calumma nasutum* group with distinct occipital lobes. Numbers at nodes are bootstrap proportions in percent (1000 replicates). EI, EII, DI, DII, DIII, FI, FII are clade numbers according to Gehring *et al*. (2012) as discussed in the text.

10.0% within *C. linotum* (Manarikoba vs. Montagne d' Ambre), 6.9% within *C. guibei,* and 2.3% within *C. boettgeri*. The new species described herein (*C. gehringi* sp. nov.) differed from all other species of the group by a minimum pairwise divergence of 12.3% (to *C. guibei*).

The data for the nuclear CMOS gene as analysed and documented by GEHRING *et al.* (2012) reveal that there

is no haplotype sharing between the four species *C. guibei, C. gehringi* sp. nov.*, C. linotum,* and *C. boettgeri* (clade F, clade E, clade DI, clade DII–III, respectively). On the contrary, the two deep mitochondrial clades observed in *C. gehringi* do share nuclear haplotypes (clades EI and EII).
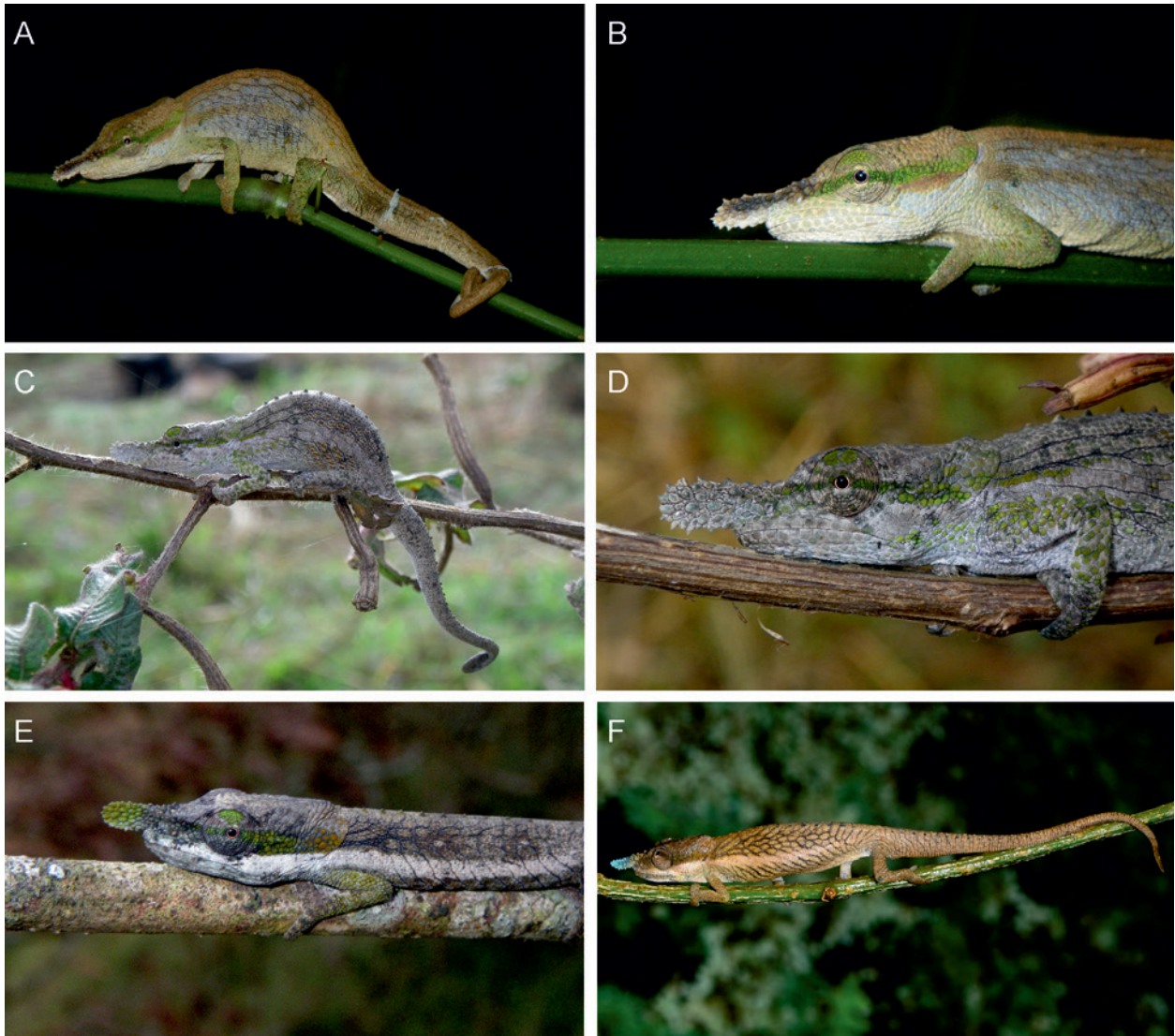
Fig. 2. Chameleon colouration in life: (**A**, **B**) *Calumma guibei*, male ZSM 2854/2010, clade FI; (**C**, **D**) *C. gehringi* sp. nov., male holotype ZSM 2851/2010, clade EII; (**E**) *C. gehringi* sp. nov., male ZSM 2843/2010; (**F**) *C. gehringi* sp. nov., male ZSM 43/2016, clade EI.

Identity and re-description of *Calumma guibei* (Hillenius, 1959)

Due to their immature state, many important characters to delimit the type series of *C. guibei* from other species are weakly developed or even lacking, e.g. several crests, adult size, sex or shape of occipital lobes. However, some characters are conspicuous (Table 1, 2): a very short rostral appendage of 0.7–1.3 mm length (2.6–3.9% of SVL), which is unusual even for juvenile specimens of the *C. nasutum* group (Table 1, Hillenius, 1959; Prötzel, unpublished data); deeply cut notch between the occipital lobes of 0.7–1.1 mm (2.6–3.3% of SVL); no traces of a dorsal crest; heterogeneous scalation of 18–22 enlarged tubercle scales from elbow to manus; a large frontoparietal fenestra; prefrontal fontanelle and naris fused; and absence of dorsal contact between squamosal and parietal, as shown for a female *C. nasutum* in

Rieppel & Crumly (1997). These osteological characters might be a result of the juvenile stage of development of the types and change in an adult organism. However, we found similar characters in an adult male specimen (ZSM 2855/2010) of clade FI (Fig. 2A, B; Fig. 3F; Fig. 4B; Fig. 5A), with a distinct frontoparietal fenestra, fused prefrontal fontanelle and naris, and a squamosal not in contact with the parietal. Radiographs taken of all male specimens from this complex confirmed a large frontoparietal fenestra also in ZSM 2853/2010 and ZSM 2854/2010.

The morphological characters that are mentioned above also support the assignment of clade FI (n = 5) to *C. guibei*: short rostral appendage in females (1.7–2.0 mm; 3.5–4.1% of SVL; n = 2), deeply cut notch completely separating the occipital lobes (1.2–1.9 mm; 2.3–3.9% of SVL; n = 5); no dorsal crest; heterogeneous scalation on arms with 16–22 enlarged tubercle scales from elbow to manus.

Fig. 3. Chameleon colouration in life: (**A**) *Calumma gehringi* sp. nov., female ZSM 41/2016, clade EII; (**B**) *C. gehringi* sp. nov., female MSZC 0049, clade EI; (**C**) *C. gehringi* sp. nov., female ZSM 2844/2010, clade EI; (**D**) *C. gehringi* sp. nov., female ZSM 38/2016, clade EI; (**E**) *C. gehringi* sp. nov., female ZSM 2852/2010, note the shape of the notch of the occipital lobes compared to (F); (**F**) *C. guibei*, male ZSM 2854/2010.

Calumma guibei (HILLENIUS, 1959)

Holotype. MNHN 50.354, juvenile, Mount Tsaratanana in the North of Madagascar at 1800 m a.s.l., collected by Paulian on an unknown date.

Paratypes. MNHN 57.115 and MNHN 57.116, both juvenile, collected by Paulian (see above).

Referred material. ZSM 2855/2010 (DRV 6140), adult male, ZSM 2857/2010 (DRV 6168), ZSM 2856/2010 (DRV 6167), both adult females, all three collected in Tsaratanana massif, camp 2 (14.1526°S, 48.9573°E, 2021 m a.s.l.) on 13 June 2010; ZSM 2853/2010 (DRV 6131), ZSM 2854/2010 (ZCMV 12325), both adult males collected in Tsaratanana massif, camp 1 (14.1741°S, 48.9452°E, 1589 m a.s.l.) on 11 and 10 June 2010; collectors are M. Vences, D. Vieites, R.D. Randrianiaina, F. Ratsoavina, S. Rasamison, A. Rakotoarison, E. & T. Rajoafiarison.

Diagnosis. *Calumma guibei* is a member of the phenetic *C. nasutum* group (PRÖTZEL *et al.*, 2016), because of the presence of a soft, dermal, unpaired rostral appendage,

absence of gular or ventral crest and heterogeneous scalation at the lower arm, consisting mostly of enlarged tubercles with a diameter of 0.3 – 0.7 mm. Within the genus it is a small sized, beige to greenish chameleon (SVL 48.1 – 53.7 mm, TL 93.6 – 115.8 mm) that is characterized by a long rostral appendage in males (4.0 – 4.5 mm) and a short rostral appendage in females (1.7 – 2.0 mm), occipital lobes that are clearly notched in V-form and completely separated, absence of axillary pits, absence of a dorsal crest in both sexes, and a unique skull morphology including a large frontoparietal fenestra (with a width of 5.0 – 8.5% of SVL).

Calumma guibei differs from *C. fallax*, *C. gallus*, *C. nasutum*, *C. peyrierasi*, *C. vatosoa* and *C. vohibola* of the *C. nasutum* group by the presence of occipital lobes; from *C. boettgeri* and *C. linotum* by the completely separated occipital lobes (vs. not or slightly notched, PRÖTZEL *et al.*, 2015), hemipenis with three pairs of ro-
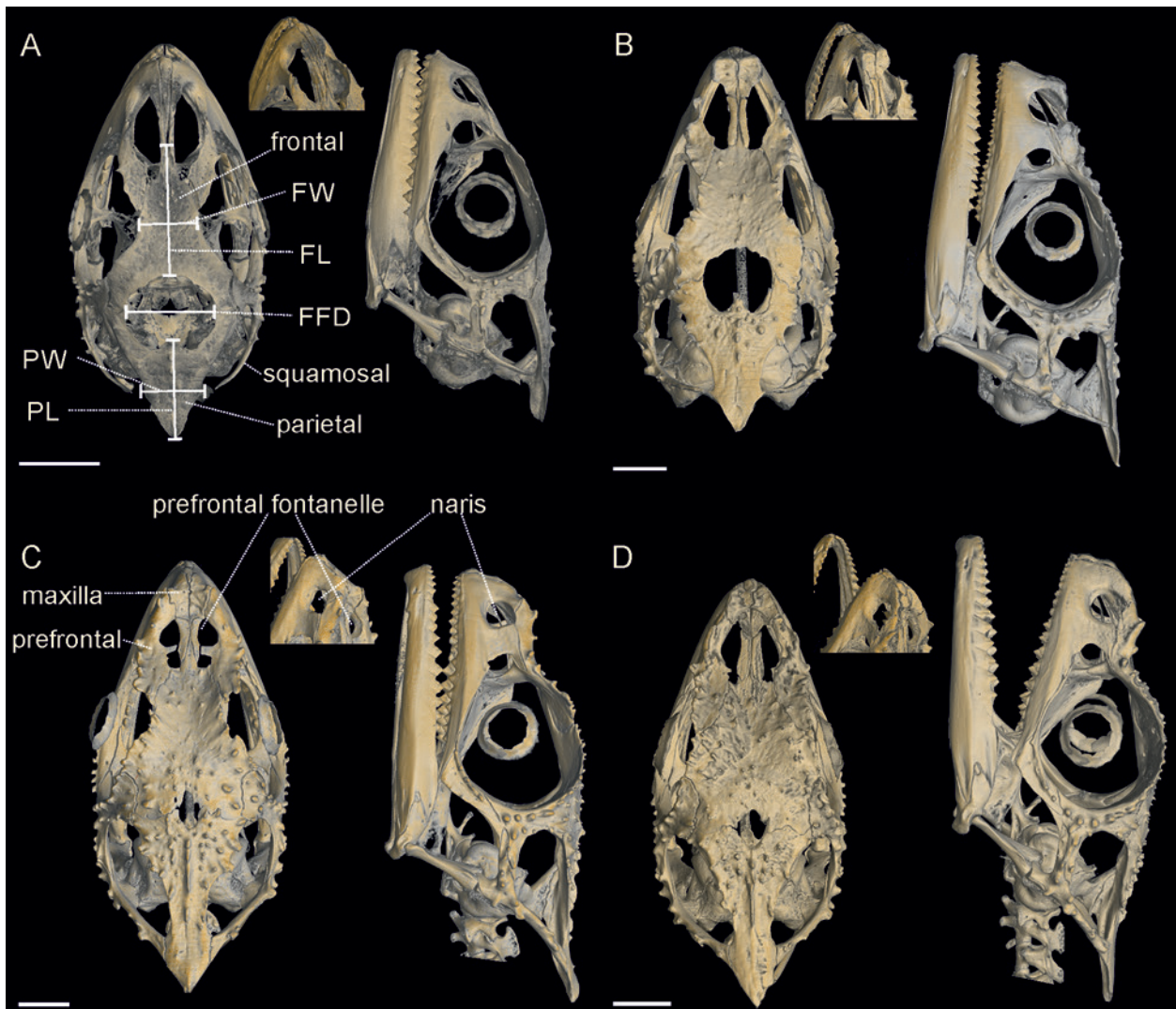
Fig. 4. Micro-CT scans of skulls of *Calumma* in dorsal and lateral view, as well as anterior parts of the skull in dorsolateral view; (**A**) holotype *C. guibei* (MNHN 50.354); (**B**) male *C. guibei* (ZSM 2855/2010); (**C**) male holotype *C. gehringi* sp. nov. (ZSM 2851/2010, clade EII); (**D**) male *C. gehringi* sp. nov. (ZSM 2840/2010, clade EII); scale bar = 2.0 mm. Abbreviations: parietal width (PW), parietal length (PL), diameter of frontoparietal fenestra (FFD), frontal width (FW), frontal length (FL).

tulae (vs. two pairs) and strongly developed cornucula gemina (vs. smaller cornucula gemina, PRÖTZEL *et al.*, 2015), presence of a large frontoparietal fenestra with a width of 5.0 – 8.5% of SVL (vs. completely closed brain case), fused prefrontal fontanelle and naris in males (vs. separated); additionally from *C. boettgeri* by larger, juxtaposed tubercle scales on the extremities (diameter 0.5 – 0.9 mm vs. small, 0.2 – 0.5 mm, and isolated from each other). For the differentiation *Calumma gehringi* sp. nov., see Diagnosis of that species.

Re-description of the holotype (Fig. 6). Juvenile, in a good state of preservation, except body completely slit on the ventral side and on left lateral side behind the occipital lobes; mouth slightly opened; SVL 33.4 mm; tail length 31.8 mm; indistinct rostral ridges that fuse on the anterior snout in a soft, laterally compressed dermal rostral appendage that projects 1.3 mm beyond the upper snout tip, rounded distally; 13 infralabial and 14 su-

pralabial scales; supralabials dorsally serrated (character 'dents de scie' in ANGEL, 1942); no supra-orbital crest; lateral crest poorly developed and pointing straight posteriorly; no temporal or parietal crests; occipital lobes clearly developed and separated by a notch of 1.1 mm; casque crest from the notch pointing towards the eye; casque not elevated from the head; no traces of gular, ventral or dorsal crest; body laterally compressed with fine homogeneous scalation with the exception of the extremities and head region; legs with small rounded tubercle scales of 0.3 mm diameter; slightly heterogeneous scalation on the head and tubercle scales on rostral appendage; no axillary or inguinal pits. Further morphological measurements are provided in Table 1.

Skull osteology of the holotype (Fig. 4A; Table 2; suppl. Fig. 1). Narrow nasal bones paired and completely separated by the frontal and the premaxilla that meet between them; prefrontal fontanelle and naris fused; smooth fron-
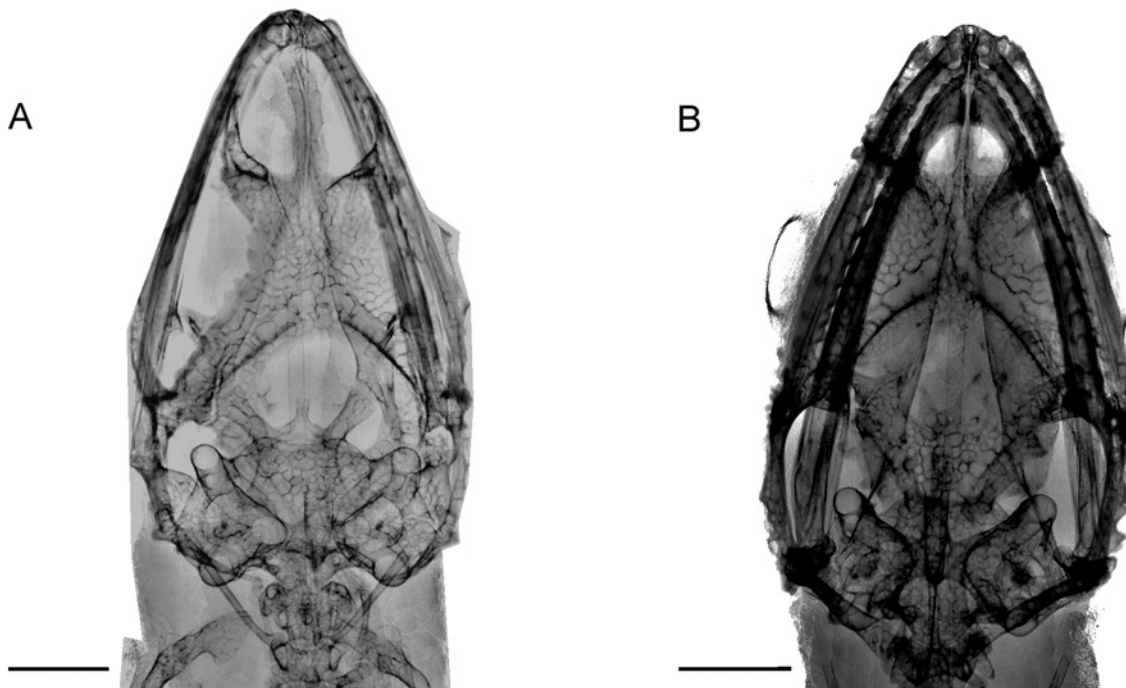
Fig. 5. Radiographs of *Calumma* in dorsal view in comparison to Fig. 3; (**A**) male *C. guibei* (ZSM 2855/2010); (**B**) male holotype *C. gehringi* sp. nov. (ZSM 2851/2010); scale bar = 2.0 mm. Note the frontoparietal fenestra in (A).

tal and parietal with only two tubercles on the parietal; frontal slim with a width of 1.7 mm (5.1% of SVL) between the orbits and a length of 3.7 mm (11.1% of SVL); large frontoparietal fenestra, lateral diameter 2.8 mm (8.5% of SVL); parietal V-shaped with straight lateral margins, tapering posteriorly; parietal 3.1 mm long at the midline (9.4% of SVL), 1.6 mm wide (4.7% of SVL); squamosal not in contact with the parietal.

Colouration of the holotype. The colour of the holotype (in 2016) is almost completely faded after storage in alcohol for more than 50 years. The body is grey-beige in colour without any recognizable pattern. The head and extremities are darkened.

Variation. For measurements of available specimens see Table 1. Within the specimens assigned to *Calumma guibei* there is only little variation: Taking into account their juvenile state, the paratypes (MNHN 57.115, 57.116) with relatively short rostral appendages (3.0 and 2.6% of SVL); male ZSM 2855/2010 is the only specimen with a lateral crest of a single tubercle on the right side; paratype MNHN 57.115 with the most supra- and infralabial scales (15 each). In skull morphology, the width of the frontoparietal fenestra of the adult specimen ZSM 2855/2010 (Fig. 4B; suppl. Fig. 2) is slightly smaller relative to its SVL (5.0%) than in the juvenile type specimens (6.6 – 8.5%).

Colouration in life. Although it can be assumed that there is variation in the colouration of *Calumma guibei*, we can only provide a description based on photographs of a single male specimen: in relaxed state with beige or light brown body colouration with an indistinct dark, net-like pattern and a beige lateral stripe; rostral appendage of same colouration as the body and with a dark brown lateral stripe that becomes green in colour over the snout, crossing the eyes and ending in the occipital lobes; extremities tending to more greenish in relation to the body and the throat to white-beige; the upper eyelid with a greenish-yellow spot.

Justification for a new species of *Calumma* and taxonomic relevance of its mitochondrial clades

After revising *Calumma boettgeri* and *C. linotum* (PRÖTZEL *et al.*, 2015) and assigning clade FI to *C. guibei* (see previous section), the status of three main lineages of *C. nasutum* group species with distinct occipital lobes remain to be clarified: clades EI, EII, and FII (sensu Gehring *et al*., 212; see Fig. 1). Only a single male specimen is available for clade FII, and it differs by genetics and morphology (GEHRING *et al.*, 2012; PRÖTZEL, unpublished data). The identity of this candidate species will be studied elsewhere.

Clades EI and EII together form a monophyletic group in the mitochondrial tree (Fig. 1). Although each is monophyletic as well, they are not very homogeneous groups, and especially EI contains various divergent haplotypes such as one from Bemanevika and a newly determined one from Andranonafindra Forest. Specimens of the two clades also share alleles in the nuclear CMOS gene (GEHRING *et al.*, 2012), and we did not observe any consistent morphological differences between them. Key

characters, used to distinguish between *C. gehringi* sp. nov. and *C. guibei* do not allow a differentiation between clade EI and EII (Table 1): males with dorsal crests of 7–15 spines and some with additional spines on the tail in EI and 13–15 spines and caudal crest in EII; distinctly elevated rostral crest and elevated casque in EI and EII; occipital lobes notched, but lobes still slightly connected or separated in EI and slightly connected in EII; in skull morphology (Fig. 4, Table 2), presence of a small frontoparietal fenestra (1.4% of SVL in EI and 1.5–2.2% of SVL in EII); prefrontal fontanelle and naris separated by contact of prefrontal with maxilla in both clades; parietal at its narrowest point (1.9% of SVL and 2.0–2.7%), and length along the midline (11.5% of SVL and 11.9–12.2%). Therefore, the available evidence suggests that these two clades are deep conspecific lineages of a single species, which we herein describe as *C. gehringi* sp. nov.

Specimens of *C. gehringi* sp. nov. differ morphologically from all other species of *Calumma* and also from its close relative *C. guibei* (see chapter 'Diagnosis' below; Table 1). Although it shares the characters of *C. gehringi* sp. nov. (long rostral appendage of 3.6 mm, occipital lobes connected, small frontoparietal fenestra), the female specimen ZSM 2845/2010 (DRV 6417) was genetically assigned to clade FI in our phylogeny of this complex (Fig. 1). This specimen was collected at 1538 m a.s.l., which is slightly lower than all other *C. guibei* (1589–2021 m) but the highest altitude of *C. gehringi* sp. nov. (1172–1538 m). It is not clear if this is a result of mitochondrial introgression in a parapatric hybrid zone or due to contamination or sequencing error, and we therefore consider this specimen putatively as *C.* sp. in need of further investigation.

There are two more nominal species of the *C. nasutum* group with soft rostral appendages and occipital lobes in Madagascar, *C. boettgeri* and *C. linotum*, whose taxonomy has been revised recently (Prötzel *et al.*, 2015). In addition to differences in distribution, these species also have no or only a slight notch between their occipital lobes and a different skull morphology.

Based on the above rationale, we here formally describe *C. gehringi* sp. nov.

Calumma gehringi sp. nov.

Remark. DNA sequences probably belonging to this species based on the tissue sample MVTIS 2001.G56 were published in the phylogeny of Tolley *et al.* (2013) under the name *C. linotum*. Sequences of OTU 10 and '*C. linotum*' of clade E in Gehring *et al.* (2012) are here assigned to *C. gehringi*, as well as the photographs of '*C. guibei*' in Glaw & Vences (2007: 290, 291).

Holotype. ZSM 2851/2010 (ZCMV 12307) adult male, collected in Antsahan'i Ledy in the Tsaratanana Massif (14.2332°S, 48.9800°E, 1207 m a.s.l.), Bealanana District, Sofia Region, Mahajanga Province, North Madagascar, on 9 June 2010 by D.R. Vieites, M. Vences, R.D. Randrianiaina, S. Rasamison, A. Rakotoarison, E. Rajeriarison, and T. Rajoafiarison (Fig. 6).

Paratypes. ZSM 1834/2010 (ZCMV 12511), ZSM 1835/2010 (ZCMV 12512), ZSM 2841/2010 (DRV 6392), ZSM 2842/2010 (DRV 6393), all four adult males, DRV 6376, 6380, 6394, ZCMV 12489 (four uncatalogued specimens in UADBA) collected near Bemanevika (14.4306°S, 48.6018°E, 1466 m a.s.l.) on 27 June 2010; ZSM 2840/2010 (DRV 6318), adult male, ZSM 2839/2010 (DRV 6316), juvenile, DRV 6320, 6321 (both uncatalogued in UADBA), all collected at Ambodikakazo (14.2098°S, 48.8982°E, 1411 m a.s.l.) on 15 June 2010; ZSM 2843/2010 (DRV 6414), adult male, ZSM 2844/2010 (DRV 6415), adult female, both collected near Bemanevika (14.3599°S, 48.5902°E, 1538 m a.s.l.) on 28 June 2010; ZSM 2846/2010 (ZCMV 12243), juvenile, ZSM 2847/2010 (ZCMV 12244), female, ZSM 2848/2010 (ZCMV 12247), subadult female, ZCMV 12245–12247, 12262 (four uncatalogued specimens in UADBA) all collected in Analabe Forest (14.5048°S, 48.8760°E, 1361 m a.s.l.) on 6 June 2010; ZSM 2850/2010 (ZCMV 12297), juvenile, ZSM 2852/2010 (ZCMV 12308), adult female, ZCMV 12296–12300, 12309 (six uncatalogued specimens in UADBA), all collected in Antsahan'i Ledy (14.2332°S, 48.9800°E, 1207 m a.s.l.) on 9 June 2010; DRV 6259, 6262 (two uncatalogued specimens in UADBA) collected in Forest Vinanitelo (14.2097°S, 48.9700°E, 1280 m a.s.l.) on 22 June 2010; collectors of the specimens above are M. Vences, D.R. Vieites, R.D. Randrianiaina, F.M. Ratsoavina, S. Rasamison, A. Rakotoarison, E. Rajeriarison, and T. Rajoafiarison; ZSM 38/2016 (MSZC 0041; 14.4231°S, 48.7189°E, 1325 m a.s.l.) on 20 December 2015, ZSM 40/2016 (MSZC 0084; 14.4163°S, 48.7181°E, 1456 m a.s.l.) on 24 December 2015, and ZSM 41/2016 (MSZC 0139; 14.4171°S, 48.7198°E, 1414 m a.s.l.) on 4 January 2016, all three adult females; MSZC 0128 (ZSM 39/2016; 14.4193°S, 48.7194°E, 1320 m a.s.l.) on 2 January 2016 and MSZC 0154 (ZSM 42/2016; 14.4159°S, 48.7210°E, 1434 m a.s.l.) on 3 January 2016, both adult males; MCSZ 0043, 0049, 0114, 0116 (four uncatalogued specimens in UADBA), all collected on the Ampotsidy Mountains by M.D. Scherz, J. Borrell, L. Ball, T. Starnes, E. Razafimandimby, D. Herizo Nomenjanahary, and J. Rabearivony; ZSM 43/2016 (MSZC 0211), adult male, collected in Andranonafindra Forest (14.7358°S, 48.5480°E, 1172 m a.s.l.) on 14 January 2016, by M.D. Scherz and M. Rakotondratsima.

Diagnosis. *Calumma gehringi* sp. nov. is a member of the phenetic *C. nasutum* group (Prötzel *et al.*, 2016), because of the presence of a soft, dermal, unpaired rostral appendage, absence of gular or ventral crest and heterogeneous scalation at the lower arm, consisting mostly of tubercles of large diameter (0.4–0.9 mm). Within the genus it is a small-sized, grey to greenish chameleon (SVL 44.7–55.5 mm, TL 92.6–123.6 mm) that is characterized by a large rostral appendage of green or blue colour in males and yellow in females when unstressed, occipital lobes that are clearly notched but usually still slightly connected, distinctly elevated rostral crest, absence of axillary pits, presence of a dorsal crest in males, and a unique skull morphology (see below).

Calumma gehringi differs from *C. fallax*, *C. gallus*, *C. nasutum*, *C. peyrierasi*, *C. vatosoa* and *C. vohibola* of the *C. nasutum* group by the presence of occipital lobes; from *C. boettgeri* and *C. linotum* by the completely separated or only slightly connected occipital lobes (vs. not or slightly notched, Prötzel *et al.*, 2015), hemipenis with three pairs of rotulae (vs. two pairs) and strongly developed cornucula gemina (vs. smaller cornucula gemina, Prötzel *et al.*, 2015), presence of a frontoparietal fenestra with a width of 1.4–2.2% of SVL (vs. completely closed brain case), frontal and parietal with many tubercles

Fig. 6. Male holotype of *Calumma gehringi* sp. nov. (ZSM 2851/2010, above) and juvenile holotype of *C. guibei* (MNHN 50.354, below) as preserved specimens. Scale bar = 10 mm.

(vs. smooth or only a few tubercles); additionally from *C. boettgeri* by larger, juxtaposed tubercle scales on the extremities (diameter 0.5–0.9 mm vs. 0.2–0.5 mm, and isolated from each other).

From the most similar taxon, *Calumma guibei*, *C. gehringi* differs most strongly in skull morphology (Fig. 4, Table 2), by possession of a smaller frontoparietal fenestra (width 1.4–2.2% of SVL vs. 5.0–8.5% of SVL); prefrontal fontanelle and naris separated by contact of prefrontal with maxilla (vs. not separated); parietal narrower at its narrowest point (1.9–2.7% of SVL vs. 3.0–4.7%) and longer along the midline (11.5–12.2% of SVL vs. 9.2–9.7%); thick squamosal (vs. thin) in broad dorsal contact with the parietal (vs. not meeting parietal), occipital lobes clearly notched but usually slightly connected (vs. completely separated, Fig. 3E, F), and presence of a dorsal crest with 7–15 tubercles in males (vs. absence). Furthermore, the new species differs from all other members of the *C. nasutum* group with occipital lobes by the possession of a distinctly elevated rostral crest, and a dorsal crest continuing on the tail in most specimens. In addition, *C. gehringi* differs from all other species of the genus *Calumma* by a substantial genetic differentiation (> 12% uncorrected pairwise distance in the mitochondrial ND2 gene; no haplotype sharing in the nuclear CMOS gene).

Description of the holotype. Adult male in a good state of preservation, its left forelimb removed for DNA analysis; mouth slightly opened with tongue between the jaws; both hemipenes incompletely everted (Fig. 6); SVL 52.6 mm; tail length 63.2 mm; distinct and elevated rostral ridges that form a concave cup on the snout and fuse on

the anterior snout in a large, laterally compressed dermal rostral appendage that projects straight forward over a length of 5.1 mm and a diameter of 3.2 mm, rounded distally with rough tubercle scales; 13 infralabial and 11 supralabial scales; supralabials dorsally serrated; no supraorbital crest; distinct lateral crest running horizontally; indistinct parietal crest, short temporal crest consisting of two tubercles on the left side and one on the right; occipital lobes clearly developed and deeply notched (0.5 mm), but not completely separated; casque raised; dorsal crest present, starting 1.6 mm from the base of the notch between the occipital lobes and continuing on the tail, consisting of a row of 13 separated conical scales spaced increasingly broadly from 1.4–2.1 mm to the cloaca and several more on the tail decreasing in size toward the tip; no traces of gular or ventral crest. Body laterally compressed with fine homogeneous scalation with the exception of the extremities and head region; limbs with large rounded tubercle scales of maximum 0.7 mm diameter; heterogeneous scalation on the head and large, oval tubercle scales on rostral appendage; no axillary or inguinal pits. Further morphological measurements are provided in Table 1.

Skull osteology of the holotype (Fig. 4C; Table 2; suppl. Fig. 3). Broad paired nasals meeting anteriorly; anterior tip of frontal exceeding more half of the naris; prefrontal fontanelle and naris separated by contact of prefrontal with maxilla; prominent prefrontals that are dorsolaterally raised; frontal and parietal with several tubercles, some forming a parietal crest; frontal with a width of 2.5 mm (4.8% of SVL) between the orbits and a length of 6.2 mm (11.8% of SVL); small frontoparietal fenestra with lat-

eral diameter of 0.8 mm (1.5% of SVL); lateral margin of parietal concave, 1.4 mm (2.7% of SVL) wide at its narrowest point; 6.4 mm (12.2% of SVL) long at the midline; posterodorsally directed parietal platform meets the squamosal laterally; squamosal thick with several tubercles.

Colouration of the holotype (Fig. 2C, D; Fig. 6). The body of the holotype in preservative is of grey-blue colour without any recognizable pattern; internal hind limbs and tail tip beige, neck region and forelimbs also of beige colour and speckled with bluish tubercle scales; rostral appendage of beige-white colour at the tip. In life, the body colouration was bright with an indistinct dark, net-like pattern, and bright green tubercle scales, also on limbs and head region; a beige lateral stripe can occur from snout tip to hip; rostral appendage same colour as the body (Fig. 2C, D); the eyelid is sectioned by a lateral stripe, crossing the eye, and a spot on the upper eyelid, that are both green in colour.

Variation. For measurements of available type specimens see Table 1. Within the clade E there is variation in colouration and morphology, but in most characters the paratypes agree well with the holotype: male ZSM 2840/2010 has the longest rostral appendage (5.4 mm), appendages of the males ZSM 2841/2010, 2842/2010, 39/2016, and 42/2016 significantly shorter (3.1–3.4 mm); the appendage of female ZSM 2844/2010 has fine tubercle scales; there is significant variation in the temporal crest, from none to two tubercles, with some individuals even having asymmetrical tubercle numbers (Table 1); in the same way, the parietal crest is absent, indistinct or present within both sexes; notch of occipital lobes in most paratypes deeper than in holotype (0.5–1.5 mm) and still slightly connected—only totally separated in ZSM 2844/2010, 38/2016, 39/2016, and 41/2016; dorsal crest present in all males, but number of cones highly variable (7–15), indistinct and small cones in ZSM 1834/2010, 39/2016, 42/2016, and 43/2016; all males with caudal crest except ZSM 1834/2010 and 2842/2010, indistinct in ZSM 43/2016; dorsal crest lacking in all females; number of supralabial and infralabial scales from 10–14. The male ZSM 43/2016 is geographically isolated and from the lowest elevation of all paratypes, and has the largest body size (55.5 SVL mm and 123.6 mm TL) and a distinct blue rostral appendage in life (Fig. 2F); it is also genetically basal to clade EI, but still strongly supported as a member of clade E, and we therefore consider its deviation from the rest of the specimens to reflect geographic variation in this species, but emphasise that more material from the Bealanana district is needed.

The three micro-CT scanned paratypes ZSM 2840/2010, 2841/2010, and 2842/2010 are more or less identical in skull osteology with the holotype (Table 2), including the prefrontal fontanelle and naris separated from each other, a small frontoparietal fenestra of 0.7–1.1 mm diameter and the squamosal meeting the parietal. The shape of the frontals is variable, with lengths of 5.5 to

6.6 mm and widths of 2.4 to 3.9 mm. In ZSM 2840/2010 the anterior tip of the frontal does not exceed more than the half of the naris.

Colouration in life. Both sexes in relaxed state have green, grey, or brown body colouration with an indistinct dark, net-like pattern; a beige-white lateral stripe can occur from snout tip to hip; males usually with a bright green rostral appendage and green-coloured extremities, the eyelid is sectioned by a lateral stripe crossing the eye, and a spot is present on the upper eyelid, both of which can be bright green in colour; additionally the temporal region and the occipital lobes can be of conspicuous green colour. Sexes are generally dichromatic, with females typically bearing a yellow, instead of a green, rostral appendage; that yellow colouration can spread over the eyelids and the temporal region to the occipital lobes. One exception is ZSM 43/2016, which had a strongly blue rostral appendage in life (as did all other males encountered in Andranonafindra; MDS pers. obs.). The extremities are usually of the same colour as the body. One gravid female was almost entirely green, including her rostral appendage.

Stress colouration is significantly darker, with a net-like black pattern of small scales on the lateral body. The rostral appendage typically becomes more distinctly bright in colouration against the darker lateral head colouration.

Hemipenial morphology based on micro-CT scans. The hemipenis of *Calumma gehringi* (Fig. 7B; suppl. Fig. 4) shows large and deep calyces with smooth ridges on the asulcal side of the truncus. The apex is ornamented with two pairs of long pointed cornucula (see discussion) and paired rotulae. The cornucula gemina rise from the sulcal side of the apex, are curved to the asulcal side and are completely everted in the investigated specimen (Fig. 7B). Two pairs of rotulae are placed on the asulcal side and are finely denticulated. Additionally on the asulcal side next to the pair of cornucula, there is a pair of rotulae with three lobes. This ornament is only recognizable when the hemipenis is fully everted.

Available names. Apart from *C. guibei* there is no other valid species or synonym in the *Calumma nasutum* group with deeply notched occipital lobes.

Etymology. We dedicate the new species to Philip-Sebastian Gehring. His comprehensive molecular phylogenetic study on the *Calumma nasutum* group was the basis for the description of the new species, and will be instrumental to the resolution of the rest of this complex. The species epithet '*gehringi*' is a patronym in the Latin genitive form.

Distribution. *Calumma gehringi* has, so far, been collected in Northern Madagascar on the Tsaratanana Massif and south of it (Fig. 8). In contrast to *C. guibei*, whtich covers the higher elevations in Tsaratanana from
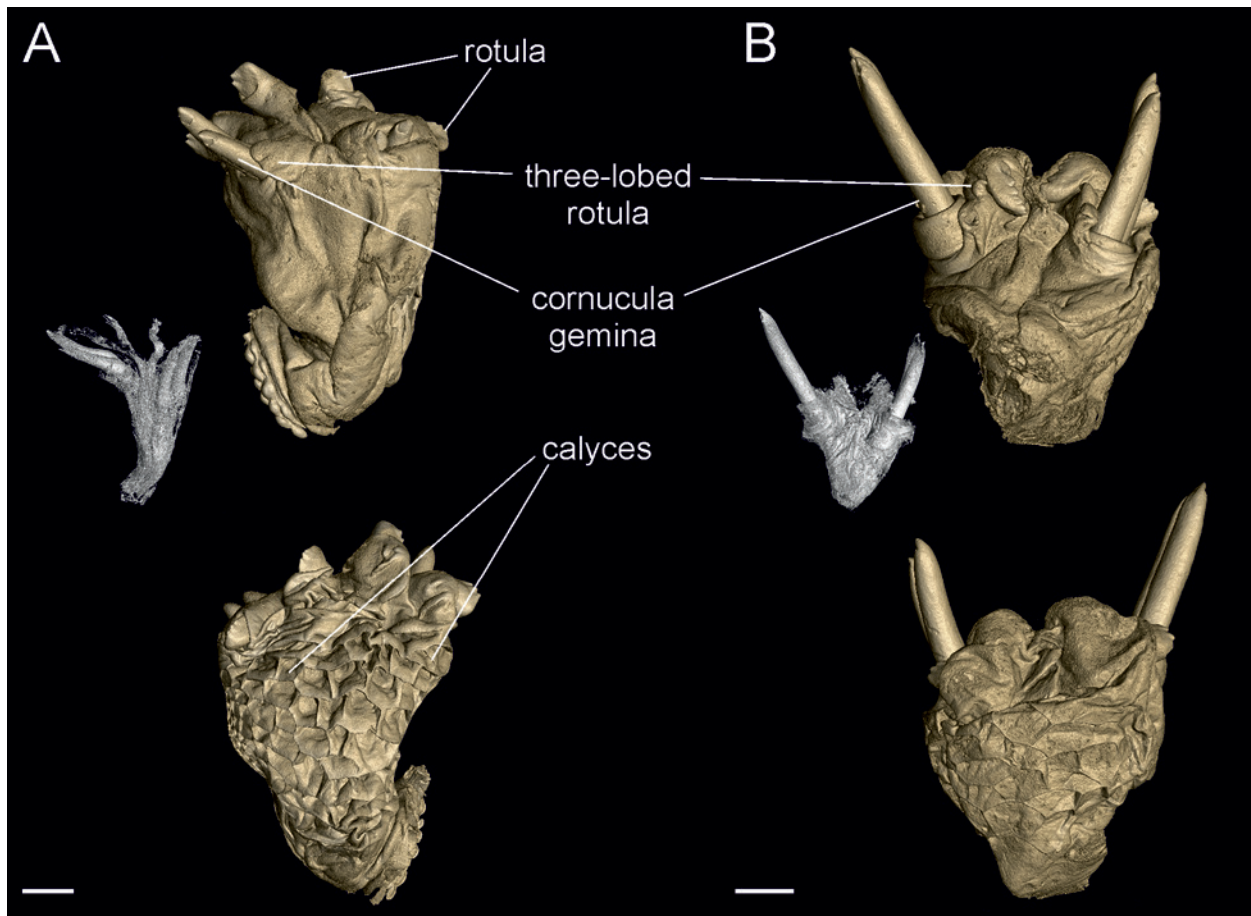
Fig. 7. Micro-CT scans of hemipenes of *Calumma* species in sulcal (above) and asulcal view (below). (**A**) *C. guibei* (ZSM 2855/2010); (**B**) *C. gehringi* sp. nov. (ZSM 2842/2010). Small images show the (everted or retracted) cornucula gemina inside of the hemipenis at a different threshold. Scale bar = 1 mm.

1590–2020 m a.s.l. (according to our data) or even up to 2250 m a.s.l. (RAXWORTHY *et al.*, 2008), *C. gehringi* lives at mid-altitudinal level from 730–1540 m a.s.l. and is recorded from Ambodikakazo, Ampotsidy, Antsahan'i Ledy, Analabe Forest, Andranonafindra Forest, Bemanevika, Manarikoba (14.0422°S, 48.7616°E, 730 m a.s.l.) and Vinanitelo Forest. The location at 730 m a.s.l. is based on a single (tissue) record; the distribution of most specimens starts from an altitude of 1200 m a.s.l. or higher. For geographic coordinates of the other localities, see chapter 'Paratypes'.

Natural history and ecology. *Calumma gehringi* is an arboreal, diurnal species occurring from 0.5 to at least 4 m above the ground in secondary, degraded primary, and pristine primary rainforest. Specimens were often observed on bushes and low branches of trees near rivers, almost always roosting at night, on leaves or thin branches/ twigs. The species can be locally abundant, often occurring in couples a few metres from one another, occasionally forming mixed-sex clusters of up to eight individuals over a few square metres. Heavily gravid females were collected from Ampotsidy in late December 2015 and early January 2016, indicating a mating season coinciding with seasonal rains. An absence of juveniles in this period

suggests that these hatch later in the season. At lower altitude, in Andranonafindra Forest (1172 m a.s.l.), hatchlings were encountered in mid-January 2016, indicating that there may be some degree of altitudinal variation in the reproductive cycle or timing of these chameleons. The following females contained well-developed eggs, that were ready to be laid: ZSM 40/2016, four eggs (dimensions from 8.3–9.6 × 5.3–5.7 mm); 41/2016, two eggs (8.1 × 4.0 mm and 7.9 × 4.9 mm); ZSM 38/2016, three eggs (8.9–9.3 × 4.2–4.7 mm); ZSM 2847/2010 (collected in June 2010), two eggs (12.1 x 5.8 mm and 11.5 × 5.9 mm). When disturbed on thin branches and vines during the day, individuals moved their bodies to the opposite side from the observer, and, if the perch was thin enough, were able to keep looking at the observer whilst being difficult to detect, by the lateral position of their eyes.

Discussion

In this work, we have taken another step towards clarifying the systematics of the *Calumma nasutum* group, by revising the identity of *C. guibei* and describing the new
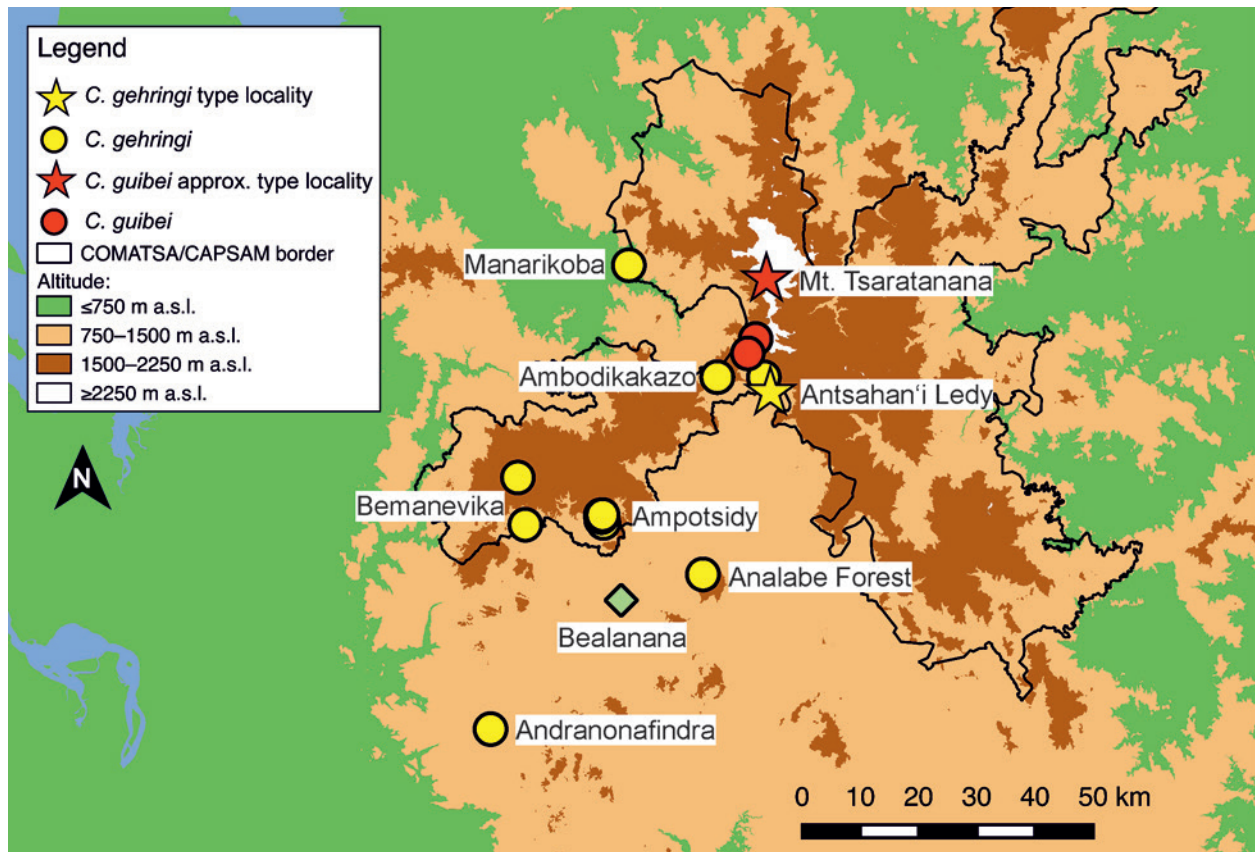
Fig. 8. Map of north-western Madagascar with localities of *Calumma guibei* and *C. gehringi* sp. nov. COMATSA/CAPAM border is that of a series of established and recently proposed protected areas. The green diamond indicates the town of Bealanana.

species *C. gehringi*. One of the several genetic lineages within the *C. guibei* complex (Gehring *et al*., 2012) must represent the true *C. guibei*, but because that species was described based on a juvenile holotype (from which genetic data are not available), assignment is difficult. After examining the holotype, the two paratypes, and specimens of the mitochondrial clades FI, EI and EII of Gehring *et al*. (2012) we have assigned *C. guibei* to clade FI and described the chameleons belonging to the clades EI and EII as a new species. No consistent differences between them in morphology or osteology were recognizable, and as mentioned above, they share haplotypes of the nuclear CMOS gene (400 bp). Additionally, two specimens (ZSM 2841/2010 and ZSM 2842/2010), representing clade EII and EI, occurred sympatrically at the same collection site in Bemanevika (camp 1, Antsirakala, 14.4306°S, 48.6018°E), without differentiation in the nuclear gene studied. Consequently, we merged these two OTUs of Gehring *et al.* (2012) to one new species, *C. gehringi*. This shows the importance of an integrative taxonomic approach to avoid over-splitting of species. However, additional work is needed in the future for better understanding of the differentiation among the various deep conspecific lineages within *C. gehringi* and to fully rule out the possibility that some of these represent cryptic species.

In conclusion, *Calumma guibei* is a species of the phenetic *C. boettgeri* complex with clearly notched and com-

pletely separated occipital lobes, a short rostral appendage in females, a unique skull morphology and lacking a dorsal crest—though this has not been a constant character in previous studies (Prötzel *et al.*, 2015). We confirm the characters stated by Hillenius (1959), specifically the separation of the occipital lobes and the lack of a dorsal crest, as diagnostic, except for the short rostral appendage that is of usual length (4.0–4.5 mm) in the males. In contrast, *C. gehringi* has notched, but not totally separated, occipital lobes, a long rostral appendage in females, and a small frontoparietal fenestra. Additionally, the species separate geographically; *C. guibei* occurs at higher elevations, from 1590–2250 m a.s.l. on the Tsaratanana Massif, and *C. gehringi* at mid-altitudes from 730–1540 m a.s.l. from Tsaratanana south and southwest to Bemanevika. Consequently, the specimens mentioned as *C. guibei* in Raxworthy & Nussbaum (1996) and Raxworthy *et al.* (2008) probably were correctly assigned to this species, while the '*C. linotum*' of Raxworthy *et al.* (2008) almost certainly refer to *C. gehringi*. The scalation of the extremities that was used to distinguish between *C. boettgeri* and *C. linotum* (Prötzel *et al.*, 2015) was not as characteristic in the present species, though *C. gehringi* has a more homogenous scalation with fewer scales in a row from elbow to manus (NSA, see Table 1). The size and shape of the rostral appendage is surprisingly variable within both species, decreasing its value as a diagnostic character. However, it is interesting that it tends to show sexual

dichromatism in *C. gehringi*, with males usually having green, and females usually yellow appendages—although some exceptions have been found.

With the aid of the micro-CT technique, we have shown that the presence and size of the frontoparietal fenestra is an informative character in this group, and particularly in the distinction of *C. guibei* from its congeners. Additionally, the squamosal is not connected with the parietal bone in *C. guibei*. These characters are reminiscent of juvenile skull morphology, and it is difficult to derive a biological function from this. Generally, cranial sutures allow small intercranial movements and if they remain open, they might allow micro-movements to dissipate forces acting on the skull (MOAZEN *et al*., 2009). RIEPPEL & CRUMLY (1997) suggest that this is a result of paedomorphosis. In chameleons, adults of small taxa often resemble juveniles of larger ones (RIEPPEL & CRUMLY, 1997). Thus, paedomorphosis is a potential explanation, but why the fenestra is so much more strongly developed in *C. guibei* than in closely related, and equally sized chameleons, remains a mystery. The skull of *C. gehringi* is more robust, with only a small frontoparietal fenestra, separated prefrontal fontanelle and naris, a strongly developed squamosal that is connected to the parietal, and differently shaped frontal and parietal bones. Though cheaper and faster in production, traditional radiography appears to be of limited use for identification of skull characters. Due to the flattening of a 3D object onto a 2D image plane, many characters overlap and are difficult to distinguish. However, the frontoparietal fenestra of *C. guibei* was recognizable as a slightly brighter grey contrast.

Although the hemipenis morphology of the two species considered here appears superficially different (Fig. 7A and B), there are in fact no substantial differences, except for the calyces on the asulcal side of the truncus, which are slightly larger in *C. gehringi*. Dice-CT scans enable a detailed view of the structure and the inside of a hemipenis and show that the two pairs of long spines, visible in Fig. 7A, are completely everted and in Fig. 7B largely retracted, but approximately of the same size. This ornament is not homologous to the papillae of e.g. Calumma brevicorne that are defined as 'fleshy and pliable projections' in KLAVER & BÖHME (1986). Due to its structure that reminds of paired, small horns we propose to name this ornament with the Latin equivalent '*cornuculum geminum*' (plural '*cornucula gemina*'). This ornament also exists in *C. boettgeri* and *C. linotum*, and we revise the description in PRÖTZEL *et al*. (2015) accordingly. The tip of a *cornuculum geminum* is also reminiscent of a hypodermic needle, and raises questions about its function, which may be to do with anchoring inside the cloaca, but further research is necessary. The fact that the *cornucula gemina* are retractable makes it even more important that conclusions from genital morphology are based on fully everted hemipenes.

The differences between clade FI and E listed in GEHRING *et al*. (2012, Table 1) concerning the presence of apical sulcal lobes and the size and position of the rotu-

lae could not be substantiated and would require further studies on a larger number of fully everted hemipenies for clarification.

Similar genital morphology also exists in the species pair *C. boettgeri* and *C. linotum* (PRÖTZEL *et al.*, 2015). However, these species differ from *C. gehringi* and *C. guibei* in having ornaments of only two pairs of rotulae, the sulcal pair enlarged, and apparently smaller cornucula gemina. Thus, in these taxa, genital morphology appears to have evolved at a slower rate than other characters, which is counter to typical expectation. According to current knowledge, both species pairs occur either allopatrically (*C. boettgeri* and *C. linotum*) or possibly parapatrically (*C. gehringi* and *C. guibei*), and their speciation may therefore have involved other selective forces than genital ornamentation.

The objective visualisation and the more detailed view of characters like hemipenes or skull structures show once again the value of X-ray micro-CT as a modern tool for integrative taxonomy. Integrating morphology, osteology, and geographic data with genetics led on the one hand to the splitting of the former species *C. guibei*, and on the other, to the lumping of two OTUs to the species *C. gehringi*. As there are still more genetic lineages within the *C. nasutum* group than currently recognised species, its resolution is far from complete, but this approach is certainly the key to unravelling its mysteries.

Acknowledgments

References

ANDREONE, F., GLAW, F., MATTIOLI, F., JESU, R., SCHIMMENTI, G., RANDRIANIRINA, J.E. & VENCES, M. (2009): The peculiar herpetofauna of some Tsaratanana rainforests and its affinities with Manongarivo and other massifs and forests of northern Madagascar. – Italian Journal of Zoology, **76**(1): 92–110.

Angel, F. (1942): Les Lézards de Madagascar. – Mémoires de l'Académie Malgache, **36**: 1–193.

Bruford, M.W., Hanotte, O., Brookfield, J.F.Y & Burke, T. (1992): Single-locus and multilocus DNA fingerprint. Pp. 225–270 in A.R. Hoelzel, ed. Molecular genetic analysis of populations: a practical approach. IRL Press, Oxford, U.K, 486 pp.

Brygoo, E.R. (1971): Reptiles Sauriens Chamaeleonidae – genre *Chamaeleo*. – Faune de Madagascar, **33**: 1–318.

Darriba, D., Taboada, G.L., Doallo, R. & Posada, D. (2012): jModelTest 2: more models, new heuristics and parallel computing. – Nature Methods, **9**: 772.

Eckhardt, F.S., Gehring, P.-S., Bartel, L., Bellmann, J., Beuker, J., Hahne, D., Korte, J., Knittel, V., Mensch, M., Nagel, D., Pohl, M., Rostosky, C., Vierath, V., Wilms, V., Zenk, J. & Vences, M. (2012): Assessing sexual dimorphism in a species of Malagasy chameleon (*Calumma boettgeri*) with a newly defined set of morphometric and meristic measurements. – Herpetology Notes, **5**: 335–344.

Gehring, P.-S., Ratsoavina, F.M., Vences, M. & Glaw, F. (2011): *Calumma vohibola*, a new chameleon species (Squamata: Chamaeleonidae) from the littoral forests of eastern Madagascar. – African Journal of Herpetology, **60**: 130–154.

Gehring, P.-S., Tolley, K.A., Eckhardt, F.S., Townsend, T.M., Ziegler, T., Ratsoavina, F., Glaw, F. & Vences, M. (2012): Hiding deep in the trees: discovery of divergent mitochondrial lineages in Malagasy chameleons of the *Calumma nasutum* group. – Ecology and Evolution, **2**: 1468–1479.

Glaw, F. (2015): Taxonomic checklist of chameleons (Squamata: Chamaeleonidae). – Vertebrate Zoology, **65**(2): 167–246.

Glaw, F. & Vences, M. (2007): A field guide to the amphibians and reptiles of Madagascar. – Vences and Glaw Verlag, Cologne, 496 pp.

Hillenius, D. (1959): The differentiation within the genus *Chamaeleo* Laurenti, 1768. – Beaufortia, **8**(89): 1–92.

Hillenius, D. (1963): Notes on chameleons I. Comparative cytology: Aid and new complications in chameleon-taxonomy. – Beaufortia, **9**(108): 201–218.

Hughes, D.F., Kusamba, C., Behangana, M. & Greenbaum, E. (2017): Integrative taxonomy of the Central African forest chameleon, *Kinyongia adolfifriderici* (Sauria: Chamaeleonidae), reveals underestimated species diversity in the Albertine Rift. – Zoological Journal of the Linnean Society, **zlx005**: 1–39.

Klaver, C.J.J. & Böhme, W. (1986): Phylogeny and classification of the Chamaeleonidae (Sauria) with special reference to hemipenis morphology. – Bonner Zoologische Monographien, **22**: 1–64.

Kumar, S., Stecher, G. & Tamura, K. (2016): MEGA7: Molecular Evolutionary Genetics Analysis Version 7.0 for bigger datasets. – Molecular Biology and Evolution, **33**(7): 1870–1874.

Macey, J.R., Larson, A., Ananjeva, N.B., Fang, Z. & Papenfuss, T.J. (1997): Two novel gene orders and the role of light-strand replication in rearrangement of the vertebrate mitochondrial genome. – Molecular Biology and Evolution, **14**: 91–104.

Macey, J.R., Schulte II, J.A., Larson, A., Ananjeva, N.B., Wang, Y., Pethiyagoda, R., Rastegar-Pouyani, N. & Papenfuss, T.J. (2000): Evaluating trans-Tethys migration: an example using acrodont lizard phylogenetics. – Systematic Biology, **49**: 233–256.

Menegon, M., Loader, S.P., Davenport, T.R., Howell, K.M., Tilbury, C.R., Machaga, S. & Tolley, K.A. (2015): A new species of chameleon (Sauria: Chamaeleonidae: *Kinyongia*) highlights the biological affinities between the Southern Highlands and Eastern Arc Mountains of Tanzania. – Acta Herpetologica, **10**(2): 111–120.

Moazen, M., Curtis, N., O'Higgins, P., Jones, M.E., Evans, S.E. & Fagan, M.J. (2009): Assessment of the role of sutures in a lizard skull: a computer modelling study. – Proceedings of the Royal Society of London B: Biological Sciences, **276**(1654): 39–46.

Nagy, Z.T., Sonet, G., Glaw, F. & Vences, M. (2012): First large-scale DNA barcoding assessment of reptiles in the biodiversity hotspot of Madagascar, based on newly designed COI primers. – PLoS ONE, **7**(3): e34506.

Prötzel, D., Ruthensteiner, B., Scherz, M.D. & Glaw, F. (2015): Systematic revision of the Malagasy chameleons *Calumma boettgeri* and *C. linotum* (Squamata: Chamaeleonidae). – Zootaxa, **4048**(2): 211–231.

Prötzel, D., Ruthensteiner, B. & Glaw, F. (2016): No longer single! Description of female *Calumma vatosoa* (Squamata, Chamaeleonidae) including a review of the species and its systematic position. – Zoosystematics and Evolution, **92**(1): 13–21.

Rabearivony, J., Rasamoelina, M., Raveloson, J., Rakotomanana, H.V., Raselimanana, A.P., Raminosoa, N.R. & Zaonarivelo, J.R. (2015): Roles of a forest corridor between Marojejy, Anjanaharibe-Sud and Tsaratanana protected areas, northern Madagascar, in maintaining endemic and threatened Malagasy taxa. – Madagascar Conservation & Development, **10**(2): 85–92.

Raxworthy, C.J. & Nussbaum, R.A. (1996): Montane amphibian and reptile communities in Madagascar. – Conservation Biology, **10**: 750–756.

Raxworthy, C.J., Pearson, R.G., Rabibisoa, N., Rakotondrazafy, A.M., Ramanamanjato, J.B., Raselimanana, A.P. & Stone, D.A. (2008): Extinction vulnerability of tropical montane endemism from warming and upslope displacement: a preliminary appraisal for the highest massif in Madagascar. – Global Change Biology, **14**(8): 1703–1720.

Rieppel, O. & Crumly, C. (1997): Paedomorphosis and skull structure in Malagasy chameleons (Reptilia: Chamaeleonidae). – Journal of Zoology, **243**(2): 351–380.

Tilbury, C.T. (2014): Overview of the systematics of the Chamaeleonidae. In: Tolley, K.A. & Herrel, A. (Eds.), The Biology of Chameleons. – University of California Press, Berkeley, pp. 151–174.

Tolley, K.A., Townsend, T.M. & Vences, M. (2013): Large-scale phylogeny of chameleons suggests African origins and Eocene diversification. – Proceedings of the Royal Society **280**(1759): 20130184.

Electronic Supplement Files
at http://www.senckenberg.de/vertebrate-zoology

File 1: Suppl. Fig. 1_skull_C_guibei_ht_MNHN 50.354.avi
File 2: Suppl. Fig. 2_skull_adult_C_guibei_ZSM_2855_2010.avi
File 3: Suppl. Fig. 3_skull_C_gehringi_ht_ZSM_2851_2010.avi
File 4: Suppl. Fig. 4_hemipenis_C_gehringi_ZSM_2842_2010.avi

3.1.3 PAPER: Endangered beauties: micro-CT cranial osteology, molecular genetics and external morphology reveal three new species of chameleons in the *Calumma boettgeri* complex (Squamata: Chamaeleonidae)

The exact definition and redescription of the species of the *Calumma boettgeri* complex in chapters 3.1.1 and 3.1.2 created the basis for the description of additional new species. These were found on recent expeditions to Madagascar in 2012 and 2015 or were already known as genetic lineages in Gehring *et al.* (2012). The descriptions of these three species followed the proven integrative approach described previously, involving dice-CT scans of hemipenes and micro-CT scans of the skulls (see supplementary materials). One of the described species, *C. lefona*, has a large frontoparietal fenestra (FF) in the skull roof, which is also present in other *Calumma* from high elevation habitats. A dice-CT scan of the head shows that the fenestra is right above the cerebrum, and raises questions as to the biological function of this opening in the skull. Frontoparietal fenestrae are common among other lizards, as Lacertidae Oppel, 1811, and some Iguania Laurenti, 1768 (Evans, 2008) and are associated with a parietal eye that functions as an extraoptic photoreceptor and is visible from the outside (Eakin, 1973, Ellis-Quinn & Simony, 1991). In *Calumma,* however, the presence of a parietal eye has not been reported so far and the FF is distinctly larger than in other lizards. Further, we found six other *Calumma* species with a FF and all of them living at an elevation above 1000 m a.s.l. with a highly significant correlation of width of the FF and elevation. We discuss a possibly selective advantage in thermoregulation for montane species. The discovery of *C. juliae*, in an easy accessible habitat next to one of the main roads in Madagascar shows that even morphological distinct chameleon species still can be discovered in well-studied areas.

Post-publication comments:
- Probably due to the spectacular display colouration of the newly-described *Calumma uetzi* this publication received significant media attention (as a Research Highlight in Nature, others see CV) and is one of the papers with the most online attention within the journal:
  - altmetric score of 120 (accessed on 14.08.2018)
  - In the top 5% of all research outputs scored by Altmetric
  - Among the highest-scoring outputs from this source (#17 of 1,171)

- The newly-described *Calumma juliae* is to date only known from a small forest fragment of 15 ha, which is highly threatened by deforestation. Currently, we are trying to protect this area as a natural reserve in cooperation with Rainer Dolch of the Association Mitsinjo.

Endangered beauties: micro-CT cranial osteology, molecular genetics and external morphology reveal three new species of chameleons in the *Calumma boettgeri* complex (Squamata: Chamaeleonidae)

DAVID PRÖTZEL[1]*, MIGUEL VENCES[2], OLIVER HAWLITSCHEK[1],
MARK D. SCHERZ[1,2], FANOMEZANA M. RATSOAVINA[3] AND FRANK GLAW[1]

[1]*Zoologische Staatssammlung München (ZSM-SNSB), Münchhausenstraße 21, 81247 München, Germany*
[2]*Zoological Institute, Technical University of Braunschweig, Mendelssohnstraße 4, 38106 Braunschweig, Germany*
[3]*Mention Zoologie et Biodiversité Animale, Département Biologie, Université d'Antananarivo, BP 906, Antananarivo, 101 Madagascar*

Based on recent discoveries and an integrative study including external morphology, osteology and molecular genetics, we continue to revise the Madagascar-endemic chameleons of the *Calumma boettgeri* complex (within the *Calumma nasutum* species group). We describe three new species of these small-sized, occipital-lobed chameleons. ***Calumma uetzi* sp. nov.** is a species from the Sorata and Marojejy massifs (northern Madagascar), with a spectacular display coloration in males, clearly notched occipital lobes, and females with a dorsal crest. ***Calumma lefona* sp. nov.** is described based on a male specimen from Tsaratanana (northern Madagascar), with widely notched occipital lobes, a long and pointed rostral appendage, a dorsal crest, and a frontoparietal fenestra in the skull roof. This last character also occurs in six other *Calumma* species, and its presence and width are correlated with the elevational distribution of the species. ***Calumma juliae* sp. nov.** is known only from a small, isolated forest fragment near Moramanga in eastern Madagascar, and only females have been found so far. It is a relatively large member of the *C. nasutum* group, with a distinct dorsal crest and numerous infralabial scales. Two of the new species are known exclusively from their type localities, and we recommend protection of the habitats of all three as soon as possible.

ADDITONAL KEYWORDS: *Calumma nasutum* species group – conservation – frontoparietal fenestra – hemipenis morphology – Madagascar.

INTRODUCTION

Madagascar is famous for its biodiversity, especially that of reptiles and amphibians. Research on the herpetofauna of the island began in the 18th century and has intensified strongly in the past 25 years (Andriamialisoa & Langrand, 2003; Glaw & Vences, 2007). Chameleons have particularly attracted the attention of biologists, and 87 endemic species (Glaw, 2015; Prötzel *et al.*, 2017) have been described so far

from the island, starting with the three impressive species *Calumma parsonii* (Cuvier, 1824), *Furcifer pardalis* (Cuvier, 1829) and *Furcifer verrucosus* (Cuvier, 1829). Almost 200 years later, saturation of species numbers in the family Chamaeleonidae is not yet in sight. Within the Madagascar-endemic genus *Calumma*, 11 (32%) of the currently recognized 34 species have been described during the last two decades (Andreone *et al.*, 2001; Raxworthy & Nussbaum, 2006; Gehring *et al.*, 2010, 2011; Prötzel *et al.*, 2017), and numerous additional deep genetic lineages of unclarified status have been identified (Boumans *et al.*, 2007; Nagy *et al.*, 2012; Gehring *et al.*, 2012; Tolley, Townsend & Vences, 2013).

*Corresponding author. E-mail: david.proetzel@mail.de

The phenetic *Calumma nasutum* group comprises small species, usually with a soft dermal appendage on the snout tip (Prötzel, Ruthensteiner & Glaw, 2016); four species in the group, *Calumma boettgeri* (Boulenger, 1888), *Calumma gehringi* (Prötzel *et al.*, 2017), *Calumma guibei* (Hillenius, 1959), and *Calumma linotum* (Müller, 1924), differ from the others by the possession of well-defined occipital lobes and are referred to as the *C. boettgeri* complex (Gehring *et al.*, 2012). Although neither the *C. nasutum* group nor the *C. boettgeri* complex was recovered as monophyletic in the multigene phylogeny of Tolley *et al.* (2013), these two phenetic clusters are easily defined by a unique combination of morphological traits. More in-depth studies with a large number of markers will be necessary to clarify the convoluted phylogeny of *Calumma* fully, but the current phenetic species groups and complexes continue to be useful units for taxonomic comparison, and we therefore restrict the present study to the *Calumma* species with a soft dermal snout appendage and occipital lobes, i.e. the *C. boettgeri* complex.

Gehring *et al.* (2012) proposed a total of 33 operational taxonomic units (OTUs) within the *C. nasutum* species group based on a comprehensive molecular study, with only nine of these corresponding to nominal species (Prötzel *et al.*, 2015, 2017). The morphologically cryptic species/OTUs within the *C. nasutum* group require an integrative approach to evaluate their taxonomic status, comparable to the recently unravelled *Kinyongia adolfifriderici* complex (Hughes *et al.*, 2017). Combining genetic data with data from osteology, external and genital morphology, OTUs 8 and 9 of Gehring *et al.* (2012) have been attributed to *C. linotum* (Prötzel *et al.*, 2015). Furthermore, *C. linotum sensu* Gehring *et al.* (2012) and OTU 10 have been lumped into one new species (Prötzel *et al.*, 2017), but all other OTUs still await a taxonomic assignment.

Based on the analysis of mitochondrial DNA sequences, Gehring *et al.* (2012) distinguished a number of main clades (A–K) in the *C. nasutum* group, of which some were further divided into subclades. Of these, the clades D–F comprise species of the *C. boettgeri* complex; *C. boettgeri* (clade DI), *C. linotum* (DII/DIII), *C. gehringi* (EI/EII), and *C. guibei* (clade FI). Clade FII is represented by a single male specimen from Andrevorevo (Antsiranana Province, northern Madagascar) that was already declared as a confirmed candidate species (CCS) by Gehring *et al.* (2012) owing to genetic and morphological differentiation. The genetic divergence of sequences (uncorrected pairwise distances; p-distances) of the mitochondrial *ND2* gene between FII and its sister species (FI; *C. guibei*) amounts to 7.6%, there is no haplotype sharing among them in the nuclear *CMOS* gene, and differences in

external and genital morphology have been identified (Gehring *et al.*, 2012).

Supplemented by further morphological and osteological data obtained by micro-computed tomography (micro-CT), in the present study we describe this OTU as a new species. We also describe two additional new species of the *C. boettgeri* complex on the basis of morphological, osteological, and molecular data sets. Both these species were discovered since the publication of Gehring *et al.* (2012) during recent expeditions: one species from the Sorata Massif (Antsiranana Province, northern Madagascar, in 2012), with a spectacular display coloration, and another species, surprisingly, collected near Moramanga (Toamasina Province, eastern Madagascar, in 2015 and 2016), an easily accessible and well-studied area located several hundred kilometres south of all hitherto known localities of the *C. boettgeri* complex.

MATERIAL AND METHODS

TAXON SAMPLING

We studied 11 specimens of the putative new species and 60 specimens of the *Calumma nasutum* group (Table 1) from the collections of the Zoologische Staatssammlung München, Germany (ZSM), the Université d'Antananarivo, Mention Zoologie et Biodiversité Animale, Département Biologie, Madagascar (UADBA), the Muséum National d'Histoire Naturelle de Paris, France (MNHN), and the Museo Regionale di Scienze Naturali, Torino, Italy (MRSN). Specimens of the new taxa described herein were collected in the field by surveying at night. They were fixed in 90% ethanol and transferred to 70% ethanol for long-term storage. Field numbers of preserved specimens and tissue samples refer to the collections of Angelica Crottini (ACZC), Frank Glaw and Miguel Vences (FGMV, FGZC and ZCMV), Mark D. Scherz (MSZC) and David R. Vieites (DRV).

EXTERNAL MORPHOLOGY

The morphological measurements taken from these specimens generally follow Eckhardt *et al.* (2012), Gehring *et al.* (2012) and Prötzel *et al.* (2015). The following characters (see also Table 1) were measured with digital callipers to the nearest 0.1 mm, counted using a binocular dissecting microscope, evaluated by eye or calculated; the data set contains 10 continuous, eight meristic and four qualitative/other characters (excluding the particular ratios): snout–vent length (SVL) from the snout tip (not including the rostral appendage) to the cloaca; tail length (TaL) from the cloaca to the tail tip; total length (TL) as a sum of SVL

Table 1. Morphological measurements of the *Calumma boettgeri* complex

Species	Sex	Collection no.	Field no.	Type status	Elevation (m)	SVL	TaL	TL	RTaSV	LRA	RRASV	DRA	RDRSV	NDRA	NSRA	RNLRA	RC
C. lefona **sp. nov.**	m	ZSM 2849/2010	DRV 6287	HT	1717	51.3	62.4	113.7	1.22	5.6	0.11	2.0	0.04	8	60	10.7	+
C. uetzi **sp. nov.**	m	ZSM 1688/2012	FGZC 3627	HT	1100	45.7	55.5	101.2	1.21	3.8	0.08	2.0	0.04	5	28	7.4	+
C. uetzi **sp. nov.**	jm	ZSM 1686/2012	FGZC 3674	PT	1396	37.3	44.0	81.3	1.18	3.9	0.10	1.8	0.05	5	19	4.9	+
C. uetzi **sp. nov.**	f	ZSM 1687/2012	FGZC 3640	PT	1516	42.0	45.3	87.3	1.08	3.1	0.07	1.6	0.04	5			+
C. uetzi **sp. nov.**	jf	ZSM 1685/2012	FGZC 3593	PT	1417	33.7	39.6	73.3	1.18	3.3	0.10	1.8	0.05	5			+
C. juliae **sp. nov.**	f	ZSM 143/2016	FGZC 5235	HT	950	55.8	55.4	111.2	0.99	2.7	0.05	2.2	0.04	6	21	7.8	+
C. juliae **sp. nov.**	f	ZSM 142/2016	FGZC 5233	PT	950	59.4	52.2	111.6	0.88	2.6	0.04	2.2	0.04	6	23	8.8	+
C. juliae **sp. nov.**	f	UADBA-R	FGZC 5232	PT	950	53.5	51.8	105.3	0.97	2.6	0.05						+
C. juliae **sp. nov.**	f	UADBA-R	FGZC 5234	PT	950	53.3	52.3	105.6	0.98	2.4	0.05						+
C. juliae **sp. nov.**	f	ZSM 254/2016	FGZC 5274	PT	950	58.4	52.6	111.0	0.90	2.3	0.04	2.1	0.04	5	22	9.6	+
C. juliae **sp. nov.**	j	ZSM 255/2016	FGZC 5275	PT	950	36.4	35.1	71.5	0.96	1.8	0.05	1.7	0.05	4			
C. boettgeri	m	Min–max:	N = 13		0–751	41.1–54.6	44.0–55.7	85.4–110.3	0.9–1.01	2.5–4.1	0.05–0.10	1.8–3.0	0.04–0.06	5–8			+
		Mean:				49.2	51.5	100.6	0.96	3.2	0.07	2.3	0.05	6.8			
		SD:				4.0	4.0	7.7	0.04	0.5	0.01	0.4	0.01	0.9			
C. boettgeri	f	Min–max:	N = 15		0–751	42.0–55.5	41.8–52.8	83.8–108.0	0.92–1.07	1.2–4.1	0.02–0.08	1.3–2.3	0.02–0.05	5–7			+
		Mean:				48.7	47.3	96.0	1.03	2.9	0.06	1.9	0.04	6.1			
		SD:				3.2	3.1	6.0	0.04	0.7	0.01	0.3	0.01	0.8			
C. gehringi	m	Min–max:	N = 9		1207–1538	49.3–53.7	55.4–68.2	105.5–121.5	1.09–1.28	3.1–5.4	0.06–0.11	2.2–3.5	0.04–0.07	5–8	20–42	6.5–9.4	+
		Mean:				51.9	60.3	112.1	1.16	4.0	0.08	2.7	0.05	5.8	30.0	7.6	
		SD:				1.5	4.0	5.0	0.06	0.9	0.02	0.5	0.01	1.0	7.6	8.5	
C. gehringi	f	Min–max:	N = 7		1207–1538	47.5–52.3	45.1–52.2	92.6–104.2	0.89–1.06	3.2–4.4	0.07–0.08	2.0–2.8	0.04–0.05	5–6			+
		Mean:				50.3	49.1	99.5	0.98	3.6	0.07	2.2	0.04	5.4			
		SD:				2.2	2.9	4.2	0.05	0.4	0.01	0.3	0.01	0.5			
C. guibei	m	Min–max:	N = 3		1589–2021	51.7–53.7	60.2–62.8	111.9–115.8	1.16–1.18	4.0–4.5	0.07–0.08	1.8–2.3	0.03–0.04	5–6	26–31	6.5–7.3	(+)
		Mean:				52.8	61.7	114.5	1.17	4.2	0.08	2.1	0.04	5.7	28.7	6.9	
		SD:				1.0	1.3	2.3	0.01	0.3	0.01	0.3	0.01	0.6	2.5	8.7	
C. guibei	f	min–max:	N = 2		1589–2021	48.1–49.1	45.5–49.6	93.6–98.7	0.95–1.01	1.7–2.0	0.04–0.04	1.5–2.0	0.03–0.04	4–5			(+)
		Mean:				48.6	47.6	96.2	0.98	1.9	0.04	1.8	0.04	4.5			
		SD:				0.7	2.9	3.6	0.05	0.2	0.00	0.4	0.01	0.7			
C. linotum	m	Min–max:	N = 8		730–1306	52.4–59.6	37.9–70.0	109.3–126.1	0.80–0.96	2.5–4.7	0.07–0.09	2.3–3.2	0.04–0.06	4–7	19–27	6.3–9.5	+
		Mean:				52.9	58.9	117.4	0.9	4.2	0.08	2.7	0.05	5.9	24.0	8.2	
		SD:				6.6	9.5	6.9	0.1	0.7	0.01	0.3	0.01	1.1	4.4	1.7	
C. linotum	f	Min–max:	N = 3		730–1306	42.7–54.5	47.4–54.9	90.1–109.4	0.90–1.00	2.0–4.1	0.04–0.08	1.9–2.3	0.04–0.04	4–6			+
		Mean:				49.3	51.0	100.3	1.0	3.1	0.06	2.1	0.04	5.0			
		SD:				6.0	3.8	9.7	0.1	1.1	0.02	0.2	0.00	1.0			

Table 1. *Continued*

Species	Sex	Collection no.	LC	TCL	TCR	PC	OL	OLND	RODSV	OLD	RODSV	OLW	ROWSV	DSOL	DSCT	DC	DSA	NSA	NSL	NIL
C. lefona **sp. nov.**	m	ZSM 2849/2010	+	2	2	+	s	1.8	0.04	4.8	0.09	2.9	0.06	0.6	0.6	23	0.5	21	11	12
C. uetzi **sp. nov.**	m	ZSM 1688/2012	+	2	2	(+)	c	1.0	0.02	3.8	0.08	2.3	0.05	0.6	1.0	13	0.5	15	11	12
C. uetzi **sp. nov.**	jm	ZSM 1686/2012	+	1	1	+	c	0.5	0.01	3.9	0.10	2.3	0.06	0.8	1.1	14	0.4	15	11	12
C. uetzi **sp. nov.**	f	ZSM 1687/2012	+	1	1	+	c	0.6	0.01	4.4	0.10	2.3	0.05	0.7	1.3	5	0.5	18	12	12
C. uetzi **sp. nov.**	jf	ZSM 1685/2012	+	2	2	+	c	0.2	0.01	4.0	0.12	2.1	0.06	0.7	1.0	3	0.3	18	10	11
C. juliae **sp. nov.**	f	ZSM 143/2016	+	—	—	—	c	0.5	0.01	4.6	0.08	3.2	0.06	0.8	1.3	12	0.7	17	13	14
C. juliae **sp. nov.**	f	ZSM 142/2016	+	—	—	—	c	0.2	0.00	3.9	0.07	3.5	0.06	0.7	1.1	14	0.7	19	15	15
C. juliae **sp. nov.**	f	UADBA-R	+	—	—	—		0.8	0.01	4.4	0.08				1.3	12			14	14
C. juliae **sp. nov.**	f	UADBA-R	+	—	—	—		0.6	0.01	4.3	0.08				1.2	12			14	15
C. juliae **sp. nov.**	f	ZSM 254/2016	+	—	—	—	c	0.6	0.01	3.9	0.07	3.6	0.06	0.8	1.4	11	0.8	17	14	15
C. juliae **sp. nov.**	j	ZSM 255/2016	+	—	—	—	c	0.2	0.01	3.3	0.09	2.8	0.08	0.7	1.0	9	0.5	13	15	15
C. boettgeri	m	min–max:	+	—	—	—	c	0–0.6	0–0.01	3.0–4.8	0.06–0.1	2.0–3.4	0.04–0.07	0.5–0.8	0.9–1.3	0–28	0.2–0.5	7–14	11–16	11–15
		mean:						0.3	0.01	3.8	0.08	2.8	0.06	0.6	1.1	11.1	0.4	9.8	12.5	12.2
		SD:						0.2	0.00	0.6	0.01	0.4	0.01	0.1	0.1	9.1	0.1	1.9	1.2	1.2
C. boettgeri	f	min–max:	+	—	—	—	c	0–0.7	0–0.01	2.7–4.6	0.05–0.09	2.3–3.2	0.04–0.07	0.5–0.9	0.7–1.2	0–11	0.2–0.4	8–14	11–17	6.1–14
		mean:						0.3	0.01	3.4	0.07	2.8	0.06	0.6	0.9	0.9	0.3	10.2	12.7	11.6
		SD:						0.2	0.00	0.6	0.01	0.3	0.01	0.1	0.2	2.9	0.0	1.7	1.7	1.9
C. gehringi	m	min–max:	+	0–2	0–1	—	c	0.5–1.5	0.01–0.03	5.1–6.1	0.1–0.12	2.8–3.5	0.05–0.07	0.8–1.3	0.7–1.1	7–15	0.5–0.9	12–20	11–13	12–14
		mean:		1.2	1			1.2	0.02	5.7	0.11	3.1	0.06	1.0	0.9	10.5	0.7	15.3	11.9	13.0
		SD:		0.4	0			0.4	0.01	0.3	0.01	0.3	0.01	0.2	0.1	3.1	0.2	2.4	0.6	0.8
C. gehringi	f	min–max:	+	0–1	0–1	—	c	0.5–1.4	0.01–0.03	4.8–5.5	0.1–0.11	2.2–3.1	0.05–0.06	0.6–1.1	0.7–1.0	0	0.5–0.6	14–23	10–13	11–14
		mean:		0.8	0.8			1.1	0.02	5.2	0.10	2.7	0.05	0.8	0.9		0.6	17.3	11.6	11.6
		SD:		0.5	0.5			0.4	0.01	0.2	0.00	0.3	0.01	0.2	0.1		0.0	2.9	1.0	1.1
C. guibei	m	min–max:	+	—	—	(+)	s	1.2–1.5	0.02–0.03	4.1–4.9	0.08–0.09	2.0–2.5	0.04–0.05	0.8–1.0	0.8–1.1	0	0.5–0.7	16–22	11–12	11–13
		mean:						1.4	0.03	4.5	0.08	2.2	0.04	0.9	0.9		0.6	19.3	11.7	12.3
		SD:						0.2	0.00	0.4	0.01	0.3	0.01	0.1	0.2		0.1	3.1	0.6	1.2
C. guibei	f	min–max:	+	—	—	+	s	1.5–1.9	0.03–0.04	5.1–5.4	0.11–0.11	2.6–2.6	0.05–0.05	0.9–1.0	0.7–1.0	0	0.5–0.5	17–19	11–11	11–12
		mean:						1.7	0.03	5.3	0.11	2.6	0.05	1.0	0.9		0.5	18.0	11.0	11.5
		SD:						0.3	0.01	0.2	0.00	0.0	0.00	0.1	0.2		0.0	1.4	0.0	0.7
C. linotum	m	min–max:	+	1	1	+	c	0–0.3	0–0.01	2.84–4.77	0.07–0.09	3–4.3	0.05–0.08	0.7–1	1–1.4	0–13	0.4–0.8	18–23	12–14	12–14
		mean:						0.1	0.00	4.2	0.079	3.6	0.06	0.8	1.2	6.8	0.7	20.4	12.7	12.8
		SD:						0.1	0.00	0.6	0.009	0.4	0.01	0.1	0.2	4.8	0.1	1.7	0.8	0.9
C. linotum	f	min–max:	+	1	1	+	c	0–0.2	0–0	3.94–5.11	0.07–0.1	3.3–3.8	0.06–0.09	0.6–1.1	0.9–1.4	0–6	0.5–0.6	16–22	12–13	12–13
		mean:						0.1	0.00	4.4	0.089	3.6	0.07	0.8	1.2	3.0	0.6	18.3	12.7	12.7
		SD:						0.1	0.00	0.6	0.014	0.3	0.01	0.3	0.3	4.2	0.0	3.2	0.8	0.6

Detailed information is provided for the three new species; ranges and mean values for the remaining four species.
F, female; j, juvenile; HT, holotype; m, male; PT, paratype; all measurements are in millimetres; further abbreviations see Material and Methods.

+ TaL; ratio of TaL and SVL (RTaSV); length of the rostral appendage (LRA) from the upper snout tip; ratio of LRA and SVL (RRASV); diameter of rostral appendage (DRA), measured dorsoventrally at the widest point; ratio of DRA and SVL (RDRSV); number of scales across DRA (NDRA); number of tubercle scales (diameter > 0.3 mm) on rostral appendage, counted on the right side (NSRA); ratio of NSRA and LRA (RNLRA); distinct rostral crest (RC) presence (+) or absence (−); lateral crest (LC), running from the posterior of the eye horizontally, presence (+) or absence (−); temporal crest, running dorsally to the LC, curving toward the midline, absence (−) or number of tubercles on left side (TCL) and right side (TCR); parietal crest (PC) presence (+) or absence (−); occipital lobes (OL) completely separated (s) or still, at least slightly, connected (c); depth of the dorsal notch in the occipital lobes (OLND); ratio of OLND and SVL (RODSV); lateral diameter of OL (OLD); ratio of OLD and SVL (RODSV); width of OL measured at the broadest point (OLW); ratio of OLW and SVL (ROWSV); diameter of largest scale on OL (DSOL); diameter of largest scale on temporal region (DSCT), measured on the right side; dorsal crest (DC) absence (−) or number of dorsal cones visible to the naked eye without the use of a binocular microscope according to Eckhardt *et al.* (2012); diameter of broadest scale on the lower arm (DSA), defined as the area from the elbow to the manus in lateral view on the right side; number of scales on lower arm in a line from elbow to manus (NSA); number of supralabial scales (NSL), counted from the first scale next to the rostral to the last scale that borders directly and entirely (with one complete side) to the mouth slit of the upper jaw on the right side; and number of infralabial scales (NIL), analogous to the definition of NSL above, on the right side.

Morphological data of the three new species were compared with data of the other species of the *C. boettgeri* complex from Prötzel *et al.* (2015, 2016, 2017). The following measurements were added to the data from 2015: DRA, NDRA, NRS, LC, TCL, TCR, OLW, OL, DSOL and DSCT, including the corresponding ratios (note that some abbreviations might have changed). The following measurement was added to the data of Prötzel *et al.* (2017): NRS. The morphological data were used only for the species diagnoses and descriptions and not analysed further. For the 'diagnosis' in the species descriptions, only adult specimens were considered.

MICRO-COMPUTED TOMOGRAPHY

For internal morphology, micro-CT scans of the head were prepared for the following: a male specimen, ZSM 2849/2010, from Andrevorevo (northern Madagascar);

the two males, ZSM 1688/2012 and ZSM 1686/2012, from Sorata; and two females, ZSM 143/2016 and ZSM 254/2016, from Moramanga (eastern Madagascar). To investigate the frontoparietal fenestra, additional scans were made of *Calumna* cf. *fallax* (Mocquard, 1900), ZSM 693/2003, male; *Calumna gallus* (Günther, 1877), ZSM 691/2009, female; *C.* cf. *nasutum* (Duméril & Bibron, 1836), ZSM 134/2005, male; ZSM 35/2016, male; ZSM 618/2009, male; ZSM 735/2003, female; ZSM 619/2009, male; ZSM 663/2014, male; ZSM 441/2005, male; ZSM 135/2005, female; ZSM 136/2005, female; ZSM 924/2003, male; ZSM 553/2001, female; ZSM 661/2014, female; ZSM 662/2014, female; *Calumna vatosoa* (Andreone *et al.*, 2001), MRSN R1628, male; and *Calumna vohibola*, ZSM 645/2009, male. Previous scans of 12 specimens of *C. boettgeri*, *C. gehringi*, *C. guibei*, and *C. linotum* produced for Prötzel *et al.* (2015, 2017) were included in the analysis. In total, the present study is based on 36 micro-CT scans of 14 (candidate) species.

For micro-CT scanning, specimens were placed in a closed plastic vessel slightly larger than the specimen, with the head oriented upwards, and stabilized with ethanol-soaked paper. To avoid scanning artefacts, it was ensured that the paper did not cover the head region. Micro-CT scanning was performed with a phoenix|x nanotom m (GE Measurement & Control, Wunstorf, Germany) using a tungsten or diamond target at a voltage of 130 kV and a current of 80 µA for 29 min (1800 projections of 1000 ms). Three-dimensional data sets were processed with VG Studio Max 2.2 (Visual Graphics GmbH, Heidelberg, Germany); the data were visualized using the Phong volume renderer to show the surface of the skull and reflect a variety of different levels of X-ray absorption. The osteological terminology follows Rieppel & Crumly (1997). The following skull characters were measured in VG Studio Max 2.2 using the calliper tool (Table 2): nasal length (NaL); frontal width measured at prefrontal border (FWPf); frontal width measured at anterior border to postorbitofrontal (FWPo); frontal width measured at frontal–parietal border (FWPa); parietal width measured at posterior border to postorbitofrontal (PWPo); parietal width at midpoint (PWm); parietal length (PL); frontal length (FL); width of the frontoparietal fenestra (FFW); snout–casque length, measured from tip of upper jaw to posterior end of parietal (SCL); and skull length, measured from tip of upper jaw to skull capsule (SkL). The respective ratios to SkL are indicated with an 'R' in front of the character abbreviations. Statistical analysis of the presence, width and elevation of the fenestra was done using the statistical analysis software PAST 3.08 (Hammer, Harper & Ryan, 2001).

Table 2. Osteological measurements of the *Calumma boettgeri* complex

Species	Collection no.	Sex	NaL	RNaL (%)	FWPf	RFWPf (%)	FWPo	RFWPo (%)	FWPa	RFWPa (%)	PWPo	RPWPo (%)	PWm	RPWm (%)	PL	RPL (%)	FL	RFL (%)	FFW	RFFD	SCL	RSCL	SkL
C. lefona sp. nov.	ZSM 2849/2010	m	2.1	16.0	2.9	22.1	4.0	30.5	4.0	30.5	3.9	29.8	2.4	18.3	5.2	39.7	5.4	41.2	1.9	14.7	15.9	121.4	13.1
C. uetzi sp. nov.	ZSM 1688/2012	m	1.0	9.2	2.8	25.7	4.3	39.4	3.8	34.9	4.2	38.5	2.7	24.8	4.7	43.1	5.9	54.1	0.0	—	12.9	118.3	10.9
C. uetzi sp. nov.	ZSM 1686/2012	jm	1.1	10.6	2.1	20.2	3.7	35.6	3.6	34.6	3.8	36.5	2.1	20.2	4.2	40.4	5.5	52.9	0.0	—	12.7	122.1	10.4
C. juliae sp. nov.	ZSM 143/2016	f	1.9	14.4	2.4	18.2	4.1	31.1	3.3	25.0	3.9	29.5	0.8	6.1	6.0	45.5	6.6	50.0	0.0	—	16.1	122.0	13.2
C. juliae sp. nov.	ZSM 254/2016	f	1.5	10.9	2.3	16.8	4.2	30.7	3.6	26.3	3.9	28.5	0.8	5.8	5.8	42.3	6.0	43.8	0.0	—	16.9	123.4	13.7
C. boettgeri	ZSM 440/2000	m	1.7	13.2	3.0	23.3	4.5	34.9	4.2	32.6	4.6	35.7	0.8	6.2	6.6	51.2	7.1	55.0	0	—	16.4	127.1	12.9
C. boettgeri	ZSM 444/2000	m	2.3	18.3	3.1	24.6	4.4	34.9	4.4	34.9	4.5	35.7	0.6	4.8	7.2	57.1	6.7	53.2	0	—	16.4	130.2	12.6
C. boettgeri	ZSM 227/2002	(f)	1.7	14.7	2.7	23.3	2.9	25.0	3.9	33.6	4.2	36.2	0.9	7.8	5.5	47.4	6.8	58.6	0	—	14.5	125.0	11.6
C. boettgeri	ZSM 441/2001	f	2.1	18.6	1.9	16.8	3.9	34.5	3.7	32.7	4.0	35.4	0.6	5.3	5.7	50.4	6.3	55.8	0	—	14.9	131.9	11.3
C. gehringi	ZSM 2842/2010	m	1.8	14.9	2.9	24.0	4.4	36.4	3.5	28.9	3.8	31.4	1.2	9.9	5.9	48.8	6.4	52.9	0.7	5.8	15.8	130.6	12.1
C. gehringi	ZSM 2840/2010	m	1.9	15.7	3.9	32.2	4.8	39.7	4.1	33.9	4.4	36.4	1.5	12.4	5.8	47.9	6.7	55.4	1.1	9.1	16.1	133.1	12.1
C. guibei	ZSM 2855/2010	m	1.8	14.5	2.6	21.0	4.4	35.5	4.1	33.1	4.2	33.9	1.9	15.3	4.7	37.9	4.6	37.1	2.6	21.0	15.1	121.8	12.4
C. linotum	ZSM 21/1923	m	2.7	19.1	3.7	26.2	5.1	36.2	4.3	30.5	4.5	31.9	1.8	12.8	4.9	34.8	8.0	56.7	0	—	16.5	117.0	14.1
C. linotum	ZSM 2073/2007	m	2.2	16.4	3.2	23.9	4.8	35.8	4.3	32.1	4.5	33.6	0.6	4.5	6.1	45.5	7.3	54.5	0	—	16.7	124.6	13.4
C. linotum	ZSM 2072/2007	m	2.4	19.4	3.4	27.4	5.0	40.3	4.3	34.7	4.5	36.3	1.5	12.1	6.0	48.4	7.1	57.3	0	—	16.4	132.3	12.4
C. linotum	ZSM 551/2001	f	1.5	11.5	2.9	22.1	4.5	34.4	4.4	33.6	4.6	35.1	1.1	8.4	4.9	37.4	6.7	51.1	0	—	14.9	113.7	13.1
C. linotum	ZSM 873/1920/2	f	2.2	17.9	3.0	24.4	4.4	35.8	4.0	32.5	4.2	34.1	0.8	6.5	5.7	46.3	6.2	50.4	0	—	15.1	122.8	12.3

All measurements are in millimetres. For abbreviations see Material and Methods.

Using diffusible iodine contrast enhanced micro-CT (diceCT; Gignac *et al.*, 2016), hemipenes of ZSM 2849/2010 from Andrevorevo and ZSM 1686/2012 from Sorata were scanned. One hemipenis was clipped off of each specimen and immersed in iodine solution (I$_2$ in 1% ethanol) for 2 days to increase X-ray absorbance. For scanning, the hemipenes were placed with their apices oriented upwards in a plastic tube, immersed in 70% ethanol. Scanning was performed for 30 min at a voltage of 60 kV and a current of 200 μA (2400 projections) using a tungsten target. The three-dimensional data were processed in VG Studio Max 2.2 as described above. Hemipenial terminology follows Klaver & Böhme (1986). Hemipenes of the remaining males were investigated using a binocular dissecting microscope.

A diceCT scan was also made for *C. gehringi* (ZSM 2840/2010) to investigate soft tissue of the head. The whole specimen was immersed in ~25% Lugol's iodine solution (I$_2$/KI in 75% ethanol) for 5 days and placed in a plastic tube for scanning (see above). Scanning was performed for 30 min at a voltage of 80 kV and a current of 240 μA (2400 projections) using a tungsten target. For an alternative scanning setting of brain tissue in chameleons, see also Hughes *et al.* (2016). In VG Studio Max 2.2, the diceCT scan was aligned and combined with an unstained micro-CT scan of the skull of the same specimen (scanned before staining) to illustrate the position of the brain in the skull.

Genetic analysis

We complemented previous molecular data on the *C. boettgeri* complex from Gehring *et al.* (2012) and Prötzel *et al.* (2017) with new sequences for specimens from Sorata, Marojejy, and Moramanga, as well as a few additional samples of *C. gehringi*. Total genomic DNA was extracted from tissue samples using proteinase K (10 mg/mL) digestion, followed by a salt extraction protocol (Bruford *et al.*, 1992). We targeted parts of the mitochondrial gene for NADH dehydrogenase subunit 2 (*ND2*) and parts of the nuclear oocyte maturation factor gene (*CMOS*). We used standard PCR protocols (Gehring *et al.*, 2012) with the primers ND2F17 (5 -TGACAAAAAAT TGCNCC-3 ; Macey *et al.*, 2000) and ALAR2 (5′-AAAATRTCTGRGTTGCATTCAG-3′; Macey *et al.*, 1997),and CO8 (5 -GCTTGGTGTTCAATAGACTGG-3) and CO9 (5 -TTGGGAGCATCCAAAGTCTC-3′; Han, Zhou & Bauer, 2004). We purified PCR products with ExoSAPIT (Thermo Fisher Scientific, Waltham, MA, USA), and sequenced these on an automated DNA sequencer (ABI 3130 XL; Applied Biosystems). The software CodonCode Aligner (CodonCode Corporation) was used to check for sequencing errors and to identify heterozygotes in nuclear DNA. All new sequences obtained in the present study were submitted to GenBank (accession numbers MG407559–MG407583); for accession numbers of previously published sequences, see Gehring *et al.* (2012) and Prötzel *et al.* (2017). We selected representative sequences of all species and intraspecific lineages of the *C. boettgeri* complex, removing most of the identical or near-identical sequences from previous studies (Gehring *et al.*, 2012; Prötzel *et al.*, 2017). Sequences were aligned manually by amino acid translation in MEGA7 (Kumar, Stecher & Tamura, 2016), and the most appropriate model of evolution under the Bayesian information criterion was determined with jModeltest 2 (Darriba *et al.*, 2012). We reconstructed a gene tree for the *ND2* gene fragment under the maximum likelihood (ML) optimality criterion in MEGA7 (Kumar, Stecher & Tamura, 2016), with a heuristic search using the subtree pruning–regrafting algorithm (SPR level 5). We calculated 2000 bootstrap replicates, as recommended by Hedges (1992) to test the robustness of nodes, and chose a sequence of *Calumma oshaughnessyi*, a distantly related congener (Tolley *et al.*, 2013), as the outgroup. We furthermore used Bayesian inference (BI) of phylogeny using MrBayes 3.2 (Ronquist *et al.*, 2012), with the same substitution model settings, to calculate the posterior probabilities of nodes. We ran two independent chains for 20 million generations each, with a sample frequency of 10 000 and a burn-in of 25%.

CMOS sequences were obtained for two of the new species described herein and compared with those of Gehring *et al.* (2012). Given that the haplotypes identified from these new species differed only by single or few substitutions from the previously defined haplotypes (no heterozygotes identified), we added them to the haplotype network of Gehring *et al.* (2012) on the basis of an ML tree calculated in MEGA7. Relationships among haplotypes were visualized in Haploviewer, following the methodological approach of Salzburger, Ewing & Von Haeseler (2011).

RESULTS

Genetic differentiation in the *C. boettgeri* complex

Our molecular analysis followed the same approach as that of Gehring *et al.* (2012) and partly of Prötzel *et al.* (2017) by analysing the mitochondrial and nuclear DNA sequences separately, as our main goal was not to reconstruct the phylogeny in the *C. boettgeri* complex but rather to ascertain concordance of differentiation in these largely independently evolving markers. We chose a model-based phylogenetic analysis to visualize variation in mitochondrial DNA (*ND2*), and a haplotype network to visualize the very limited variation in nuclear DNA (*CMOS*).

For the *ND2* gene fragment, the Bayesian information criterion in jModeltest selected the Hasegawa-Kishino-Yano model with gamma distributed rate variation among sites (HKY+G) substitution model as best fitting the data. The trees obtained by ML and BI analysis of the *ND2* alignment showed an identical topology (Fig. 1A), with *C. guibei* branching off at the basal node of the complex and supporting a sister group relationship of *C. boettgeri* and *C. linotum*. The recently described *C. gehringi* (Prötzel *et al.*, 2017) is a sister species to the clade containing *C. boettgeri* and *C. linotum*, but with low support, and contains several
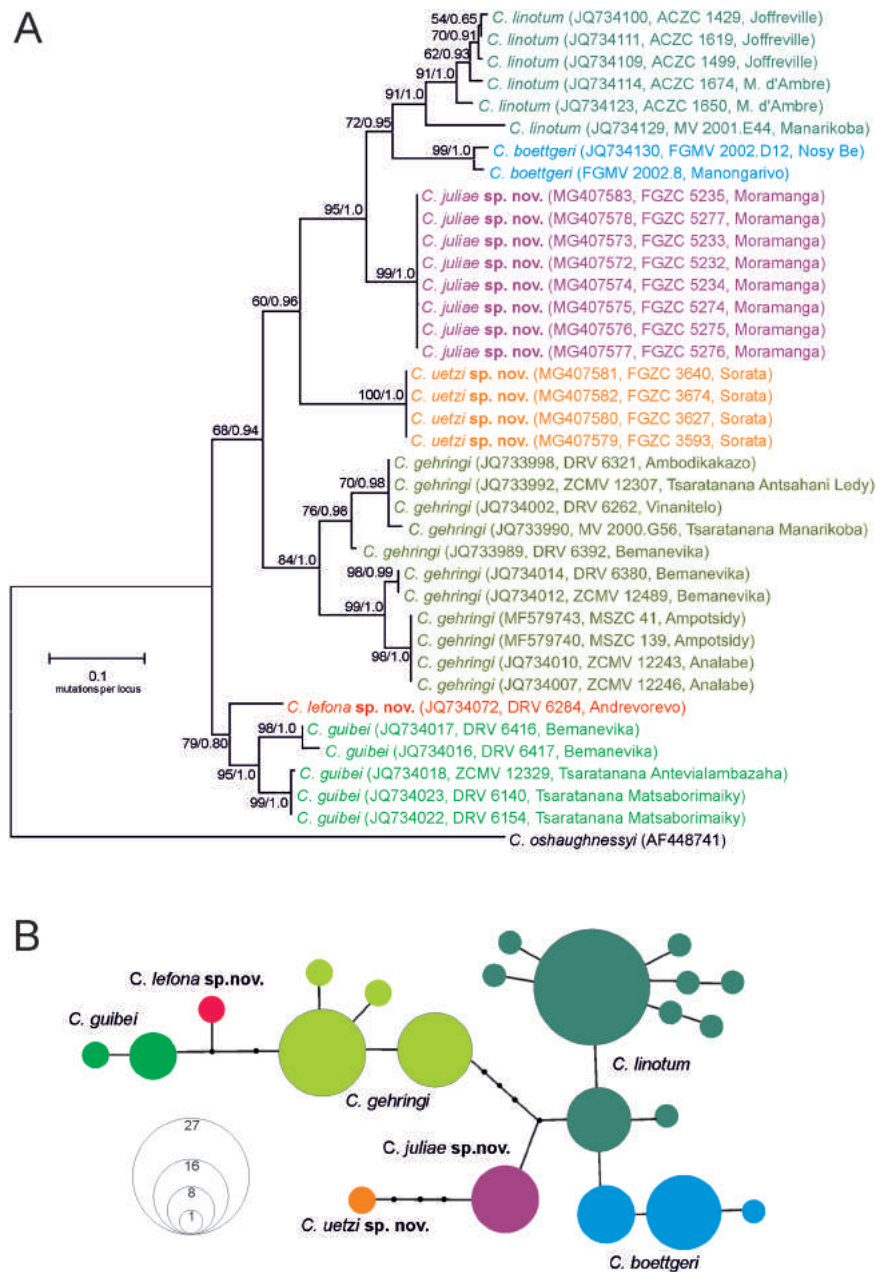
Figure 1. Molecular differentiation of species in the *Calumma boettgeri* complex. A, maximum likelihood tree based on DNA sequences of the mitochondrial *ND2* gene (515 bp). Numbers at nodes are bootstrap proportions expressed as a percentage (2000 replicates) followed by posterior probabilities from an independent Bayesian inference analysis of the same data set. GenBank accession numbers are given for each sequence included. B, haplotype network estimated from sequences of the nuclear *CMOS* gene (410 bp). Black dots represent additional mutational steps, and species are assigned the same colours as in the mitochondrial DNA tree.

deep conspecific lineages (Prötzel *et al.*, 2017). The following three deep lineages were identified, which are not currently associated with known species: (1) a specimen from Andrevorevo, already included in a previous study, that formed the sister lineage of *C. guibei*; (2) a lineage containing various individuals from near Moramanga in eastern Madagascar, which formed the sister group to the *C. boettgeri*/*C. linotum* clade; and (3) a lineage from the northern Sorata Massif placed sister to the *C. boettgeri*/*C. linotum*/Moramanga clade. Each of these species-level lineages was supported by high bootstrap values and posterior probabilities (for support values, see Fig. 1A). *ND2* divergences (between-group mean uncorrected pairwise p-distances) among single samples of the described species in the *C. nasutum* group range from 9.2 to 19.0% (Table 3), whereas maximal intraspecific distances are 2.1, 11.4 and 6.8% in *C. boettgeri*, *C. linotum* and *C. guibei*, respectively.

A comparison with the haplotype network of the nuclear *CMOS* gene (Fig. 1B) shows that each major mitochondrial lineage consists of exclusive haplotypes, with no indication of haplotype sharing. This suggests that the three undescribed lineages from Andrevorevo, Moramanga, and Sorata are probably following independent evolutionary trajectories, and there is no evidence of gene flow among them. Given that they are also differentiated in morphological characters as reported below, we consider these three lineages as new species and provide formal descriptions.

SPECIES DESCRIPTIONS

FAMILY CHAMAELEONIDAE RAFINESQUE, 1815

GENUS *CALUMMA* GRAY, 1865

CALUMMA UETZI SP. NOV.

urn:lsid:zoobank.org:act:C13858A2-8989-475E-9679-F96F283E34D7

Holotype: ZSM 1688/2012 (FGZC 3627), adult male with completely everted hemipenes (hemipenis on the right removed for micro-CT scanning), collected in the Sorata massif (13.6944°S, 49.4441°E, 1100 m a.s.l.), Antsiranana Province, northern Madagascar, on 27 November 2012 by F. Glaw, O. Hawlitschek, T. Rajoafiarison, A. Rakotoarison, F. M. Ratsoavina, and A. Razafimanantsoa.

Paratypes: ZSM 1686/2012 (FGZC 3674), subadult male, collected in Sorata above the campsite (13.6804°S, 49.4395°E, 1396 m a.s.l.) on 28 November 2012; ZSM 1685/2012 (FGZC 3593), adult female, collected in Sorata above the campsite (13.6805°S, 49.4451°E, 1417 m a.s.l.) on 26 November 2012; ZSM 1687/2012 (FGZC 3640), adult female, collected in Sorata, bamboo forest above the campsite (13.6746°S, 49.4406°E, 1516 m a.s.l.) on 28 November 2012; UADBA-R uncatalogued (FGZC 3628), adult female, collected in Sorata (13,6944°S, 49,4441°E, 1100 m a.s.l.) on 27 November 2012; all collected by F. Glaw, O. Hawlitschek, T. Rajoafiarison, A. Rakotoarison, F. M. Ratsoavina, and A. Razafimanantsoa.

Referred material: ZSM 450/2016 (ZCMV 15287), juvenile, collected in Marojejy National Park at Camp 3 'Simpona' (14.43661°S, 49.74335°E, 1325 m a.s.l.) on 18 November 2016 by M. D. Scherz, A. Rakotoarison, M. Bletz, M. Vences, A. Razafimanantsoa, and J. Razafindraibe. This juvenile specimen was recently identified by DNA barcoding to be conspecific with *Calumma uetzi* but is not figured above.

Diagnosis: Calumma uetzi sp. nov. is a member of the phenetic *C. nasutum* species group (Prötzel, Ruthensteiner & Glaw, 2016), on the basis of the presence of a soft, dermal unpaired rostral appendage, absence of gular or ventral crests, and heterogeneous scalation on the lower arm, consisting mostly of tubercles of diameter 0.3–0.5 mm. Within the group, it is one of the smallest species, at 42.0–45.7 mm SVL and 87.3–101.2 mm total length. The brown to olive-green chameleon is characterized by a long and distally rounded rostral appendage, occipital lobes that are clearly notched but not completely separated, a distinctly elevated rostral

Table 3. Mean interspecific genetic distances, and mean and maximal intraspecific genetic distances between species of the *Calumma boettgeri* complex (uncorrected pairwise distances of a fragment of the mitochondrial *ND2* gene, expressed as a percentage)

	C. boettgeri	C. gehringi	C. guibei	C. juliae	C. lefona	C. linotum	C. uetzi
C. boettgeri	2.1/2.1						
C. gehringi	17.1	6.6/11.4					
C. guibei	19.0	14.8	4.1/6.8				
C. juliae	11.2	12.6	15.4	0.0/0.0			
C. lefona	17.4	14.2	9.2	14.5	NA		
C. linotum	12.1	15.4	17.7	10.9	15.1	4.6/10.1	
C. uetzi	15.3	12.2	14.9	12.2	13.5	12.4	0.0/0.0

crest, a dorsal crest in both sexes, absence of axillary pits and unique skull morphology.

Calumma uetzi sp. nov. differs from *C. fallax*, *C. gallus*, *C. nasutum*, *Calumma peyrierasi* (Brygoo, Blanc & Domergue, 1974), *C. vatosoa,* and *C. vohibola* of the *C. nasutum* group by the presence of occipital lobes; from *C. linotum* and *C. boettgeri* in the clearly notched occipital lobes with a depth of 0.5–1.0 mm (vs. not or slightly notched with 0–0.3 mm and 0–0.6 mm); additionally, from *C. boettgeri* by the higher number of large juxtaposed tubercle scales on the extremities (15–18 in line vs. 7–14, isolated from each other). From the most similar taxa, *C. gehringi* and *C. guibei* (Prötzel *et al.*, 2017), *C. uetzi* sp. nov. differs in the smaller body size of 42.0–45.7 mm SVL in adults (vs. 47.5–53.7 mm in *C. gehringi* and 48.1–53.7 mm in *C. guibei*); a longer tail relative to SVL in females of 108–118% (vs. 89–106% in *C. gehringi* and 95–101% in *C. guibei*); the presence of a dorsal crest in females (vs. absence); a straight-lined dorsal margin of the supralabial scales vs. serrated (character 'en dents de scie' of Angel, 1942); furthermore, in skull morphology of adult males of *C. gehringi* and *C. guibei* (Prötzel *et al.*, 2017), by a completely closed brain case in adults (vs. presence of a frontoparietal fenestra with a diameter of 0.7–2.6 mm); elevated protuberances at the anterior end of the maxillae in males (vs. absence); and in a broadened parietal with a width at its midpoint of 24.8% related to skull length (vs. 9.9–15.3%). Furthermore, *C. uetzi* sp. nov. differs from all other species by a unique coloration of males in life.

Description of the holotype (Figs 2, 3A): Adult male, in a good state of preservation; mouth slightly opened, with tongue tip between the jaws; originally, both hemipenes completely everted, but right hemipenis removed for micro-CT scanning and stored in a separate Eppendorf tube alongside the specimen; SVL 45.7 mm, tail length 55.5 mm; for other measurements, see Table 1; distinct and elevated rostral ridges that form a concave cup on the snout and fuse on the anterior snout at the base of a tapering, laterally compressed dermal rostral appendage that projects straight forward over a length of 3.8 mm beyond the snout tip with a diameter of 2.0 mm, rounded distally; 12 infralabial and 11 supralabial scales; supralabials with a straight dorsal margin; no supra-orbital crest; distinct lateral crest running horizontally; short temporal crest consisting of two tubercles per side; indistinct parietal crest; occipital lobes clearly developed and separated, but still slightly connected, by a deep, V-shaped notch (1.0 mm); casque raised; dorsal crest present, starting 0.9 mm from the base of the notch between the occipital lobes, consisting of a row of 13 separated, small conical scales spaced at irregular intervals from 0.1 to 1.8 mm; no

caudal crest; no traces of gular or ventral crest. Body laterally compressed, with fine homogeneous scalation with the exception of the extremities and head region; limbs with rounded tubercle scales having a maximal diameter of 0.5 mm; heterogeneous scalation on the head, with largest scale on temporal region with diameter of 1.0 mm; 28 oval tubercle scales (diameter > 0.3 mm) per side on rostral appendage; no axillary or inguinal pits.

Skull osteology of the holotype (Fig. 4A; Supporting information, Video S1): Skull length 10.9 mm; snout–casque length 12.9 mm; maxillae with elevated protuberances at the anterior end; narrow paired nasals separated from each other; anterior tip of frontal exceeding more than half of the naris and meeting the premaxilla; prefrontal fontanelle and naris separated by contact of prefrontal with maxilla; prominent prefrontal with laterally raised tubercles; frontal and parietal with several tubercles; frontal with a width of 2.8 mm (25.7% of skull length) at border to prefrontal, extending to 4.3 mm (39.4%) at border to postorbitofrontal; broad parietal, tapering more or less constantly from a width of 4.2 mm (38.5%) at the border to frontal and still broad at midpoint with 2.7 mm (24.8%) until it meets the squamosals, then narrowing rapidly to a tip; posterodorsally directed parietal meets the squamosal laterally; squamosal thick, with several tubercles. For further measurements, see Table 2.

Coloration of the holotype in preservative (Fig. 3A): The body of the holotype in preservative is of grey–blue colour, with an indistinct beige lateral stripe and a light blueish stripe above it; ventral and temporal region and gular folds also beige; extremities speckled with blue to light blue tubercle scales; tail irregularly annulated beige and grey.

Variation: The three ZSM paratypes agree well with the holotype in most characters of morphology and osteology: male ZSM 1686/2012 with a dorsal crest of elongated spines (Fig. 3A; vs. conical scales in holotype) and a small number of tubercle scales on the rostral appendage (19 per side); temporal crest varies between the specimens from one to two tubercles; depth of notch of occipital lobes is smaller in paratypes (0.2–0.6 mm; juvenile specimens included); number of dorsal cones in males is distinctly higher (13–14) than in females (three to five; juvenile ZSM 1685/2012 assumed as female). The skull of a second micro-CT-scanned specimen (ZSM 1686/2012) differs by the smooth frontal and parietal that is also narrower at its midpoint (3.2% of SVL, vs. 4.4% of SVL in the holotype). Both characters can be attributed to the subadult developmental stage of the specimen.

Coloration in life (based on observations and photographs of the type specimens only; Fig. 2): Sexes are dichromatic, with males in relaxed state generally greenish beige and females with brown body coloration; a beige–white lateral stripe may occur from the occipital lobes to the hip. In males, the stripe is distinct and framed by a violet line. Throat and ventral region white in males, beige in females; rostral appendage not contrasted and of same colour as the body; dark lateral stripe from nostrils, crossing the eyes to the base of the occipital lobes; cheek region highlighted in blue (males) or green (females) colour; large scales on temporal region of males of bluish colour.

Signalling males show a spectacular coloration of bright yellow all over the body, tail, extremities and eyelids, a red lateral stripe that is framed in violet, light blue cheek region, violet temporal region and a bluish–green rostral appendage; the eye-stripe darkens and contrasts the remaining head coloration. The stress coloration of females focuses only on the head region, with distinct yellow spots on the rostral appendage, rostral crest, dorsal head side and temporal crest; eyelids with radially aligned blue spots, also on occipital lobes; colourful spots contrasted by dark brown head coloration; rest of body uniformly brown (Fig. 2C).

Hemipenial morphology based on diceCT scans (Fig. 5A; Supporting information, Video S2): The hemipenis of *Calumma uetzi* sp. nov. shows large and deep calyces, with smooth ridges on the asulcal side of the truncus. The apex is ornamented with two pairs of pointed cornucula (recently described hemipenial ornament; see Prötzel *et al.* (2017) and paired rotulae. The cornucula rise from the sulcal side of the apex, are curved to the asulcal side and are not completely everted in the investigated specimen. A pair of rotulae, with four and six tips, respectively, is placed on the asulcal side. Additionally, on the asulcal side there is a pair of larger rotulae that are curved and bear 12 and 13 tips. The top of the apex has a papillary field of several fleshy papillae.

Available names: Apart from *C. gehringi* and *C. guibei*, there is no other valid species or synonym in the *C. nasutum* group with deeply notched occipital lobes.

Figure 2. *Calumma uetzi* **sp. nov.** in life. A, male (ZSM 1686/2012) in slightly stressed coloration. B, subadult female (ZSM 1685/2012) relaxed. C, male holotype (ZSM 1688/2012, left) in spectacular display, with adult female (right, UADBA-R-FGZC 3628) in stress coloration, repelling the male.

Etymology: This species is dedicated to our colleague and friend Peter Uetz, who developed and has maintained the Reptile Database (http://www.reptile-database.org/) voluntarily for > 20 years. This database is the most important online resource for information on reptile species, thereby providing a priceless service to herpetology and a model for what should be available for all organism groups.

Distribution: *Calumma uetzi* sp. nov. was originally discovered in northern Madagascar, in the area of the Sorata massif (Antsiranana Province) from elevations of 1100–1500 m a.s.l., but new DNA barcoding results revealed that a juvenile chameleon recently collected in Marojejy National Park (14.43661°S, 49.74335°E, 1325 m a.s.l.; Fig. 6) also belongs to *C. uetzi* sp. nov.

Natural history and ecology: The principal habitat of *Calumma uetzi* sp. nov. is primary mid-elevation rainforest that has recently been degraded at different levels. Most individuals were found at night roosting in the vegetation on thin branches or on the tip of leaves ~1–3 m above the forest floor and had red mites between the fingers and toes. When a male and a female were put in close proximity on the same branch, both sexes quickly changed colour and became brightly coloured (Fig. 2), and the female threatened the male with an open mouth. In other cases, one of the individuals moved away to avoid closer contact. In one, case the artificial encounter led to a possible mating attempt.

Recommended IUCN status: Given the limited data available on *C. uetzi* sp. nov., specifically no data pertaining to the size of its population or probability of extinction, it cannot currently be assessed under any criterion other than B of the IUCN Red List Criteria (IUCN, 2012). A minimal convex polygon of the Sorata and Marojejy massifs, corresponding to the estimated extent of occurrence (EOO) of the species (criterion B1), covers an area of ~2500 km². It is currently known from two threat-defined locations (as defined by the IUCN, 2012; criterion B, subcriterion a), one of which is well protected (Marojejy National Park). The other location (Sorata) is not yet protected, but is currently included in a planned protected area, COMATSA Nord (corridor between Marojejy, Anjanaharibe-Sud and Tsaratanana protected areas, WWF Madagascar, 2015). At present, Sorata is experiencing high deforestation pressure, and forest has been largely eradicated from sea level to ~1200 m a.s.l. As such, the deforestation pressure is directly impacting the distribution range of *C. uetzi* sp. nov. in this area [criterion B, subcriterion b(iii)]. As the EOO of the

species is < 5000 km², and the number of threat-defined locations is fewer than five, the species qualifies as Endangered under IUCN criterion B1ab(iii).

FAMILY CHAMAELEONIDAE RAFINESQUE, 1815

GENUS *CALUMMA* GRAY, 1865

CALUMMA LEFONA SP. NOV.

urn:lsid:zoobank.org:act:99AF4F23-EBDF-4276-AE41-3C04E7443FD8

Remark: This species was considered as clade FII by Gehring *et al.* (2012).

Holotype: ZSM 2849/2010 (DRV 6287), adult male with incompletely everted hemipenes, left hemipenis removed for micro-CT scanning, collected in Andrevorevo southeast of Tsaratanana Massif (14.3464°S, 49.1028°E, 1717 m a.s.l.), Mahajanga Province, northern Madagascar, on 21 June 2010 by F. M. Ratsoavina and F. Randrianasola.

Paratypes: None.

Diagnosis: *Calumma lefona* sp. nov. is a member of the phenetic *C. nasutum* species group (Prötzel, Ruthensteiner & Glaw, 2016), on the basis of the presence of a soft, dermal, unpaired rostral appendage, absence of gular or ventral crests, and heterogeneous scalation on the lower arm, consisting mostly of tubercles of ~0.5 mm diameter. Within the genus, it is a small sized chameleon (SVL 51.3 mm, TL 113.7 mm) that is characterized by a long and pointed rostral appendage, occipital lobes that are widely notched and completely separated, a distinctly elevated rostral crest, a dorsal and caudal crest, absence of axillary pits and unique skull morphology.

Calumma lefona sp. nov. differs from *C. fallax*, *C. gallus*, *C. nasutum*, *C. peyrierasi*, *C. vatosoa,* and *C. vohibola* of the *C. nasutum* group by the presence of occipital lobes; from *C. boettgeri* and *C. linotum* in the clearly notched occipital lobes with a depth of 1.8 mm (vs. not or slightly notched with 0–0.7 mm), presence of a frontoparietal fenestra with a width of 1.9 mm (14.7% of skull length; vs. completely closed brain case), prefrontal, frontal and parietal with many tubercles (vs. smooth or only a few tubercles); additionally, from *C. boettgeri* by the higher number (21 in line) of large, juxtaposed tubercle scales on the extremities (vs. seven to 14 isolated tubercles).

From the other three taxa with notched occipital lobes, *C. gehringi*, *C. guibei,* and *C. uetzi* sp. nov., *C. lefona* sp. nov. differs by the long (5.6 mm) and pointed rostral appendage (vs. 3.1–5.4 mm in males, rounded), with 60 large scales (diameter > 0.3 mm)

on the right side of the rostral appendage (vs. 20–42 in males), dorsal crest of 23 small conical scales (vs. absence or 5–15 large conical scales), clearly and widely separated occipital lobes with a notch of 1.8 mm (vs. tightly separated or connected with a notch of 0.5–1.5 mm in males); furthermore, in skull morphology by a narrower frontal, e.g. at the border to the postorbitofrontal with 30.5% of SkL (vs. 35.5–39.7%) and strongly raised maxillae; from *C. gehringi* and *C. guibei* in a broader parietal at midpoint with 18.3% of SkL (vs. 9.9–15.3%); from *C. uetzi* sp. nov. by possession of a frontoparietal fenestra (vs. completely closed brain case) and a narrower head (e.g. RFWPo of 30.5 vs. 35.6–39.4%); from *C. guibei* by a smaller frontoparietal fenestra with 14.7% of SkL (vs. 21.0%), prefrontal fontanelle and naris separated by contact of prefrontal with maxilla (vs. fused), thick squamosal (vs. thin) in broad dorsal contact with the parietal (vs. not meeting parietal or only in weak contact); and from *C. gehringi* by possession of a larger frontoparietal fenestra (21.0% of SkL vs. 5.8–9.1%).

Description of the holotype (Fig. 3B): Adult male, in a good state of preservation, left forelimb removed for DNA analysis, left hemipenis removed for micro-CT scanning; mouth slightly opened with tongue between the jaws; originally both hemipenes incompletely everted (Fig. 5B), but left hemipenis cut off for micro-CT scanning and stored in a separate Eppendorf tube alongside the specimen; SVL 51.3 mm, tail length 62.4 mm; see Table 1 for other measurements; distinct and elevated rostral ridges that form a concave cup on the snout and fuse on the anterior snout at the base of a tapering, laterally compressed dermal rostral appendage that projects straight forward over a length of 5.6 mm with a diameter of 2.0 mm, pointed distally; 12 infralabial and 11 supralabial scales; supralabials dorsally serrated; no supra-orbital crest; distinct lateral crest running horizontally; short temporal crest consisting of two tubercles per side; indistinct parietal crest; occipital lobes clearly developed and completely separated by a deep, 'U'-shaped notch (1.8 mm); casque raised; dorsal crest present, starting 0.8 mm from the base of the notch between the occipital lobes, consisting of a row of 23 separated, small conical scales spaced at irregular intervals from 0.1 to 0.9 mm, and several more on the tail decreasing in size towards the tip; no traces of gular or ventral crest. Body laterally compressed, with fine homogeneous scalation with the exception of the extremities and head region; limbs with rounded tubercle scales with a maximal diameter of 0.5 mm; heterogeneous scalation on the head, with largest scale on temporal region with diameter of 0.6 mm and 60 oval tubercle scales (diameter > 0.3 mm) on the right side of the rostral appendage; no axillary or inguinal pits.

Figure 3. Holotypes of the three new *Calumma* species as preserved specimens. A, **C. uetzi sp. nov.** (ZSM 1688/2012). B, **C. lefona sp. nov.** (ZSM 2849/2010). C, **C. juliae sp. nov.** (ZSM 143/2016). Scale bar: 20 mm.
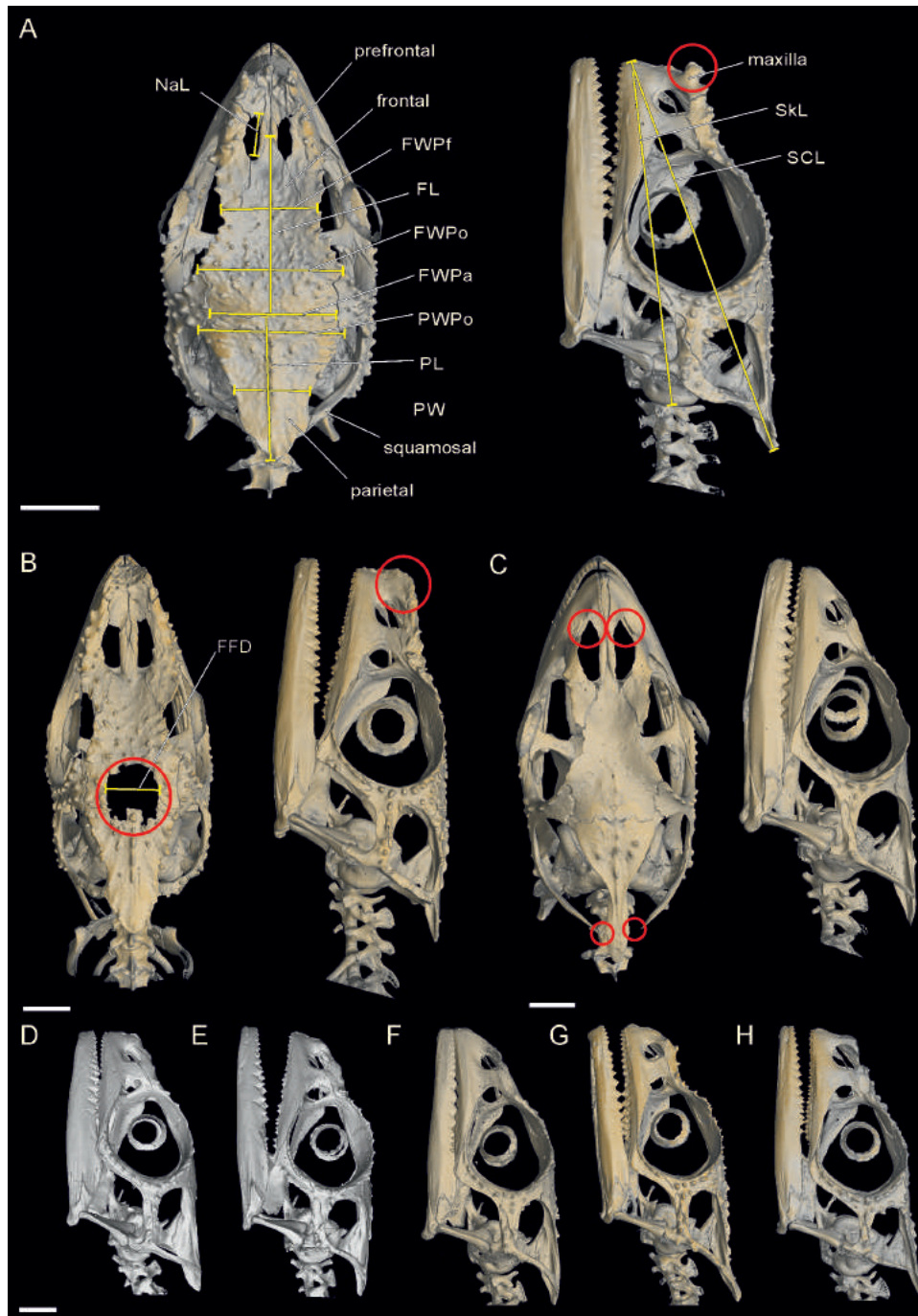
Figure 4. Micro-computed tomography scans of the skulls of the three holotypes in dorsal and lateral view. A, male *Calumma uetzi* **sp. nov.** (ZSM 1688/2012). B, male *C. lefona* **sp. nov.** (ZSM 2849/2010). C, female *C. juliae* **sp. nov.** (ZSM 143/2016). D, male *C. boettgeri* (ZSM 440/2000). E, male *C. linotum* holotype. F, female *C. linotum* (ZSM 551/2001). G, male *C. gehringi* holotype (ZSM 2851/2010). H, male *C. guibei* (ZSM 2855/2010). Diagnostic characters are encircled in red. Abbreviations are given in the Material and Methods. Scale bars: 2.0 mm.

Skull osteology of the holotype ([Fig. 4B, Supporting information, Video S3](#)): Skull length 13.1 mm; snout–casque length 15.9 mm; broad paired nasals meeting anteriorly, anterior tip of frontal exceeding more than half of the naris; prefrontal fontanelle and naris separated by contact of prefrontal with maxilla;

elevated maxillae building a rectangular edge at anterior margin; prominent prefrontals with laterally raised tubercles; frontal and parietal with several tubercles, five on the midline forming a parietal crest; frontal with a width of 2.9 mm (22.1% of SkL) at border to prefrontal extending to 4.0 mm (30.5% of SkL) at border to postorbitofrontal; frontoparietal fenestra with transverse diameter of 1.9 mm (14.7% of SkL); parietal tapering more or less constantly, with a width of 3.9 mm (29.8% of SkL) at the border to frontal and 2.4 mm (18.3% of SkL) at its midpoint, and then tapering rather strongly to the posterior tip; posterodorsally directed parietal meets the squamosal laterally; squamosal thick, with several tubercles. For further measurements, see Table 2.

Coloration of the holotype in preservative (Fig. 3B): The body of the holotype in preservative is of a grey–blue colour, with an indistinct beige lateral stripe; ventral and temporal regions and throat also beige; dark blue line from dorsal part of rostral appendage crossing the eyes and the lateral crest, ending in occipital lobes; extremities speckled with bluish tubercle scales. The coloration in life is unknown.

Hemipenial morphology based on diceCT scans: The hemipenis of the holotype was incompletely everted, and a diceCT scan resulted in an inadequate illustration (Fig. 5B). Apparently, it showed deep calyces and two pairs of rotulae; changing the threshold revealed two pairs of cornucula that were not everted.

Available names: Apart from *C. gehringi*, *C. guibei,* and *C. uetzi* sp. nov., there is no other valid species or synonym in the *C. nasutum* group with deeply notched occipital lobes.

Etymology: *Calumma lefona* sp. nov. is the only species in the *C. nasutum* group with a relatively long and pointed/constantly tapering rostral appendage (with the exception of *C. gallus*). This shape reminds of a spearhead; accordingly, we chose the Malagasy word 'lefona' (meaning 'spear') as its species epithet. It is used as an invariable noun in apposition to the genus name.

Distribution: *Calumma lefona* sp. nov. is, so far, known from only a single location in northern Madagascar, southeast of the Tsaratanana Massif, called Andrevorevo, at 1717 m a.s.l. (Fig. 6; for geographical coordinates see the 'holotype' details above). It lives within the lower elevational range of its sister taxon *C. guibei* (from 1590–2250 m a.s.l.) and at higher elevation than *C. gehringi* (730–1540 m a.s.l.).

Natural history and ecology: *Calumma lefona* sp. nov. was found roosting at night on tree branches ~2 m above the ground. The habitat consisted of primary forest with closed canopy cover and small streams. During the nocturnal observations on 20 and 21 June 2010, two adults and two juveniles were found along the forest path, but only one adult (the holotype) was collected.

Recommended IUCN status: Practically no data are available on the distribution and condition of *C. lefona* sp. nov., and the species is known from a single specimen and a few additional observations. To avoid inflation of perceived risk, we recommend that this species be considered Data Deficient by the IUCN until more data become available.

FAMILY CHAMAELEONIDAE RAFINESQUE, 1815
GENUS *CALUMMA* GRAY, 1865
***CALUMMA JULIAE* SP. NOV.**

urn:lsid:zoobank.org:act:6A92C95D-6383-45DC-9FFC-0943B08F064F

Remark: Despite intensive research at the type locality in January (by L. Randriamanana, F.G. and D.P.), August (by N. Raharinoro, K. Glaw, T. Glaw, J. Forster, F.G. and D.P.) and November 2016 (by A. Rakotoarison and M.D.S.) in the rainy and dry seasons, only female specimens of this new species were found. In total, eight adult females, two subadult females and two juveniles were encountered (but not all of them collected).

Holotype: ZSM 143/2016 (FGZC 5235), adult female, collected in small forest fragment 5 km east of Moramanga, just south of the Route Nationale 2 (18.9520°S, 48.2707°E, at 950 m a.s.l.), Toamasina Province, eastern Madagascar on 6 January 2016 by F. Glaw, D. Prötzel and L. Randriamanana.

Paratypes: ZSM 142/2016 (FGZC 5233), FGZC 5232 and FGZC 5234 (two uncatalogued specimens in UADBA), all three adult females, collected from the same location as the holotype (18.9519°S, 48.2705°E, within a radius of 50 m, at 950 m a.s.l.) on 6 January 2016 by F. Glaw, D. Prötzel, and L. Randriamanana. ZSM 254/2016 (FGZC 5274), adult female, and ZSM 255/2016 (FGZC 5275) and FGZC 5276 (uncatalogued specimen in UADBA), both juveniles, all three collected on 30 July 2016; FGZC 5277 (uncatalogued specimen in UADBA), subadult, collected on 31 July 2016 at the same location as above by F. Glaw, D. Prötzel, and N. Raharinoro.

Diagnosis: Male specimens are unknown so far, hence the diagnosis refers only to females of this species. *Calumma juliae* sp. nov. is a member of the phenetic *C. nasutum* species group (Prötzel, Ruthensteiner & Glaw, 2016), on the basis of the presence of a soft,
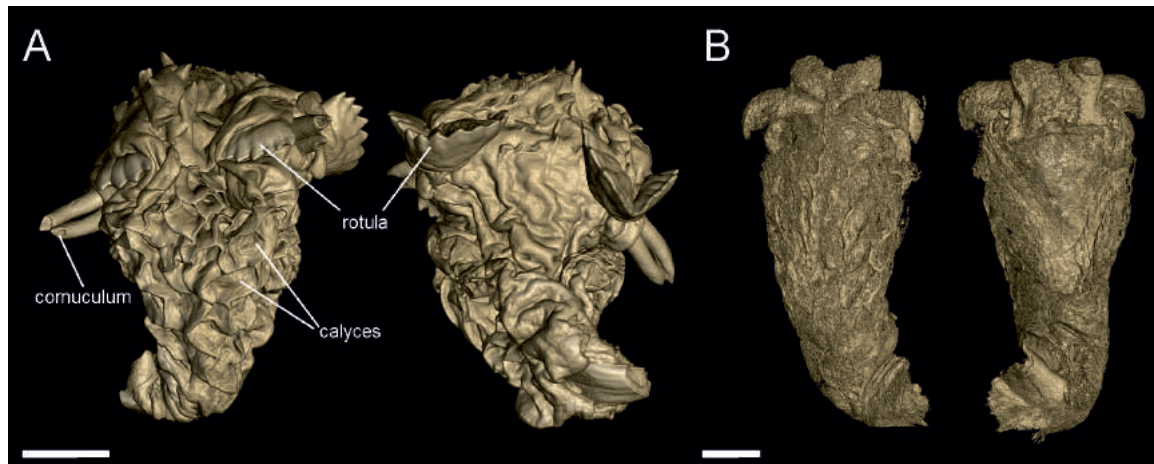
Figure 5. DiceCT scans of hemipenes. A, right hemipenes of ***Calumma uetzi* sp. nov.** in asulcal (left) and sulcal (right) view. B, left hemipenes (incompletely everted) of ***C. lefona* sp. nov.** in asulcal (left) and sulcal (right) view; note that characters can be seen only in completely everted hemipenes. Scale bars: 1.0 mm.

dermal unpaired rostral appendage, absence of gular or ventral crests, and heterogeneous scalation on the lower arm, consisting mostly of tubercles of a diameter of 0.7–0.8 mm. Within the group, it is a large (TL 105.3–111.6 mm), grey–beige chameleon that is characterised by a long and distally rounded rostral appendage, a dorsal crest of 11–14 tubercles, occipital lobes that are clearly notched but not completely separated, and absence of axillary pits.

Calumma juliae sp. nov. differs from *C. fallax*, *C. gallus*, *C. nasutum*, *C. peyrierasi*, *C. vatosoa,* and *C. vohibola* of the *C. nasutum* group by the presence of occipital lobes; from *C. gehringi*, *C. guibei,* and *C. lefona* sp. nov. in the completely closed brain case (vs. frontoparietal fenestra); additionally, from female *C. gehringi* and *C. guibei* in body size of 53.3–59.4 mm SVL (vs. 47.5–52.3 mm); from female *C. gehringi* in the shorter rostral appendage of 2.3–2.7 mm (vs. 3.2–4.4 mm); from *C. guibei* (both sexes) in the notch between the occipital lobes of 0.2–0.8 mm (vs. completely separated with notch of 1.2–1.9 mm; see [Brygoo, 1971](#)); from *C. lefona* sp. nov. (one male) in the shorter (2.3–2.7 mm) and rounded rostral appendage (vs. 5.6 mm, pointed), the absence of a temporal and parietal crest (vs. presence) and the number of dorsal cones of 11–14 (vs. 23); from *C. boettgeri* (both sexes) by the higher number of large (0.7–0.8 mm diameter) juxtaposed tubercle scales on the extremities (17–19 in line vs. 7–14, diameter of 0.2–0.5 mm and isolated from each other); from female *C. uetzi* sp. nov. in the larger body size of 53.3–59.4 mm SVL (vs. 42.0 mm SVL in females), the absence of a temporal and parietal crest (vs. presence of both) and the higher number of infralabial scales of 14–15 (vs. 11–12); from its most

similar taxon *C. linotum* by the clearly notched occipital lobes with a depth of 0.2–0.8 mm (vs. not or slightly notched with depth 0–0.2 mm), presence of a dorsal crest in females consisting of 11–14 conical scales in *C. juliae* sp. nov. (vs. zero in *C. linotum* and six in *C.* cf. *linotum*; one specimen from Andampy), higher number of infralabial scales in females of 14–15 (vs. 12–13), absence of temporal and parietal crest in females (vs. both present), and in generally larger body size in females of 53.3–59.4 mm SVL (vs. 42.7–54.5 mm). In skull morphology, the squamosal and parietal do not meet in female *C. juliae* sp. nov. (vs. broad in contact in male and female *C. linotum* ([Prötzel *et al.*, 2015](#)); frontal of triangular shape and narrower, e.g. 16.8–18.2% of SkL at border to prefrontal (vs. 22.1–24.4%), 30.7–31.1% of SkL at border to postorbitofrontal (vs. 34.4–35.8%) and 25.0–26.3% of SkL bordering the parietal (vs. 32.5–33.6%); also, parietal is narrower at border to frontal with 28.5–29.5% of SkL (vs. 34.1–35.1%).

Description of the holotype ([Fig. 3C](#)): Adult female, in a good state of preservation; SVL 55.8 mm, tail length 55.4 mm; for other measurements, see [Table 1](#); distinct rostral crest, laterally compressed dermal rostral appendage that projects forward of the snout tip over a length of 2.7 mm with a diameter of 2.2 mm, rounded distally; 14 infralabial and 13 supralabial scales; supralabials dorsally serrated; no supra-orbital crest; distinct lateral crest running horizontally; no temporal crest; occipital lobes clearly developed and separated but still slightly connected by a notch of 0.5 mm; casque raised; dorsal crest present, starting 4.3 mm from the base of the notch between the occipital lobes, consisting of a row of 12 separated, small conical scales
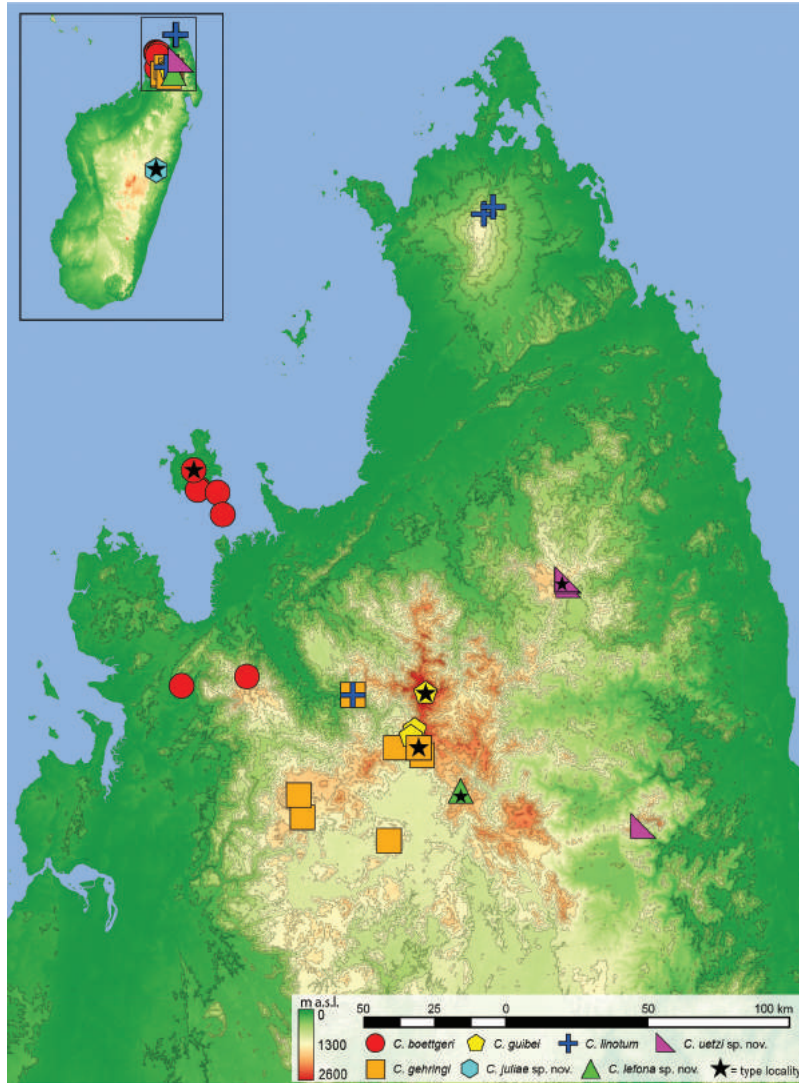
Figure 6. Distribution map of seven species of the *Calumma boettgeri* complex in Madagascar. The type locality is unknown for *Calumma linotum.* Contour lines indicate steps of 200 m elevation. The record from Nosy Komba is based on Hyde Roberts & Daly (2014). Coordinates for *Calumma boettgeri*, Maromiandra (Nagy *et al.*, 2012) in Prötzel *et al.* (2015) are corrected to 13.9965°S, 48.2177°E.

spaced at regular intervals of ~2 mm, continuing on the tail with smaller and narrower spaced cones; no traces of gular or ventral crest. Body laterally compressed, with fine homogeneous scalation with the exception of the extremities and head region; limbs with rounded tubercle scales of maximal diameter 0.7 mm; heterogeneous scalation on the head, with largest scale on temporal region having a diameter of 1.3 mm; no axillary or inguinal pits.

Skull osteology of the holotype (Fig. 4C, Supporting information, Video S4): Skull length 13.2 mm; snout–casque length 16.1 mm; broad paired nasals meeting

each other; anterior tip of frontal exceeding less than half of the naris and separated from premaxilla; prefrontal fontanelle and naris fused; frontal smooth, and parietal with only a few tubercles; frontal with width of 2.4 mm (18.2% of SkL) at border to prefrontal extending to 4.1 mm (31.1% of SkL) at border to postorbitofrontal; broad parietal tapering strongly from a width of 3.9 mm (29.5% of SkL) at the border to frontal to 0.8 mm (6.1% of SkL) at midpoint, then extending mostly straight beyond the posterodorsal extension of the squamosals, and finally tapering again at its tip; posterodorsally directed parietal does
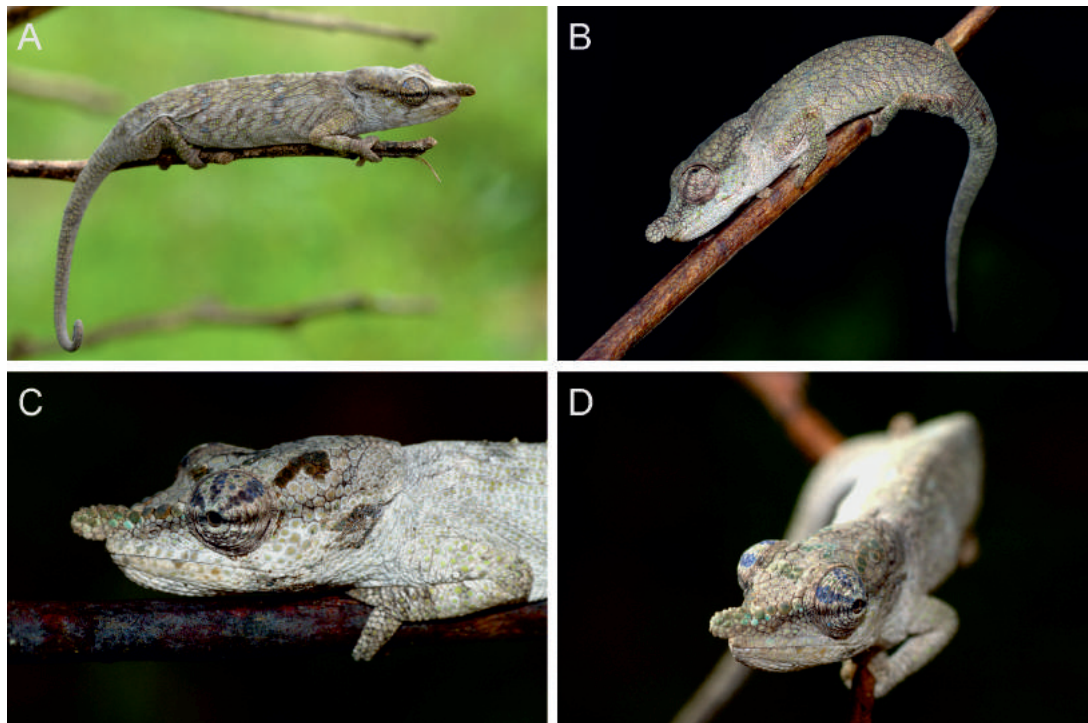
Figure 7. *Calumma juliae* **sp. nov.** coloration in life during day. A, female holotype ZSM 143/2016 relaxed. B, juvenile ZSM 254/2016 relaxed. C, D, portrait of female ZSM 254/2016 with stress pattern (C) and slightly displaying (D).

not meet the squamosal; squamosal thin without tubercles. For further measurements, see Table 2.

Coloration of the holotype in preservative (Fig. 3C): The body of the holotype in preservative is of dark grey colour without any distinct pattern; inner side of extremities and tail beige; extremities and temporal and postocular region of the head speckled with greyish–blue tubercle scales.

Variation: All adult female *C. juliae* sp. nov. that have been found so far show a consistent morphology and consequently agree well with the holotype. ZSM 254/2016 and FGZC 5234 have a slightly shorter rostral appendage than the holotype, at 2.4 and 2.3 mm (vs. 2.7 mm); the notch between the occipital lobes is deeper in FGZC 5232 at 0.8 mm and less deep in ZSM 142/2016 at 0.2 mm (vs. 0.5 mm); the dorsal crest of ZSM 255/2016 consists of only nine tubercles (vs. 12); this might be referred to its juvenile developmental stage. In osteology, no significant variations were found.

Coloration in life (Fig. 7): Females are indistinctly grey–beige coloured; a netlike dark brown pattern on the skin between the scales and two dorsoventrally compressed blue blotches may occur on the body; tubercle scales on extremities and body may be bright green; rostral appendage not highlighted and of same

colour as the body; a dark lateral stripe may stretch from the rostral appendage across the eyes to the occipital lobes. If stressed, only the head coloration changes to dark brown or green pattern at the dorsal head region, eyelids with radially aligned blue/violet spots, and rostral crest and appendage of turquoise/green colour.

Available names: Apart from *C. boettgeri* and *C. linotum*, there is no other valid species or synonym in the *C. nasutum* group with slightly notched occipital lobes.

Etymology: D.P. dedicates the first new species he discovered himself to Julia Forster, in recognition of her generous support and understanding of our research on Madagascan chameleons and her help in collecting specimens of this species.

Distribution: *Calumma juliae* sp. nov. has so far been recorded only from a fragment of degraded primary rainforest, covering an area of just 15 ha, east of Moramanga (Toamasina Province, eastern Madagascar; Figs 6, 8A); for geographical coordinates, see the descriptions in the subsections 'Holotype' and 'Paratypes' above. The forest fragment spreads over a hill that rises to a maximum elevation of 1010 m a.s.l.; specimens were found only along the trail at 950 m a.s.l., but we expect them to occur on the hill as well.
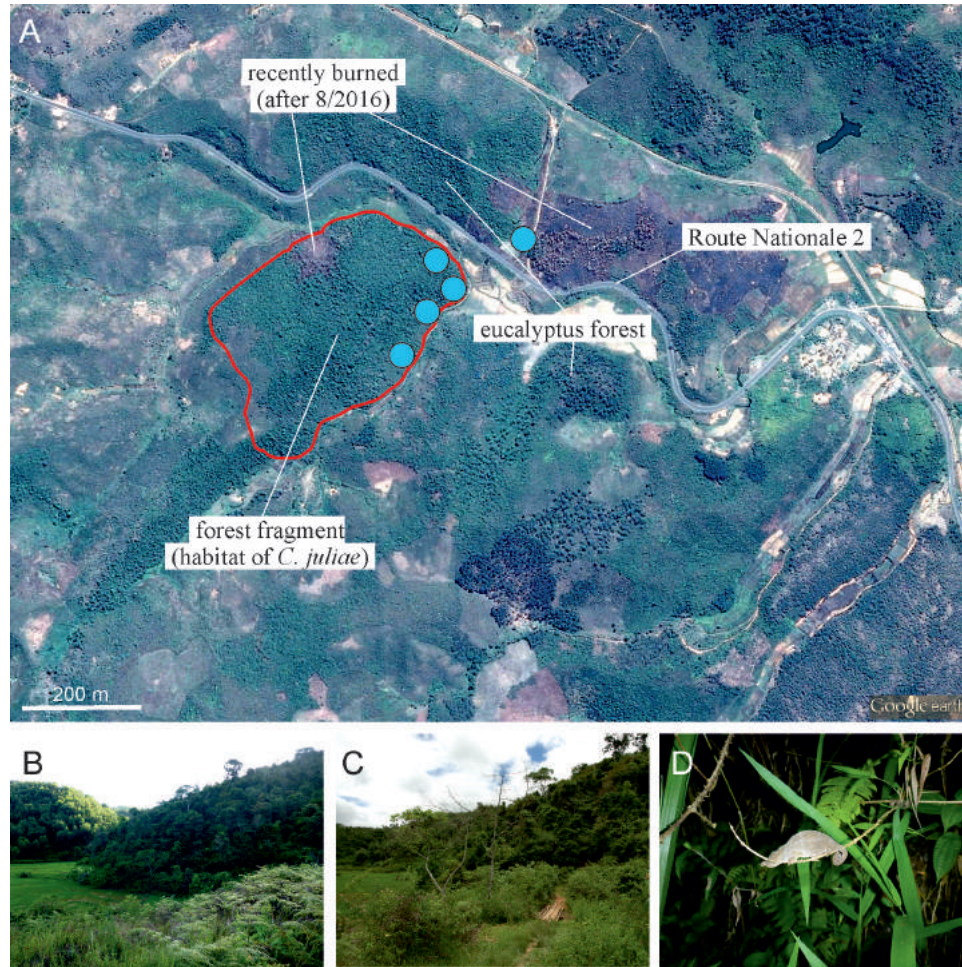
Figure 8. Distribution and habitat of *Calumma juliae* **sp. nov.** A, fragment of degraded primary forest of 15 ha next to Route Nationale 2; blue dots indicate records of *C. juliae* **sp. nov.** B, small fragment of primary forest (on the right) between rice fields and eucalyptus forest (on the left, behind). C, habitat of *C. juliae* **sp. nov.** next to rice fields; view from Route Nationale 2 in August 2016. D, *C. juliae* **sp. nov.** in sleeping position photographed at night. Satellite imagery from Google Earth (17 December 2016).

A further specimen was observed just north of the Route Nationale 2 (18.9513°S, 48.2721°E, 950 m a.s.l.) in secondary bushes.

Natural history and ecology: *Calumma juliae* sp. nov. is an arboreal, diurnal species found in bushes and trees in a small forest fragment of degraded primary rainforest. Roosting sites at night were thin branches or, rarely, leaves that were not exposed, but hidden inside tree/bush cover 0.3–2 m above the ground. In contrast to the syntopically occurring population of *C.* cf. *nasutum*, the present species preferred a horizontal sleeping position (vs. head pointing downwards). When disturbed, some specimens dropped immediately and stayed curled and motionless on the ground. In appropriate habitat, specimens occurred a few metres from one another. In January 2016, only adult females were collected; in August 2016, additionally subadult and juvenile specimens; in November 2016, only one adult female was found. None of the collected females showed signs of being gravid. The size of the juveniles suggests that they hatched during the rainy season from approximately January to March. Under the occipital lobes of two specimens (ZSM 143/2016 and 142/2016) we found three and two mites, respectively; the lobes might function as mite pockets comparable to axillary pits in other chameleon species to limit and locate the damage caused by these ectoparasites (Arnold, 1986).

Recommended IUCN status: As no attempts have yet been made to estimate the population size or status of

C. juliae sp. nov. directly, we suggest that it should be assessed under the IUCN Red List criterion B (IUCN, 2012). The distribution area of the single known forest in which the species occurs has an area of ~0.15 km², which we interpret as the area of occupancy (AOO) of the species as defined by the IUCN (2012), but which at present is also equivalent to the EOO of the species (criterion B1). This constitutes a single threat-defined location (criterion B, subcriterion a). The forest in which it occurs is under heavy active anthropogenic pressure and is, in our opinion, in imminent danger of disappearance [criterion B, subcriterion b(iii)]. As the AOO of the species is considerably < 10 km², consists of a single threat-defined location, and is experiencing on-going decline in its quality and extent, the species qualifies as Critically Endangered under IUCN criterion B1ab(iii).

OSTEOLOGY

Using micro-CT scans, we compared the skull morphology of the currently seven species of the *C. boettgeri* complex. Osteological measurements proved to be a useful tool to delimit these rather cryptic species. As a further important taxonomic character, *C. gehringi* (Fig. 10A–C), *C. guibei,* and *C. lefona* sp. nov. have a distinct frontoparietal fenestra (FF; also pineal or parietal foramen of other authors; see Eakin, 1973) that differs in size between the species. This fenestra also occurs in other species of the *C. nasutum* group, e.g. *C. fallax* (Rieppel & Crumly, 1997) and *C. cf. nasutum* (Table 4). Compared with the elevational distribution of the species, a highly significant correlation [$P = 3.8207 \times 10^{-6}$, r (Pearson) = 0.67] was found with presence/width of the fenestra and elevation (Fig. 10D). None of the

species that live < 1000 m a.s.l. has an FF, and all those > 1500 m a.s.l. have one. Additionally, FF also occur in *C. peyrierasi* and *C. tsaratananense* (Prötzel *et al.*, 2018; A. van't Padje *et al.*, unpublished observations); both are montane species that occur > 1900 m a.s.l. (Brygoo, 1971, 1978), the latter of which is certainly not closely related to the *C. nasutum* group (Tolley *et al.*, 2013). All other investigated *Calumma* species have a closed skull roof (Prötzel *et al.*, 2018; van't Padje *et al.*, unpubl.).

DISCUSSION

DIVERSITY OF THE *CALUMMA BOETTGERI* COMPLEX

With the description of *C. lefona* sp. nov., *C. juliae* sp. nov., and *C. uetzi* sp. nov., the number of species within the *C. boettgeri* complex increases from four to seven. These species have some overlapping characteristics, which makes them difficult to identify confidently based on external morphology alone; therefore, a key is provided to assist with their identification (see above and Fig. 9). Only one of these species (*C. lefona* sp. nov.) was known before as a candidate species in the study by Gehring *et al.* (2012); the others represent additional species above and beyond that already known for the *C. nasutum* species group, highlighting how much remains unknown about this group. An update of the phylogeny of the genus *Calumma* is clearly a necessary future project.

In several species of the *C. boettgeri* complex, genetic intraspecific distances for the mitochondrial *ND2* gene are high, sometimes exceeding those among species. This applies, for instance, to *C. guibei* and *C. gehringi* (Table 3). As discussed by Prötzel *et al.* (2017), current evidence suggests that these divergent sequences in fact represent intraspecific variation, exemplifying
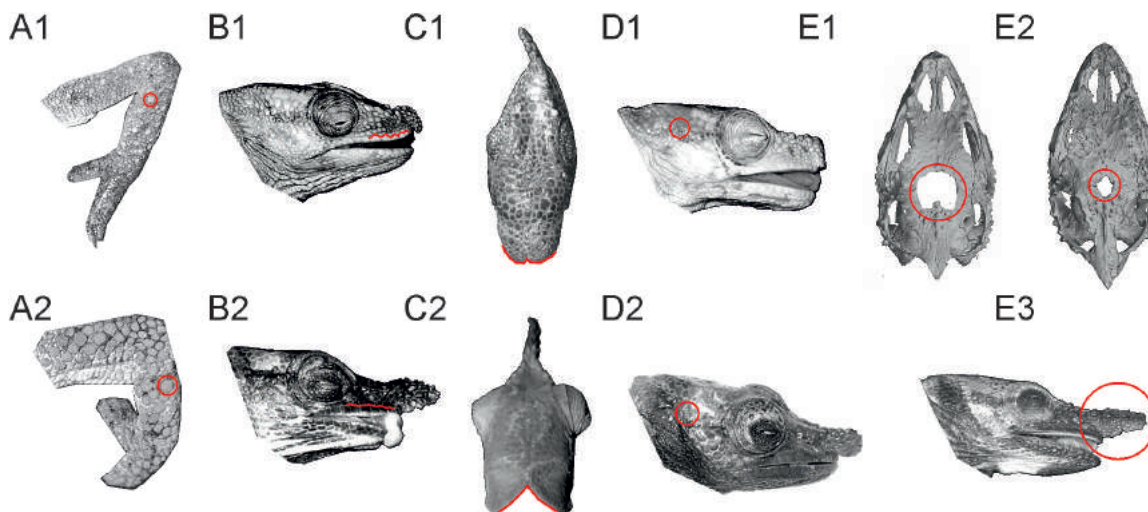

Figure 9. Identification key to the species of the *Calumma boettgeri* complex, including the three new species described here. Diagnostic characters are marked in red. For a comparison of diagnostic characters, see also Table 5.
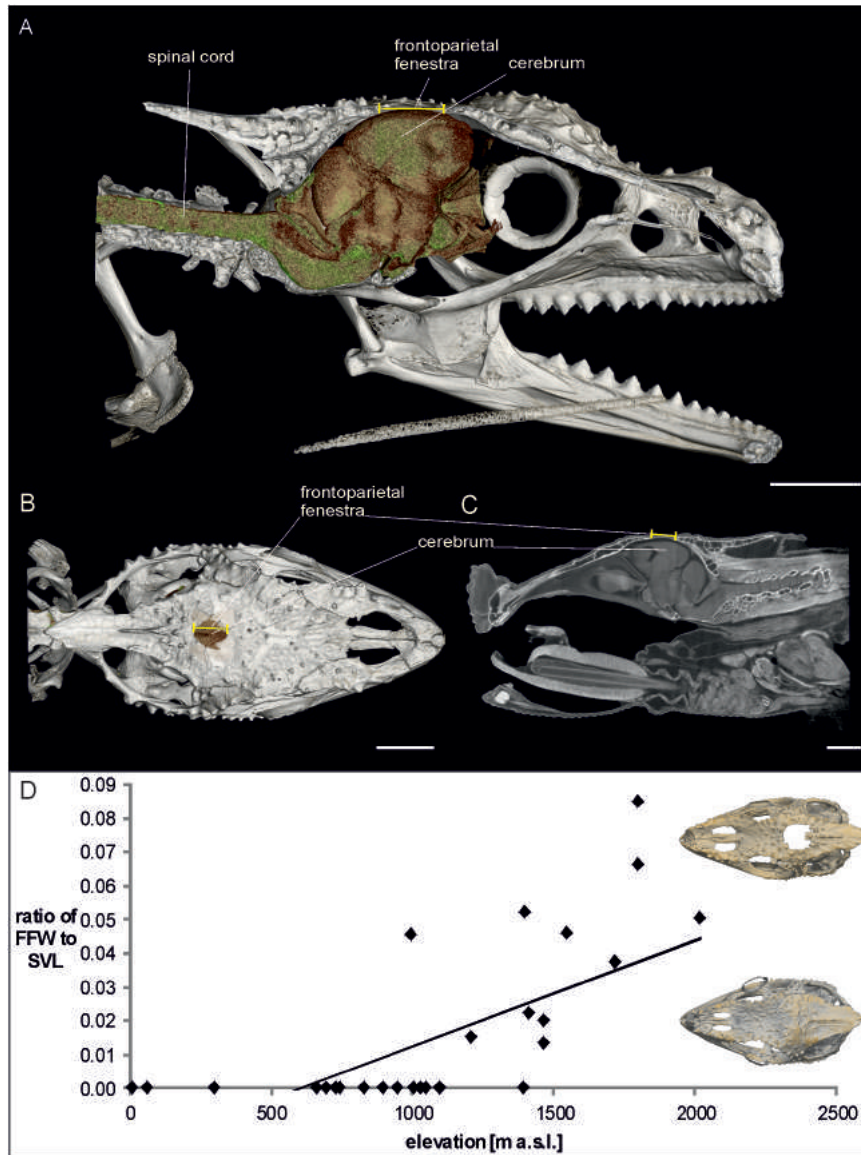
Figure 10. DiceCT scan integrated into micro-CT scan of the skull of *Calumma gehringi* (ZSM 2840/2010), showing the position of the brain below the frontoparietal fenestra. A, lateral view on midsagittal section of three-dimensional model. B, dorsal view on three-dimensional model. C, lateral view on midsagittal section (diceCT only). D, correlation of elevation and presence/width of the frontoparietal fenestra in the *Calumma nasutum* group, based on data in Table 4. Scale bars: 2.0 mm.

that high genetic distances alone should not be a decisive criterion for species delimitation but can serve only as a first step in an integrative species delimitation pipeline (Padial *et al.*, 2010). However, we cannot exclude the possibility that future, detailed studies of gene flow in the contact zones between these sublineages will reveal that they represent independent evolutionary lineages.

The smallest species within the *C. boettgeri* complex so far is *C. uetzi* sp. nov., with a total length of ~10 cm

in an adult male. Based on the clearly notched occipital lobes and its distribution north of Tsaratanana, it appears phenotypically similar to *C. gehringi* and *C. guibei*, but in contrast to those species it has no frontoparietal fenestra but a completely closed cranium. The species has an impressive display coloration in males (Fig. 2C). Sexual selection is probably responsible for the expression of conspicuous, contrasting colours in the males, as has been reported from some *Bradypodion* chameleons from South Africa (Stuart-Fox & Moussalli,

Table 4. Species and taxonomic units of *Calumma nasutum* group checked for frontoparietal fenestra

Species	Collection number	Clade (Gehring *et al.*, 2012)	Elevation (m)	Locality	Sex	SVL	FFW	RFWSL
C. boettgeri	ZSM 440/2000	D	65	Nosy Be	m	50.1	0	0
C. boettgeri	ZSM 444/2000	D	65	Nosy Be	m	51.9	0	0
C. boettgeri	ZSM 441/2000	D	65	Nosy Be	f	45.5	0	0
C. fallax (cf.)	ZSM 693/2003	H	1000	Ranomafana	m	46.2	2.1	0.045
C. gallus	ZSM 691/2009	A	300	Ambatoroma	f	44.1	0	0
C. gehringi	ZSM 2851/2010	E	1207	Antsahani Ledy	m	52.6	0.8	0.015
C. gehringi	ZSM 2840/2010	E	1411	Ambodikakazo	m	49.3	1.1	0.022
C. gehringi	ZSM 2841/2010	E	1466	Bemanevika	m	44.7	0.9	0.020
C. gehringi	ZSM 2842/2010	E	1466	Bemanevika	m	51.6	0.7	0.014
C. guibei	MNHN 50.354	—	1800	Tsaratanana	—	33.4	2.8	0.085
C. guibei	MNHN 57.115	—	1800	Tsaratanana	—	33.3	2.2	0.066
C. guibei	ZSM 2855/2010	F	2021	Tsaratanana	m	51.7	2.6	0.050
C. juliae sp. nov.	ZSM 143/2016	—	950	Moramanga	f	55.8	0	0
C. juliae sp. nov.	ZSM 254/2016	—	950	Moramanga	f	58.4	0	0
C. lefona sp. nov.	ZSM 2849/2010	F	1717	Andrevorevo	m	51.3	1.92	0.037
C. linotum	ZSM 1683/2012	D	830	M. d'Ambre	m	53.0	0	0
C. linotum	ZSM 2073/2007	D	1050	M. d'Ambre	m	59.6	0	0
C. linotum	ZSM 2072/2007	D	1050	M. d'Ambre	m	53.7	0	0
C. linotum	ZSM 551/2001	D	730	Andampy	f	50.6	0	0
C. nasutum	ZSM 134/2005	J	1548	Andohahela	m	50.1	2.3	0.046
C. nasutum	ZSM 35/2016	I	1400	Bealanana	m	48.3	2.5	0.052
C. nasutum	ZSM 618/ 2009	B	1100	Makira Plateau	m	47.9	0	0
C. nasutum	ZSM 735/2003	J	900	Ranomafana	f	45.5	0	0
C. nasutum	ZSM 619/ 2009	G	1009	Makira Plateau	m	49.2	0	0
C. nasutum	ZSM 663/2014	B	1009	Makira Plateau	m	48.7	0	0
C. nasutum	ZSM 441/2005	G	746	Marojejy	m	48.9	0	0
C. nasutum	ZSM 135/2005	B	700	Vohidrazana	f	47.6	0	0
C. nasutum	ZSM 136/2005	B	700	Vohidrazana	f	47.1	0	0
C. nasutum	ZSM 924/2003	K	900	Andasibe	m	43.7	0	0
C. nasutum	ZSM 553/2001	B	900	Andasibe	f	49.1	0	0
C. nasutum	ZSM 661/2014	B	1032	Ambodisakoa	f	45.0	0	0
C. nasutum	ZSM 662/2014	B	1032	Ambodisakoa	f	40.1	0	0
C. uetzi sp. nov.	ZSM 1688/2012	—	1100	Sorata	m	45.7	0	0
C. uetzi sp. nov.	ZSM 1686/2012	—	1396	Sorata	jm	37.3	0	0
C. vatosoa	MRSN R1628	—	665	Foret de Tsararano	m	57.9	0	0
C. vohibola	ZSM 645/2009	C	9	Vohibola	m	46.9	0	0

The presence and measurements of the frontoparietal fenestra are based on micro-CT scans.
F, female; FFW, width of the frontoparietal fenestra; m, male; RFWSL, ratio of FFW and SVL; SVL, snout–vent length.

2008). Females, however, do not invest as much in social signalling and only show yellow and blue dots on their heads to reject the males. The rest of the body is an indistinct brown colour and well camouflaged.

Calumma lefona sp. nov. has some intermediate morphological and ecological features of *C. gehringi* and *C. guibei* (Prötzel *et al.*, 2017) with regard to elevational distribution and morphology, e.g. the diameter of the frontoparietal fenestra. It differs clearly in size and the number of tubercle scales on the rostral appendage, as already mentioned by Gehring *et al.*

(2012). Unfortunately, no photographs of this species in life are available.

Despite intense searches on three different expeditions at different seasons of the year, no male individual of *C. juliae* sp. nov. has yet been found. Given that chameleons in general exhibit strong sexual dimorphism (Stuart-Fox *et al.*, 2006; Karsten *et al.*, 2009; da Silva *et al.*, 2014), females show fewer diagnostic characters than males, in the *C. nasutum* group, for example, in terms of coloration, length of the rostral appendage, casque height and some osteological

Table 5. Diagnostic characters of species of the *Calumma boettgeri* group supplementary to the identification key (Fig. 9)

Species	Total length	Snout–vent length	Diameter of tubercle scales on extremities	Parietal crest	Temporal crest	Notch of occipital lobes	Fronto-parietal fenestra	Dorsal crest (number of cones)	Shape of rostral appendage
C. boettgeri	83.8–110.3	41.1–55.5	≤ 0.5	–	–	0–0.7	–	0–28	Rounded
C. gehringi	92.6–121.5	45.1–55.4	0.5–0.9	–	+/–	0.5–1.5	+	0–15	Rounded
C. guibei	93.6–115.8	48.1-53-7	0.5–0.7	+	–	1.2–1.9	+	0	Rounded
C. juliae **sp. nov.**	105.3–111.6	53.3–59.4	0.5–0.8	–	–	0.2–0.8	–	11–14	Rounded
C. lefona **sp. nov.**	113.7	51.3	0.5	+	+	1.8	+	23	Pointed
C. linotum	90.1–126.1	42.7–59.6	0.4–0.8	+	+	0–0.3	–	0–13	Rounded
C. uetzi **sp. nov.**	87.3–101.2	42.0–45.7	0.4–0.5	+	+	0.5–1.0	–	5–14	Rounded

All measurements are in millimetres.

characters. Nevertheless, it was possible to delimit the specimens from female *C. linotum* and *C. boettgeri*, which are the closest related taxa (Fig. 1), primarily focusing on the clearly notched occipital lobes and the presence of a dorsal crest of 11–14 cones. Additionally, the morphology of the skull, investigated by micro-CT scans, differs in the shape of the frontal and parietal, and the squamosal not meeting the parietal. Although the observed females of *C. juliae* sp. nov. were genetically very similar (all *ND2* sequences were identical; Table 3), we still suspect that males exist but have gone undetected until now, and consider it unlikely that our sex ratio is a result of an unusual reproductive mode, such as parthenogenesis. Parthenogenetic reproduction has been reported recently for different squamate taxa, but not for chameleons so far (Booth *et al.*, 2012). Pasteur & Blanc (1991) also hypothesized parthenogenesis for *Lygodactylus pauliani* Pasteur & Blanc, 1991, which is also known only from female specimens. This might be an interesting project for further studies. Furthermore, the disjunct distribution of *C. juliae* sp. nov. relative to *C. linotum* and *C. boettgeri* with a distance of ~600 km raises questions regarding the biogeography of this clade, but interpretation on this matter should be forestalled until better sampling is attained in forests of the northern east and eastern north of Madagascar.

MICRO-COMPUTED TOMOGRAPHY AS A TAXONOMIC TOOL

Micro-CT scans have proved once more (Prötzel *et al.*, 2015, 2017) to be a helpful tool for taxonomy to uncover diagnostic characters of the skull in rather cryptic species (Bickford *et al.*, 2007). Osteological measurements appear to be more reliable for diagnosis than some external morphological characters, e.g. length and shape of rostral appendage or number of dorsal cones (Table 1), although at present sample sizes per species

are low. The osteology of males and females within one species is also similar to the sexual dimorphism in their external appearance. DiceCT scans of the hemipenis (Fig. 5) are a helpful addition for species delimitation (Klaver & Böhme, 1986; Prötzel *et al.*, 2015), but their value was again hampered by the incompleteness of eversion. Nevertheless, the scans provide an objective illustration that is largely free of interpretation compared with the usual drawings of hemipenes. Apparently, the description of the hemipenis of the holotype of *C. lefona* sp. nov. (ZSM 2849/2010) by Gehring *et al.* (2012), with 'much smaller and shallower calyces' and the absence of cornucula, resulted from an incompletely everted hemipenis, as shown in the scan (Fig. 5B). Furthermore, the morphology and functionality of such minuscule organs can be investigated conveniently using this approach. Upon changing the threshold in processing the scan, we found that the cornuculum is a structure of high density that can be retracted and everted, and its absence is thus easily misjudged (Fig. 5; Prötzel *et al.*, 2015, 2017).

FRONTOPARIETAL FENESTRA

Micro-CT scans revealed a frontoparietal fenestra in *C. lefona* sp. nov., which is an important diagnostic character in the *Calumma nasutum* group but also raises the question of its biological function. An FF has already been described for *C. fallax* and was explained as a variable degree of ossification or a variety of paedomorphism (Rieppel & Crumly, 1997). Some species of Lacertidae and the infraoder Iguania [e.g. *Acanthodactylus* sp.; *Basiliscus basiliscus* (Linnaeus, 1758); *Chalarodon madagascariensis* Peters, 1854; *Gallotia galloti* (Oudart, 1839); *Petrosaurus* sp.; *Uromastyx* sp. (Evans, 2008)] have a similar parietal foramen either within the frontal or parietal or within the suture of both bones. The foramen or fenestra in the roof of the skull locates the so-called 'third eye' or 'parietal eye' (Eakin, 1973).

This extraoptic photoreceptor is a part of the pineal complex and helps in orientation, in some instances by detection of polarization patterns of the sun/sky (Adler & Phillips, 1985; Ellis-Quinn & Simony, 1991). Although a parietal eye is well developed only in some species (see above), the pineal organ exists in all lizard species. In chameleons, a parietal spot, associated with the parietal organ, is visible in some genera, e.g. *Bradypodion*, *Chamaeleo* and *Furcifer* (Anderson & Higham, 2014) and absent in other genera, e.g. *Trioceros*. According to an investiagtion of Gundy & Wurst (1976b), *Chamaeleo chamaeleon* (Linnaeus, 1758), *Ch. gracilis* Hallowell, 1842 and *Furcifer pardalis* have a 'regressed' parietal eye that is lacking a distinct lens and retina, in contrast to most other investigated lizard species with a well-developed parietal eye. Histologically, the parietal eye appears as a hollow vesicle that is located in the parietal foramen and connected with the cerebrum via the pineal (Gundy & Wurst, 1976b). For *Calumma* no data are available, and we did not find any parietal spot *sensu* Gundy & Wurst (1976a) in the investigated specimens. However, the function of the pineal gland and the parietal organ, when present, is still unclear in chameleons (Nečas, 2004).

The opening in the skull roof in *Calumma* is considerably larger than the parietal foramen in lizards of the families Iguanidae or Lacertidae. The presence of this character in seven montane *Calumma* species suggests some evolutionary pressure towards its development and/or its retention. As shown in a diceCT scan, the chameleon brain is located directly below the FF (Fig. 10A–C). The FF presumably uncovers the cerebellum and/or the bordering optic lobe (Vitt & Caldwell, 2013). Chameleons are known for their excellent eyesight, with a relatively higher image magnification than other vertebrates (Ott & Schaeffel, 1995) and fast and independent eye movements (El Hassni *et al.*, 2000). We speculate that the optic sensory system of chameleons of the genus *Calumma* at high elevation might benefit from a skull opening for thermoregulative or light receptive reasons. Parts of the brain or the large optic root ganglion (Shanklin, 1930) might heat up faster in the sun than under a closed roof. The presence or absence of a fenestra in other chameleon genera in relationship to their elevational distribution remains to be assessed.

IMPLICATIONS FOR CONSERVATION

Two of the three chameleon species described here are known from a only single location, confirming the trend that many newly described lizard species have very small distribution ranges (Meiri *et al.*, 2018). Species with small geographical ranges bear a high risk of extinction by anthropogenic disturbances. This is also true for the three chameleon species described here

and puts them at potential risk, as reflected by our preliminary assessment of *C. uetzi* sp. nov. as Endangered and *C. juliae* sp. nov. as Critically Endangered. Both these species occur at least in part in unprotected forests that require urgent conservation efforts.

Calumma juliae sp. nov. is known from only a single small fragment of forest with an area of ~0.5 km × 0.3 km (0.15 km²), which is surrounded by rice fields, eucalyptus forests, and secondary habitats, where *C. juliae* sp. nov. is, as far as we know, not able to survive. This would give it the smallest known distribution of all chameleons so far, even smaller than *Rhampholeon chapmanorum* with a total range of 0.6 km² (Tolley, Menegon & Plumptre, 2014), and is reminiscent of the situation of the restricted (< 10 km²) and isolated habitat of *Calumna tarzan* (Gehring *et al.*, 2010; Jenkins *et al.*, 2011). Several paths through the forest and logged big trees indicate that the forest is already used for firewood by the local community, and its area is diminishing continuously; in 2016, a small area of the forest was burned (Fig. 8A). We recommend that this forest be protected as a nature reserve as soon as possible. The forest is located some 15 m from the Route Nationale 2, one of Madagascar's busiest tourist roads. Aside from *C. juliae* sp. nov., the forest is home to several other charismatic reptile and amphibian species, including the chameleons *Calumma gastrotaenia* (Boulenger, 1888), *C.* cf. *nasutum*, *Furcifer lateralis* (Gray, 1831), *Furcifer oustaleti* (Mocquard, 1894), *Furcifer willsii* (Günther, 1890); other lizards, e.g. the leaf-tailed gecko *Uroplatus phantasticus* Boulenger, 1888; and frogs, e.g. *Boophis erythrodactylus* (Guibé, 1953). These and other species would naturally benefit from the protection of the forest, as well as providing additional attraction for tourists.

The Sorata massif in northern Madagascar with an area of ~250 km² (as estimated in Google Earth) is the type locality of *Calumma uetzi* sp. nov. It is considerably larger and not as isolated from other similar forest habitats as the location of *C. juliae* sp. nov., and it harbours a much more diverse herpetofauna. In addition to *C. uetzi* sp. nov., several locally endemic frog species have been described recently or are currently under description: *Rhombophryne longicrus*, *Rhombophryne diadema* (Scherz *et al.*, 2015, 2017), two new *Stumpffia* species (Rakotoarison *et al.*, 2017) and other new species (e.g. *Gephyromantis* sp., *Uroplatus* sp.) still awaiting scientific description. Sorata is an extremely remote area, and as far as we know there has been only one other biodiversity survey in this area, which identified ten species of tenrecs and rodents from the area (Maminirina, Goodman & Raxworthy, 2008). The survival of the locally endemic species is threatened by deforestation, which is rampant in Madagascar (Harper *et al.*, 2007), and particularly serious on the Sorata massif. Fortunately, Sorata has already been included in plans to extend the

protected areas in this region of Madagascar, named COMATSA Nord (WWF Madagascar, 2015), which would extend protection also to cover the type locality of *C. lefona* sp. nov. and, in part, the distribution range of the recently described *C. gehringi* (Prötzel *et al.*, 2017). The second location of *C. uetzi* sp. nov. in Marojejy is already protected as a National Park. COMATSA will essentially connect Marojejy with Sorata through a conservation corridor (WWF Madagascar, 2015) and will therefore be an important addition to the network of protected areas in northern Madagascar.

The new species described here show that there are still new chameleon species left to discover in Madagascar, in remote areas like Sorata, as well as in comfortably accessible places, such as next to the Route Nationale 2, one of Madagascar's most heavily driven roads. If the rate of deforestation of Madagascan rainforests continues at the same rate as seen over the last decades (Harper *et al.*, 2007), it must be feared that some chameleon or other species will go extinct before their discovery (Costello, May & Stork, 2013), or that they already have done. Continued ambitious taxonomic investigations on Madagascar are required to assess the herpetofaunal biodiversity more completely and to provide a basis for sustainable, directed conservation efforts (Jenkins *et al.*, 2014).

KEY TO THE *CALUMMA BOETTGERI* COMPLEX

1a Small tubercle scales (diameter ≤ 0.5 mm) on extremities (Fig. 9A1), small body size (< 110 mm total length, ≤ 45 mm SVL) 2
1b Large tubercle scales (diameter 0.5–0.9 mm) on extremities (Fig. 9A2), large body size (generally > 110 mm total length, > 45 mm SVL)..3
2a Tubercle scales on extremities isolated from each other, supralabial scales serrated (Fig. 9B1), no temporal crest..***Calumma boettgeri***
2b Tubercle scales on extremities bordering each other, supralabial scales plain (Fig. 9B2), temporal crest present ....***Calumma uetzi* sp. nov.**
3a Occipital lobes not or only slightly separated (notch 0–0.8 mm; Fig. 9C1), no frontoparietal fenestra (closed skull roof)..4
3b Occipital lobes clearly separated (notch > 0.5 mm; Fig. 9C2), frontoparietal fenestra present (can be felt through the skin in alcohol-preserved specimens)..5
4a Temporal crest of one or two tubercles present (Fig. 9D1), zero to six dorsal cones in females, in life blue rostral appendage and green tubercles on extremities..***Calumma linotum***
4b Temporal crest absent (Fig. 9D2), dorsal crest in females of nine to 14 cones, in life rostral appendage and extremities beige or light green..***Calumma juliae* sp. nov.**
5a Large frontoparietal fenestra (Fig. 9E1), occipital lobes widely separated, dorsal and caudal crest absent, rostral appendage rounded..***Calumma guibei***
5b Small frontoparietal fenestra (Fig. 9E2), occipital lobes slightly connected, dorsal crest of seven to 15 distinct cones in males, no caudal crest, rostral appendage rounded ....***Calumma gehringi***
5c Medium-sized frontoparietal fenestra, occipital lobes completely separated, dorsal crest of > 20 small conical scales, caudal crest present, rostral appendage pointed > 5.5 mm (Fig. 9E3)...... ***Calumma lefona* sp. nov.**

REFERENCES

Adler K, Phillips JB. 1985. Orientation in a desert lizard (*Uma notata*): time-compensated compass movement and polarotaxis. *Journal of Comparative Physiology A* **156:** 547–552.

Anderson CV, Higham TE. 2014. Chameleon anatomy. In: Tolley KA, Herrel A, eds. *The biology of chameleons*. Berkeley: University of California Press, 7–55.

Andreone F, Mattioli F, Jesu R, Randrianirina JE. 2001. Two new chameleons of the genus *Calumma* from northeast Madagascar, with observations on hemipenial morphology in the *Calumma furcifer* group (Reptilia, Squamata, Chamaeleonidae). *Herpetologial Journal* **11:** 53–68.

Andriamialisoa F, Langrand O. 2003. The history of zoological exploration of Madagascar. In: Goodman SM, Benstead JP, eds. *The natural history of Madagascar*. Chicago and London: The University of Chigaco Press, 1–15.

Angel F. 1942. Les lézards de Madagascar. *Mémoires de l'Académie Malgache* **36:** 1–193.

Arnold EN. 1986. Mite pockets of lizards, a possible means of reducing damage by ectoparasites. *Biological Journal of the Linnean Society* **29:** 1–21.

Bickford D, Lohman DJ, Sodhi NS, Ng PK, Meier R, Winker K, Ingram KK, Das I. 2007. Cryptic species as a window on diversity and conservation. *Trends in Ecology and Evolution* **22:** 148–155.

Booth W, Smith CF, Eskridge PH, Hoss SK, Mendelson JR 3rd, Schuett GW. 2012. Facultative parthenogenesis discovered in wild vertebrates. *Biology Letters* **8:** 983–985.

Boulenger GA. 1888. Descriptions of two new chamaeleons from Nossi-Bé, Madagascar. *Annals and Magazine of Natural History* **6:** 22–23.

Boumans L, Vieites DR, Glaw F, Vences M. 2007. Geographical patterns of deep mitochondrial differentiation in widespread Malagasy reptiles. *Molecular Phylogenetics and Evolution* **45:** 822–839.

Bruford M, Hanotte O, Brookfield J, Burke T. 1992. Single-locus and multilocus DNA fingerprint. In: Hoelzel AR, ed. *Molecular genetic analysis of populations: a practical approach*. Oxford: IRL Press, 225–270.

Brygoo ER. 1971. Reptiles sauriens Chamaeleonidae. Genre *Chamaeleo. Faune de Madagascar* **33:** 1–318.

Brygoo ER. 1978. Reptiles Sauriens Chamaeleonidae. Genre *Brookesia* et complément pour le genre *Chamaeleo. Faune de Madagascar* **47:** 1–173.

Brygoo ER, Blanc CP, Domergue CA. 1974. Notes sur les *Chamaeleo* de Madagascar XII. Caméléons du Marojezy. *C. peyrierasi* n. sp. et *C. gastrotaenia guillaumeti* n. subsp. *Bulletin Academie Malgache* **51**(1973)**:** 151–166.

Costello MJ, May RM, Stork NE. 2013. Can we name Earth's species before they go extinct? *Science* **339:** 413–416.

Cuvier G. 1824. *Recherches sur les ossements fossiles, de quadrupèdes, où l'on rétablit les caractères du plusieurs espèces d'animaux que les révolutions du globe paroissent avoir détruites*. Paris: Dufour & d'Ocagne.

Cuvier G. 1829. *Règne animal*, 2: 60, note 1.

Darriba D, Taboada GL, Doallo R, Posada D. 2012. jModel-Test 2: more models, new heuristics and parallel computing. *Nature Methods* **9:** 772.

da Silva JM, Herrel A, Measey GJ, Tolley KA. 2014. Sexual dimorphism in bite performance drives morphological variation in chameleons. *PLoS One* **9:** e86846.

Duméril A, Bibron G. 1836. Erpétologie Générale ou Histoire Naturelle Complete des Reptiles. In: *Librairie encyclopédique de Roret*, Paris.

Eakin RM. 1973. *The third eye*. Berkely and Los Angeles: University of California Press.

Eckhardt FS, Gehring P-S, Bartel L, Bellmann J, Beuker J, Hahne D, Korte J, Knittel V, Mensch M, Nagel D, Pohl M, Rostosky C, Vierath V, Wilms V, Zenk J, Vences M. 2012. Assessing sexual dimorphism in a species of Malagasy chameleon (*Calumma boettgeri*) with a newly defined set of morphometric and meristic measurements. *Herpetology Notes* **5:** 335–344.

El Hassni M, Bennis M, Rio JP, Repérant J. 2000. Localization of motoneurons innervating the extraocular muscles in the chameleon (*Chamaeleo chameleon*). *Anatomy and Embryology* **201:** 63–74.

Ellis-Quinn BA, Simony CA. 1991. Lizard homing behavior: the role of the parietal eye during displacement and radio-tracking, and time-compensated celestial orientation in the lizard *Sceloporus jarrovi. Behavioral Ecology and Sociobiology* **28:** 397–407.

Evans S. 2008. The skull of lizards and tuatara. *Biology of the Reptilia* **20:** 1–347.

Gehring P-S, Pabijan M, Ratsoavina FM, Köhler J, Vences M, Glaw F. 2010. A Tarzan yell for conservation: a new chameleon, *Calumma tarzan* sp. n., proposed as a flagship species for the creation of new nature reserves in Madagascar. *Salamandra* **46:** 167–179.

Gehring P-S, Ratsoavina FM, Vences M, Glaw F. 2011. *Calumma vohibola*, a new chameleon species (Squamata: Chamaeleonidae) from the littoral forests of eastern Madagascar. *African Journal of Herpetology* **60:** 130–154.

Gehring PS, Tolley KA, Eckhardt FS, Townsend TM, Ziegler T, Ratsoavina F, Glaw F, Vences M. 2012. Hiding deep in the trees: discovery of divergent mitochondrial lineages in Malagasy chameleons of the *Calumma nasutum* group. *Ecology and Evolution* **2:** 1468–1479.

Gignac PM, Kley NJ, Clarke JA, Colbert MW, Morhardt AC, Cerio D, Cost IN, Cox PG, Daza JD, Early CM, Echols MS, Henkelman RM, Herdina AN, Holliday CM, Li Z, Mahlow K, Merchant S, Müller J, Orsbon CP, Paluh DJ, Thies ML, Tsai HP, Witmer LM. 2016. Diffusible iodine-based contrast-enhanced computed tomography (diceCT): an emerging tool for rapid, high-resolution, 3-D imaging of metazoan soft tissues. *Journal of Anatomy* **228:** 889–909.

Glaw F. 2015. Taxonomic checklist of chameleons (Squamata: Chamaeleonidae). *Vertebrate Zoology* **65:** 167–246.

Glaw F, Vences M. 2007. *A field guide to the amphibians and reptiles of Madagascar*. Cologne: Vences & Glaw Verlag.

Gray JE. 1831. A synopsis of the species of Class Reptilia. In: Griffith E, Pidgeon E. *The animal kingdom arranged in conformity with its organisation by the Baron Cuvier, with additional descriptions of all the species hitherto named, and of many not before noticed*. London: Whittaker, Treacher and Co.

Guibé J. 1953. Deux Hyperolius nouveaux pour la faune malgache (Batraciens). *Le Naturaliste Malgache* **5:** 101–103.

Gundy GC, Wurst GZ. 1976a. The occurrence of parietal eyes in recent Lacertilia (Reptilia). *Journal of Herpetology* **10:** 113–121.

Gundy GC, Wurst GZ. 1976b. Parietal eye-pineal morphology in lizards and its physiological implications. *The Anatomical Record* **185:** 419–431.

Günther A. 1877. Descriptions of some new species of reptiles from Madagascar. *Annals and Magazine of Natural History* **4:** 313–317.

Günther A. 1890. Tenth contribution to the knowledge of the fauna of Madagascar. *Annals and Magazine of Natural History* **6:** 69–72.

Hallowell E. 1842. Description of a new species of *Chameleon* from Western Africa. *Journal of the Academy of Natural Sciences of Philadelphia* **8:** 324–329.

Hammer Ø, Harper D, Ryan P. 2001. PAST: paleontological statistics software package for education and data analysis. *Palaeontolia Electronica* **4:** 9.

Han D, Zhou K, Bauer AM. 2004. Phylogenetic relationships among gekkotan lizards inferred from C-*mos* nuclear DNA sequences and a new classification of the Gekkota. *Biological Journal of the Linnean Society* **83:** 353–368.

Harper GJ, Steininger MK, Tucker CJ, Juhn D, Hawkins F. 2007. Fifty years of deforestation and forest fragmentation in Madagascar. *Environmental Conservation* **34:** 325–333.

Hedges SB. 1992. The number of replications needed for accurate estimation of the bootstrap P value in phylogenetic studies. *Molecular Biology and Evolution* **9:** 366–369.

Hillenius D. 1959. The differentiation within the genus *Chamaeleo* Laurenti, 1768. *Beaufortia* **8:** 1–92.

Hughes DF, Kusamba C, Behangana M, Greenbaum E. 2017. Integrative taxonomy of the Central African forest chameleon, *Kinyongia adolfifriderici* (Sauria: Chamaeleonidae), reveals underestimated species diversity in the Albertine Rift. *Zoological Journal of the Linnean Society* **181:** 1–39.

Hughes DF, Walker EM, Gignac PM, Martinez A, Negishi K, Lieb CS, Greenbaum E, Khan AM. 2016. Rescuing perishable neuroanatomical information from a threatened biodiversity hotspot: remote field methods for brain tissue preservation validated by cytoarchitectonic analysis, immunohistochemistry, and X-ray microcomputed tomography. *PLoS One* **11:** e0155824.

Hyde Roberts S, Daly C. 2014. A rapid herpetofaunal assessment of Nosy Komba Island, northwestern Madagascar, with new locality records for seventeen species. *Salamandra* **50:** 18–26.

IUCN. 2012. *IUCN red list categories and criteria: version 3.1.* Gland, Switzerland and Cambridge, UK: IUCN.

Jenkins RKB, Andreone F, Andriamazava A, Anjeriniaina M, Brady L, Glaw F, Griffiths RA, Rabibisoa N, Rakotomalala D, Randrianantoandro JC, Randrianiriana J, Randrianizahana H, Ratsoavina F, Robsomanitrandrasana E. 2011. *Calumma tarzan. The IUCN red list of threatened species*: e.T193482A8862229.

Jenkins RK, Tognelli MF, Bowles P, Cox N, Brown JL, Chan L, Andreone F, Andriamazava A, Andriantsimanarilafy RR, Anjeriniaina M, Bora P, Brady LD, Hantalalaina EF, Glaw F, Griffiths RA, Hilton-Taylor C, Hoffmann M, Katariya V, Rabibisoa NH, Rafanomezantsoa J, Rakotomalala D, Rakotondravony H, Rakotondrazafy NA, Ralambonirainy J, Ramanamanjato JB, Randriamahazo H, Randrianantoandro JC, Randrianasolo HH, Randrianirina JE, Randrianizahana H, Raselimanana AP, Rasolohery A, Ratsoavina FM, Raxworthy CJ, Robsomanitrandrasana E, Rollande F, van Dijk PP, Yoder AD, Vences M. 2014. Extinction risks and the conservation of Madagascar's reptiles. *PLoS One* **9:** e100173.

Karsten KB, Andriamandimbiarisoa LN, Fox SF, Raxworthy CJ. 2009. Sexual selection on body size and secondary sexual characters in two closely related, sympatric chameleons in Madagascar. *Behavioral Ecology* **20:** 1079–1088.

Klaver C, Böhme W. 1986. Phylogeny and classification of the Chamaeleonidae (Sauria) with special reference to hemipenis morphology. *Bonner Zoologische Monographien* **22:** 1–64.

Kumar S, Stecher G, Tamura K. 2016. MEGA7: Molecular Evolutionary Genetics Analysis Version 7.0 for Bigger Datasets. *Molecular Biology and Evolution* **33:** 1870–1874.

Linnaeus C. 1758. *Systema naturæ per regna tria naturæ, secundum classes, ordines, genera, species, cum characteribus, differentiis, synonymis, locis*. Laurentii Salvii, Holmiæ.

Macey JR, Larson A, Ananjeva NB, Fang Z, Papenfuss TJ. 1997. Two novel gene orders and the role of light-strand replication in rearrangement of the vertebrate mitochondrial genome. *Molecular Biology and Evolution* **14:** 91–104.

Macey JR, Schulte JA 2nd, Larson A, Ananjeva NB, Wang Y, Pethiyagoda R, Rastegar-Pouyani N, Papenfuss TJ. 2000. Evaluating trans-tethys migration: an example using acrodont lizard phylogenetics. *Systematic Biology* **49:** 233–256.

Maminirina CP, Goodman SM, Raxworthy CJ. 2008. Les micro-mammifères (Mammalia, Rodentia, Afrosoricida et Soricomorpha) du massif du Tsaratanana et biogéographie des forêts de montagne de Madagascar. *Zoosystema* **30:** 695–721.

Meiri S, Bauer AM, Allison A, Castro-Herrera F, Chirio L, Colli G, Das I, Doan TM, Glaw F, Grismer LL, Hoogmoed M, Kraus F, LeBreton M, Meirte D, Nagy ZT, de C. Nogueira C, Oliver P, Pauwels OSG, Pincheira-Donoso D, Shea G, Sindaco R, Tallowin OJS, Torres-Carvajal O, Trape JF, Uetz P, Wagner P, Ziegler T, Roll U. 2018. Extinct, obscure or imaginary: The lizard species with the smallest ranges. *Diversity & Distributions* **24:** 262–273.

Mocquard F. 1900. Diagnose d'espèces nouvelles de reptiles de Madagascar. *Bulletin du Muséum national d'Histoire naturelle* **6:** 345–348.

Müller L. 1924. Ueber ein neues Chamaeleon aus Madagaskar. *Mitteilungen aus dem Zoologischen Museum in Berlin* **11:** 95–96.

Nagy ZT, Sonet G, Glaw F, Vences M. 2012. First large-scale DNA barcoding assessment of reptiles in the biodiversity hotspot of Madagascar, based on newly designed COI primers. *PLoS One* **7:** e34506.

Nečas P. 2004. *Chameleons: nature's hidden jewels.* Frankfurt am Main: Edition Chimaira.

Ott M, Schaeffel F. 1995. A negatively powered lens in the chameleon. *Nature* **373:** 692–694.

Oudart PL, Barker-Webb P, Berthelot S. 1839. *Histoire Naturelle des Iles Canaries*. Tome deuxieme, deuxieme partie, Paris (Bethune).

Padial JM, Miralles A, De la Riva I, Vences M. 2010. The integrative future of taxonomy. *Frontiers in Zoology* **7:** 16.

Pasteur G, Blanc C. 1991. Un lézard parthénogénétique à Madagascar? Description de *Lygodactylus pauliani* sp. nov. (Reptilia, Gekkonidae). *Bulletin du Muséum national d'Histoire Naturelle Paris (4ème série)* **13:** 209–215.

Peters WCH. 1854. *Diagnosen neuer Batrachier, welche zusammen mit der früher (24. Juli und 17. August) gegebenen Übersicht der Schlangen und Eidechsen mitgetheilt werden*. Bericht über die zur Bekanntmachung geeigneten Verhandlungen der Königlichen Preussischen Akademie der Wissenschaften zu Berlin: 614–628.

Prötzel D, Heß M, Scherz MD, Schwager M, van't Padje A, Glaw F. **2018.** Widespread bone-based fluorescence in chameleons. *Scientific Reports*. 8(1): 698.

Prötzel D, Ruthensteiner B, Glaw F. 2016. No longer single! Description of female *Calumma vatosoa* (Squamata, Chamaeleonidae) including a review of the species and its systematic position. *Zoosystematics and Evolution* **92:** 13–21.

Prötzel D, Ruthensteiner B, Scherz MD, Glaw F. 2015. Systematic revision of the Malagasy chameleons *Calumma boettgeri* and *C. linotum* (Squamata: Chamaeleonidae). *Zootaxa* **4048:** 211–231.

Prötzel D, Vences M, Scherz MD, Vieites DR, Glaw F. 2017. Splitting and lumping: an integrative taxonomic assessment of Malagasy chameleons in the *Calumma guibei* complex results in the new species C. *gehringi* sp. nov. *Vertebrate Zoology* **67:** 231–249.

Rakotoarison A, Scherz MD, Glaw F, Köhler J, Andreone F, Franzen M, Glos J, Hawlitschek O, Jono T, Mori A, Ndriantsoa SH, Raminosoa N, Riemann JC, Rödel M-O, Rosa GM, Vieites DR, Crottini A, Vences M. 2017. Describing the smaller majority: integrative taxonomy reveals twenty-six new species of tiny microhylid frogs (genus *Stumpffia*) from Madagascar. *Vertebrate Zoology* **67:** 271–398.

Raxworthy CJ, Nussbaum RA. 2006. Six new species of occipital-lobed *Calumma* chameleons (Squamata: Chamaeleonidae) from montane regions of Madagascar, with a new description and revision of *Calumma brevicorne*. *Copeia* **2006:** 711–734.

Rieppel O, Crumly C. 1997. Paedomorphosis and skull structure in Malagasy chamaeleons (Reptilia: Chamaeleoninae). *Journal of Zoology* **243:** 351–380.

Ronquist F, Teslenko M, van der Mark P, Ayres DL, Darling A, Höhna S, Larget B, Liu L, Suchard MA, Huelsenbeck JP. 2012. MrBayes 3.2: efficient Bayesian phylogenetic inference and model choice across a large model space. *Systematic Biology* **61:** 539–542.

Salzburger W, Ewing GB, Von Haeseler A. 2011. The performance of phylogenetic algorithms in estimating haplotype genealogies with migration. *Molecular Ecology* **20:** 1952–1963.

Scherz MD, Hawlitschek O, Andreone F, Rakotoarison A, Vences M, Glaw F. 2017. A review of the taxonomy and osteology of the *Rhombophryne serratopalpebrosa* species group (Anura: Microhylidae) from Madagascar, with comments on the value of volume rendering of micro-CT data to taxonomists. *Zootaxa* **4273:** 301–340.

Scherz MD, Rakotoarison A, Hawlitschek O, Vences M, Glaw F. 2015. Leaping towards a saltatorial lifestyle? An unusually long-legged new species of *Rhombophryne* (Anura, Microhylidae) from the Sorata massif in northern Madagascar. *Zoosystematics and Evolution* **91:** 105–114.

Shanklin W. 1930. The central nervous system of *Chameleon vulgaris*. *Acta Zoologica* **11:** 425–490.

Stuart-Fox D, Firth D, Moussalli A, Whiting MJ. 2006. Multiple signals in chameleon contests: designing and analysing animal contests as a tournament. *Animal Behaviour* **71:** 1263–1271.

Stuart-Fox D, Moussalli A. 2008. Selection for social signalling drives the evolution of chameleon colour change. *PLoS Biology* **6:** e25.

Tolley KA, Menegon M, Plumptre A. 2014. *Rhampholeon chapmanorum. The IUCN red list of threatened species 2014: e.T172568A1345654.*

Tolley KA, Townsend TM, Vences M. 2013. Large-scale phylogeny of chameleons suggests African origins and Eocene diversification. *Proceedings of the Royal Society of London B: Biological Sciences*, **280:** 20130184.

Vitt LJ, Caldwell JP. 2013. *Herpetology: an introductory biology of amphibians and reptiles*. London, Waltham and San Diego: Academic Press.

WWF Madagascar. 2015. *Plan d'amenagement et de gestion integre du complexe d'aires protegées Ambohimirahavavy Marivorahona, Report Draft*. Available at: http://www.mrpa.mg/sites/default/files/download/Etudes/PAG/PAG%20CAPAM.pdf.

SUPPORTING INFORMATION

Additional Supporting Information may be found in the online version of this article at the publisher's web-site:

Video S1. 360° rotation of a micro-CT scan of the skull of the holotype of ***Calumma uetzi* sp. nov.** (ZSM 1688/2012).

Video S2. 360° rotation of a micro-CT scan of the hemipenis of the holotype of ***Calumma uetzi* sp. nov.** (ZSM 1688/2012).

Video S3. 360° rotation of a micro-CT scan of the skull of the holotype of ***Calumma lefona* sp. nov.** (ZSM 2849/2010).

Video S4. 360° rotation of a micro-CT scan of the skull of the holotype of ***Calumma juliae* sp. nov.** (ZSM 143/2016).

3.1.4 PAPER: The smallest 'true chameleon' from Madagascar: a new, distinctly colored species of the *Calumma boettgeri* complex (Squamata: Chamaeleonidae)

On a field trip to eastern Madagascar, the US-American and Malagasy students SML, GTA, and CRH (see below) found a novel-looking chameleon. They contacted our working group at the ZSM and sent us specimens for closer examination. Their discovery resulted in a new species of the *Calumma boettgeri* complex that was named *Calumma roaloko* referring to its characteristic two-toned body coloration. This species is apparently the smallest chameleon of all members of the Chamaeleoninae from Madagascar, though only five specimens are known to date. Further, the species is unique among Madagascan chameleons with its two-toned body colouration and it has surprisingly not been discovered at an earlier date although living in the highly frequented Andasibe region. Together with its sister taxon *C. uetzi* it is the only species within the *C. nasutum* group with a clear sexual dichromatism. This makes the group an interesting model to study the evolution of signals resulting from sexual versus natural selection as has been conducted by Stuart-Fox *et al.* (2007) in *Bradypodion.*

Prötzel, D, Lambert, SM, Andrianasolo, GT, Hutter, CR, Cobb, KA, Scherz, MD, Glaw, F (2018): The smallest 'true chameleon' from Madagascar: a new, distinctly colored species of the *Calumma boettgeri* complex (Squamata: Chamaeleonidae). *Zoosystematics and Evolution (94),* 409–423.

PENSOFT.

MUSEUM FÜR
NATURKUNDE
BERLIN

The smallest 'true chameleon' from Madagascar:
a new, distinctly colored species of the *Calumma boettgeri* complex
(Squamata, Chamaeleonidae)

David Prötzel[1], Shea M. Lambert[2], Ginah Tsiorisoa Andrianasolo[3], Carl R. Hutter[4], Kerry A. Cobb[5], Mark D. Scherz[1,6], Frank Glaw[1]

1   *Zoologische Staatssammlung München (ZSM-SNSB), Münchhausenstr. 21, 81247 München, Germany*

2   *Department of Ecology and Evolutionary Biology, University of Arizona, Tucson, AZ 85721, USA*

3   *Mention Zoologie et Biodiversité Animale, Université d'Antananarivo, BP 906, Antananarivo 101, Madagascar*

4   *Biodiversity Institute and Department of Ecology and Evolutionary Biology, University of Kansas, Lawrence, KS 66045–7561, USA*

5   *Department of Biological Sciences, Auburn University, Auburn, AL 36849, USA*

6   *Zoologisches Institut, Technische Universität Braunschweig, Mendelssohnstr. 4, 38106 Braunschweig, Germany*

http://zoobank.org/2433A9DD-8AC1-4139-A639-E24053D5C33F

Corresponding author: *David Prötzel* (david.proetzel@mail.de)

Abstract

On a recent expedition to eastern Madagascar, we discovered a distinct new species of the genus *Calumma* that we describe here using an integrative approach combining morphology, coloration, osteology and molecular genetics. *Calumma roaloko* **sp. n.** has a dermal rostral appendage and occipital lobes, and belongs to the *C. boettgeri* complex, within the Madagascar-endemic phenetic *C. nasutum* species group. It is readily distinguished from other species of the *C. boettgeri* complex by a characteristic two-toned body coloration and small body size with a snout-vent length of 45.6 mm in an adult male. The osteology of the skull, with a prominent maxilla and broad parietal, is similar to the closest related species, *C. uetzi*. Analysis of uncorrected genetic distances within the *C. nasutum* group using the mitochondrial gene ND2 shows a minimum pairwise distance of 11.98% to *C. uetzi* from the Sorata massif and Marojejy National Park >500 km north of the type locality of *C. roaloko* **sp. n.**. Given an apparently small range (potentially <300 km²), located entirely outside of any nationally-protected areas, we recommend this new species be classified as Endangered under criterion B1ab(iii) of the IUCN Red List. The discovery of clearly distinct species like *C. roaloko* **sp. n.** in an area of Madagascar that is comparatively thoroughly surveyed highlights the critical role of continued field surveys for understanding the true extent of Madagascar's spectacular biodiversity.

Introduction

The biota of Madagascar is recognized as exceptional, both in terms of endemism and density of species (Myers et al. 2000). In recent years, revised estimates of species richness for the island have revealed a significant underestimation of animal species richness by current taxonomy, e.g., in primates (Yoder et al. 2000), anurans (Vieites et al. 2009) and squamates (Nagy et al. 2012). In addition to the recognition of many morphologically

'cryptic' species (Bickford et al. 2006), often identified by the application of integrative taxonomy (Dayrat 2005, Padial et al. 2010), biodiversity field surveys in Madagascar continue to reveal morphologically distinct and often deeply divergent species, frequently characterized by restricted ranges and/or highly secretive habits (e.g., among herpetofauna, Nussbaum and Raxworthy 1994, Glaw et al. 1998, 2006, Vieites et al. 2010, Gehring et al. 2011, Rosa et al. 2014, Scherz et al. 2015, 2017, Lambert et al. 2017).

With currently 90 endemic species (Glaw 2015, Prötzel et al. 2017, 2018) chameleons are among the most diverse squamate families on Madagascar. The application of widespread genetic sampling and species delimitation methods (Gehring et al. 2012) confirmed long-standing suspicions that *Calumma nasutum* and other species are actually complexes of species (e.g., Hillenius 1959, Brygoo 1971, Glaw and Vences 2007). As many as 33 potential species (OTUs) were identified by Gehring et al. (2012) in the *C. nasutum* species group, but a higher taxonomic resolution awaits the completion of ongoing detailed morphological and genetic analyses (Prötzel et al. 2015, 2016, 2017, 2018).

The small-bodied chameleons of the *Calumma nasutum* group, usually characterized by their dermal rostral appendages, are distributed across the forests of eastern and northern Madagascar. Within this group, the species *C. boettgeri* (Boulenger, 1888), *C. guibei* (Hillenius, 1959) and *C. linotum* (Müller, 1924) differ from the others by the possession of well-defined occipital lobes and are referred to as the *C. boettgeri* complex (Gehring et al. 2012). Recently the number of species in the *C. boettgeri* complex has more than doubled with the description of *C. gehringi* Prötzel et al., 2017, *C. juliae* Prötzel et al., 2018, *C. lefona* Prötzel et al., 2018, and *C. uetzi* Prötzel et al., 2018 due to discoveries on recent expeditions. So far, *C. juliae* has been the only member of the *C. boettgeri* complex that occurs in eastern Madagascar; the other species are from northern Madagascar.

During fieldwork in a forest fragment within the Réserve de Ressources Naturelles du Corridor Ankeniheny-Zahamena just south of Andasibe-Mantadia National Park in 2015/2016, we discovered a small-bodied chameleon with distinct coloration belonging to the *Calumma nasutum* group. Integrating morphological, molecular, and osteological data, we describe this new species of the *C. boettgeri* complex.

Materials and methods

Specimen collection

We located specimens at night using targeted searches of arboreal habitats during the rainy season, using flashlights to locate sleeping individuals. Following euthanasia, we removed a portion of liver tissue and transferred it immediately into 95% ethanol for use in DNA extractions for genetic analyses. Specimens were fixed in 10% formalin (buffered to pH 7.0 with sodium phosphate), and transferred to 75% ethanol for long-term storage after approximately two weeks. We deposited the holotype and four paratypes at the University of Kansas Biodiversity Institute, Lawrence, KS (KU). Two of the paratypes will be repatriated to the Université d'Antananarivo, Mention de Zoologie et Biologie Animale (UADBA) probably during 2018 and one paratype was exchanged with the Zoologische Staatssammlung München (ZSM). All type specimens

will maintain their original KU museum number so that they can more easily be referenced in the future. SML refers to field numbers of S. M. Lambert.

Morphological investigation

Terms of morphological measurements taken on these specimens were adapted from previous studies (Prötzel et al. 2015, 2017). The following characters (Table 1) were measured with a digital caliper to the nearest 0.1 mm, counted using a binocular dissecting microscope, evaluated by eye or calculated: snout-vent length (SVL) from the snout tip (not including the rostral appendage) to the cloaca; tail length (TaL) from the cloaca to the tail tip; total length (TL) as a sum of SVL + TaL; ratio of TaL and SVL (RTaSV); length of the rostral appendage (LRA) from the upper snout tip; ratio of LRA and SVL (RRASV); diameter of rostral appendage (DRA), measured dorsoventrally at the widest point; ratio of DRA and SVL (RDRSV); number of scales across DRA (NDRA); number of tubercle scales (diameter >0.3 mm) on rostral appendage, counted on the right side (NSRA); ratio of NSRA and LRA (RNLRA); distinct rostral crest (RC) presence (+) or absence (–); lateral crest (LC), running from the posterior of the eye horizontally, presence (+) or absence (–); temporal crest, running dorsally to the LC, curving toward the midline, absence (–) or number of tubercles on left side (TCL) and right side (TCR); parietal crest (PC) presence (+) or absence (–); occipital lobes (OL) completely separated (s) or still, at least slightly, connected (c); depth of the dorsal notch in the occipital lobes (OLND); ratio of OLND and SVL (ROLSV); lateral diameter of OL (OLD); ratio of OLD and SVL (RODSV); width of OL measured at the broadest point (OLW); ratio of OLW and SVL (ROWSV); diameter of largest scale on OL (DSOL); diameter of largest scale on temporal region (DSCT), measured on the right side; dorsal crest (DC) absence (–) or number of dorsal cones visible to the naked eye without the use of a binocular microscope according to Eckhardt et al. (2012); diameter of broadest scales on the lower arm (DSA), defined as the area from the elbow to the manus in lateral view on the right side; number of scales on lower arm in a line from elbow to manus on the right side (NSA); number of supralabial scales (NSL), counted from the first scale next to the rostral to the last scale that borders directly and entirely (with one complete side) to the mouth slit of the upper jaw on the right side; and number of infralabial scales (NIL), analogous to the definition of NSL above, on the right side. Terminology of hemipenial structures follows Klaver and Böhme (1986) and Prötzel et al. (2017). For the "diagnosis", only adult specimens were considered. "Adult" is defined for specimens with 90–100% SVL of the largest specimen and additionally for males with completely developed hemipenes; "subadult" (subad.) refers to specimens with 70–90% of SVL and already developed hemipenes; "juvenile" is defined as <70% of SVL without any distinct sexual characteristics.

Table 1. Morphological measurements of *Calumma roaloko* sp. n. All measurements in mm. For abbreviations, see Materials and methods.

Final museum no.	KU 343178	KU 343168	ZSM 244/2018	UADBA-R (uncatalogued)	UADBA-R (uncatalogued)
original museum no.	KU 343178	KU 343168	KU 343177	KU 343176	KU 343167
field no.	SML 213	SML 177	SML 210	SML 178	SML 166
sex	adult male	adult female	subad. male	subad. male	subad. female
type status	holotype	paratype	paratype	paratype	paratype
altitude [m]	1100	1100	1100	1100	1100
SVL	45.6	44.5	37.6	38.6	40.0
TaL	48.1	41.0	44.3	42.3	34.8
TL	93.7	85.5	81.9	80.9	74.8
RTaSV	105%	92%	118%	110%	87%
LRA	5.2	2.3	4.6	3.9	2.7
RRASV	11.4%	5.2%	12.2%	10.1%	6.8%
DRA	2.6	1.9	2.3	2.7	1.6
RDRSV	5.7%	4.3%	6.1%	7.0%	4.0%
NDRA	5	6	4	5	7
NSRA	16	29	28	33	31
RNLRA	3.1	12.6	6.1	8.5	11.5
RC	+	+	+	+	+
LC	+	+	+	+	+
TCL	–	–	–	–	–
TCR	–	–	–	–	–
PC	+	–	–	–	–
OL	c	c	c	c	c
OLND	0.4	0.2	0.3	0.2	0.3
RODSV	8.8%	10.1%	10.4%	10.6%	10.3%
OLD	4.0	4.5	3.9	4.1	4.1
ROLSV	4.6%	4.3%	5.1%	5.2%	4.5%
OLW	2.1	1.9	1.9	2.0	1.8
ROWSV	0.9%	0.4%	0.8%	0.5%	0.8%
DSOL	0.7	0.5	0.7	0.6	0.7
DSCT	0.7	0.6	0.7	0.6	0.6
DC	2	0	1	0	0
DSA	0.7	0.5	0.5	0.4	0.4
NSA	11	14	13	15	15
NSL	13	13	13	13	13
NIL	13	14	13	13	12

Micro-CT

For internal morphology, micro-Computed Tomography (micro-CT) scans of the head were prepared for the male holotype KU 343178 and the female paratype KU 343168. For micro-CT scanning, specimens were placed in a closed plastic vessel slightly larger than the specimen with the head oriented upwards and stabilized with ethanol-soaked paper. To avoid artifacts, it was ensured that the paper did not cover the head region. Micro-CT scanning was performed with a phoenix|x nanotom m (GE Measurement & Control, Wunstorf, Germany) using a tungsten or diamond target at a voltage of 130 kV and a current of 80 µA for 29 minutes (1800 projections). 3D data sets were processed with VG Studio Max 2.2 (Visual Graphics GmbH, Heidelberg, Germany); the data were visualized using the Phong volume renderer to show the surface of the skull and reflect a variety of different levels of x-ray absorption following recommendations of Scherz et al. (2017). Osteological terminology follows Rieppel and Crumly (1997). Measurements were taken in VG Studio Max 2.2 using the caliper tool, given the following abbreviations (Table 2, Fig. 1): nasal length (NaL); frontal width measured at prefrontal border (FWPf); frontal width measured at anterior border to postorbitofrontal (FWPo); frontal width measured at frontal-parietal-border (FWPa); parietal width measured at posterior border to postorbitofrontal (PWPo); parietal width at midpoint (PWm); parietal length (PL); frontal length (FL); snout-casque length, measured from tip of upper jaw to posterior end of parietal (SCL); skull length, measured from tip of upper jaw to skull capsule (SkL); the respective ratios, divided by SkL, are indicated with an 'R' in front of the character-abbreviations.
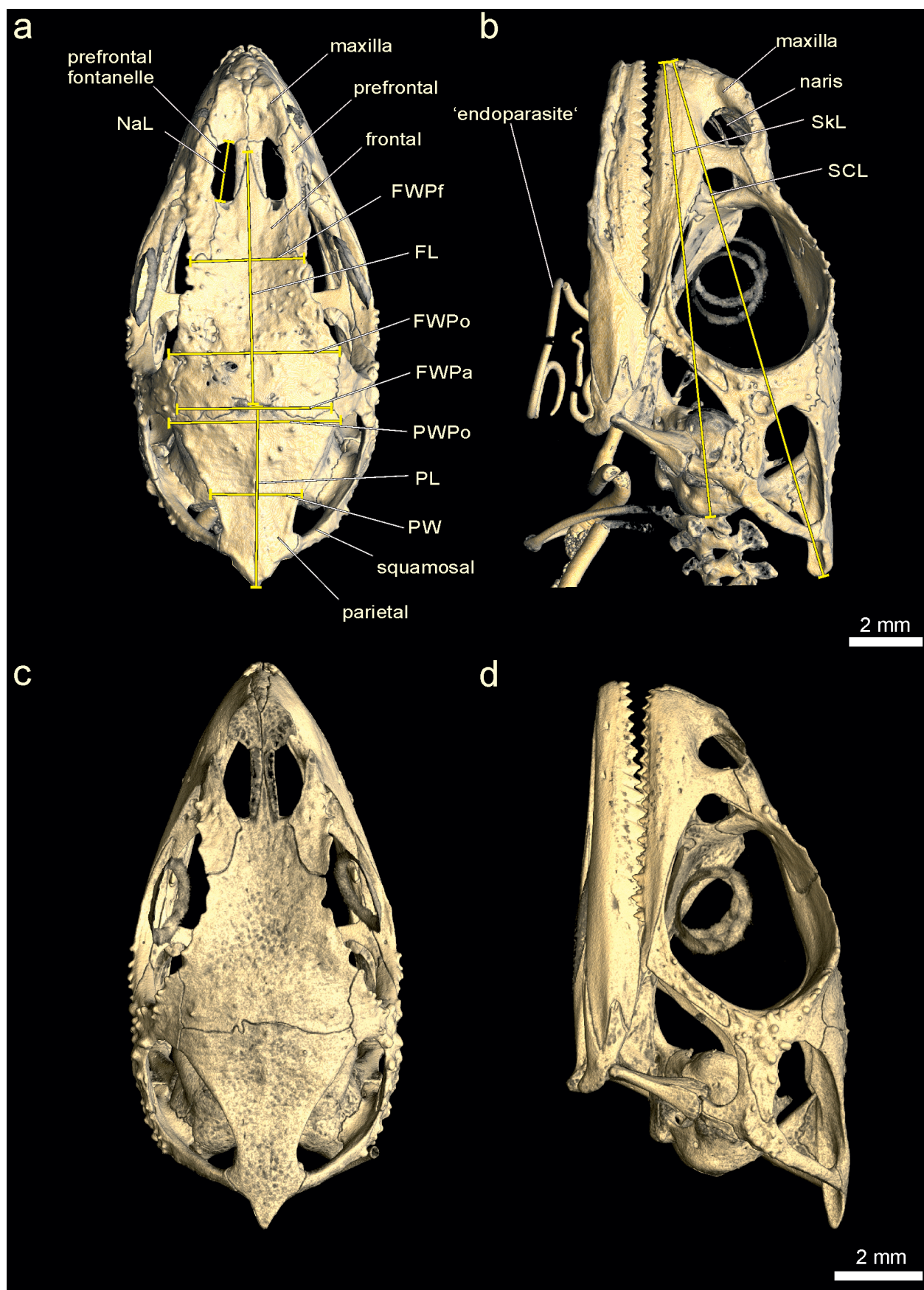
Figure 1. Micro-CT scans of skulls of *Calumma roaloko* sp. n. Male holotype KU 343178 in dorsal view (**a**) and lateral view (**b**), note the worm-like structure (presumably an endoparasite) in the throat of the holotype; female KU 343168 in dorsal view (**c**) and lateral view (**d**). See Materials and methods for abbreviations. See also Suppl. material 3 and 4 for a 360° movie of the skull.

Table 2. Osteological measurements based on micro–CT scans of the skulls of the male holotype and an adult female of *Calumma roaloko* sp. n. All measurements in mm. For abbreviations, see Materials and methods.

Collection no.	KU 343178	KU 343168
field no.	SML 213	SML 177
sex	male	female
type status	holotype	paratype
NaL	1.4	1.8
RNaL	11.6%	15.7%
FWPf	3.2	2.8
RFWPf	26.4%	24.3%
FWPo	4.5	4.1
RFWPo	37.2%	35.7%
FWPa	4.1	3.9
RFWPa	33.9%	33.9%
PWPo	4.7	4.0
RPWPo	38.8%	34.8%
PWm	2.7	2.2
RPWm	22.3%	19.1%
PL	5.1	4.9
RPL	42.1%	42.6%
FL	7.0	6.0
RFL	57.9%	52.2%
SCL	14.5	13.5
RSCL	119.8%	117.4%
SkL	12.1	11.5

DNA sequencing and phylogenetic analysis

We extracted genomic DNA from tissue samples at the KU Biodiversity Institute using a phenol-chloroform protocol. We amplified two mitochondrial gene fragments, COI and ND2, using standard protocols. Primers and protocols used for ND2 are described in Gehring et al. (2011) for ND2 and in Nagy et al. (2012) for COI. For ND2 alignments, we used previously published sequences from Gehring et al. (2012) and Prötzel et al. (2018), supplemented by sequences of the new species described herein (Fig. 2). For COI alignments, we downloaded all available sequences for the *C. nasutum* group taxa from GenBank. All newly generated sequences were submitted to GenBank (accession numbers MH668289–MH668297). We aligned sequences using MUSCLE (Edgar 2004) in Geneious version 6 (Kearse et al. 2012), under default settings. We manually inspected alignments for accuracy and open reading frames, but no changes were necessary. We calculated uncorrected pairwise genetic distances from our alignments in R v3.3.2 (R Development Core Team 2017), using the dist.dna function of the ape package (Paradis et al. 2004), with deletion of non-shared sites for each pairwise comparison. We used *C. oshaughnessyi* (FGZC 4577) as an outgroup.

Prior to phylogenetic analysis of the ND2 gene, conducted using maximum-likelihood in RAxML 8.2.6 (Stamatakis 2014), we used PartitionFinder2 (Lanfear et al. 2012) to select an optimal partitioning scheme. We provided the first, second, and third positions as initial partitions. As RAxML can only use a single model across all partitions, we evaluated only the 'GTR+G' model of sequence evolution. We then used the '-f a' option in RAxML to run 1000 rapid bootstraps and searched for the best-scoring maximum-likelihood tree, providing the optimal partitioning scheme identified by PartitionFinder2 using the '-q' option.

Registration of nomenclature

The electronic version of this article in Portable Document Format (PDF) will represent a published work according to the International Commission on Zoological Nomenclature (ICZN), and hence the new names contained in the electronic version are effectively published under that Code from the electronic edition alone. This published work and the nomenclatural acts it contains have been registered in ZooBank, the online registration system for the ICZN. The ZooBank LSIDs (Life Science Identifiers) can be resolved and the associated information viewed through any standard web browser by appending the LSID to the prefix http://zoobank.org/. The LSID for this publication is: urn:lsid:zoobank.org:pub:2433A9DD-8AC1-4139-A639-E24053D5C33F. The online version of this work will be archived and made available from the following digital repositories: CLOCKSS and Zenodo.

Results

Genetic differentiation in the *Calumma boettgeri* complex

The ND2 alignment contained 513 sites and a total of 235 variable sites, of which 177 were parsimony informative. The genetic analysis of the ND2 gene fragment (Fig. 2) revealed strong differences of the newly discovered form to all other species of the *C. boettgeri* complex including the three recently described species. Comparisons of genetic distance using mitochondrial genes show minimum distances of 11.98% in ND2 to *C. uetzi,* a species from Sorata and Marojejy (>500 km north from the type locality of our novel species) that was described only recently (Prötzel et al. 2018), and maximum distances to *C. boettgeri* and *C. gehringi* (>17%, Suppl. material 1). The intraspecific variation is small at 0.00–0.19%. In the COI sequences there is at least 12.20% distance between the collected specimens and all sequences available for the *C. nasutum* group, however *C. uetzi* is not included in this dataset (Suppl. material 2). According to the ND2 phylogeny (Fig. 2) *C. uetzi* is the sister taxon to the new species and together they form a clade which is sister to a clade including *C. boettgeri*, *C. linotum* and *C. juliae*. However, bootstrap values are relatively low, possibly due to the limited number of informative base-pairs. Supported by the genetic data provided we describe the following new species:
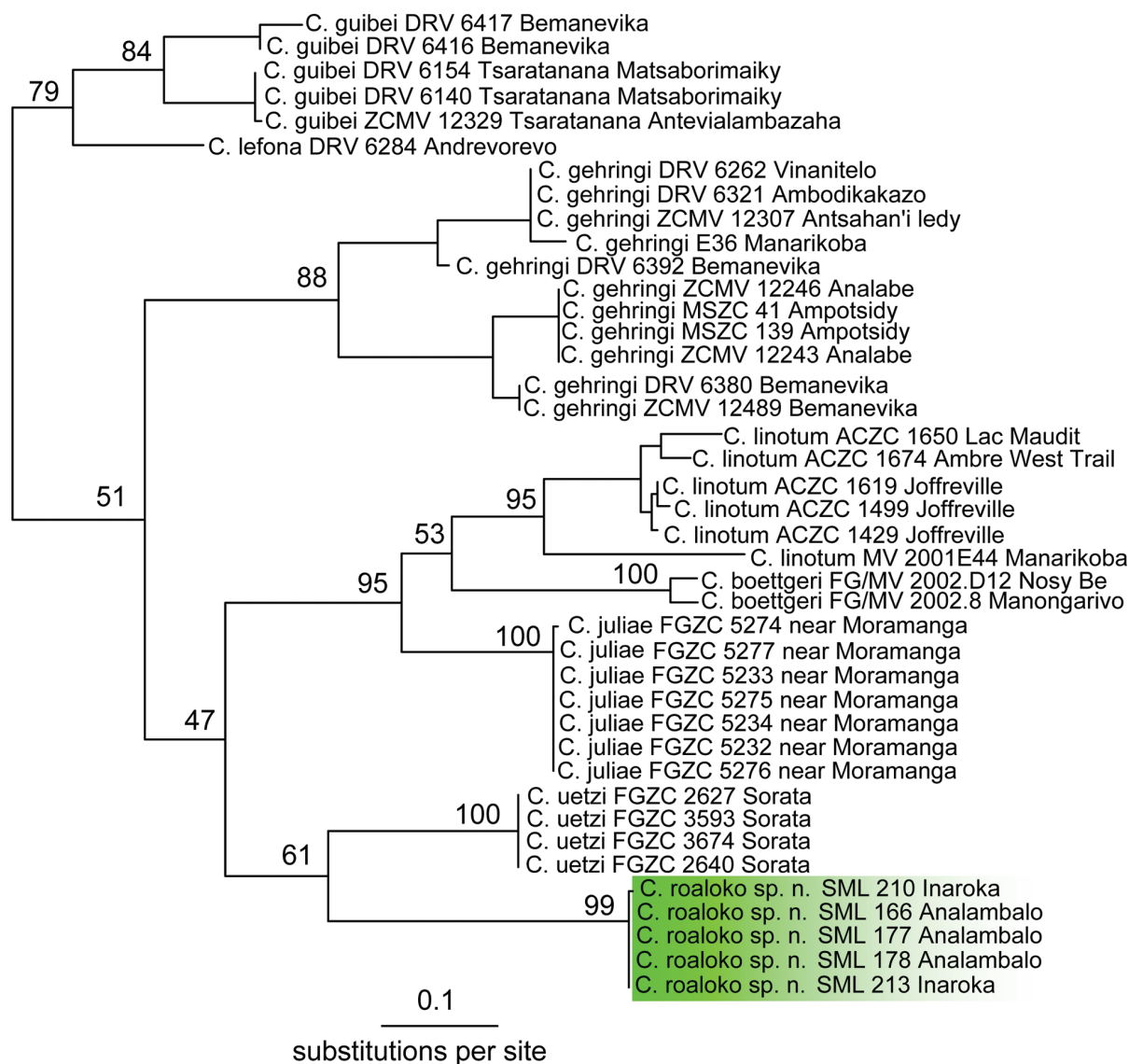
Figure 2. Maximum-likelihood tree of the *Calumma boettgeri* complex, based on 513 base-pairs of the mitochondrial ND2 gene. Nodal support values indicate the proportional support from 1000 rapid bootstrap replicates. Support values for intra-specific relationships are not shown. Outgroup (*C. oshaughnessyi* FGZC 4577) not shown for graphical reasons.

Calumma roaloko sp. n.

http://zoobank.org/B2018AA8-8C9A-4F1C-8B18-FA49ADA627EA

Suggested common English name: The two-toned soft-nosed chameleon
Suggested common Malagasy name: Tanalahy roa loko

Holotype. KU 343178 (field number SML 213), adult male in a good state of preservation with incompletely everted hemipenes (Fig. 3), collected on January 12th, 2016 by Shea M. Lambert, Carl R. Hutter, Kerry A. Cobb and Ginah Tsiorisoa Andrianasolo in mid-altitude rainforest, locally known as Inaroka (ca. 19.0050°S, 48.4613°E, ca. 1100 m a.s.l., Fig. 4) near Vohidrazana, Alaotra-Mangoro Region, in central-eastern Madagascar.

Paratypes. ZSM 244/2018 (KU 343177, field number SML 210), subadult male, same locality and collectors

as holotype; KU 343168 (field number SML 177), adult female, UADBA-R uncatalogued (KU 343176, field number SML 178), subadult male, and UADBA-R uncatalogued (KU 343167, field number SML 166), subadult female, all three collected on December 28th, 2015 (SML 166) and December 29th, 2015 (SML 177, 178) by Shea M. Lambert, Carl R. Hutter, Kerry A. Cobb and Ginah Tsiorisoa Andrianasolo in mid-elevation rainforest, locally known as Analambalo (ca. 18.9659°S, 48.4888°E, ca. 1100 m a.s.l., Figs 4–6) near Vohidrazana, Alaotra-Mangoro Region, in central-eastern Madagascar.

Diagnosis. *Calumma roaloko* sp. n. is a member of the phenetic *C. nasutum* species group (Prötzel et al. 2016), on the basis of the presence of a soft, dermal unpaired rostral appendage, absence of gular and ventral crests, and heterogeneous scalation on the lower
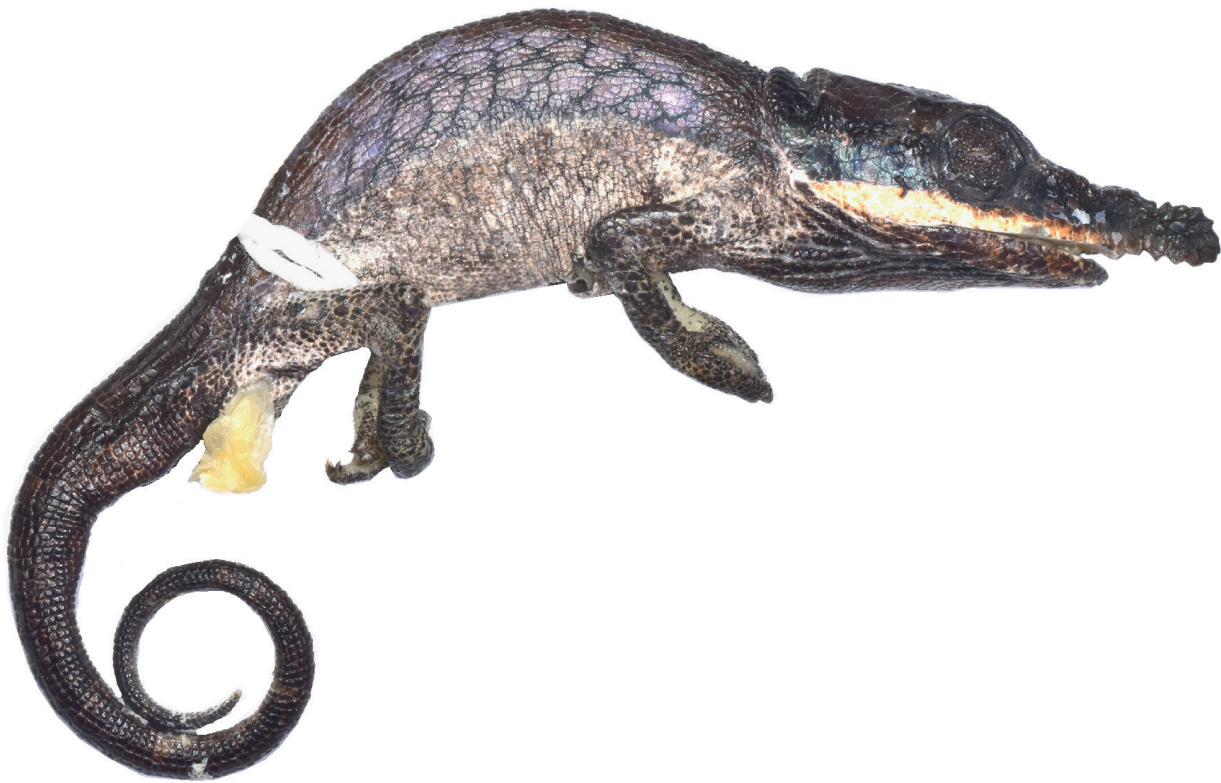
Figure 3. Preserved holotype (KU 343178) of *Calumma roaloko* sp. n. Scale bar = 10 mm.

arm, consisting mostly of tubercles of 0.4–0.7 mm diameter. With 44.5–45.6 mm SVL and 85.5–93.7 mm total length in adult specimens it is currently the smallest known species in the genus *Calumma*. The body of the chameleon is uniquely two-colored with beige/white on the ventral and bright green on the dorsal half. Furthermore, it is characterized by a prominent and distally rounded rostral appendage, occipital lobes that are slightly notched, a distinctly elevated rostral crest, absence of a dorsal crest (or presence of at most two cones) in both sexes, absence of axillary pits, and a unique skull morphology.

Calumma roaloko sp. n. differs from *C. fallax*, *C. gallus*, *C. nasutum*, *C. peyrierasi*, *C. vatosoa* and *C. vohibola* of the *C. nasutum* group by the presence of occipital lobes; from *C. boettgeri*, *C. gehringi*, *C. guibei*, *C. lefona*, *C. linotum* and *C. juliae* in the generally smaller body size with a maximum SVL of 45.6 mm and a maximum TL of 93.7 mm (vs. a range of SVL maxima in the former species of 49.1–59.6 mm and TL maxima of 98.7–126.1 mm), and a straight-lined dorsal margin of the supralabial scales vs. serrated (character 'en dents de scie' in Angel 1942); additionally from *C. gehringi*, *C. guibei*, and *C. lefona* in the slightly notched occipital lobes of 0.2–0.4 mm (vs. clearly notched with 0.5–1.8 mm) and in the absence of frontoparietal fenestra; from *C. boettgeri* by the large juxtaposed tubercle scales on the extremities (vs. isolated from each other).

From the most similar taxon *Calumma uetzi*, *C. roaloko* sp. n. differs in the absence of a dorsal crest or presence of at most two cones (vs. presence of 5–14 cones), absence of a temporal crest (vs. presence of 1–2 temporal tubercles), greater number of supralabial scales (13 vs. 10–12) and infralabial scales (12–14 vs. 11–12), a longer rostral appendage in adult males of 5.2 mm with large tubercle scales (vs. 3.8 mm, small and smooth tubercle scales; note: n = 1 each), and less heterogeneous scalation on the head with diameter of largest scale in temporal region of 0.6–0.7 mm (vs. 1.0–1.3 mm). The osteology of the skull is similar in both species; *C. roaloko* sp. n. differs from *C. uetzi* only in the absence of elevated protuberances at the anterior end of the maxilla that characterize the skull of male *C. uetzi*. *Calumma roaloko* sp. n. furthermore differs from all other species by distinct differences in the mitochondrial genes ND2 and COI and a unique two-colored life-coloration.

Description of the holotype. Adult male (Figs 3, 5b) in a good state of preservation; mouth slightly open; both hemipenes incompletely everted; SVL 45.6 mm, tail length 48.1 mm, for further measurements see Table 1; distinct and elevated rostral ridges that form a concave cup on the snout and fuse on the anterior snout at the base of a tapering, laterally compressed dermal rostral appendage that projects straight forward over a length of 5.2 mm with a diameter of 2.6 mm, rounded distally; 13 infralabi-
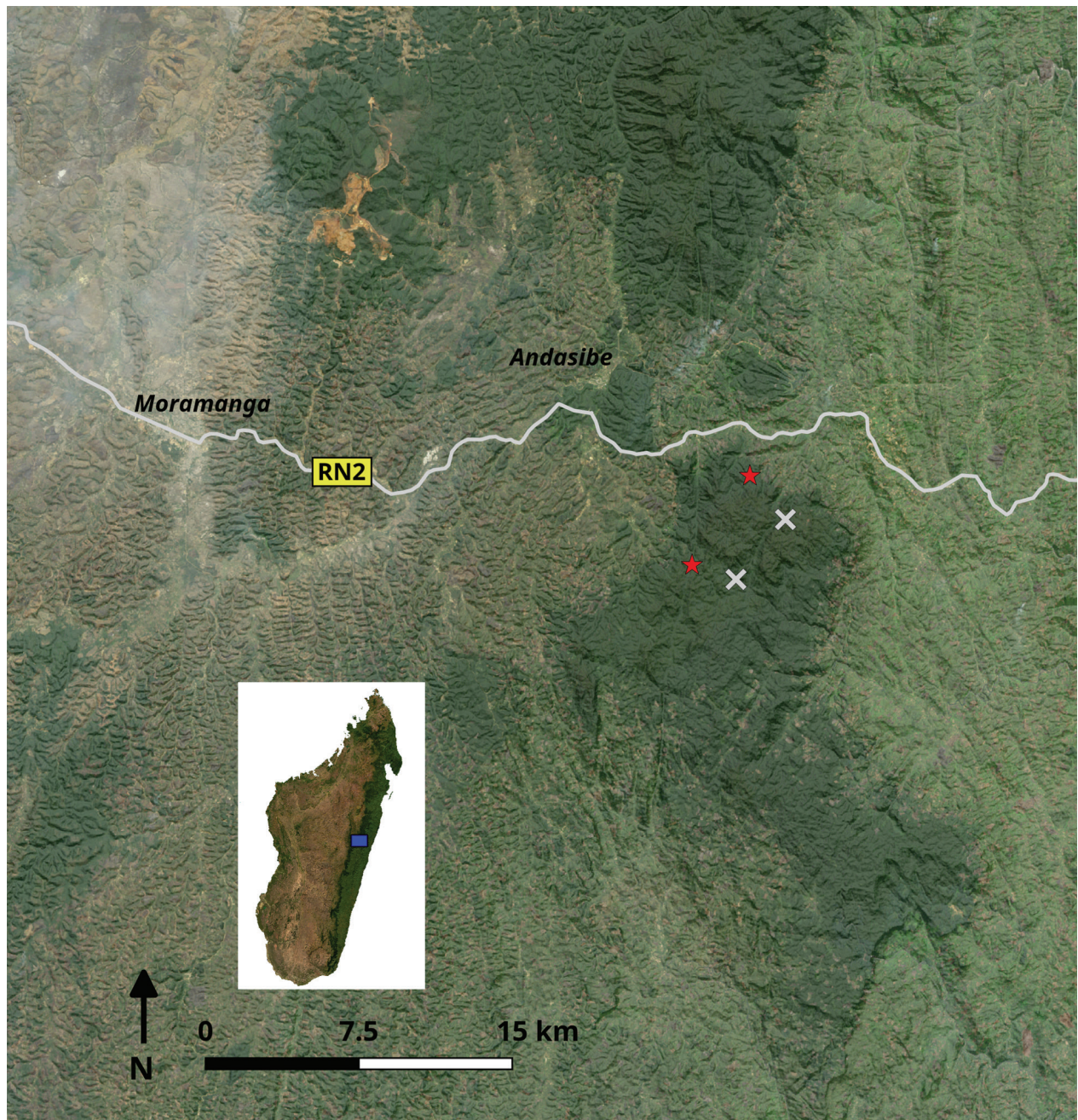
Figure 4. Map showing the location of the known range of *Calumma roaloko* sp. n. in central-eastern Madagascar. Red stars indicate localities where *C. roaloko* sp. n. was found, gray "X" indicate localities surveyed but with no detection of the species. The map is a composite of Landsat 7 and SRTM (Shuttle Radar Topographic Mission; Farr and Kobrick 2000) digital elevation data (U.S. Geological Survey (USGS) Earth Resources Observation and Science (EROS) Center) created in QGIS v2.18.

al and 13 supralabial scales; supralabials with a straight dorsal margin; no supra-orbital crest; distinct lateral crest running horizontally; no temporal crest; indistinct parietal crest; occipital lobes clearly developed and slightly notched (0.4 mm); casque raised; dorsal crest absent, only two single cones 0.7 and 1.1 mm from the base of the notch between the occipital lobes; no caudal crest; no traces of gular or ventral crest. Body laterally compressed with fine homogeneous scalation, slightly more heterogeneous on the extremities and head region; limbs with rounded tubercle scales with maximum of 0.7 mm diame-

ter; heterogeneous scalation on the head with largest scale on temporal region with diameter of 0.7 mm; 16 large, oval tubercle scales (diameter >0.3 mm) on the right side of the rostral appendage; no axillary or inguinal pits.

Skull osteology of the holotype. Description based on a micro-CT scan (Fig. 1a, b). Skull length 12.1 mm; snout-casque length 14.5 mm; maxillae dorsolaterally forming ridges—externally seen as rostral crest; narrow paired nasals tightly bordering anteriorly and separating frontal from maxillae; anterior tip of frontal exceeding more than
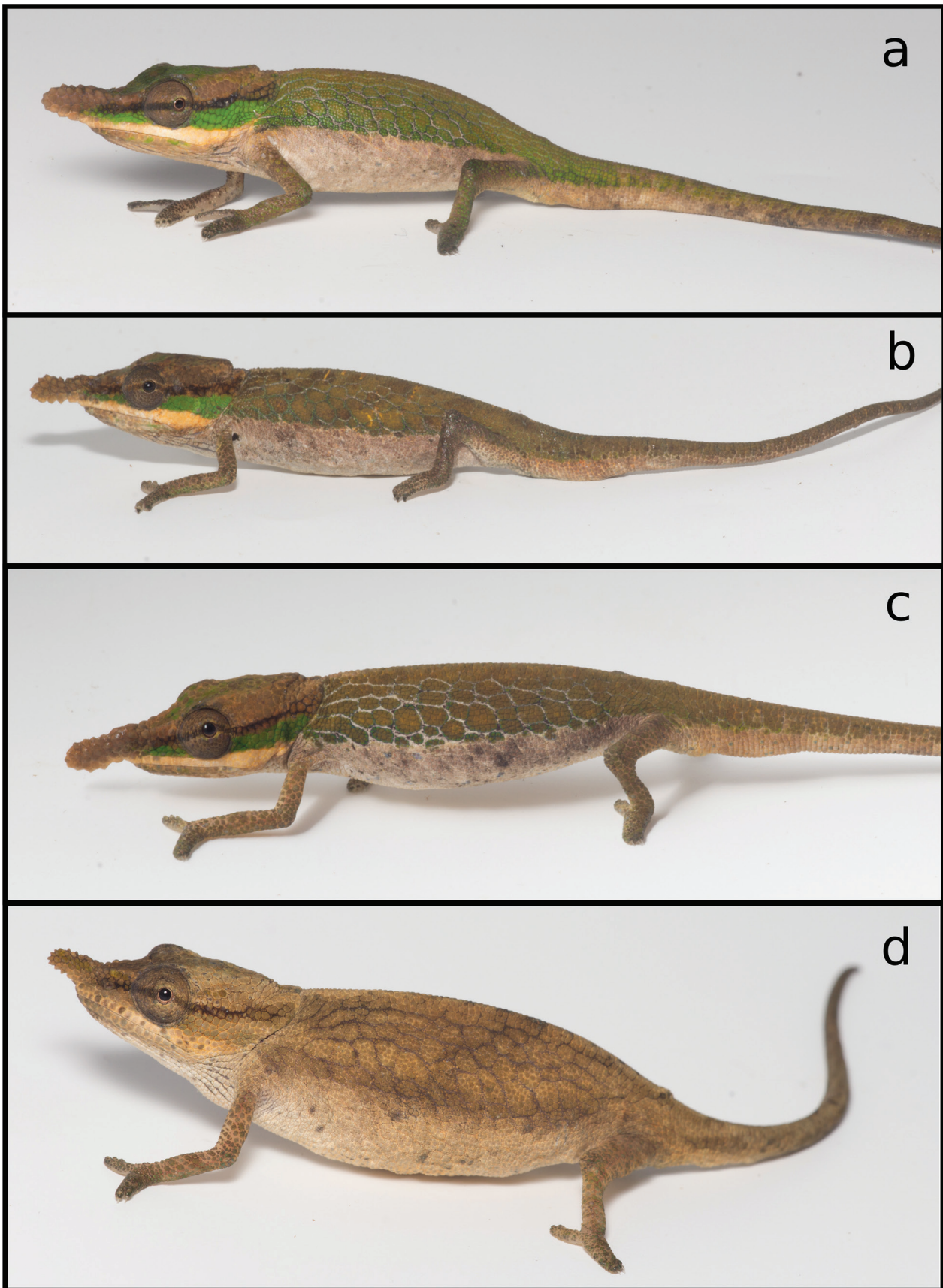
Figure 5. In-life photos of four specimens of *Calumma roaloko* sp. n.; (**a**) subadult male (ZSM 244/2018, KU 343177); (**b**) the holotype, adult male (KU 343178); (**c**) subadult male (UADBA-R, KU 343167); (**d**) adult female (KU 343168).

Figure 6. Posed photos of a subadult male specimen of *Calumma roaloko* sp. n. (ZSM 244/2018, KU 343177); (**a**) Indigo coloration on the rostral appendage and head scalation is apparent; (**b**) portrait of the same specimen.

half of the naris; prefrontal fontanelle and naris separated by contact of prefrontal with maxilla; frontal and parietal smooth with few tubercles; frontal with a width of 3.2 mm (26.4% of skull length) at border to prefrontal, extending to 4.5 mm (37.2%) at border to postorbitofrontal; broad parietal tapering more or less constantly from a width of 4.7 mm (38.8%) at the border to frontal and still broad at midpoint at 2.7 mm (22.3%) until it meets the squamosals, then narrowing to a tip; posterodorsally directed parietal in broad lateral contact with the squamosal; squamosal

thick with a few tubercles. For further measurements, see Table 2 and also Suppl. material 3 for a 360° video of the skull. The skull of *Calumma roaloko* sp. n. shows notable similarity to *C. uetzi* except for the shape of the maxilla.

The micro-CT scan uncovered a worm-like structure that lies curled and fractured in the throat and proceeds posteriorly into the chameleon's body presumably via the esophagus. We suppose that this shows an endoparasite trying to leave the dying chameleon after the processing, but note that it is remarkably strongly mineralized.

Coloration of the holotype in preservative. The body of the holotype in preservative (Fig. 3) is of gray and blue/violet color; the rostral appendage and the head are dark brown with a beige stripe from the snout tip via the supralabial scales to the ventral margin of the occipital lobes and a dark blue temporal region; broad lateral stripe on the body violet with a diffuse net-like pattern, tubercles on extremities also violet; ventral half of the body and inner side of extremities beige-white, dorsal margin of the body and tail of same dark brown color as the head.

Variation. The four paratypes agree well with the holotype in most characters of morphology and osteology. However, all four paratypes have more tubercle scales on rostral appendage on right side (28–33 vs. 16) and all paratypes lack a parietal crest (vs. indistinctly present); dorsal crest absent in UADBA-R (KU 343167), KU 343168, and UADBA-R (KU 343176). In osteology of the skull the only other micro-CT scanned specimen (the female KU 343168; Fig. 1c, d, Suppl. material 4) differs by the fused prefrontal fontanelle and naris, and the slightly narrower parietal with 34.8% of skull length at postorbitofrontal border (vs. 38.8%) and 19.1% of skull length at midpoint (vs. 22.3%). Both osteological characters can be attributed to sexual dimorphism or intraspecific variation.

Coloration in life. Based on observations and photographs of the type specimens (Figs 5–7) the species is sexually dichromatic, with males showing a body coloration with an olive green to bright green dorsal half of the body and beige to white ventral half that is continuing on the tail. Females are generally brown and tan or cream ventrally. Both sexes can display a netlike pattern caused by skin between scales in dark brown or beige. Extremities indistinct brown or beige; throat and upper labial scales beige in both sexes; rostral appendage of same brown color as the upper head region, can turn violet in males (Fig. 6a), as well as the eyes, with a beige line on ventral side; in females the appendage can turn yellowish (Fig. 7); dark lateral stripe from the base of the appendage crossing the eyes and ending at the occipital lobes; cheek region highlighted in bright green in the males, continued anteriorly to the base of the appendage.

Hemipenial morphology. The hemipenes of the three male specimens (the holotype KU 343178, UADBA-R (KU 343176), and ZSM 244/2018) are not completely everted and consequently we can only provide a preliminary and possibly incomplete description. On the asulcal side of the truncus the hemipenis shows large calyces with smooth ridges. The apex is ornamented with two pairs of rotulae, which are larger on the sulcal side (with 12–14 tips) and with 8–10 tips on asulcal side. In the holotype KU 343178 and UADBA-R (KU 343176) there is a small peak between the lobes on the posterior side that might be the tip of a cornuculum (Prötzel et al. 2017), but this interpretation is in need

of confirmation due to the incomplete eversion of the hemipenes. The top of the apex has a papillary field of several fleshy papillae.

Available names. There are no available names that could be attributed to a species of the *C. nasutum* group with occipital lobes.

Etymology. The specific epithet "roaloko" is a combination of the Malagasy words "roa" meaning "two" and "loko" meaning "color", in reference to the characteristic two-toned body colorations of males (green and white) and females (brown and tan) of this species. The epithet is to be treated as an invariable noun in apposition.

Natural history. The specific natural history of *C. roaloko* sp. n. is little-known, but assumed to be similar to other small-bodied *Calumma*. As with other *C. nasutum* group species, individuals of *C. roaloko* sp. n. were encountered sleeping at night on leaves (Fig. 7) or small branches, and most often spotted ~2–5 m above the ground. *Calumma roaloko* sp. n. may be restricted to higher-elevation habitats, as it has only been found at ca. 1100 m a.s.l., although this is difficult to determine with certainty as most forests below ~1000 m a.s.l. in the area have been cleared. Interestingly, it is known from only two sites, both on the periphery of the forest fragment, and characterized by qualitatively more degraded habitat and/or secondary forest growth as compared to two sites located with more intact primary forest, where it was not encountered (Fig. 4). In summary, either *C. roaloko* sp. n. may have a higher detection probability in disturbed habitats, and/or may be out-competed in primary forest by close relatives (e.g., *C. nasutum* complex species that we found in all four sites). Several specimens were observed to have small red acarid ectoparasites (visible on the hindlimb in Fig. 6a).

Distribution. Given current evidence, the distribution of *C. roaloko* sp. n. is potentially restricted to a small fragment (~300 km²) of mid-elevation rainforest that lies outside of nearby Analamazaotra Special Reserve and Andasibe-Mantadia National Park in central-eastern Madagascar (Fig. 4), but within the Réserve de Ressources Naturelles du Corridor Ankeniheny-Zahamena newly protected area. However, we believe that *C. roaloko* sp. n. may still be discovered in nearby areas, including Andasibe-Mantadia National Park, although it has never been found over dozens of surveys in nearby protected areas over the last century, including our own surveys (Hutter, Lambert, Scherz, Prötzel, Glaw, etc. unpubl. data). It is also possible that *C. roaloko* sp. n. could be found in other smaller and more fragmented forests located to the west of the type locality of *C. roaloko* sp. n., south of the city of Moramanga, but recent work in one remnant forest fragment in that area discovered *C. juliae* there, and no specimens of *C. roaloko* sp. n. were found (Prötzel et al. 2018).

Figure 7. In-situ photograph of an uncollected (in sleeping position) female of *Calumma roaloko* **sp. n.**, from the same locality as KU 343168.

Suggested Conservation Status. The ~300 km² fragment of mid-elevation rainforest from which *C. roaloko* sp. n. is known is managed by several local government councils, and has recently been established as a new protected area (Réserve de Ressources Naturelles du Corridor Ankeniheny-Zahamena) within the scope of the expansion of Madagascar's national parks (Gardner et al. 2018). Forest in this area is dramatically fragmented and its area is decreasing. We suggest to evaluate the species as Endangered under the IUCN Red List criterion B1 (Extent of occurrence <5000 km²) subcriteria a (severely fragmented or known from fewer than five threat-defined locations) and b(iii) (continuing decline in the area, extent, and/or quality of habitat). However, potentially suitable habitat for *C. roaloko* sp. n. also exists in other nearby protected areas (Andasibe-Mantadia, Analamazaotra) and private reserves (Vohimana). Although field surveys to these areas have not yet uncovered *C. roaloko* sp. n., they have revealed the presence of several other undescribed species of amphibians and reptiles, found originally in the same forest fragment as *C. roaloko* sp. n. (Hutter, unpubl. data). Furthermore, current evidence suggests that *C. roaloko* sp. n. is amenable to disturbed habitat (see Natural History). As such, the conservation status of *C. roaloko* sp. n. as suggested herein may need revision pending future survey work, particularly in nearby protected areas.

Discussion

The discovery of *C. roaloko* adds to a growing understanding of the diversity of small-bodied *Calumma* in Madagascar (Gehring et al. 2011, 2012, Prötzel et al. 2015, 2016, 2017, 2018). The *C. nasutum* group has grown significantly over the past few years, and is likely to continue to grow as taxonomic revision on it continues, and given the number of OTUs identified for the group by Gehring et al. (2012). Yet with this contribution and those of Prötzel et al. (2017, 2018), the *C. boettgeri* complex has expanded from three known species (Prötzel et al. 2015) to eight.

Biogeographically the pattern of diversity in the *C. nasutum* group currently suggests a complex history, possibly involving several major dispersal events, especially within the *C. boettgeri* complex, with *C. roaloko* being

sister to *C. uetzi*, a species found >500 km to the north in the Sorata massif and Marojejy NP (Prötzel et al. 2018), and a similar situation in the recently described *C. juli-ae*, whose sister species are *C. boettgeri* and *C. linotum*, separated also by over 500 km. These distributions highlight the north central east of Madagascar as an important biogeographic gap in the *C. boettgeri* complex that may yield intermediate members connecting these species over their long sister-pair distances.

With a total length of 93.7 mm and a body size of 45.6 mm in the largest specimen (the male holotype), *C. roaloko* represents the smallest member of the "true" chameleons, subfamily Chamaeleoninae, (excluding the small, mostly ground dwelling species of the subfamily Brookesiinae) on Madagascar, and one of the smallest members of the Chamaeleoninae in the world. Within the *C. nasutum* group *C. uetzi* (with maximum TL of 101.2 mm and maximum SVL of 45.7 mm) and *C. vohibola* (with maximum TL of 90.5 mm – resulting from a measuring error due to a cut-off tail for DNA analysis – and maximum SVL of 49.8 mm, Gehring et al. 2011) are only slightly larger. Other small species are *C. guillaumeti* and *C. peyrierasi* with below 110 mm (TL), but all of these data are based on relatively small sample sizes (Prötzel et al. 2016).

Interestingly, *Calumma roaloko* and its sister taxon *C. uetzi* are among the only species within the *C. nasutum* group with strong sexual dichromatism. Males of both species differ clearly from the females by a conspicuous display coloration that contrasts well from the green and brown overall background of their habitat as shown for some chameleon species of the genus *Bradypodion* (Stuart-Fox et al. 2007). Displaying male *C. roaloko* are still well-camouflaged however when seen from above due to the green color on the dorsal part of their bodies. Laterally, from a conspecific's eye perspective, they may signal with the white ventral body part and the violet rostral appendage—a strategy employed still more strongly in several other lizards, e.g. *Algyroides*, *Sceloporus*, *Uta* (Ossip-Drahos et al. 2016).

The increase in species richness in chameleons may come not only from the splitting of currently recognized and often widespread species (e.g., in the African chameleon genus *Kinyongia*, Hughes et al. 2017), but from the continued discovery of clearly distinct, previously unknown species, often with geographically or elevationally restricted ranges, and/or low detection probabilities, such as *C. roaloko* (see also Gehring et al. 2011 and Prötzel et al. 2018). Such discoveries highlight the unabated importance of field research for phylogenetic systematics. Indeed, far more examples of "unexpected" species discoveries, also revealed by recent field surveys, are found in other squamate lineages and tropical regions (Welton et al. 2010, Mahler et al. 2016), but also occur in other Malagasy herpetofauna (e.g. Glaw et al. 2006), as well as in other tropical vertebrate clades (e.g., in mammals, Helgen et al. 2013, Hrbek et al. 2014). Clearly, if we are to understand the evolutionary extent of Madagascar's many endemic radiations, and of biodiversity in the tropics generally, a great deal of basic field survey work yet remains.

Acknowledgements

References

Angel F (1942) Les lézards de Madagascar. Mémoires de l'Académie Malgache 36: 1–193.

Bickford D, Lohman DJ, Sodhi NS, Ng PKL, Meier R, Winker K, Ingram KK, Das I (2006) Cryptic species as a window on diversity and conservation. Trends in Ecology & Evolution 22(3): 148–155. https://doi.org/10.1016/j.tree.2006.11.004

Brygoo ER (1971) Reptiles Sauriens Chamaeleonidae – Genre *Chamaeleo*. Faune de Madagascar 33: 1–318.

Dayrat B (2005) Towards integrative taxonomy. Biological Journal of the Linnean Society 85(3): 407–415. https://doi.org/10.1111/j.1095-8312.2005.00503.x

Eckhardt FS, Gehring PS, Bartel L, Bellmann J, Beuker J, Hahne D, Korte J, Knittel V, Mensch M, Nagel D, Pohl M, Rostosky C, Vierath V, Wilms V, Zenk J, Vences M (2012) Assessing sexual dimorphism in a species of Malagasy chameleon (*Calumma boettgeri*) with a newly defined set of morphometric and meristic measurements. Herpetology Notes 5: 335–344.

Edgar RC (2004) *MUSCLE*: multiple sequence alignment with high accuracy and high throughput. Nucleic Acids Research 32(5): 1792–1797. https://doi.org/10.1093/nar/gkh340

Farr TG, Kobrick M (2000) Shuttle Radar Topography Mission produces a wealth of data. Eos, Transactions American Geophysical Union 81: 583–585. https://doi.org/10.1029/EO081i048p00583

Gardner CJ, Nicoll ME, Birkinshaw C, Harris A, Lewis RE, Rakotomalala D, Ratsifandrihamanana AN (2018) The rapid expansion of Madagascar's protected area system. Biological Conservation 220: 29–36. https://doi.org/10.1016/j.biocon.2018.02.011

Gehring P-S, Ratsoavina FM, Vences M, Glaw F (2011) *Calumma vohibola*, a new chameleon species (Squamata: Chamaeleonidae) from the littoral forests of eastern Madagascar. African Journal of Herpetology 60(2): 130–154. https://doi.org/10.1080/21564574.2011.628412

Gehring P-S, Tolley KA, Eckhardt FS, Townsend TM, Ziegler T, Ratsoavina F, Glaw F, Vences M (2012) Hiding deep in the trees: discovery of divergent mitochondrial lineages in Malagasy chameleons of the *Calumma nasutum* group. Ecology and Evolution 2(7): 1468–1479. https://doi.org/10.1002/ece3.269

Glaw F (2015) Taxonomic checklist of chameleons (Squamata: Chamaeleonidae). Vertebrate Zoology 65: 167–246.

Glaw F, Hoegg S, Vences M (2006) Discovery of a new basal relict lineage of Madagascan frogs and its implications for mantellid evolution. Zootaxa 1334: 27–43.

Glaw F, Vences M (2007) A Field Guide to the Amphibians and Reptiles of Madagascar. Third Edition. Vences & Glaw Verlag, Köln, 496 pp.

Glaw F, Vences M, Böhme W (1998) Systematic revision of the genus *Aglyptodactylus* Boulenger, 1919 (Anura: Ranidae) and analysis of its phylogenetic relationships with other ranid genera from Madagascar (*Tomopterna*, *Boophis*, *Mantidactylus* and *Mantella*). Journal of Zoological Systematics and Evolutionary Research 36: 17–37. https://doi.org/10.1111/j.1439-0469.1998.tb00775.x

Helgen KM, Pinto, CM, Kays R, Helgen LE, Tsuchiya MTN, Quinn A, Wilson DE, Maldonado JE (2013) Taxonomic revision of the olingos (*Bassaricyon*), with description of a new species, the Olinguito. ZooKeys 324: 1–83. https://doi.org/10.3897/zookeys.324.5827

Hillenius D (1959) The differentiation within the genus *Chamaeleo* Laurenti, 1768. Beaufortia 8: 1–92.

Hrbek T, da Silva VMF, Dutra N, Gravena W, Martin AR, Farias IP (2014) A new species of river dolphin from Brazil or: How little do we know our biodiversity. PLoS ONE 9 (1): e83623. https://doi.org/10.1371/journal.pone.0083623

Hughes DF, Kusamba C, Behangana M, Greenbaum E (2017) Integrative taxonomy of the Central African forest chameleon, *Kinyongia adolfifriderici* (Sauria: Chamaeleonidae), reveals underestimated species diversity in the Albertine Rift. Zoological Journal of the Linnean Society 181: 1–39. https://doi.org/10.1093/zoolinnean/zlx005

Kearse M, Moir R, Wilson A, Stones-Havas S, Cheung M, Sturrock S, Buxton S, Cooper A, Markowitz S, Duran C, Thierer T, Ashton B, Mentjies P, Drummond A (2012) Geneious Basic: an integrated and extendable desktop software platform for the organization and analysis of sequence data. Bioinformatics 28(12): 1647–1649. https://doi.org/10.1093/bioinformatics/bts199

Klaver C, Böhme W (1986) Phylogeny and classification of the Chamaeleonidae (Sauria) with special reference to hemipenis morphology. Bonner Zoologische Monographien 22: 1–64.

Lambert SM, Hutter CR, Scherz MD (2017) Diamond in the rough: a new species of fossorial diamond frog (*Rhombophryne*) from Ranomafana National Park, southeastern Madagascar. Zoosystematics and Evolution 93(1): 143–155. https://doi.org/10.3897/zse.93.10188

Lanfear R, Calcott B, Ho SY, Guindon S (2012) PartitionFinder: combined selection of partitioning schemes and substitution models for phylogenetic analyses. Molecular Biology and Evolution 29(6): 1695–1701. https://doi.org/10.1093/molbev/mss020

Mahler DL, Lambert SM, Geneva AJ, Ng J, Hedges SB, Losos JB, Glor RE (2016) Discovery of a giant chameleon-like lizard (*Anolis*) on Hispaniola and its significance to understanding replicated adaptive radiations. The American Naturalist 188(3): 357–364. https://doi.org/10.1086/687566

Myers N, Mittermeier RA, Mittermeier CG, da Fonseca GAB, Kent J (2000) Biodiversity hotspots for conservation priorities. Nature 403: 853–858. https://doi.org/10.1038/35002501

Nagy ZT, Sonet G, Glaw F, Vences M (2012) First large-scale DNA barcoding assessment of reptiles in the biodiversity hotspot of Madagascar, based on newly designed COI primers. PLoS ONE 7(3): e34506. https://doi.org/10.1371/journal.pone.0034506

Nussbaum RA, Raxworthy CJ (1994) A new rainforest gecko of the genus *Paroedura* Günther from Madagascar. Herpetological Natural History 2(1): 43–49.

Ossip-Drahos AG, Morales JRO, Vital-García C, Zúñiga-Vega JJ, Hews DK, Martins EP (2016) Shaping communicative colour signals over evolutionary time. Royal Society Open Science, 3(11): 160728. https://doi.org/10.1098/rsos.160728

Padial JM, Miralles A, De la Riva I, Vences M (2010) The integrative future of taxonomy. Frontiers in Zoology 7: 16. https://doi.org/10.1186/1742-9994-7-16

Paradis E, Claude J, Strimmer K (2004) APE: analyses of phylogenetics and evolution in R language. Bioinformatics 20(2): 289–290. https://doi.org/10.1093/bioinformatics/btg412

Prötzel D, Ruthensteiner B, Glaw F (2016) No longer single! Description of female *Calumma vatosoa* (Squamata, Chamaeleonidae) including a review of the species and its systematic position. Zoosystematics and Evolution 92(1): 13–21. https://doi.org/10.3897/zse.92.6464

Prötzel D, Ruthensteiner B, Scherz MD, Glaw F (2015) Systematic revision of the Malagasy chameleons *Calumma boettgeri* and *C. linotum* (Squamata: Chamaeleonidae). Zootaxa 4048(2): 211–231. https://doi.org/10.11646/zootaxa.4048.2.4

Prötzel D, Vences M, Hawlitschek O, Scherz MD, Ratsoavina FM, Glaw F (2018) Endangered beauties: micro-CT cranial osteology, molecular genetics and external morphology reveal three new species of chameleons in the *Calumma boettgeri* complex (Squamata: Chamaeleonidae). Zoological Journal of the Linnean Society zlx112. https://doi.org/10.1093/zoolinnean/zlx112

Prötzel D, Vences M, Scherz MD, Vieites DR, Glaw F (2017) Splitting and lumping: an integrative taxonomic assessment of Malagasy chameleons in the *Calumma guibei* complex results in the new species *C. gehringi* sp. nov. Vertebrate Zoology 67(2): 231–249.

R Development Core Team (2017) R: A language and environment for statistical computing. R Foundation for Statistical Computing, Vienna, Austria. Available from http://www.R–project.org.

Rieppel O, Crumly C (1997) Paedomorphosis and skull structure in Malagasy chamaeleons (Reptilia: Chamaeleoninae). Journal of Zoology 243(2): 351–380. https://doi.org/10.1111/j.1469-7998.1997.tb02788.x

Rosa GM, Crottini A, Noël J, Rabibisoa N, Raxworthy CJ, Andreone F (2014) A new phytotelmic species of *Platypelis* (Microhylidae: Cophylinae) from the Betampona Reserve, eastern Madagascar. Salamandra 50(4): 201–214.

Scherz MD, Hawlitschek O, Andreone F, Rakotoarison A, Vences M, Glaw F (2017) A review of the taxonomy and osteology of the *Rhombophryne serratopalpebrosa* species group (Anura: Microhylidae) from Madagascar, with comments on the value of volume rendering of micro-CT data to taxonomists. Zootaxa 4273(3): 301–340. https://doi.org/10.11646/zootaxa.4273.3.1

Scherz MD, Rakotoarison A, Hawlitschek O, Vences M, Glaw F (2015) Leaping towards a saltatorial lifestyle? An unusually long-legged new species of *Rhombophryne* (Anura, Microhylidae) from the Sorata massif in northern Madagascar. Zoosystematics and Evolution 91(2): 105–114. https://doi.org/10.3897/zse.91.4979

Stamatakis A (2014) RaxML version 8: a tool for phylogenetic analysis and post-analysis of large phylogenies. Bioinformatics 30(9): 1312–1313. https://doi.org/10.1093/bioinformaics/btu033

Stuart-Fox D, Moussalli A, Whiting MJ (2007) Natural selection on social signals: signal efficacy and the evolution of chameleon display coloration. The American Naturalist 170(6): 916–930. https://doi.org/10.1086/522835

Vieites DR, Ratsoavina FM, Randrianiaina R-D, Nagy ZT, Glaw F, Vences M (2010) A rhapsody of colours from Madagascar: discovery of a remarkable new snake of the genus *Liophidium* and its phylogenetic relationships. Salamandra 46(1): 1–10.

Vieites DR, Wollenberg KC, Andreone F, Köhler J, Glaw F, Vences M (2009) Vast underestimation of Madagascar's biodiversity evidenced by an integrative amphibian inventory. Proceedings of the National Academy of Sciences of the USA 106(20): 8267–8272. https://doi.org/10.1073/pnas.0810821106

Welton LJ, Siler CD, Bennett D, Diesmos A, Duya MR, Dugay R, Rico ELB, Van Weerd M, Brown RM (2010) A spectacular new Philippine monitor lizard reveals a hidden biogeographic boundary and a novel flagship species for conservation. Biology Letters 6(5): 654–658. https://doi.org/10.1098/rsbl.2010.0119

Yoder AD, Rasoloarison RM, Goodman SM, Irwin JA, Atsalis S, Ravosa MJ, Ganzhorn JU (2000) Remarkable species diversity in Malagasy mouse lemurs (primates, *Microcebus*). Proceedings of the National Academy of Sciences of the USA 97(21): 11325–11330. https://doi.org/10.1073/pnas.200121897

Supplementary material 1

Genetic distances of ND2

Authors: David Prötzel, Shea M. Lambert, Ginah Tsiorisoa Andrianasolo, Carl R. Hutter, Kerry A. Cobb, Mark D. Scherz, Frank Glaw

Data type: .ods spreadsheet

Explanation note: Uncorrected genetic distances for all pairwise comparisons of ND2.

Link: https://doi.org/10.3897/zse.94.27305.suppl1

Supplementary material 2

Genetic distances of COI

Authors: David Prötzel, Shea M. Lambert, Ginah Tsiorisoa Andrianasolo, Carl R. Hutter, Kerry A. Cobb, Mark D. Scherz, Frank Glaw

Data type: .ods spreadsheet

Explanation note: Uncorrected genetic distances for all pairwise comparisons of COI.

Link: https://doi.org/10.3897/zse.94.27305.suppl2

Supplementary material 3

Movie of 3D model of the skull

Authors: David Prötzel, Shea M. Lambert, Ginah Tsiorisoa Andrianasolo, Carl R. Hutter, Kerry A. Cobb, Mark D. Scherz, Frank Glaw

Data type: .avi video file

Explanation note: Movie of micro-CT scan of the skull of the male holotype of *Calumma roaloko* (KU 343178).

Link: https://doi.org/10.3897/zse.94.27305.suppl3

Supplementary material 4

Movie of 3D model of the skull

Authors: David Prötzel, Shea M. Lambert, Ginah Tsiorisoa Andrianasolo, Carl R. Hutter, Kerry A. Cobb, Mark D. Scherz, Frank Glaw

Data type: .avi video file

Explanation note: Movie of micro-CT scan of the skull of the female *Calumma roaloko* (KU 343168).

Link: https://doi.org/10.3897/zse.94.27305.suppl4

3.1.5 MANUSCRIPT (in prep.): Revision of the *Calumma nasutum* group

After thorough revision of the *Calumma boettgeri* complex, the species of the remaining *C. nasutum* group (those lacking occipital lobes) were revised. The identity of the nominate species *C. nasutum* has been poorly defined and Gehring *et al.* (2012) showed that this species, thought to occur all over eastern and northern Madagascar, consists of several mitochondrial lineages. The precise definition of *C. fallax* was similarly unclear. Based on external and hemipenial morphology, osteology, and genetic data, both species are redescribed and *C. radamanus* is resurrected from synonymy with *C. nasutum.* Additionally, three species, that were indicated as genetic lineages in Gehring *et al.* (2012) and supplemented with further sampling on recent expeditions to Madagascar, are newly described. With a large data set of more than 200 specimens and about 300 genetic samples we could evaluate the species calculation based on lineage diversification of the mitochondrial ND2 gene of Gehring *et al.* (2012). With five newly described species out of 18 taxonomic units from Gehring *et al.* (2012) we found the species delimitation algorithms as highly overestimating the number of species. With the help of micro-CT scans osteology is accessible for species delimitation and proved to be less variable than external morphology. The hemipenial morphology was not useful as diagnostic characters because it is quite conservative within the group. Only the *C. radamanus* complex is lacking the cornucula gemina (Prötzel *et al.,* 2017).

Prötzel, D, Scherz, MD, Ratsoavina, F, Vences, M & Glaw, F (in prep.): Revision of the *Calumma nasutum* group. *Vertebrate Zoology*.

Revision of the *Calumma nasutum* complex (Squamata: Chamaeleonidae)

DAVID PRÖTZEL[1,*] MARK D. SCHERZ[1,2], FANOMEZANA M. RATSOAVINA[3], MIGUEL VENCES[2] & FRANK GLAW[1]

[1]*Zoologische Staatssammlung München (ZSM-SNSB), Münchhausenstr. 21, 81247 München, Germany*
[2]*Zoological Institute, Technical University of Braunschweig, Mendelssohnstr. 4, 38106 Braunschweig, Germany*
[3]*Mention Zoologie et Biodiversité Animale, Département Biologie, Université d'Antananarivo, BP 906, Antananarivo, 101 Madagascar*

[*]*Corresponding author, e-mail: david.proetzel@mail.de*

ABSTRACT

Based on a large number of specimens and genetic samples we revise the *Calumma nasutum* species group using an integrative taxonomic approach including external and hemipenial morphology, osteology, and sequences of a mitochondrial (ND2) and a nuclear gene (CMOS). After more than 180 years of taxonomic uncertainty, the eponymous species of the group, *C. nasutum*, is re-described and assigned to a genetic clade that occurs from Eastern Madagascar (Anosibe An'Ala, Andasibe) to Nothern Madagascar (Sorata) based on morphology and osteology. The identity of *C. fallax* is also clarified; it occurs at high elevation along the East coast from Andohahela (south) to Mandraka (central East). *Calumma radamanus* is resurrected from synonymy with *C. nasutum*; it lives at low elevations in Eastern Madagascar from Tampolo (south) to its type locality Ambatond'Radama (north). However, up to five deep mitochondrial lineages and strong morphological lineages are identified within this species and we still consider *C. radamanus* to constitute a species complex. Further, three new species are described: *C. emelinae* sp. nov. is distributed from Eastern Madagascar (Anosibe An'Ala in the South to Makira in the West), *C. tjiasmantoi* sp. nov. lives in Southern Madagascar (from Andohahela in the South to Ranomafana NP in the North), and *C. ratnasariae* sp. nov. is known from the Bealanana District in Northern Madagascar. Hemipenial morphology shows only little variation in this group; only the *C. radamanus* complex lacks the cornucula gemina, which are present in all the other taxa. Due to this taxonomic revision the protection status of the treated six chameleon species needs to be newly assessed.

INTRODUCTION

As one of the first ever chameleon species from Madagascar, *Calumma nasutum* was described by Duméril & Bibron in 1836. Since then several new discoveries have followed and 93 chameleon species are currently recognised from the island so far (Glaw, 2015; Prötzel *et al.*, 2018a; Prötzel *et al.*, 2018b; Prötzel *et al.*, 2017; Scherz *et al.*, 2018; Sentís *et al.*, 2018). Among the four Madagascan chameleon genera *Brookesia*, *Calumma*, *Furcifer*, and *Palleon*, especially *Calumma* has contributed to the increase in species numbers, with 12 new species described within the last 15 years (Gehring *et al.*, 2010; Gehring *et al.*, 2011; Prötzel *et al.*, 2018b; Prötzel *et al.*, 2017; Raxworthy & Nussbaum, 2006). This is a result of intensified fieldwork, including also remote areas, in Madagascar on the one hand, but also the use of new methods to detect cryptic diversity. Uncovering cryptic species is crucial for conservation reasons (Bickford *et al.*, 2006) and only a few cases have been reported of the Madagascan reptile fauna so far (Hawlitschek *et al.*, 2018). A species thought to be widespread over a great distribution range could in fact be a complex of several species, each of which inhabits only small and isolated forest fragments which are highly threatened by deforestation (Harper *et al.*, 2007), as already shown for *Calumma tarzan* (Gehring *et al.*, 2010) and *C. juliae* (Prötzel *et al.*, 2018b). Public attention and touristic development can help to protect the habitats of micro-endemic chameleon species.

Calumma nasutum was long thought to be a common species distributed across most of Madagascar's humid and sub-humid forests, until a genetic analysis of the phenetic *C. nasutum* species group revealed 33 operational taxonomic units (OTUs) based on a mitochondrial gene fragment of ND2 (Gehring *et al.*, 2012). Until that date the group consisted of seven described species: *C. boettgeri* (Boulenger, 1888), *C. fallax* (Mocquard, 1900), *C. gallus* (Günther, 1877), *C. guibei* (Hillenius, 1959), *C. linotum* (Müller, 1924), *C. nasutum* (Duméril & Bibron, 1836), and *C. vohibola* Gehring, Ratsoavina, Vences & Glaw, 2011. The species *C. vatosoa* Andreone, Mattioli, Jesu & Randrianirina, 2001 and *C. peyrierasi* (Brygoo, Blanc & Domergue, 1974) were only later transferred to the *C. nasutum* group (Prötzel *et al.*, 2016), and were not included in the study of Gehring *et al.* (2012). After having clarified the taxonomic status of *C. boettgeri, C. guibei*, and *C. linotum* of the *C. boettgeri* species group in previous works (Prötzel *et al.*, 2015; Prötzel *et al.*, 2017) the identity of *C. nasutum* is still unclear—even ~180 years after its description. The lack of a type locality, conservative morphology within the group, and the absence of genetic data from the type specimens due to their age and their temporary storage in formalin, has prevented the re-definition and re-description of *C. nasutum* so far.

In this work, however, we assign *Calumma nasutum* to a genetic clade, based on a large number of specimens using an integrative taxonomic approach including genetic analyses of mitochondrial and nuclear gene sequences, osteology and external and hemipenial morphology.

Further, we clarify the identity of *C. fallax*, resurrect the species *C. radamanus* from synonymy with *C. nasutum* and describe three additional new species.

MATERIAL AND METHODS

Taxon sampling

We studied 150 specimens of the different species/genetic clades of the *Calumma nasutum* group, excluding species with occipital lobes of the *C. boettgeri* complex, from the collections of the Zoologische Staatssammlung München, Germany (ZSM), the Museum National d'Histoire Naturelle de Paris, France (MNHN), the Senckenberg Naturmuseum, Frankfurt, Germany (SMF), the Museo Regionale di Scienze Naturali, Torino, Italy (MRSN), the Université d'Antananarivo, Département de Biologie Animale (now Mention Zoologie et Biodiversité Animale), Antananarivo, Madagascar (UADBA), and the Zoologische Forschungsmuseum Alexander Koenig, Bonn, Germany (ZFMK). Data of all these specimens are provided in suppl. Table 1. The names of the mitochondrial clades used throughout this paper follow Gehring *et al.* (2012) and clades studied here are Clade B, G, H, I, J, and K. Clade A (*C. gallus* complex), clade C (*C. vohibola*), clade D (*C. boettgeri* and *C. linotum*), clade E (*C. gehringi*), and clade F (*C. guibei*) were studied elsewhere or will be studied in future projects.

Specimens of the new taxa described herein were collected in the field by surveying mostly at night. They were fixed in 90% ethanol and transferred to 70% ethanol for long-term storage. Field numbers of preserved specimens and tissue samples refer to the collections of Frank Glaw and Miguel Vences (FGMV, FGZC, MV and ZCMV), Mark D. Scherz (MSZC) and David R. Vieites (DRV), and Franco Andreone (FN).

External morphology

The morphological measurements taken from these specimens follow largely Eckhardt *et al.* (2012); (Gehring *et al.*, 2012; Prötzel *et al.*, 2018b). The following characters (see also Table 1) were measured with a digital calliper to the nearest 0.1 mm, counted using a binocular dissecting microscope, evaluated by eye or calculated; the dataset contains 6 continuous, 3 meristic, and 8 qualitative/other characters (excluding the particular ratios): snout-vent length (SVL) from the snout tip (not including the rostral appendage) to the cloaca; tail length (TaL) from the cloaca to the tail tip; total length (TL) as a sum of SVL + TaL; ratio of TaL and SVL (RTaSV); length of the rostral appendage (LRA) from the upper snout tip; ratio of LRA and SVL (RRS); diameter of rostral appendage (DRA), measured dorsoventrally at the widest point; rostral scale integrated in rostral appendage (RSI) presence (–) or absence (+); distinct rostral

crest (RC) presence (+) or absence (–); lateral crest (LC), running from the posterior of the eye horizontally, presence (+) or absence (–); temporal crest, running dorsally to the LC, curving toward the midline, presence (+) or absence (–); casque crest (CC) bordering the casque, presence (+) or absence (–); parietal crest (PC) presence (+) or absence (–); casque height (CH); dorsal crest (DC) absence (–) or number of dorsal cones visible to the naked eye without the use of a binocular microscope according to Eckhardt *et al.* (2012); number of supralabial scales (NSL), counted from the first scale next to the rostral to the last scale that borders directly and entirely (with one complete side) to the mouth slit of the upper jaw on the right side; and number of infralabial scales (NIL), analogous to the definition of NSL above, on the right side; upper margin of supralabial scales (UMS) serrated (s) or straight in line (l); axillary pits presence (+) or absence (–); diameter of largest scale on temporal region (DSCT), measured on the right side. Diagnostic characters are indicated with a red number in Table 1. For a better traceability these numbers are also listed in the diagnoses together with the respective characters.

Diagnoses are not provided against each single species of the *Calumma boettgeri* group due to their clear identification by their occipital lobes. However, the frontoparietal fenestra (FF), already used as diagnostic character in Prötzel *et al.* (2018b) for the *Calumma boettgeri* complex, is included in the diagnosis because *C. fallax* is known to have a FF in contrast to *C. nasustum* (Rieppel & Crumly, 1997). We structure this paper in dealing first with species with a closed cranial roof, and then with the two species with a significant FF.

Micro-CT

For internal morphology, micro-Computed Tomography (micro-CT) scans of the head were prepared for 23 specimens. Specimens were placed in a closed plastic vessel slightly larger than the specimen with the head oriented upwards and stabilized with ethanol-soaked paper. To avoid scanning artefacts, it was ensured that the paper did not cover the head region. Micro-CT scanning was performed with a phoenix|x nanotom m (GE Measurement & Control, Wunstorf, Germany) using a tungsten or diamond target at a voltage of 130 kV and a current of 80 µA for 29 minutes with 1800 projections à 1000 ms or 15 minutes with 1800 projections à 500 ms. 3D data sets were processed with VG Studio Max 2.2 (Visual Graphics GmbH, Heidelberg, Germany); the data were visualized using the Phong volume renderer to show the surface of the skull and reflect a variety of different levels of x-ray absorption. The osteological terminology follows Rieppel & Crumly (1997). We base our interpretation of skull morphology on volume rendering, following the recommendations of Scherz *et al.* (2017). The following skull characters were measured in VG Studio Max 2.2 using the calliper tool, (Table 2): absence (–) or width of the frontoparietal fenestra (FFW); nasal length (NaL); frontal width measured at prefrontal border (FWPf); frontal width measured at anterior border to postorbitofrontal (FWPo); frontal width

measured at frontal-parietal-border (FWPa); parietal width measured at posterior border to postorbitofrontal (PWPo); parietal and squamosal in contact (PSC, +) or not connected (−); parietal width at midpoint (PWm); parietal length (PL); frontal length (FL); snout-casque length, measured from tip of upper jaw to posterior end of parietal (SCL); skull length, measured from tip of upper jaw to skull capsule (SkL); the respective ratios to SkL are indicated with an 'R' in front of the character-abbreviations.

Hemipenes of five males, from clade B (ZSM 663/2014), clade GII (ZSM 443/2005), clade H (ZSM 694/2003), clade I (ZSM 1724/2010), and clade K (ZSM 924/2003) were diceCT (diffusible iodine contrast enhanced micro-CT) scanned following largely Gignac *et al.* (2016). One hemipenis was clipped off from each specimen and immersed in iodine solution (I_2 in 1% ethanol) for seven days to increase X-ray absorbance. For scanning, the hemipenes were placed with their apices oriented upwards in a plastic tube immersed in 70% ethanol. Scanning was performed for 18 min at a voltage of 60 kV and a current of 200 µA (1800 projections). 3D data were processed in VG Studio Max 2.2 as described above. Hemipenial terminology largely follows Klaver and Böhme (1986) with the addition of the cornucula gemina, a structure named by Prötzel *et al.* (2017). Hemipenes of the remaining males were investigated using a binocular dissecting microscope for consistency and variability.

Genetic analysis

For this study, we complemented sequences of a segment of the mitochondrial gene for NADH dehydrogenase subunit 2 (ND2), and of the nuclear gene for oocyte maturation factor (CMOS) from previous studies (Gehring *et al.*, 2011; Gehring *et al.*, 2012; Prötzel *et al.*, 2018a; Prötzel *et al.*, 2018b; Prötzel *et al.*, 2017) with sequences of additional samples. Total genomic DNA from tissue samples using proteinase K digestion (10 mg/mL concentration) followed by a salt extraction protocol (Bruford et al., 1992). For PCR amplifications we used primers ND2F17 (5'-TGACAAAAAAT TGCNCC-3') (Macey et al., 2000) and ALAR2 (5'-AAAATRTCTGRGTTGCATTCAG-3') (Macey et al., 1997) for ND2, and CO8 (5'-CTTGGTGTTCAATAGACTGG-3') and CO9 (5'-TTTGGGAGCATCCAAAGTCTC-3') (Han et al., 2004) for CMOS. PCR products were purified using ExoSAPIT (USB) and sequenced on automated DNA sequencers. Chromatograms of newly determined DNA sequences were checked for sequencing errors in CodonCode Aligner (CodonCode Corporation), and submitted to GenBank (accession numbers #####-##### to be added upon manuscript acceptance).

Our sampling includes all available ND2 and CMOS sequences, plus complementary new sequences, for all species of the *Calumma nasutum* group sensu lato, i.e., all Malagasy chameleon species with soft dermal flaps on their snout tips. Phylogenetic analyses have suggested that this group might be paraphyletic with respect to the species of the *C. brevicorne*

group (Tolley et al., 2013), but clarifying this question is beyond the scope of the present study. As discussed below, all species of the *C. brevicorne* group can be easily distinguished morphologically by the absence of a dermal snout flap, and for the purpose of taxonomic revision herein, their omission is therefore justified.

Sequences were aligned in MEGA 7 (Kumar et al., 2016). We used the ND2 alignment (582 bp) in a Maximum Likelihood (ML) phylogenetic analysis under a GTR + G model as selected by the Bayesian Informaction Criterion implemented in MEGA7. 500 full heuristic bootstrap replicates were run in MEGA7, with subtree-pruning-regrafting (SPR level 5) branch swapping. A sequence of *Calumma oshaughnessyi* was used as an outgroup.

In our species delimitation rationale, we rely on concordance of the differentiation in mitochondrial DNA represented by the ND2 gene, with differentiation in the nuclear CMOS gene. Therefore, the CMOS sequences (360 bp) were analysed independently. We first separated sequences into haplotypes using the Phase algorithm (Stephens et al., 2001) as implemented in DNASp 5 (Librado & Rozas, 2009). We then used the phased sequences to construct a haplotype network following the approach of (Salzburger et al., 2011) with the program Haplotype Viewer (http://www.cibiv.at/~greg/haploviewer) based on an ML tree reconstructed in MEGA7 under the Jukes Cantor substitution model.

RESULTS

Genetic differentiation in the *Calumma nasutum* group

The ML analysis of ND2 sequences of 303 individuals of the *C. nasutum* group provided a tree (Fig. 1) largely in agreement with that of Gehring *et al.* (2012). All species recognized by Gehring *et al.* (2012) and described in subsequent studies forming monophyletic groups. In addition, the group also contains various other deep clades already recognized by Gehring *et al.* (2012) and not yet taxonomically resolved, i.e., clades B, G, H, I, J, and K. All of these clades received substantial bootstrap support in the mitochondrial analyses, and they are characterized by high ND2 divergences to each other and to the taxonomically well understood species (Table 3). Mean uncorrected pairwise distances ranged from 9.1% between *C. guibei* and *C. lefona*, to 20.5% between *C. boettgeri* and *C. guibei*. However, substantial genetic divergences were also found within species and main clades, as already discussed previously (Gehring *et al.*, 2012; Prötzel *et al.*, 2018b; Prötzel *et al.*, 2017). Intra-clade pairwise distances amounted up to 11.6% in clade G and *C. gehringi*, 11.8% in clade H, and 12.2% in *C. gallus*.

A haplotype network based on CMOS sequences of 114 individuals of the *C. nasutum* group revealed that most of the recognized species and taxonomically unresolved deep

mitochondrial clades also show divergence in this nuclear gene (Fig. 2). Haplotype sharing was exceedingly rare and only observed between *C. vohibola* and clade B, although in some other species and clades, the reconstructed haplotypes did not form clearly delimited phylogroups (clade I, clade J).

General diagnosis of the *Calumma nasutum* group to all other chameleons

All species described or re-described in the following belong to the phenetic *Calumma nasutum* species group. Therefore, a general delimitation of the *C. nasutum* group to the other Chameleoninae from Madagascar is provided here: The phenetic *Calumma nasutum* group comprises small species, with a total length of about 100–130 mm, usually bearing a soft dermal appendage on the snout tip (Fig. 3). Species of the genus *Furcifer* are larger and their rostral processes, if present at all, are of bony origin. The smallest species, *F. campani* with a maximum TL of 135 mm (Glaw & Vences, 2007), lacks a rostral appendage. In *Calumma* only species of the *C. furcifer* group, largely following Glaw and Vences (1994), are of similar size and morphology. However, the *C. nasutum* group differs from them by a thin body shape (vs. higher body shape), heterogeneous scalation on the extremities (vs. homogeneous), a lower number of supra- and infralabials, and a shorter distance from snout tip to the anterior margin of the orbit (concisely: a shorter snout); for more details and measurements, see Prötzel *et al.* (2016). Furthermore we revise the assignment of *C. peyrierasi* (Brygoo, Blanc & Domergue, 1974), which was assigned to this group in Prötzel *et al.* (2016) and exclude the species again. It lacks most of the features that characterize the group (soft rostral appendage, heterogeneous scalation on the extremities, etc.), is larger, and has a different casque form (data not shown). Its assignment remains somewhat unclear, but will be revised in future work on the phylogeny of *Calumma*.

Within the *C. nasutum* group eight species, *C. boettgeri* (Boulenger, 1888), *C. gehringi* Prötzel et al., 2017, *C. guibei* (Hillenius, 1959), *C. juliae* Prötzel et al., 2018, *C. lefona* Prötzel et al., 2018, *C. linotum* (Müller, 1924), *C. roaloko* Prötzel et al., 2018, and *C. uetzi* Prötzel et al., 2018 differ from the others by the possession of well-defined occipital lobes and are referred to as the *C. boettgeri* complex. Another complex within the group refers to *C. gallus* (Günther, 1877), which lacks occipital lobes and is characterized by a long, spear-like rostral appendage of 5–11 mm length in males and a short and rounded appendage of distinct red colour in females (Glaw & Vences, 2007); clade A in Gehring *et al.* (2012). The taxonomy of *C. gallus* is in need of revision and will be treated elsewhere. Including the remaining species *C. nasutum* (Duméril & Bibron, 1836), *C. vohibola* Gehring, Ratsoavina, Vences & Glaw, 2011*,* and *C. vatosoa* Andreone, Mattioli, Jesu & Randrianirina, 2001, the *C. nasutum* group contains at present twelve described species.

<u>Hemipenis morphology of the *Calumma nasutum* group (Fig. 4)</u>

The genital morphology within the group is conservative and differs only in a few characters between the species. Therefore, a description of the general morphology is provided here and only specific characters are listed in the respective species descriptions.

The general form of the hemipenis of the *Calumma nasutum* group is subcylindrical and symmetric with a slightly bilobed apex; calyces on the truncus are distinct and clearly reduced on the sulcal side, but similar on the upper truncus and pedicel (the *C. gallus* complex has reduced calyces on the pedicel), size of calyces can differ (hemipenial character A); calyx ridges are smooth and not serrated; two pairs of rotulae that are finely denticulated; both pairs of rotulae can be small, or one pair can be larger than the other (hemipenial character B); between the rotulae a papillary field of small, unpaired papillae can be present or absent (hemipenial character C); a pair of cornucula gemina, as defined in Prötzel *et al.* (2017), rising from the sulcal side and curved to the asulcal side can be present or absent (hemipenial character D); no other ornamentations (e.g. fleshy papillae, horns, pedunculi) occur in this species group.

<u>Identity and re-description of *Calumma nasutum* (Duméril & Bibron, 1836)</u>

For a complete synonymy list, see Glaw (2015). We here consider *C. radamanus* as a valid species, and resurrect it from synonymy below with a full justification.

Syntypes: Following Duméril and Bibron (1836) and Klaver and Böhme (1997), we consider the syntypes of the species to be MNHN 6643 (no field number), adult female, MNHN 6643A (1994/608), adult female, MNHN 6643B (1994/609), adult male, and MNHN 6643C (1994/610), adult male, collected by Alphonse Charles Bernier, with the type locality 'Madagascar'. Additional material that was considered to be part of this series by Mocquard (1900b) (five additional specimens) are not among the four types mentioned by Duméril and Bibron (1836) and therefore are here considered referred material, listed below.

Lectotype designation: Due to the need for a fixed, single specimen to represent the complicated taxonomy of these chameleons we designate MNHN 6643C (1994/610), an adult male syntype, as the lectotype of *C. nasutum* (Fig. 2A). This specimen is the larger of the two males in the syntype series. The remaining syntypes, MNHN 6643, 6643A, and 6643B, become paralectotypes.

Type locality discussion: Bernier collected plants, insects, lemurs and birds in Madagascar, and also plants in Réunion (Dorr, 1997). Species collected by him and named after him are

distributed all over Madagascar (e.g. the snake species *Dromicodryas bernieri* (Duméril *et al.*, 1854) and a couple of bird and plant species), so no clear conclusions about the collection locality of *C. nasutum* can be drawn. However, only a few rainforest regions were accessible on Madagascar at that time, and two areas are the most likely sources of the specimens: Nosy Be, an island off the north-western coast of Madagascar, and the National Road between the capital Antananarivo and Toamasina (Tamatave) on the East coast, which passes through the rainforests of the Moramanga-Andasibe region. As discussed below, the type series most closely resembles specimens of clade K, and differs from specimens of clade B in a number of characters. Clade K is known from the vicinity of Andasibe and from Sorata in Northern Madagascar. We tentatively conclude that the Andasibe region is the likely source of the type series.

Our assignment to the genetic clade K is based on comparison of the lectotype and one male paralectotype with two available males (with only one male sequenced and the other morphologically and geographically assigned to clade K): the length of the rostral appendage (2.6 vs. 2.0–2.2 mm), the high casque (1.7–2.0 vs. 1.5–1.7 mm), a similar number of infra- and supralabial scales (infralabials 13–15 vs. 13–14, supralabials 14–15 vs. 12–14), and similar skull morphology with the absence of a FF, parietal and squamosal connected, and similarly shaped parietals. Thus, the only available recently collected and sequenced male specimen from clade K (ZSM 924/2003) differs in some characters from the type series with a characteristically pointed casque, the presence of a parietal crest, presence of a dorsal crest (variable character), and the absence of axillary pits. The specimens from Sorata form a subclade within K and the only two adult females (ZSM 1699/2012 and ZSM 1700/2012) were available for a closer investigation; the specimens in the UADBA collection were not available for loan. These females show variation in morphology and osteology (see "Variation") and also photographs from specimens in life, including a juvenile male, suggest some differentiation between the subclade from Sorata and that from Andasibe. Furthermore, there remains the possibility that clade K is not conspecific with *C. nasutum* and represents another new species. However, given the current state of knowledge, the assignment to *C. nasutum* appears to be the most reasonable and most parsimonious solution in order to avoid over-splitting and the unlikely assumption that the 'true' *C. nasutum* still awaits its rediscovery. Further research and collection of more specimens may result in the need to re-evaluate this decision, but in the interest of resolving this complex, a pragmatic approach is required.

Referred material: ZSM 924/2003 (FG/MV 2002-0984), adult male, with completely everted hemipenes, collected in Andasibe (18.9333°S, 48.4167°E, 937 m a.s.l.), Toamasina Region, Eastern Madagascar, on 18 February 2013 by G. Aprea et al.; ZSM 454/2010 (FGZC 4506), adult male, collected in forest near Tarzanville (19.3244°S, 48.21988°E, 881 m a.s.l.), Anosibe An'Ala Region, on 13 April 2010 by F. Glaw, J. Köhler, P.-S. Gehring, K. Mebert, E. Rajeriarison,

and F.M. Ratsoavina (not sequenced, assigned based on morphology only); ZSM 1699/2012 (FGZC 3711), adult female, collected in Sorata massif at high elevation (about 13.68–13.69°S, 49.44°E, about 1060–1485 m a.s.l.), former Antsiranana Province, Northern Madagascar, on 29 November 2012; ZSM 1700/2012 (FGZC 3744) adult female; UADBA uncatalogued (FGZC 3740), adult male; UADBA uncatalogued (FGZC 3636), subadult male; UADBA uncatalogued (FGZC 3708), juvenile; all four collected in the Sorata massif (13.6772°S, 49.4413°E, 1394 m a.s.l.) on 30. November 2012 by F. Glaw, O. Hawlitschek, T. Rajoafiarison, A. Rakotoarison, F. M. Ratsoavina, A. Razafimanantsoa.

Diagnosis (based on the type series and the referred material, see above; osteology based on micro-CT scans of the three males MNHN 6643C, MNHN 6643B, and ZSM 924/2003, and two females MNHN 6643 and ZSM 1699/2012): *Calumma nasutum* is characterised by (1) a medium size (male SVL 43.7–49.0 mm, female SVL 43.0–49.4 mm; male TL 89.0–100.8 mm, female 80.7–95.1 mm), (2) a medium sized (2.2–2.6 mm, 1.2–1.5 mm in females) and distally rounded rostral appendage, (3) rostral scale not integrated into the rostral appendage, (4–7) rostral, lateral, temporal (consisting of one tubercle), and casque crests present, (8) parietal crest indistinct or present, (9) a distinct casque in males with a height of 1.5–2.0 mm, (10) dorsal crest can be present in males, (11) 12–15 supralabial scales, (12) axillary pits generally present, (13) diameter of the largest scale in the temporal region of the head 0.8–1.6 mm, (14) no frontoparietal fenestra, (15) parietal and squamosal in contact, (16) parietal bone width at midpoint 9.8–17.9% of skull length; colour in life based on clade KI: (17) a generally green to brown body colouration, (18) a typically olive green to brown nose in non-stressed colouration, (19) a green cheek colouration, (20) three to four diffuse dorsoventral blotches of variable colour on the body and a light lateral stripe, and (21) eventually a dark stripe crossing the eye.

Calumma nasutum can easily be distinguished from *C. vatosoa* by presence of a rostral appendage (vs. absence); from *C. vohibola* by the rostral appendage length (1.2–2.6 mm vs. 0.0–0.8 mm) and a high casque (0.6 mm vs. 0.7–2.0 mm); for diagnosis against *C. fallax*, see below. For diagnosis against the species described and revalidated herein, see their respective (re-)descriptions below.

Re-description of the lectotype (Fig. 3): Adult male, with mouth slightly opened and tip of tongue between the jaws, in good state of preservation, hemipenes not everted. SVL 45.7 mm, tail length 55.5 mm, for other measurements, see Table 1; rostral ridges that form the snout in a right angle, laterally compressed dermal rostral appendage of oval tubercle scales that projects straight forward over a length of 2.6 mm with a diameter of 2.2 mm, rounded distally and not including the rostral scale; 15 infralabial and 15 supralabial scales, both relatively small; supralabials with a serrated dorsal margin; indistinct lateral crest running horizontally; indistinct and short temporal crest consisting of one tubercles per side; indistinct cranial crest; no parietal crest; no occipital lobes; highly elevated (2.0 mm) and rounded casque; dorsal crest absent; no

traces of gular or ventral crest. Body laterally compressed with fine homogeneous scalation with slightly larger scales on extremities and head region, largest scale on temporal region with diameter of 0.9 mm; deep axillary and less distinct inguinal pits.

Skull osteology of the lectotype (Fig. 5): Skull length 12.3 mm; snout-casque length 15.6 mm; narrow paired nasals completely separated from each other by the anterior tip of frontal that meets the premaxilla; prefrontal fontanelle and naris separated by contact of prefrontal with maxilla; prominent prefrontal with laterally raised tubercles; frontal and parietal smooth with only a few tubercles; frontal with a width of 2.4 mm (19.5% of skull length) at border to prefrontal extending to 4.9 mm (39.8%) at border to postorbitofrontal; no frontoparietal fenestra; slightly curved parietal tapering strongly from a width of 5.0 mm (40.7%) at the border to postorbitofrontal to a width at midpoint of 1.2 mm (9.8%); posterodorsally directed parietal laterally in weak contact with the squamosals; squamosals thin without any tubercles. For further measurements, see Table 2.

Colouration in life (based on photographs, Fig. 6): Females generally browner and less colourful than males; in both sexes olive green to brown body colouration, males can be yellowish in display, extremities and tail of same colour as the body; three to four diffuse dorsoventral blotches of variable colour on the body and a light lateral stripe; throat and ventral region white or beige; rostral appendage typically olive green to brown; cheek region in olive to green colour; eyelids can be crossed by a dark brown stripe and with radiating turquoise stripes in displaying males.

Hemipenial morphology (based on clade KI, Fig. 4): small calyces (hemipenial character A); two pairs of rotulae of different size, on sulcal side large with about 11 tips, on asulcal side small with about 5 tips (B); no papillary field (C); pair of short cornucula gemina (D) anterior and posterior, only visible when hemipenis fully everted.

Variation: For variation in measurements, see Table 1. For variation in colouration in life, see Fig. 6 and Fig. 7. The type series is morphologically highly homogeneous, and we therefore consider it likely that all of the type series belongs to a single species. However the expression of the axillary pits varies between the specimens, possibly due to different fixation processes or the long period of storage in alcohol. The tail length of MNHN 6643B is exceptionally short in comparison to the other specimens. Specimens ZSM 924/2003 (genetic voucher) and ZSM 454/2010 differ from the other available material in a number of characters (see Assignment to genetic clade, above). Specimens from Sorata differ from the type series of *C. nasutum* and specimens from the Andasibe region by a distinct parietal crest over the whole length of the parietal bone (vs. absence or short parietal crest), general absence of a cranial crest (vs. generally present), the fine-scaled rostral appendage is oriented downwards vs. of large tubercles and straight, low rounded casque (vs. high and pointed). The species shows sexual

dimorphism in tail length which is longer in males than in females (RTaSV >100% vs. <100%). The relative rostral appendage length does not differ.

Etymology: the Latin adjective *nasutum* meaning 'big-nosed,' in the neuter nominative singular; obviously in reference to the characteristic rostral appendage.

Distribution (Fig. 8)*: Calumma nasutum* as redefined here, is known from Eastern Madagascar between Anosibe An'ala (19.3244°S, 48.2199°E) and Andasibe in the South to Sorata, more than 600 km further north (see coordinates above), from an elevation of 880–1400 m a.s.l.

Identity, revalidation, and re-description of *Calumma radamanus* (Mertens, 1933)

Chamaeleo radamanus Mertens, 1933; synonymy fide Angel (1942) with *Chamaeleo nasutus* Duméril & Bibron,1836; accepted and also listed as synonym in Mertens (1966).

Taxonomic notes and justification of revalidation: Chamaeleo radamanus was described by Mertens (1933) on the basis of 17 adult and three subadult specimens. Measurements, however, were only provided from two adult males and one female. These three individuals are still present in the collection of the Senckenberg Museum of Frankfurt (SMF) and were analysed here. Several of the paratypes were exchanged with other museums and their whereabouts remain unknown; we were able to trace only three of these specimens, which are housed in the Naturhistorisches Museum Wien (NMW), see below.

Chamaeleo radamanus was synonymized with *Ch. nasutus* by Angel (1942) based on the establishment of the former based on variable characters that are sexually dimorphic—we note that Angel himself apparently did not examine any of the type material of *C. radamanus*, but based this assessment on the photos presented by Mertens (1933). As is explained in greater detail in the re-description below, the members of this species differ from *C. nasutum sensu stricto* (as redefined here) in several characteristics, as the rostral scale integration into the rostral appendage (integrated vs. not integrated), direction of the rostral appendage (down vs. up or straight), shorter rostral appendage in males (2.9–3.6% of SVL vs. 4.5–5.3% of SVL) squamosal shape (short posterior process of squamosal widely separated from parietal vs. meeting the parietal), and frontal width (very broad vs. narrow at midpoint). Given these differences, we consider the morphology of *C. radamanus* to be sufficiently different from *C. nasutum* as to warrant treatment as a separate species. Additionally, the morphology of the holotype closely matches specimens of clade GII (Fig. 1); a specimen of that clade has been depicted before in Gehring *et al.* (2011) as *Calumma* sp. aff. *nasutum*, Tampolo. We therefore here attribute *C. radamanus* to clade GII, resurrect the species from synonymy, and re-describe it here.

Holotype: SMF 22132, adult male, collected in 1931 by Hans Bluntschli in Col Pierre Radama 1000 m a.s.l. (=Ambatond'Radama or Ambatoledama, 35–40 km north-east of Maroantsetra, N.E. Madagascar according to (Viette, 1991); coordinates approximately: 15.29°S, 50.00°E, ca. 547 m a.s.l.; see also Gehring *et al.* (2011).

Paratypes: At least the following five specimens: SMF 26394 (female), NMW 15999:1 (male with everted hemipenes), NMW 15999:2 (female) and NMW 15999:3 (female), all with presumably the same collection data as the holotype. The current whereabouts and institutional numbers of the remaining 13 type specimens are unknown.

Assignment to genetic clade (based on a comparison of the holotype with all specimens from clade G, Fig. 1): On the basis of the short, downward oriented rostral appendage which has the rostral scale integrated into it and the relatively short tail length, and on the basis of its skull osteology, in particular the broad frontal and parietal bones, the relatively short postparietal process, the short posterior process of the squamosal that does not contact the parietal, and the broad and crenate lateral margins of the prefrontals *C. radamanus* belongs to clade G. This clade is divided into five subclades genetically that are morphologically quite strongly conserved, see Fig. 1.

To maximise the precision of our definition, we tentatively assign the holotype to subclade GII (based on the holotype and specimens of clade GII = referred material, for osteology SFM 22132, ZSM 619/2009, ZSM 475/2010, all three males): the type series of *Calumma radamanus* and clade GII has an overlapping size of, for example, the rostral appendage in males of 1.6 vs. 1.4–1.7 mm, a short tail (96% of SVL vs. 90–99% of SVL), and the most similar osteology (e.g. relative parietal width 19.3% vs. 16.1–22.4%). This clade also makes sense biogeographically, being the nearest of the members of the G clade to the type locality of the species.

We here delimit *Calumma radamanus* (n = 7 + type series of 3) from specimens of clade GI (Nosy Komba, Fig. 1, n = 4), GIII (Vohimana, Vohidrazana, Sahafina, Moramanga, n = 5), GIV (Marojejy, n = 6), and GV (Sorata, Fanamabana, n = 15), with the aid osteological data (for *C. radamanus* ZSM 619/2009 and ZSM 475/2010, both males) from the following specimens: ZSM 88/2015, female of clade GI, ZSM 145/2016 and ZSM 451/2016, both males of clade GIII, ZSM 441/2005, male of clade GIV, and ZSM 1694/2012 and ZSM 1691/2012, both males of clade GV. The subclade GII differs from GIII by a shorter rostral appendage (in males 1.4–1.7 mm vs. 3.0–3.3 mm, in females 0.2–1.6 mm vs. 1.6–2.5 mm), dorsal crest occasionally present in males and absent in females vs. present in males and generally present in females, and a relatively wider frontal (RFWPo 38.1–42.2% vs. 36.2–36.3%); from clade GIV by a shorter rostral appendage (in males 1.4–1.7 mm vs. 3.0–3.1 mm, in females 0.2–1.6 mm vs. 1.7–2.4 mm), shorter relative parietal length (RPL 37.3–40.5% vs. 44.2%), and shorter relative snout-casque length (RSCL 114.4–119.0% vs. 123.3%); from clade GV by shorter rostral appendage in males

(1.4–1.7 mm vs. 1.8–3.4 mm), temporal crest usually present vs. absent, shorter relative parietal length (RPL 37.3–40.5% vs. 40.5–47.0%), and shorter relative snout-casque length (RSCL 114.4–119.0% vs. 121.4–126.5%).

In order to avoid over-splitting in the absence of adequate data, and despite our relatively large sample size, we here refrain from a taxonomic assignment of the remaining genetic lineages within clade G to any taxon, and instead refer these to unconfirmed candidate species within the *C. radamanus* species complex, that will certainly need a future taxonomic revision with a considerably bigger dataset.

Referred material (specimens of the clade GII): ZSM 443/2005 (ZCMV 2169), adult male, collected on Nosy Mangabe (about 15.50°S, 49.76°E, about 50–100 m a.s.l.) on 22 February 2005 by F. Glaw, M. Vences, R.D. Randrianiaina; ZSM 619/2009 (ZCMV 11293), adult male, collected in Makira Plateau (about 15.44°S, 49.12°E, about 1000 m a.s.l.) on 22–25 June 2009 by M. Vences, D.R. Vieites, F. Ratsoavina, R.D. Randrianiaina, E. Rajeriarison, T. Rajofiarison, J. Patton; ZSM 475/2010 (FGZC 4313), adult male, collected in Ambodivoahangy (15.2899°S, 49.6202°E, about 100 m a.s.l.) on 03 April 2010 by F. Glaw, J. Köhler, P.-S. Gehring, M. Pabijan, F.M. Ratsoavina; ZSM 152/2016 (FGZC 5152), adult female, collected near Analalava (17.7070°S, 49.4598°E, about 30 m a.s.l.) on 01 January 2016 by F. Glaw, D. Prötzel, L. Randriamanana; ZSM 646/2009 (ZCMV 8957), juvenile female, collected in Tampolo forest, Analanjirofo (17.2886°S, 49.4115°E, 7 m a.s.l.) on 26 April 2009 by P.-S. Gehring, F. Ratsoavina, E. Rajeriarison; ZSM 259/2016 (FGZC 5433), adult female, collected in Masoala near Eco-Lodge Chez Arol (15.7121°S, 49.9639°E, 21 m a.s.l.) on 10 August 2016; ZSM 260/2016 (FGZC 5453), juvenile male, collected in Masoala near Eco-Lodge Chez Arol (15.7247°S, 49.9599°E, 14 m a.s.l.) on 14 August 2016, both by F. Glaw, D. Prötzel, J. Forster, K. Glaw, T. Glaw.

Diagnosis (based on the type series and the referred material, see above; osteology based on SFM 22132, ZSM 619/2009, and ZSM 475/2010, all three males): *Calumma radamanus* is characterised by (1) a medium size (male SVL 42.6–49.2 mm, female SVL 43.0–49.2 mm; male TL 84.9–93.5 mm, female TL 77.0–92.9 mm), tail length shorter than body length, (2) a short (1.4–1.7 mm in males, 0.2–1.6 mm in females) and distally rounded, downward oriented rostral appendage, (3) rostral scale generally integrated into the rostral appendage, (4) rostral crest present, (5) lateral crests present, (6) temporal crest generally present, (7) casque crest present, (8) parietal crest absent, (9) an indistinct casque in males with a height of 0.8–1.5 mm, (10) a dorsal crest of 6–8 spines sometimes present in males, absent in females, (11) 11–15 supralabial scales with a serrated upper margin, (12) general absence of axillary pits, (13) diameter of the largest scale in the temporal region of the head 0.6–0.9 mm, (14) no frontoparietal fenestra in the skull, (15) posterior process of squamosal widely separated from parietal, (16) parietal bone width at midpoint 16.1–22.4% of skull length, (17) a generally

greenish body colouration, (18) a typically turquoise nose in non-stressed colouration, (19) a turquoise cheek colouration, (20) three royal blue dorsoventral blotches on the body and a white lateral stripe, and (21) a dark brown to black stripe running from rostral appendage across the eye to the casque.

Calumma radamanus can easily be distinguished from all species of the *C. boettgeri* complex (see above) by the absence of occipital lobes; from *C. gallus* by different length, shape and colour of its rostral appendage (see above); from *C. vatosoa* by presence of a rostral appendage (vs. absence); from *C. vohibola* by generally longer relative rostral appendage length (RRS 0.5–3.6% vs. 0.1–1.4%), rostral scale generally integrated into rostral appendage (vs. not integrated), squamosal and parietal not in contact (vs. in contact), wider frontal bone, crenate prefrontals (vs. smooth), greenish body colouration (vs. greyish to brownish), presence of large blue lateral blotches (vs. absence); from *C. nasutum* as redefined herein generally by rostral scale integrated into the rostral appendage (vs. not integrated), shorter rostral appendage in males (2.9–3.2% of SVL vs. 4.5–5.3%), male casque lower (0.8–1.5 mm vs. 1.5–2.0 mm), occasional presence of dorsal crest consisting of spines (vs. generally absence or consisting of cones if present), squamosal and parietal not in contact (vs. in contact); for diagnosis against *C. fallax*, see below. For diagnosis against the species described herein, see their respective descriptions below.

Description of the holotype (Fig. 3): Adult male, with mouth closed, in good state of preservation except for the ventrally sliced body, hemipenes not everted. SVL 44.5 mm, tail length 42.6 mm, for other measurements, see Table 1; rostral ridges that form the snout in a right angle, laterally compressed dermal rostral appendage of oval tubercle scales that projects downwards over a length of 1.6 mm with a diameter of 1.8 mm and includes the rostral scale; 11 infralabial and 13 supralabial scales, both rather small; supralabials with a serrated dorsal margin; distinct lateral crest running horizontally; temporal crest consisting of one tubercle per side; distinct cranial crest; no parietal crest; no occipital lobes; medium sized (1.5 mm height) and rounded casque; no trace of a dorsal or gular or ventral crest. Body laterally compressed with fine homogeneous scalation and larger scales on extremities and head region, largest scale on temporal region with diameter of 0.8 mm and in cheek region with 1.1 mm; no axillary or inguinal pits.

Skull osteology of the holotype (Fig. 5): Skull length 11.9 mm; snout-casque length 14.1 mm; narrow paired nasals completely separated from each other by the anterior tip of frontal that meets the premaxilla; prefrontal fontanelle and naris fused; prominent prefrontal with laterally raised tubercles exceeding more than the half of the prefrontal fontanelle; frontal and parietal smooth without any tubercles; frontal with a width of 3.4 mm (28.6% of skull length) at border to prefrontal extending to 4.8 mm (40.3%) at border to postorbitofrontal; no frontoparietal fenestra; triangular shaped parietal with a width of 4.0 mm (33.6%) at the border to postorbitofrontal and a

width at midpoint of 2.3 mm (19.3 %) tapering down continuously in posterodorsal direction; short squamosals far from meeting the parietal. For further measurements, see Table 2.

Colouration in life (Fig. 9)*:* No strong dichromatism between sexes; green to beige body colouration, extremities and tail of same colour as the body; a beige-white (can be inverted to black) lateral stripe may occur from the casque to the hip that crosses the three lateral blotches of distinct blue or violet colour; throat and ventral region white or beige; rostral appendage turquoise or blue; in males, a dark lateral stripe from nostrils, crossing the eyes and fading towards the tip of the casque; cheek region highlighted in turquoise or bright green colour; males appear to be more brightly coloured.

Hemipenial morphology, based on ZSM 443/2005: large calyces (hemipenial character A); two pairs of small rotulae on apex of about the same size (B), finely denticulated with about 12–15 tips each; papillary field of small, unpaired papillae (C); cornucula gemina absent (D).

Variation: For variation in measurements, see Table 1. For variation in colouration in life, see Fig. 9.

Sexual dimorphism: Males are slightly larger than females and they have a relatively longer tail (RTaSV 90–100% vs. 79–89%). However, the relative length of the rostral appendage does not differ. A dorsal crest occurs only in males, if present at all.

Etymology: Radamanus means 'from Radama' or 'Ramanaian' in Latin (-anus declension meaning 'of' or 'pertaining to'), and clearly refers to the origin of specimens from Col Pierre Radama. However, it is not clear from the word 'radamanus' nor from the original description whether this is to be treated as a substantive noun or an adjective. Thus article 31.2.2 of The International Code of Zoological Nomenclature (Ride, 1999) has to be applied: 'Where the author of a species-group name did not indicate whether he or she regarded it as a noun or as an adjective, and where it may be regarded as either and the evidence of usage is not decisive, it is to be treated as a noun in apposition to the name of its genus.' Given that the taxon *Chamaeleo radamanus* disappeared soon after its description into the synonymy of *C. nasutum*, there was no decisive usage of this name (see synonymy above). Therefore, the name is to be considered an invariable noun in apposition, and its declension is not changed.

Distribution (Fig. 8)*: Calumma radamanus* as redefined here, is known from Eastern Madagascar between Tampolo and the type locality Ambatond'Radama about 250 km further north (for coordinates, see above), from an elevation of about 7–500 m a.s.l. (see MAP).

Description of *Calumma emelinae* sp. nov.

Remark: This new species refers to clade B of Fig. 1 and Gehring *et al.* (2012).

Holotype: ZSM 618/2009 (ZCMV 11292), adult male with completely everted hemipenes, right hemipenis cut off for micro-CT scanning, collected in the Makira plateau, Angozongahy or Ampofoko (about 15.44°S, 49.12°E, 1000 m a.s.l.), in the Mahajanga Region, Northern Madagascar, on 22–25 June 2009 by M. Vences, D.R. Vieites, F. Ratsoavina, R.D. Randrianiaina, E. Rajeriarison, T. Rajofiarison, J. Patton.

Paratypes: ZSM 660/2014 (DRV 5899), ZSM 663/2014 (DRV 5898), both adult males, collected in Angozongahy, western side of Makira plateau camp 1 (15.4370°S, 49.1186°E, 1009 m a.s.l.) on 26 June 2009 by M. Vences, D.R. Vieites, F. Ratsoavina, R.D. Randrianiaina, E. Rajeriarison, T. Rajofiarison, J. Patton; ZSM 553/2001 (MV 2001-239), adult female, collected in Andasibe (about XXX, 900 m a.s.l.) on 16–18 February 2001 by M. Vences, D.R. Vieites; ZSM 135/2005 (FGZC 2692) and ZSM 136/2005 (FGZC 2693), both adult females and collected in Vohidrazana (about 18.95°S, 48.50°E, 700–800 m a.s.l.) on 09 February 2005 by F. Glaw, R.R. Randrianiaina, R. Dolch; ZSM 661/2014 (DRV 5677) and ZSM 662/2014 (DRV 5708), both adult females, collected in Mahasoa campsite near Ambodisakoa village (NE Vohimena, NE Lake Alaotra, 17.2977°S, 48.7019°E, 1032 m a.s.l.) on 13–15 February 2008 by D.R. Vieites, J. Patton, P. Bora, M. Vences; ZSM 148/2016 (FGZC 5236), adult female, collected east of Moramanga in 'Julia Forest' (18.9511°S, 48.2719°E, 941 m a.s.l.) on 6 January 2015; ZSM 147/2016 (FGZC 5175), adult female collected south of Moramanga (19.0192°S, 48.2341°E, 903 m a.s.l.) on 04 January 2016, both by F. Glaw, D. Prötzel, L. Randriamanana.

Diagnosis (based on the type series; osteology based on micro-CT scan of ZSM 618/2009, male): *Calumma emelinae* sp. nov. is characterised by (1) a medium size (male SVL 46.6–48.7 mm, female SVL 40.1–49.1 mm; male TL 93.6–103.2 mm, female TL 82.7–95.8 mm), (2) a medium (2.3–2.9 mm in males 1.5–1.8 mm in females) and distally rounded rostral appendage, (3) rostral scale not integrated into the rostral appendage, (4) rostral crest present, (5) lateral crest present, (6) temporal crest present, (7) casque crest variable, (8) parietal crest usually absent, (9) casque low in males with a height of 0.5–1.1 mm, (10) a dorsal crest of 7–10 spines in males, absent in females, (11) 12–16 supralabial scales with a mostly straight upper margin, serrated anteriorly, (12) absence of axillary pits, (13) diameter of the largest scale in the temporal region of the head 0.6–1.0 mm, (14) no frontoparietal fenestra, (15) parietal and squamosal in contact, (16) parietal bone width at midpoint 16.2% of skull length (n = 1), (17) a generally greyish to greenish body colouration, (18) rostral appendage colour generally unremarkable, (19) a green cheek colouration, (20) suggestions of two weak bluish lateral blotches, and (21) no strong eye colouration.

Calumma emelinae sp. nov. can easily be distinguished from all species of the *C. boettgeri* complex (see above) by the absence of occipital lobes; from *C. gallus* by different length, shape

and colour of its rostral appendage (see above); from *C. vatosoa* by presence of a rostral appendage (vs. absence); from *C. vohibola* by generally longer relative rostral appendage length (RRS 3.1–6.1% vs. 0.1–1.4%), dorsal crest always present in males (vs. generally absent), and pointed tip of postparietal process (vs. relatively broad), and crenate prefrontal (vs. smooth); from *C. nasutum* as redefined herein by a lower casque in males (0.5–1.1 mm vs. 1.5–2.0 mm), dorsal crest present in males consisting of spines (vs. general absence or consisting of cones if present), and scales more homogeneous (largest temporal scale in males 0.7 mm vs. 0.9–1.6 mm); from *C. radamanus* by relatively longer tail in males (longer than SVL vs. shorter), longer rostral appendage in males (RRS 4.7–6.1% vs. 2.9–3.6%), rostral scale not integrated into rostral appendage (vs. integrated), supralabials with a largely straight upper margin (vs. serrated), and parietal and squamosal in contact (vs. widely separated); from *C. nasutum* by much less pronounced and raised casque in males (CH 0.5–1.1 vs. 1.5–2.0), dorsal crest consisting of spines (vs. absent or broad cones), more homogeneous scalation, e.g. temporal scale in males (0.7 mm vs. 0.9–1.6 mm); for diagnosis against *C. fallax*, see below. For diagnosis against the other species described herein, see their respective descriptions below.

Description of the holotype (Fig. 3): Adult male, with mouth closed, in good state of preservation, both hemipenes fully everted. SVL 47.9 mm, tail length 50.7 mm, for other measurements, see Table 1; rostral ridges that form the snout in a right angle; laterally flattened and distally rounded rostral appendage of small tubercle scales that projects straight forward over a length of 2.9 mm with a diameter of 2.4 mm not including the rostral scale; 14 infralabial and 15 supralabial scales, both rather small; supralabials with a straight upper margin; distinct lateral crest running horizontally; no temporal or cranial crest; low parietal crest; no occipital lobes; very low casque of 0.5 mm height; dorsal crest consisting of 10 spines; no gular or ventral crest. Body laterally compressed with fine homogeneous scalation and slightly larger scales on extremities and head region, largest scale on temporal region with diameter of 0.7 mm and in cheek region with 0.9 mm; no axillary or inguinal pits.

Skull osteology of the holotype (Fig. 10): Skull length 11.7 mm; snout-casque length 13.8 mm; narrow paired nasals anterior still slightly connected; anterior tip of frontal exceeding about the half of the prefrontal fontanelle that is fused with the naris; prominent and broad prefrontal with laterally raised tubercles; frontal and parietal covered with a few tubercles; frontal with a width at border to prefrontal of 3.0 mm (25.6% of skull length) extending to 4.4 mm (37.6%) at border to postorbitofrontal; no frontoparietal fenestra; narrow parietal with a width at the border to postorbitofrontal of 4.2 mm (35.9%) and a width at midpoint of 1.9 mm (16.2%) tapering strongly in posterodorsal direction; parietal laterally in strong contact with the squamosals; squamosals relatively thick and covered with several tubercles. For further measurements, see Table 2.

Hemipenial morphology, based on ZSM 618/2009, ZSM 660/2014 and ZSM 663/2014: small calyces (hemipenial character A); two pairs of small rotulae on apex of about the same size (B),

more roughly denticulated with about 9–12 tips each; papillary field of small, unpaired papillae (C); pair of short cornucula gemina (D), only visible when hemipenis fully everted.

Sexual dimorphism: Males are usually larger than females (mean TL of 98.5 mm vs. 88.3 mm). Tail length is generally longer in males than in females (RTaSV >100% vs. <100%), as well as the length of the rostral appendage (>2.0 mm vs. <2.0 mm).

Colouration in life (Fig. 11): Both sexes with an indistinct brown to beige body colouration, extremities and tail of same colour as the body; three diffuse/scattered dark dorsoventral blotches can occur on the body without any lateral stripe; throat and ventral region beige; rostral appendage not accentuated; cheek region can be light green; eyelids crossed by a dark brown stripe and occasionally with radiating dark green stripes in both sexes.

Variation: For variation in measurements, see Table 1. For variation in colouration in life, see Fig. 12.

Etymology: The specific epithet is named after Emelina Widjojo, the mother of Wewin Tjiasmanto, in recognition of her support for taxonomic research and nature conservation projects in Madagascar through the BIOPAT initiative (http://biopat.de/).

Distribution (Fig. 8): *Calumma emelinae* sp. nov. is known in Eastern Madagascar from Anosibe An'Ala to Angozongahy (Makira) about 500 km further north (for coordinates, see above), from an altitude of 750–1030 m a.s.l.

Description of *Calumma tjiasmantoi* sp. nov.

Remark: This new species refers to clade J of Fig. 1 and Gehring *et al.* (2012). Due to uncertainties about the collection data of the only male specimen we designate a well-documented female as the holotype.

Holotype: ZSM 735/2003 (FG/MV 2002-497), adult female collected in Ranomafana National Park in Fianarantsoa Region (21.2639°S, 47.4194°E, 983 m a.s.l.) on 23 January 2003 by F. Glaw, M. Puente, L. Raharivololoniaina, M. Thomas, D.R. Vieites.

Paratypes: ZSM 312/2006 (ZCMV 2896), adult male, collected in Ranomafana, probably Ambatolahy (21.2439°S, 47.4262°E, 919 m a.s.l.) on 21 February 2006 by M. Vences and team; ZSM 723/2003 (FG/MV 2002-0396) and ZSM 736/2003 (FG/MV 2002-0498), both adult females, same collection data as holotype; ZSM 380/2016 (ZCMV 14835), adult female, collected in Sampanandrano (24.1399°S, 49.0742°E, 539 m a.s.l.) on 16 December 2016 by A. Rakotoarison, E. Rajeriarison, J.W. Ranaivosolo.

Diagnosis (based on the type series, osteology based on micro-CT scan of ZSM 735/2003, female): *Calumma tjiasmantoi* sp. nov. is characterised by (1) a small size (SVL 43.9–46.8 mm, female TL 84.1–94.8 mm); (2) a medium sized (1.1–2.1 mm) and distally rounded rostral appendage, (3) rostral scale not integrated into the rostral appendage, (4) rostral crest present, (5) lateral crest present, (6) temporal crest present, (7) casque crest present, (8) parietal crest present, (9) casque medium sized in males (1.3 mm), (10) a dorsal crest of 7–9 spines can be present in males (based additionally on photographs), absent in females, (11) 15–17 supralabial scales with a mostly straight upper margin, (12) general absence of axillary pits, (13) diameter of the largest scale in the temporal region of the head 0.6–0.8 mm, (14) frontoparietal fenestra absent, (15) parietal and squamosal in contact, (16) parietal bone width at midpoint 16.1% of skull length (n = 1) with a characteristic broad tip to the postparietal process, (17) a generally greyish, greenish, or brownish body colouration, (18) rostral appendage colour generally unremarkable, (19) cheek colouration not accentuated, (20) five characteristic lateral stripes of blue or brown colour, and (21) no distinct stripe crossing the eye.

Calumma tjiasmantoi sp. nov. can easily be distinguished from all species of the *C. boettgeri* complex (see above) by the absence of occipital lobes; from *C. gallus* by different length, shape and colour of its rostral appendage (see above); from *C. vatosoa* by presence of a rostral appendage (vs. absence); from *C. vohibola* by longer rostral appendage in females (RRS 2.4–4.6% vs. 0.2–0.7%), parietal crest present (vs. absent), smaller temporal scale (0.6–0.8 mm vs. 1.0 mm); from *C. nasutum* as redefined herein by the higher number of supralabials (15–17 vs. 12–15), a shorter rostral appendage (4.3% of SVL vs. 4.5–5.3% of SVL), a shorter parietal (36.3% of skull length vs. 41.0–44.3%), broad postparietal process (vs. narrow); from *C. radamanus* by a relatively longer tail in females (RTaSV 92–95% vs. 79–89%), rostral scale not integrated in rostral appendage (vs. generally integrated), parietal crest present (vs. absent), more supralabials (15–17 vs. 11–15) with a generally straight upper margin (vs. serrated), parietal and squamosal in contact (vs. widely separated); from *C. emelinae* sp. nov. by presence of parietal crest (vs. usually absent), and broader postparietal process; for diagnosis against *C. fallax*, see below. For diagnosis against the other species described herein, see their respective descriptions below.

Description of the holotype (Fig. 3): Adult female, with mouth closed, in good state of preservation except for a ventrally sliced body, with four eggs still fixed in the oviduct; SVL 45.5 mm, tail length 42.5 mm, for other measurements, see Table 1; bulging rostral ridges; laterally flattened and distally rounded rostral appendage of tubercle scales that projects straight forward over a length of 1.7 mm with a diameter of 1.4 mm not including the rostral scale; 15 infralabial and 15 supralabial scales, both rather small; most of the supralabials with a straight upper margin, only anterior scales serrated; distinct lateral crest running horizontally; temporal crest consisting of two tubercles; short cranial crest; short parietal crest; no occipital lobes; medium

sized casque of 1.1 mm height; no dorsal, gular or ventral crest. Body laterally compressed with fine homogeneous scalation and only slightly larger scales on extremities and head region, largest scale on temporal region with diameter of 0.6 mm and in cheek region with 0.6 mm; no axillary or inguinal pits.

Skull osteology of the holotype (Fig. 10): Skull length 12.4 mm; snout-casque length 14.4 mm; narrow paired nasals anterior still in contact; anterior tip of frontal exceeding less than the half diameter of the prefrontal fontanelle that is fused with the naris; prominent and broad prefrontal with laterally raised tubercles; frontal and parietal smooth with only a few tubercles; frontal with a width of 2.4 mm (19.4% of skull length) at border to prefrontal extending to 4.3 mm (34.7%) at border to postorbitofrontal; no frontoparietal fenestra; broad parietal with distinct parietal crest tapering slightly from a width of 4.3 mm (34.7%) at the border to postorbitofrontal to a width at midpoint of 2.0 mm (16.1%); the posterodorsally broadened end is in strong contact with the squamosals; squamosals broad with several tubercles. For further measurements, see Table 2.

Colouration in life: Strong sexual dichromatism with males of bright green or yellowish body colouration and turquoise extremities and females generally browner and less conspicuous. In both sexes five diffuse dorsoventral stripes on the body—in males of blue colour with light spots, in females of brown colour; no lateral stripe across the body; tail annulated, continuing the blotches from the body; throat and ventral region can be beige or of same colour as the body; indistinct rostral appendage not accentuated from the head; cheek region turquoise in males; a diffuse dark stripe may cross the eye.

Hemipenial morphology based on ZSM 312/2006: medium sized calyces (hemipenial character A); two pairs of small rotulae on apex of about the same size (B), finely denticulated with about 7–9 tips each; papillary field of small, unpaired papillae (C); pair of medium sized cornucula gemina (D), only visible when hemipenis fully everted.

Variation: For variation in measurements, see Table 1. For variation in colouration in life, see Fig. 12. The female ZSM 134/2005 (FGZC 2508) from Andohahela at high altitude (1548 m a.s.l.) belongs genetically to clade J but shows substantial morphological differences so that we do not designate it as a paratype. Next to a larger total length (97.0 mm), a longer rostral appendage (2.6 mm), and a low number of supralabials (12) it also has a unique skull morphology with a FF. This correlates well with a previous study where only high elevation species tend to have a FF (Prötzel *et al.*, 2018b) but does not fit in the general pattern of *C. tjiasmantoi* sp. nov. Further studies are necessary to clarify this apparent contradiction in our dataset and potential taxonomic conclusions.

Sexual dimorphism: Body size (SVL and TL) is slightly larger in males than females, tail length is longer in males than in females (RTaSV 103% vs. 92–95%), and a dorsal crest is only present in males.

Etymology: The specific epithet is a patronym honouring Wewin Tjiasmanto in recognition of his support for taxonomic research and nature conservation projects in Madagascar through the BIOPAT initiative (http://biopat.de/).

Distribution (Fig. 8): *Calumma tjiasmantoi* sp. nov. is known from Eastern Madagascar from Andohahela in the South to Ranomafana NP about 400 km further north (for coordinates, see above), from an altitude of 267 to 983 m a.s.l. (see Fig. 8).

Identity and re-description of *Calumma fallax*

Syntypes: Following Gehring *et al.* (2011) and Brygoo (1971) we consider the syntypes of the species to be MNHN 1899.317, adult male, locality Forêt d'Ikongo, collected in 1898–1899 by Guillaume Grandidier, and MNHN 1899.318 (female), locality Forêt d'Ikongo, collected in 1898–1899 by Guillaume Grandidier; Mocquard (1900a) and (Mocquard, 1900b) did not specify the specimen numbers of the types, but these were deduced based on their collection dates.

Lectotype designation: We designate MNHN 1899.317, the adult male syntype, as the lectotype of the species, the remaining syntype, MNHN 1899.318, becoming the paralectotype.

Assignment to genetic clade (based on a comparison of the lectotype with the male specimens assigned to clade H, ZSM 693/2003, ZSM 286/2010, ZSM 312/2006, ZSM 685/2003, and ZSM 694/2003): *Calumma fallax* belongs to clade H, according to the high casque (2.1 mm in the lectotype vs. 1.3–2.5 mm), rounded, oval rostral appendage with a length of (2.7 mm vs. 1.8–4.3 mm), heterogeneous scalation in head region with diameter of largest scale in temporal region of 1.6 mm vs. 0.8–1.5 mm, distinct parietal crest ending in the casque, temporal crest present consisting of 1 or 2 tubercles (2 vs. 1–2); osteology of the skull is almost identical, e.g. width of the frontoparietal fenestra with 16.4% of skull length vs. 13.9–15.4%.

Referred material: Accordingly, the specimens MNHN 1890.430, MNHN 1890.431, MNHN 1890.432, all three adult males, and MNHN 1888.24, adult female, are non-type specimens. In addition, in anticipation of our conclusions on the taxonomic identity of the species, we here refer the following specimens to *C. fallax* as it is here re-defined:

ZSM 685/2003 (FG/MV 2002-0291), ZSM 693/2003 (FG/MV 2002-0317) and ZSM 694/2003 (FG/MV 2002-0318), all three adult males, collected in Ranomafana NP, Vohiparara, near Kidonavo-bridge (about 21.22°S, 47.37°E, about 1000 m a.s.l.) on 16–20 January 2003 by F. Glaw, M. Puente, L. Raharivololoniaina, M. Thomas, D.R. Vieites; ZSM 134/2005 (FGZC 2508), female, collected in Andohahela NP (24.5440°S, 46.7141°E, 1548 m a.s.l.) on 27 January 2005 by F. Glaw, M. Vences, and P. Bora; ZSM 286/2010 (FGZC 4588), adult male, collected east of Tsinjoarivo, between camps 2 and 1 (19.7103°S, 47.8182°E, 1465 m a.s.l.) on 23 April 2010 by

F. Glaw, J. Köhler, P.-S. Gehring, J.L. Brown, E. Rajeriarison; ZSM 313/2006 (ZCMV 2930), adult female, collected in Ranomafana NP, Vohiparara river and stream/swamp (about 21.25°S, 47.40°E, about 1100 m a.s.l.) on 20 February 2006 by M. Vences, E. Rajeriarison, Y. Chiari, E. Balian; ZSM 476/2010 (FGZC 4352), adult female, collected in Anjozorobe region, Mananara Lodge (18.4629°S, 47.9381°E, 1298 m a.s.l.) on 06 April 2010, ZSM 479/2010 (FGZC 4575), adult female, collected east of Tsinjoarivo, camp 1 (19.6800°S, 47.7706°E, 1607 m a.s.l.) on 19 April 2010, both by F. Glaw, J. Köhler, P.-S. Gehring, M. Pabijan, K. Mebert, E. Rajeriarison, F. Randrianasolo, S. Rasamison; ZSM 149/2016 (FGZC 5226) and ZSM 150/2016 (FGZC 5225), both adult females, collected in Mandraka (18.9122°S, 47.9144°E, 1235 m a.s.l.) on 05 January 2016 by F. Glaw, D. Prötzel, L. Randriamanana; ZSM 258/2016 (FGZC 5291), adult female, collected in Mandraka (18.9133°S, 47.9145°E, 1260 m a.s.l.) on 03 August 2016 by F. Glaw, D. Prötzel, J. Forster, N. Raharinoro.

Diagnosis (based on the type series and the referred material, see above; osteology based on micro-CT scans of MNHN 1899.317, MNHN 1890.430, ZSM 693/2003, and ZSM 286/2010, all four males): *Calumma fallax* is characterised by (1) a medium size (male SVL 42.9–50.6 mm, female SVL 40.8–50.7 mm; male TL 90.9–107.3 mm, female TL 77.3–99.8 mm), (2) a long (1.8–4.3 mm in males, 1.7–3.2 mm in females) and distally rounded rostral appendage, (3) rostral scale not integrated into the rostral appendage, (4) prominent rostral crest forming a concave cup on the snout, (5) lateral crests present, (6) temporal crest generally present, (7) casque crest generally absent, (8) parietal crest generally present but short, (9) a distinct casque in males with a height of 1.3–2.5 mm, (10) a dorsal crest of 6–11 cones in males, generally absent in females (one specimen with five cones), (11) 10–16 supralabial scales with a straight upper margin, (12) absence of axillary pits, (13) diameter of the largest scale in the temporal region of the head 0.8–1.8 mm, (14) a frontoparietal fenestra in the skull, (15) parietal and squamosal generally in contact, (16) parietal bone width at midpoint 6.7–15.7% of skull length, (17) a generally greenish, greyish, or brownish body colouration, (18) a typically blue nose in non-stressed colouration, (19) a green cheek colouration, (20) three blue dorsoventral stripes on the body and a white lateral stripe, and (21) a diffuse dark strip crossing the eye.

C. fallax can be distinguished from all species of the *C. boettgeri* complex (see above) by the absence of occipital lobes; from *C. gallus* by different length, shape and colour of its rostral appendage (see above); from all other species of the *C. nasutum* group without occipital lobes by the presence of a frontoparietal fenestra.

In addition, it can be distinguished from *C. vatosoa* by the presence of a rostral appendage (vs. absence); from *C. vohibola* by longer rostral appendage (RRS 4.2–8.5% vs. 0.2–3.1%), supralabials with a straight upper margin (vs. serrated), parietal crest generally present (vs. absent); from *C. nasutum* as here redefined by general absence of casque crest (vs. present), a shorter frontal (39.4–50.4% of skull length vs. 51.2–82.1%), blue rostral appendage (vs. brown),

and three blue lateral blotches (vs. four brown blotches with light spots); from *C. radamanus* by rostral scale not integrated into the rostral appendage (vs. generally integrated), parietal crest generally present (vs. absent), supralabials with a straight upper margin (vs. serrated), parietal and squamosal in contact or closely approaching (vs. widely separated), and width of parietal at midpoint (6.7–15.7% vs. 16.1–22.4%); from *C. emelinae* sp. nov. by general presence of parietal crest (vs. general absence), higher casque in males (1.3–2.5 mm vs. 0.5–1.1 mm), dorsal crest consisting of cones (vs. spines) in males; larger temporal scale in males (0.8–1.6 mm vs. 0.7 mm); from *C. tjiasmantoi* sp. nov. by fewer supralabials (10–15 vs. 15–17), larger diameter of temporal scale (1.0–1.8 mm vs. 0.6–0.8 mm), and slightly narrower postparietal process.

Re-description of the lectotype (Fig. 3): Adult male, with mouth slightly opened, in good state of preservation, hemipenes not everted. SVL 42.9 mm, tail length 53.2 mm, for other measurements, see Table 1; distinct rostral ridges that form the snout to a concave cup, laterally compressed dermal rostral appendage of oval tubercle scales that projects straight forward over a length of 2.7 mm with a diameter of 3.4 mm, in a shape of a taller than long oval; 11 infralabial and 11 supralabial scales, both relatively large; supralabials with a smooth dorsal margin; distinct lateral crest running horizontally; distinct temporal crest consisting of two tubercles per side; no cranial crest; distinct parietal crest; no occipital lobes; highly elevated (2.1 mm) and rather acute casque; dorsal crest present, consisting of 11 spines that decrease posteriorly; no traces of gular or ventral crest. Body laterally compressed with fine homogeneous scalation and distinctly larger scales on extremities and head region, largest scale on temporal region with diameter of 1.6 mm and in cheek region with 1.4 mm; no axillary or inguinal pits.

Skull osteology of the lectotype (Fig. 13): Skull length 12.0 mm; snout-casque length 14.6 mm; narrow paired nasals completely separated from each other by the anterior tip of frontal that meets the premaxilla; prefrontal fontanelle and naris fused; prominent prefrontal with laterally raised tubercles exceeding more than the half of the prefrontal fontanelle; frontal and parietal smooth without any tubercles; frontal with a width of 2.7 mm (22.5% of skull length) at border to prefrontal extending to 4.4 mm (36.7%) at border to postorbitofrontal; large frontoparietal fenestra with a width of 2.4 mm (20.0%); curved parietal tapering strongly from a width of 3.9 mm (32.5%) at the border to postorbitofrontal to a width at midpoint of 0.8 mm (6.7%) and broadening slightly posterodorsally, where it is in weak contact with the squamosals; squamosals thin without any tubercles. For further measurements, see Table 3.

Colouration in life (Fig. 14): Weak sexual dichromatism, males slightly more colourful. In both sexes grey/beige body colouration with three bright blue dorsoventral stripes on the body that can be crossed by a broad white lateral stripe; extremities and tail of same colour as the body, tail in males can be diffusely annulated; rostral appendage grey or blue; cheek region can be bright green; a diffuse dark stripe may cross the eye.

Hemipenial morphology, based on the lectotype: large calyces (hemipenial character A); two pairs of finely denticulated rotulae of different size, on sulcal side large with about 16 tips, on asulcal side small with about 8 tips (B); papillary field of few, unpaired papillae (C); pair of short cornucula gemina (D), only visible when hemipenis fully everted.

Variation: For variation in measurements, see Table 1. For variation in colouration in life, see Fig. 14.

Sexual dimorphism: Body size (SVL and TL) is slightly larger in males than females. Tail length is longer in males than in females (RTaSV 102–124% vs. 89–104%). Relative rostral appendage length does not differ. Dorsal crest is more pronounced in males than females.

Etymology: a Latin adjective meaning 'deceptive' or 'fallacious' in the neutral nominative, with unclear justification.

Distribution (Fig. 8): *Calumma fallax* as redefined here, occurs in Eastern Madagascar from Andohahela in the South to Mandraka about 650 km further north (coordinates, see above), from an altitude of 922–1781 m a.s.l.

Description of *Calumma ratnasariae* sp. nov.

Remark: This new species refers to clade I of Fig. 1 and (Gehring *et al.*, 2012).

Holotype: ZSM 35/2016 (MSZC 0066), adult male in a good state of preservation with everted hemipenes, one completely (on the left) and one incompletely everted (on the right), collected in the Ampotsidy mountains (14.4146°S, 48.7115°E, 1400 m a.s.l.), in the Bealanana District, Northern Madagascar, on 22 December 2015 by M.D. Scherz, J. Borrell, L. Ball, T. Starnes, T.S.E. Razafimandimby, D.H. Nomenjanahary, J. Rabearivony.

Paratypes: ZSM 1724/2010 (ZCMV 12483), adult male and ZSM 2884/2010 (ZCMV 12273), adult female, both collected in Analabe Forest, near Antambato village (Ambodimanga mountain, 14.5048°S, 48.8760°E, 1361 m a.s.l.) on 24 June 2010, ZSM 517/2014 (DRV 6283), adult male collected in Andrevorevo (14.3464°S, 49.1028°E, 1717 m a.s.l.) on 21 June 2010, all three by M. Vences, D. Vieites, R.D. Randrianiaina, F. Ratsoavina, S. Rasamison, A. Rakotoarison, E. Rajeriarison, T. Rajoafiarison; ZSM 36/2016 (MSZC 0140), adult female, collected in the Ampotsidy mountains (14.4099°S, 48.7155°E, 1647 m a.s.l.) on 3 January 2016, and ZSM 37/2016 (MSZC 0169), adult female, collected in the Ampotsidy mountains (14.4193°S, 48.7193°E, 1337 m a.s.l.), on 8 January 2016 both by M.D. Scherz, J. Borrell, L. Ball, T.S.E. Razafimandimby, D.H. Nomenjanahary, J. Rabearivony.

Diagnosis (based on the type series; osteology based on micro-CT scans of ZSM 35/2016 and ZSM 517/2014, both males): *Calumma ratnasariae* sp. nov. is characterised by (1) a large size (male SVL 43.9–52.0 mm, female SVL 48.7–51.5 mm; male TL 97.1–110.7, female TL 95.3–101.0); (2) a short (1.8–2.3 mm in males, 2.1–2.2 mm in females) and distally rounded rostral appendage, (3) rostral scale not integrated into the rostral appendage, (4–7) rostral, lateral, temporal (one tubercle on either side), and casque crests present, (8) parietal crest distinct and running the length of the parietal bone, (9) a distinct casque in males with a height of 1.3–1.5 mm, (10) a dorsal crest of 7–12 cones in males, generally present in females (6–8 cones), (11) 10–13 supralabial scales with a straight upper margin, (12) absence of axillary pits, (13) diameter of the largest scale in the temporal region of the head 1.2–1.6 mm, (14) a frontoparietal fenestra in the skull, (15) parietal and squamosal in contact (n = 2), (16) parietal bone width at midpoint 17.8–18.5% of skull length, (17) a generally yellowish body colouration in males, greyish body colouration in females, (18) rostral appendage not accentuated from the body colouration, (19) a blue and yellow cheek colouration, (20) yellow in males and beige in females, and (21) brown stripe crossing the eye. *Calumma ratnasariae* sp. nov. is unique among the *C. nasutum* complex in having an elevated bony knob on the anterodorsal edge of the maxillary facial process (this character is similar to that seen in *C. uetzi*).

Calumma ratnasariae sp. nov. can be distinguished from all species of the *C. boettgeri* complex (see above) by the absence of occipital lobes; from *C. gallus* by different length, shape and colour of its rostral appendage (see above); from all other species of the *C. nasutum* group without occipital lobes except *C. fallax* by the presence of a frontoparietal fenestra. It is also quite unusual in having an overall yellowish body colouration in males. In addition, it can be distinguished from *C. vatosoa* easily by the presence of a rostral appendage (vs. absence); from *C. vohibola* by longer rostral appendage (RRS 3.8–4.8% vs. 0.2–3.1%), parietal crest present (vs. absent), fewer supralabials (10–13 vs. 13–16) with a straight upper margin (vs. serrated), larger temporal scale (1.2–1.6 mm vs. 1.0 mm), broader parietal bone with a continuous parietal crest (vs. smooth parietal); from *C. nasutum* as here redefined by a larger maximum total length in males (110.7 mm vs. 89.0–100.8 mm), a distinct parietal crest (vs. absent or indistinct), dorsal crest generally present in both sexes (vs. generally absent and absent in females); from *C. radamanus* by larger total length (95.3–110.7 mm vs. 77.0–93.5 mm), tail length in males longer than SVL (vs. shorter), rostral scale not integrated into the rostral appendage (vs. generally integrated), parietal crest present (vs. absent), supralabials with a straight upper margin (vs. serrated), larger temporal scale (1.2–1.6 mm vs. 0.6–0.9 mm), and parietal and squamosal in contact (vs. widely separated); from *C. emelinae* sp. nov. by parietal crest distinct (vs. general absence), higher casque in males (1.3–1.5 mm vs. 0.5–1.1 mm), dorsal crest consisting of cones (vs. spines) in males; larger temporal scale (1.2–1.6 mm vs. 0.6–1.0 mm), and broad postparietal process (vs. strongly tapering); from *C. tjiasmantoi* sp. nov. by larger body length of females (SVL 48.7–51.5 mm vs. 43.9–46.1 mm), dorsal crest generally present in females (vs.

absent), fewer supralabials (11–12 vs. 15–17), and larger diameter of temporal scale (1.2–1.6 mm vs. 0.6–0.8 mm); and from *C. fallax* by generally shorter relative rostral appendage length in females (RRS 4.1–4.5% vs. 4.2–7.6%), casque crest present (vs. generally absent), parietal crest longer and more distinct, dorsal crest generally present in females (vs. generally absent), and a wider mid-parietal width (17.8–18.5% of skull length vs. 6.7–15.7%).

Description of the holotype (Fig. 3): Adult male, with mouth closed, in good state of preservation, with everted hemipenes, one completely (on the left) and one incompletely (on the right); SVL 48.2 mm, tail length 54.2 mm, for other measurements, see Table 1; distinct rostral ridges that form the snout in a right angle; laterally compressed dermal rostral appendage of oval tubercle scales that projects slightly downwards over a length of 2.3 mm with a diameter of 1.9 mm; 13 infralabial and 12 supralabial scales, both relatively large; supralabials with a smooth dorsal margin; distinct lateral crest running horizontally; temporal crest consisting of one tubercle per side; short cranial crest; distinct and long parietal crest ending in the tip of the casque with a height of 1.5 mm; no occipital lobes; dorsal crest present, consisting of 7 broad cones; no traces of gular or ventral crest. Body laterally compressed with fine homogeneous scalation and distinctly larger scales on extremities and head region, largest scale on temporal region with diameter of 1.3 mm and in cheek region with 1.1 mm; no axillary or inguinal pits.

Skull osteology of the holotype (Fig. 13): Skull length 11.9 mm; snout-casque length 14.4 mm; narrow paired nasals anterior slightly connected; anterior tip of frontal exceeding the prefrontal fontanelle that is fused with the naris; prominent and broad prefrontal; frontal and parietal smooth without any tubercles; frontal with a width of 2.6 mm (21.8% of skull length) at border to prefrontal extending to 4.4 mm (37.0%) at border to postorbitofrontal; large frontoparietal fenestra with a width of 2.5 mm (21.0%); broad parietal with distinct parietal crest tapering slightly from a width of 4.0 mm (33.6%) at the border to postorbitofrontal to a width at midpoint of 2.2 mm (18.6%); the posterodorsally broadened end is in weak contact with the squamosals; squamosals thin with a few tubercles. For further measurements, see Table 2.

Colouration in life (Fig. 15): Strong sexual dichromatism with males of yellow body colouration and turquoise stripes and females generally uniformly beige. Males with turquoise annulated tail and extremities and two brown blotches on the body side that is crossed by a diffuse white lateral stripe; no pattern in females; throat and ventral region slightly brighter than the flank; indistinct rostral appendage not accentuated from the body/head, can be spotted with blue or yellow dots; in males cheek region and eyelids with turquoise dots, in females blue dots can occur on rostral ridges and eyelids when stressed; a diffuse brown stripe crosses the eye in both sexes.

Hemipenial morphology, based on ZSM 1724/2010, ZSM 517/2014, and ZSM 35/2016: small calyces (hemipenial character A); two pairs of finely denticulated rotulae of different size, on

sulcal side large with about 12–15 tips, on asulcal side small with about 5–7 tips (B); papillary field of small, unpaired papillae (C); pair of short cornucula gemina (D), only visible when hemipenis fully everted.

Variation: For variation in measurements, see Table 1. For variation in colouration in life, see Fig. 15. The osteology of the male ZSM 693/2003 differs from the other specimens in having the parietal and squamosal bone not connected; probably this is due to its juvenile state.

Sexual dimorphism: Males and females do not seem to differ in body size. Tail length is longer in males than in females (RTaSV 112–121% vs. 94–98%). Relative rostral appendage length does not differ. Dorsal crest does not differ between males and females.

Etymology: The specific epithet is named after Yulia Ratnasari, in recognition of her support for taxonomic research and nature conservation projects in Madagascar through the BIOPAT initiative (http://biopat.de/).

Distribution (Fig. 8): *Calumma ratnasariae* sp. nov. is only known from the Bealanana District of Northern Madagascar. It is distributed from Analabe Forest in the South to Andrevorevo, about 20 km further north (for coordinates, see above), from an altitude of 1337–1717 m a.s.l.

DISCUSSION

As already suggested by Gehring *et al.* (2012), *Calumma nasutum* turned out to be a complex of several species. Excluding the OTUs assigned to the *C. boettgeri* complex and *C. gallus* complex, Gehring *et al.* (2012) calculated six OTUs within *C. fallax* (OTU 17–21, plus '*C. fallax*') and even twelve OTUs (6, 7, 13–16, 22–26, plus '*C. nasutum*') that formerly all belonged to the single species *C. nasutum.* The OTUs were calculated using three different approaches (net p-distances, SpeciesIdentifier and GMYC model) all based on divergences of a ND2 gene fragment. Using integrative taxonomy we consider 18 OTUs 'within' the two described species to be an overestimation. However, the classification into different clades based on ND2 divergences of >8.2% proved to be a helpful orientation to evaluate taxonomic units. Following our integrative revision, the clades B, G, H, I, J, and K resulted in one (new) species each. The 18 OTUs from Gehring *et al.* (2012) constitute six (newly described or resurrected) species. For the whole *C. nasutum* group (including the *C. boettgeri* complex but excluding the *C. gallus* complex) Gehring *et al.* (2012) calculated a total of 27 OTUs that resulted in 12 described species to date, not considering the only recently discovered species *C. juliae, C. uetzi, C. roaloko* (Prötzel *et al.*, 2018a) which were not studied by Gehring *et al.* (2012). This fits the general pattern of overestimation of species based on species delimitation algorithms (Leaché *et*

al., 2018). There are other examples of mitochondrial divergence exceeding 10% between apparently conspecific populations of anole lizard species (Jackman *et al.*, 2002; Thorpe *et al.*, 2005). The comparison of different groups of chameleons confirms also the phenomenon that morphological and mitochondrial variation or differentiation are not necessarily correlated, as shown, e.g. in *Anolis roquet* on Martinique (Losos, 2009; Thorpe *et al.*, 2008). The deep mitochondrial lineages within the *C. nasutum* group, which is morphological relatively conserved contrasts for example with species within the genus *Bradypodion* where some morphologically distinct species differ genetically by only 5% in the ND2 gene or less (Branch *et al.*, 2006; Tilbury & Tolley, 2009). Additionally, it is not reliable to compare the percentage only without giving an indication of the number of sites used in the comparison.

Again, we want to state the importance of an integrative approach in taxonomy with as many methods as possible. Miralles *et al.* (2011) and Vasconcelos *et al.* (2012) for example used three lines of evidence (mtDNA, nDNA, and morphology) and described a species if at least two lines showed clear differences. In this work we additionally use micro-CT scans for skull morphology and diceCT scans (Gignac *et al.*, 2016) for detailed hemipenial morphology as emerging methods in taxonomy. Most of the chameleon species described here differ in four (mtDNA, nDNA, external morphology, and skull morphology) of five lines of evidence; only the morphology of the hemipenis is conservative in the *C. nasutum* group. In *C. radamanus* however, the hemipenes have larger calyces and are lacking the cornucula gemina (Prötzel *et al.*, 2017), which makes the species unique in all five lines of evidence. Other characters show a great variability, such as the dorsal crest, which can be present or absent in males of *C. linotum* (Prötzel *et al.*, 2015), *C. nasutum, C. radamanus* or *C. vohibola* (Gehring *et al.*, 2011). More constant is the shape of the dorsal crest, consisting either of spines, e.g. in *C. radamanus*, or cones, e.g. in *C. fallax,* and *C. ratnasariae* sp. nov.. Another character that usually is diagnostic is the presence or absence of axillary pits (Andreone *et al.*, 2001) which are also present in the type series of *C. nasutum* and were also mentioned by Gehring *et al.* (2011). Thus, axillary pits are lacking in the specimens of clade K, which *C. nasutum* was assigned to, following Gehring *et al.* (2012). So far we cannot tell whether the presence of axillary pits also varies, perhaps depending on the presence or number of mites in the habitat, or if the structure of the skin might be have changed during the long period of storage and the axillary pits are an artefact. As mentioned above, the assignment of *C. nasutum* to clade K was partly made owing to the lack of better alternatives and to avoid over-splitting of species. The attempt to isolate DNA from the holotype using a target enrichment approach in development by Straube et al. (unpubl. data) failed, but might be repeated once this promising method is better established. The assignment of *C. fallax* to clade H, again following Gehring *et al.* (2012), is strongly supported by morphological and osteological characters, e.g. presence of a FF, and also by the knowledge of the type locality which is in South-eastern Madagascar within the distribution of clade K specimens.

With 16 described species to date the *C. nasutum* group is surprisingly diverse compared to other groups within the genus. The species of the *C. furcifer* group for example are of similar body size (Prötzel *et al.*, 2016) and their genetic clades radiated at about the same time (Tolley *et al.*, 2013) but the group contains only eight described species to date (Glaw, 2015). The species are morphologically conservative and all are more or less uniformly green coloured and lacking any conspicuous colour signals. Signalling structures may promote speciation by enhancing sexual selection or species recognition, and in some lizards, it has been hypothesised that signalling structures, e.g. dewlaps in *Anolis*, have contributed to increased speciation and diversification rates (Ingram *et al.*, 2016; Losos, 2009). The rostral appendage of the *C. nasutum* group is also used for intraspecific communication (Parcher, 1974) and might accelerate the rate of speciation as well. Within the group the prominence of the rostral appendage is highly variable. It ranges from very large in *C. gallus, C. gehringi*, and *C. lefona* to almost completely absent in *C. vohibola* or completely absent in *C. vatosoa.* In contrast to anoles there are no studies about the signalling function of colour variation of the rostral appendages in chameleons. It would be interesting to check whether there is a correlation of the prominence of the rostral appendage with the presence of syntopic species of the group. There is certainly a great deal of potential for future studies on this fascinating group of lizards.

Supplement Files

File 1: Supplementary Table 1. Morphological measurments of all investigated specimens of the *Calumma nasutum* group.
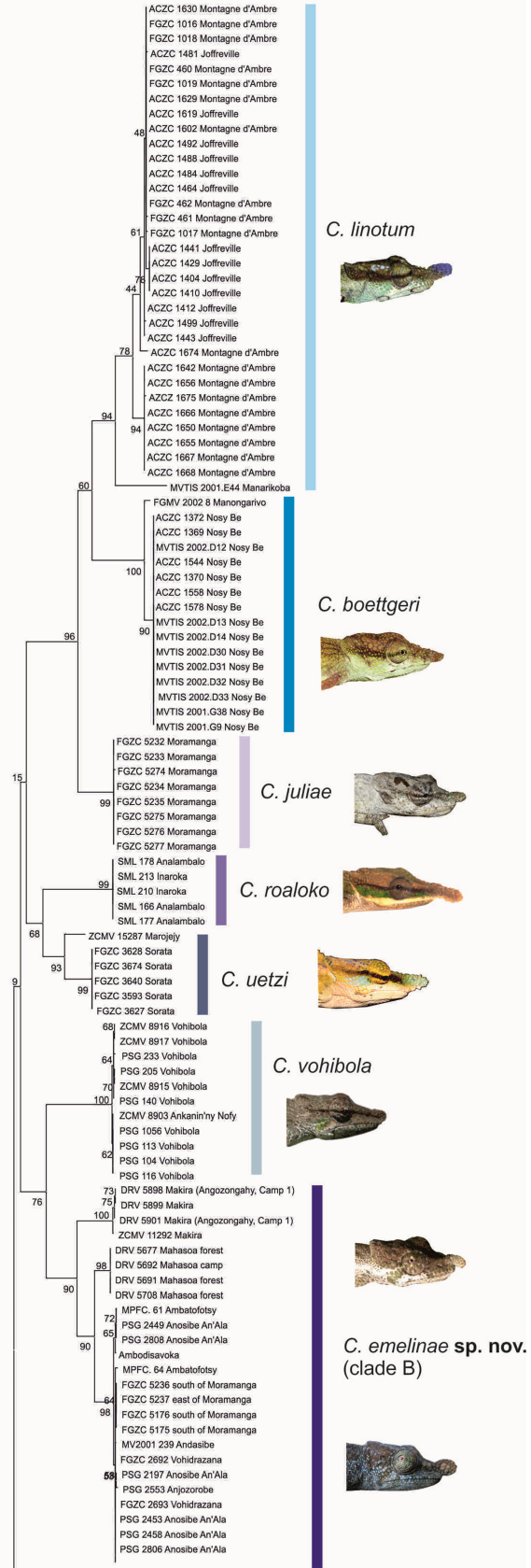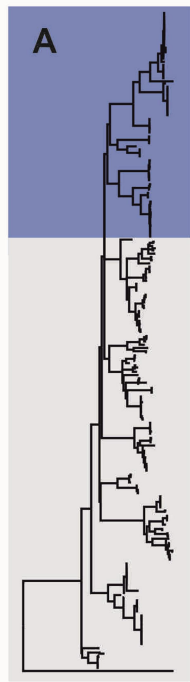
References

Andreone, F, Mattioli, F, Jesu, R & Randrianirina, JE (2001): Two new chameleons of the genus *Calumma* from north-east Madagascar, with observations on hemipenal morphology in the *Calumma furcifer* group (Reptilia, Squamata, Chamaeleonidae). *Journal of Herpetology, 11*, 53–68.

Angel, F (1942): Les lézards de Madagascar. *Mémoires de l'Académie Malgache, 36*, 1–193.

Bickford, D, Lohman, DJ, Sodhi, NS, Ng, PK, Meier, R, Winker, K, Ingram, KK & Das, I (2006): Cryptic species as a window on diversity and conservation. *Trends in ecology & evolution, 22*, 148–155.

Branch, W, Tolley, KA & Tilbury, CR (2006): A new Dwarf Chameleon (Sauria: *Bradypodion* Fitzinger, 1843) from the Cape Fold Mountains, South Africa. *African Journal of Herpetology, 55*, 123–141.

Bruford, M, Hanotte, O, Brookfield, J & Burke, T (1992): Single-locus and multilocus DNA fingerprint. *In:* A Hoelzel (Ed), *Molecular genetic analysis of populations: a practical approach*. Oxford University Press, Oxford, pp. 225–270.

Brygoo, ER (1971): Reptiles Sauriens Chamaeleonidae. Genre *Chamaeleo. Faune de Madagascar, 33*, 1–318.

Dorr, LJ (1997): *Plant collectors in Madagascar and the Comoro Islands*. Kew: Royal Botanic Gardens, pp. 524.

Duméril, A & Bibron, G (1836): *Erpétologie Générale ou Histoire Naturelle Complete des Reptiles* (Vol. 3). Paris: Librairie encyclopédique de Roret, pp. 517

Duméril, A, Bibron, G & Duméril, A (1854): *Erpétologie Genérale ou Histoire Naturelle Complète des Reptiles. Tome Septième, Duexiéme Partie* (Vol. XII). Paris: Librairie Encyclopédique de Roret

Eckhardt, FS, Gehring, P-S, Bartel, L, Bellmann, J, Beuker, J, Hahne, D, Korte, J, Knittel, V, Mensch, M, Nagel, D, Pohl, M, Rostosky, C, Vierath, V, Wilms, V, Zenk, J & Vences, M (2012): Assessing sexual dimorphism in a species of Malagasy chameleon (*Calumma boettgeri*) with a newly defined set of morphometric and meristic measurements. *Herpetology Notes, 5*, 335–344.

Gehring, P-S, Pabijan, M, Ratsoavina, FM, Köhler, J, Vences, M & Glaw, F (2010): A Tarzan yell for conservation: a new chameleon, *Calumma tarzan* sp. n., proposed as a flagship species for the creation of new nature reserves in Madagascar. *Salamandra, 46*, 167–179.

Gehring, P-S, Ratsoavina, FM, Vences, M & Glaw, F (2011): *Calumma vohibola*, a new chameleon species (Squamata: Chamaeleonidae) from the littoral forests of eastern Madagascar. *African Journal of Herpetology, 60*, 130–154.

Gehring, P-S, Tolley, KA, Eckhardt, FS, Townsend, TM, Ziegler, T, Ratsoavina, F, Glaw, F & Vences, M (2012): Hiding deep in the trees: discovery of divergent mitochondrial lineages in Malagasy chameleons of the *Calumma nasutum* group. *Ecology and Evolution, 2*, 1468–1479.

Gignac, PM, Kley, NJ, Clarke, JA, Colbert, MW, Morhardt, AC, Cerio, D, Cost, IN, Cox, PG, Daza, JD & Early, CM (2016): Diffusible iodine-based contrast-enhanced computed tomography (diceCT): An
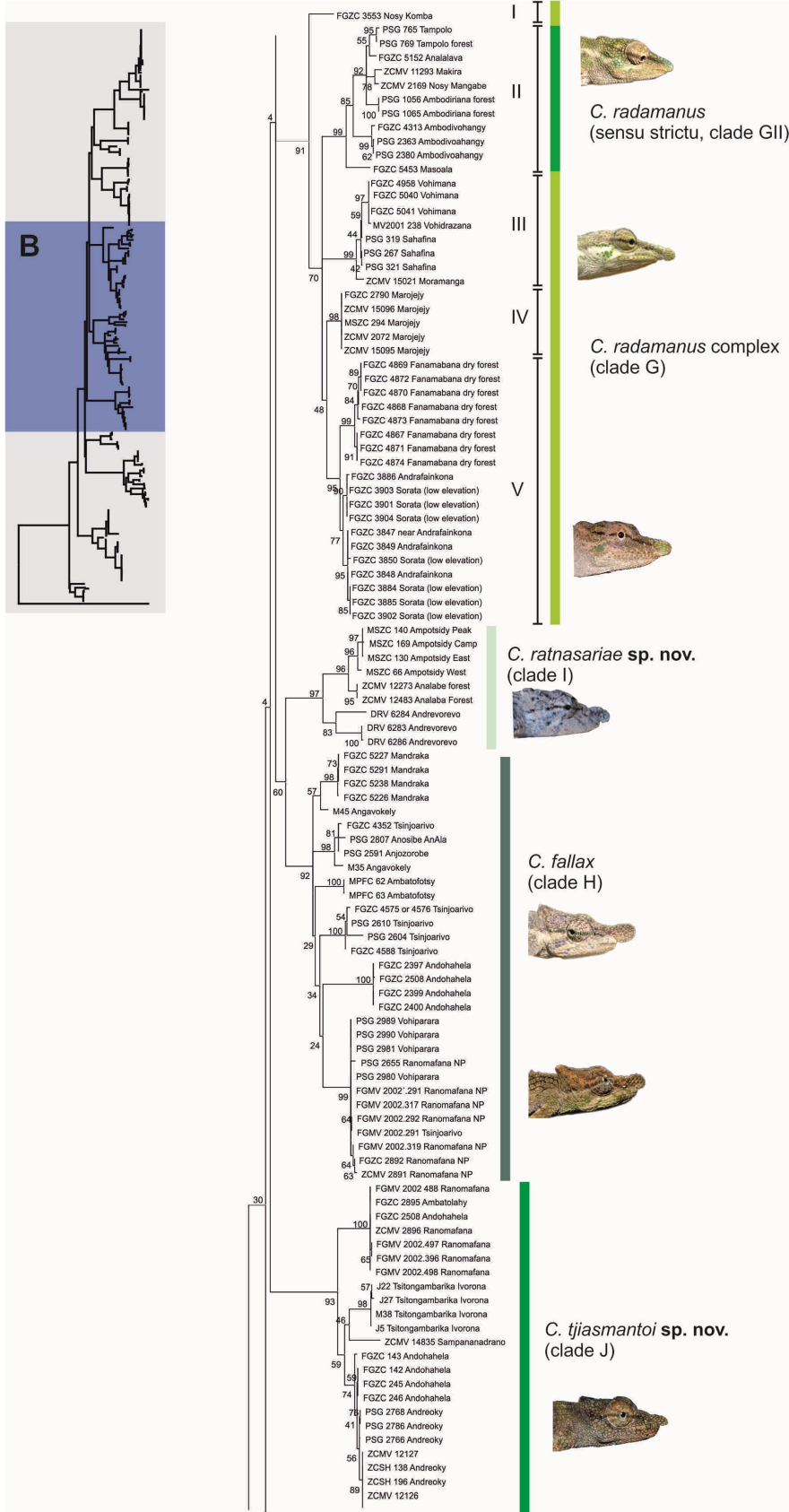
emerging tool for rapid, high-resolution, 3-D imaging of metazoan soft tissues. *Journal of anatomy, 228*, 889–909.

Glaw, F (2015): Taxonomic checklist of chameleons (Squamata: Chamaeleonidae). *Vertebrate Zoology, 65*, 167–246.

Glaw, F & Vences, M (1994): *A fieldguide to the amphibians and reptiles of Madagascar* (2 ed.). Cologne: Vences & Glaw Verlag, pp. 480.

Glaw, F & Vences, M (2007): *A field guide to the amphibians and reptiles of Madagascar* (3 ed.). Cologne: Vences & Glaw Verlag, pp. 496.

Han, D, Zhou, K & Bauer, AM (2004): Phylogenetic relationships among gekkotan lizards inferred from C-mos nuclear DNA sequences and a new classification of the Gekkota. *Biological Journal of the Linnean Society, 83*, 353–368.

Harper, GJ, Steininger, MK, Tucker, CJ, Juhn, D & Hawkins, F (2007): Fifty years of deforestation and forest fragmentation in Madagascar. *Environmental Conservation, 34*, 325–333.

Hawlitschek, O, Scherz, MD, Ruthensteiner, B, Crottini, A & Glaw, F (2018): Computational molecular species delimitation and taxonomic revision of the gecko genus Ebenavia Boettger, 1878. *The Science of Nature, 105*, 1–21.

Ingram, T, Harrison, A, Mahler, DL, del Rosario Castañeda, M, Glor, RE, Herrel, A, Stuart, YE & Losos, JB (2016): Comparative tests of the role of dewlap size in Anolis lizard speciation. *Proceedings of the Royal Society of London B: Biological Sciences, 283*, 1–9.

Jackman, TR, Irschick, DJ, De Queiroz, K, Losos, JB & Larson, A (2002): Molecular phylogenetic perspective on evolution of lizards of the Anolis grahami series. *Journal of Experimental Zoology Part A: Ecological Genetics and Physiology, 294*, 1–16.

Klaver, C & Böhme, W (1997): *Chamaeleonidae. Das Tierreich. Part 112*: Verlag Walter de Gruyter & Co, Berlin and New York.

Klaver, C & Böhme, W (1986): Phylogeny and classification of the Chamaeleonidae (Sauria) with special reference to hemipenis morphology. *Bonner Zoologische Monographien, 22*, 1–64.

Kumar, S, Stecher, G & Tamura, K (2016): MEGA7: Molecular Evolutionary Genetics Analysis Version 7.0 for Bigger Datasets. *Molecular biology and evolution, 33*, 1870–1874.

Leaché, AD, Zhu, T, Rannala, B & Yang, Z (2018): The spectre of too many species. *Systematic biology*, syy051.

Librado, P & Rozas, J (2009): DnaSP v5: a software for comprehensive analysis of DNA polymorphism data. *Bioinformatics, 25*, 1451–1452.

Losos, JB (2009): *Lizards in an Evolutionary Tree* (Vol. 10). Berkeley: University of California Press, pp. 509.

Macey, JR, Larson, A, Ananjeva, NB, Fang, Z & Papenfuss, TJ (1997): Two novel gene orders and the role of light-strand replication in rearrangement of the vertebrate mitochondrial genome. *Molecular biology and evolution, 14*, 91–104.

Macey, JR, Schulte, JA, Larson, A, Ananjeva, NB, Wang, Y, Pethiyagoda, R, Rastegar-Pouyani, N & Papenfuss, TJ (2000): Evaluating trans-Tethys migration: an example using acrodont lizard phylogenetics. *Systematic biology, 49*, 233–256.

Mertens, R (1933): Die Reptilien der Madagaskar-Expedition Prof. Dr. H. Bluntschli's. *Senckenbergiana biologica, 15*, 260–274.

Mertens, R (1966): Chamaeleonidae. *Das Tierreich, 83*, 1–37.

Miralles, A, Vasconcelos, R, Perera, A, Harris, DJ & Carranza, S (2011): An integrative taxonomic revision of the Cape Verdean skinks (Squamata, Scincidae). *Zoologica Scripta, 40*, 16–44.

Mocquard, MF (1900a): Diagnoses d'espèces nouvelles de reptiles de Madagascar. *Bulletin du Muséum national d'histoire naturelle, 6*, 344–345.

Mocquard, MF (1900b): Nouvelle contribution a` la faune herpe´tologique de Madagascar. *Bulletin de la Société philomathique de Paris, 9*, 93–111.

Parcher, SR (1974): Observations on the natural histories of six Malagasy Chamaeleontidae. *Zeitschrift für Tierpsychologie, 34*, 500–523.

Prötzel, D, Lambert, S, Andrianasolo, G, Hutter, C, Cobb, K, Scherz, M & Glaw, F (2018a): The smallest 'true chameleon' from Madagascar: a new, distinctly colored species of the *Calumma boettgeri* complex (Squamata: Chamaeleonidae) *Zoosystematics and Evolution, 94*, 409–423.

Prötzel, D, Ruthensteiner, B & Glaw, F (2016): No longer single! Description of female *Calumma vatosoa* (Squamata, Chamaeleonidae) including a review of the species and its systematic position. *Zoosyst. Evol., 92*, 13–21.

Prötzel, D, Ruthensteiner, B, Scherz, MD & Glaw, F (2015): Systematic revision of the Malagasy chameleons *Calumma boettgeri* and *C. linotum* (Squamata: Chamaeleonidae). *Zootaxa, 4048*, 211–231.

Prötzel, D, Vences, M, Hawlitschek, O, Scherz, MD, Ratsoavina, FM & Glaw, F (2018b): Endangered beauties: Micro-CT cranial osteology, molecular genetics and external morphology reveal three new species of chameleons in the *Calumma boettgeri* complex (Squamata: Chamaeleonidae). *Zoological Journal of the Linnean Society, 184*, 471–498.

Prötzel, D, Vences, M, Scherz, MD, Vieites, DR & Glaw, F (2017): Splitting and lumping: An integrative taxonomic assess-ment of Malagasy chameleons in the *Calumma guibei* complex results in the new species *C. gehringi* sp. nov. *Vertebrate Zoology, 67*, 231-249.

Raxworthy, CJ & Nussbaum, RA (2006): Six new species of occipital-lobed *Calumma* chameleons (Squamata: Chamaeleonidae) from montane regions of Madagascar, with a new description and revision of *Calumma brevicorne*. *Copeia, 2006*, 711–734.

Ride, W (1999): *International code of zoological nomenclature*: International Trust for Zoological Nomenclature

Rieppel, O & Crumly, C (1997): Paedomorphosis and skull structure in Malagasy chamaeleons (Reptilia: Chamaeleoninae). *Journal of Zoology, 243*, 351–380.

Salzburger, W, Ewing, GB & Von Haeseler, A (2011): The performance of phylogenetic algorithms in estimating haplotype genealogies with migration. *Molecular ecology, 20*, 1952–1963.

Scherz, MD, Glaw, F, Rakotoarison, A, Wagler, M & Vences, M (2018): Polymorphism and synonymy of *Brookesia antakarana* and *B. ambreensis*, leaf chameleons from Montagne d'Ambre in north Madagascar. *Salamandra, 54*, 259–268.

Scherz, MD, Hawlitschek, O, Andreone, F, Rakotoarison, A, Vences, M & Glaw, F (2017): A review of the taxonomy and osteology of the *Rhombophryne serratopalpebrosa* species group (Anura: Microhylidae) from Madagascar, with comments on the value of volume rendering of micro-CT data to taxonomists. *Zootaxa, 4273*, 301–340.

Sentís, M, Chang, Y, Scherz, MD, Prötzel, D & Glaw, F (2018): Rising from the ashes: resurrection of the Malagasy chameleons *Furcifer monoceras* and *F. voeltzkowi* (Squamata: Chamaeleonidae), based on micro-CT scans and external morphology. *Zootaxa, 4483*, 549–566.

Stephens, M, Smith, NJ & Donnelly, P (2001): A new statistical method for haplotype reconstruction from population data. *The American Journal of Human Genetics, 68*, 978–989.

Thorpe, R, Leadbeater, D & Pook, C (2005): Molecular clocks and geological dates: cytochrome b of Anolis extremus substantially contradicts dating of Barbados emergence. *Molecular ecology, 14*, 2087–2096.

Thorpe, R, Surget-Groba, Y & Johansson, H (2008): The relative importance of ecology and geographic isolation for speciation in anoles. *Philosophical Transactions of the Royal Society B: Biological Sciences, 363*, 3071–3081.

Tilbury, C & Tolley, KA (2009): A new species of dwarf chameleon (Sauria; Chamaeleonidae, *Bradypodion* Fitzinger) from KwaZulu Natal South Africa with notes on recent climatic shifts and their influence on speciation in the genus. *Zootaxa, 2226*, 43–57.

Tolley, K, Townsend, TM & Vences, M (2013): Large-scale phylogeny of chameleons suggests African origins and Eocene diversification. *Proceedings of the Royal Society of London B: Biological Sciences, 280*, 11–21.

Vasconcelos, R, Perera, A, Geniez, P, Harris, DJ & Carranza, S (2012): An integrative taxonomic revision of the *Tarentola* geckos (Squamata, Phyllodactylidae) of the Cape Verde Islands. *Zoological Journal of the Linnean Society, 164*, 328–360.

Viette, P (1991): Principales localités où des insectes ont été recueillis à Madagascar: Chief field stations where insects were collected in Madagascar. *Faune de Madagascar, supplement, 2*, 1–88.

A

ACZC 1630 Montagne d'Ambre
FGZC 1016 Montagne d'Ambre
FGZC 1018 Montagne d'Ambre
ACZC 1481 Joffreville
FGZC 460 Montagne d'Ambre
FGZC 1019 Montagne d'Ambre
ACZC 1629 Montagne d'Ambre
ACZC 1619 Joffreville
ACZC 1602 Montagne d'Ambre
ACZC 1492 Joffreville
ACZC 1488 Joffreville
ACZC 1484 Joffreville
ACZC 1464 Joffreville
FGZC 462 Montagne d'Ambre
FGZC 461 Montagne d'Ambre
FGZC 1017 Montagne d'Ambre
ACZC 1441 Joffreville
ACZC 1429 Joffreville
ACZC 1404 Joffreville
ACZC 1410 Joffreville
ACZC 1412 Joffreville
ACZC 1499 Joffreville
ACZC 1443 Joffreville
ACZC 1674 Montagne d'Ambre
ACZC 1642 Montagne d'Ambre
ACZC 1656 Montagne d'Ambre
AZCZ 1675 Montagne d'Ambre
ACZC 1666 Montagne d'Ambre
ACZC 1650 Montagne d'Ambre
ACZC 1655 Montagne d'Ambre
ACZC 1667 Montagne d'Ambre
ACZC 1668 Montagne d'Ambre
MVTIS 2001.E44 Manarikoba

C. linotum

FGMV 2002 8 Manongarivo
ACZC 1372 Nosy Be
ACZC 1369 Nosy Be
MVTIS 2002.D12 Nosy Be
ACZC 1544 Nosy Be
ACZC 1370 Nosy Be
ACZC 1558 Nosy Be
ACZC 1578 Nosy Be
MVTIS 2002.D13 Nosy Be
MVTIS 2002.D14 Nosy Be
MVTIS 2002.D30 Nosy Be
MVTIS 2002.D31 Nosy Be
MVTIS 2002.D32 Nosy Be
MVTIS 2002.D33 Nosy Be
MVTIS 2001.G38 Nosy Be
MVTIS 2001.G9 Nosy Be

C. boettgeri

FGZC 5232 Moramanga
FGZC 5233 Moramanga
FGZC 5274 Moramanga
FGZC 5234 Moramanga
FGZC 5235 Moramanga
FGZC 5275 Moramanga
FGZC 5276 Moramanga
FGZC 5277 Moramanga

C. juliae

SML 178 Analambalo
SML 213 Inaroka
SML 210 Inaroka
SML 166 Analambalo
SML 177 Analambalo

C. roaloko

ZCMV 15287 Marojejy
FGZC 3628 Sorata
FGZC 3674 Sorata
FGZC 3640 Sorata
FGZC 3593 Sorata
FGZC 3627 Sorata

C. uetzi

ZCMV 8916 Vohibola
ZCMV 8917 Vohibola
PSG 233 Vohibola
PSG 205 Vohibola
ZCMV 8915 Vohibola
PSG 140 Vohibola
ZCMV 8903 Ankanin'ny Nofy
PSG 1056 Vohibola
PSG 113 Vohibola
PSG 104 Vohibola
PSG 116 Vohibola

C. vohibola

DRV 5898 Makira (Angozongahy, Camp 1)
DRV 5899 Makira
DRV 5901 Makira (Angozongahy, Camp 1)
ZCMV 11292 Makira
DRV 5677 Mahasoa forest
DRV 5692 Mahasoa camp
DRV 5691 Mahasoa forest
DRV 5708 Mahasoa forest
MPFC. 61 Ambatofotsy
PSG 2449 Anosibe An'Ala
PSG 2808 Anosibe An'Ala
Ambodisavoka
MPFC. 64 Ambatofotsy
FGZC 5236 south of Moramanga
FGZC 5237 east of Moramanga
FGZC 5176 south of Moramanga
FGZC 5175 south of Moramanga
MV2001 239 Andasibe
FGZC 2692 Vohidrazana
PSG 2197 Anosibe An'Ala
PSG 2553 Anjozorobe
FGZC 2693 Vohidrazana
PSG 2453 Anosibe An'Ala
PSG 2458 Anosibe An'Ala
PSG 2806 Anosibe An'Ala

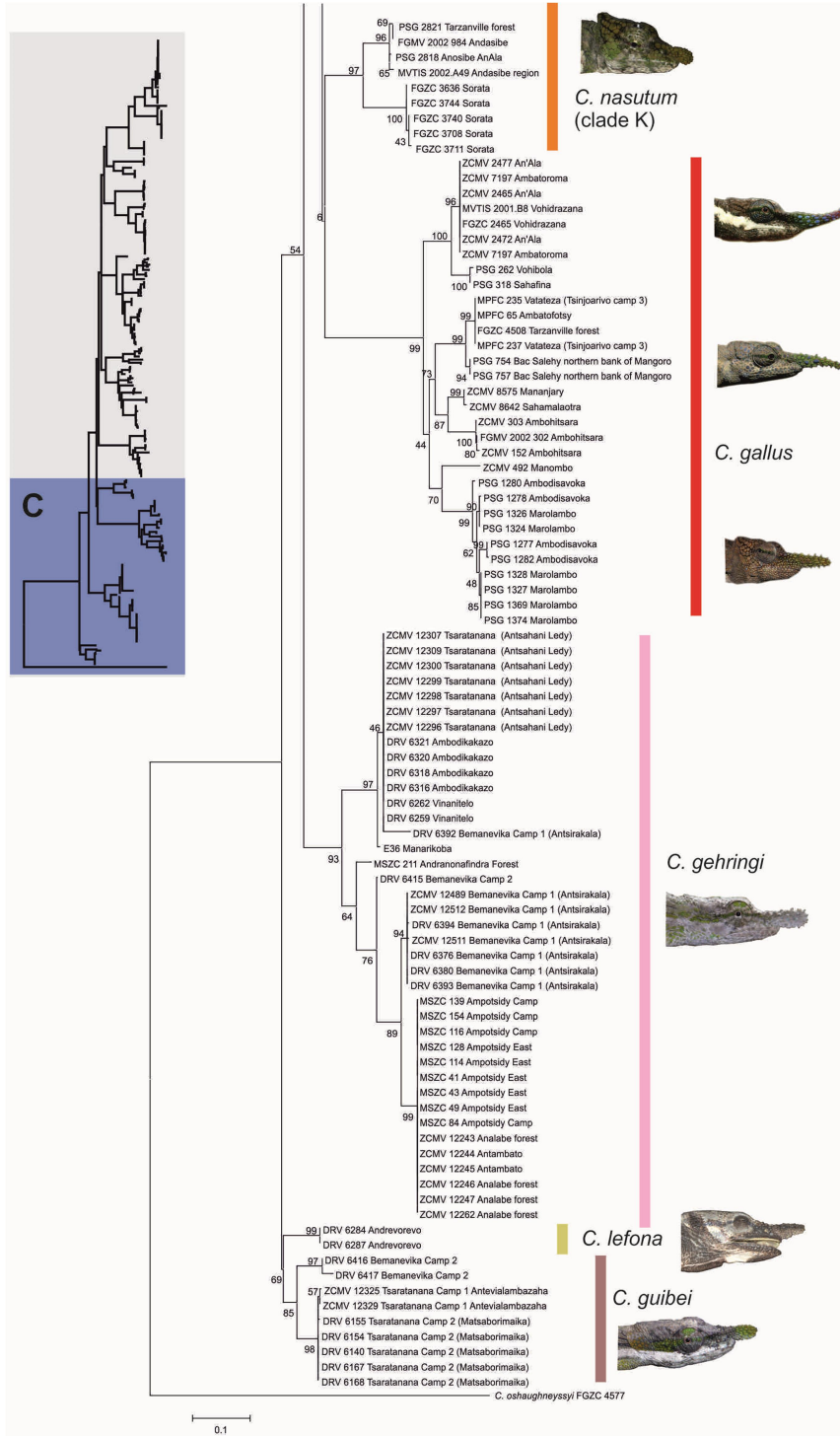*C. emelinae* **sp. nov.**
(clade B)

35

I

Fig. 1. Maximum likelihood tree based on DNA sequences of the mitochondrial *ND2* gene (582 bp) of species of the *Calumma nasutum* group. Numbers at nodes are bootstrap proportions expressed as a percentage (500 replicates).
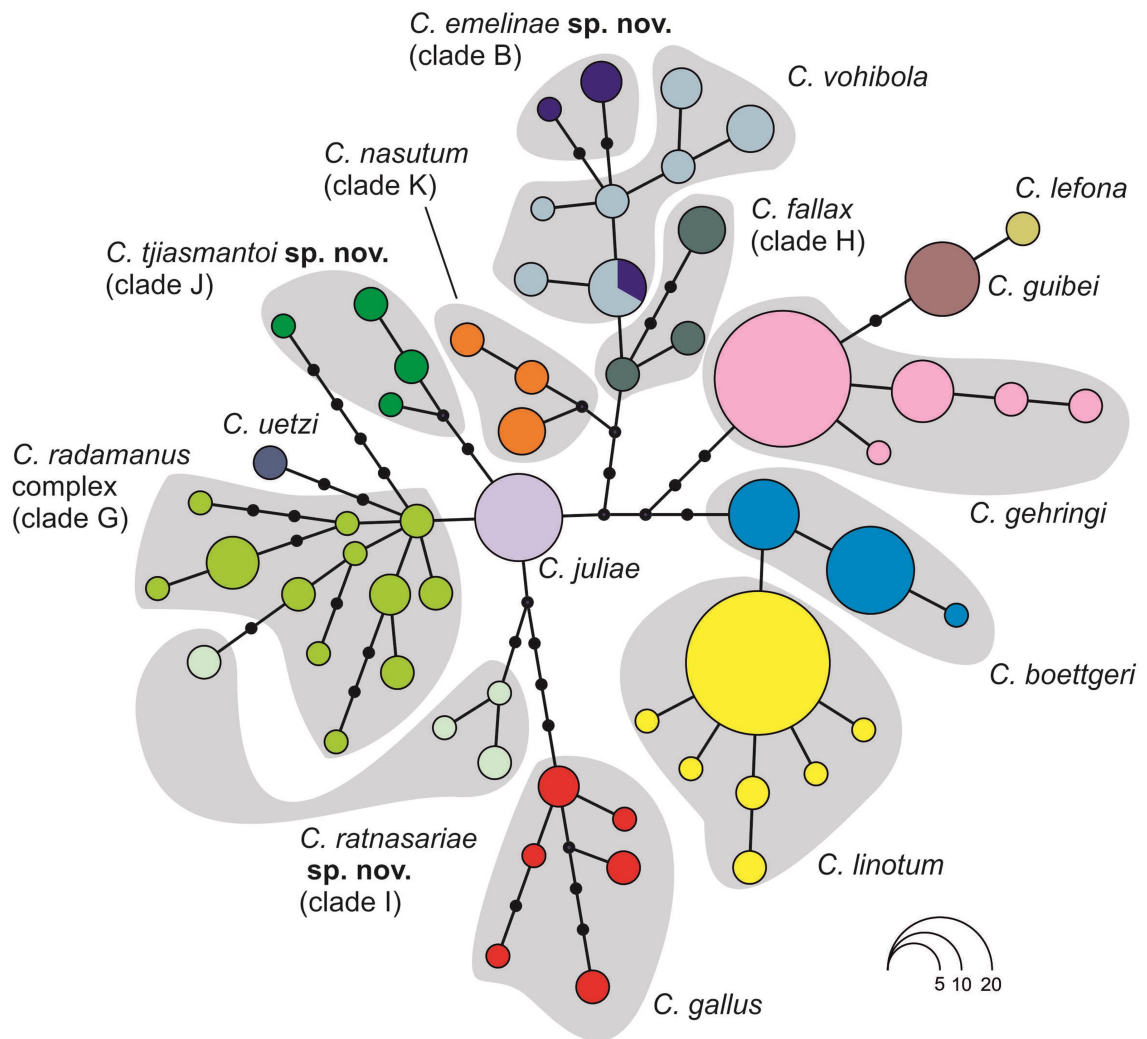
Fig. 2. Haplotype network estimated from sequences of the nuclear *CMOS* gene (360 bp). Black dots represent additional mutational steps, the size of a coloured circle correlates with the species number, see scale.
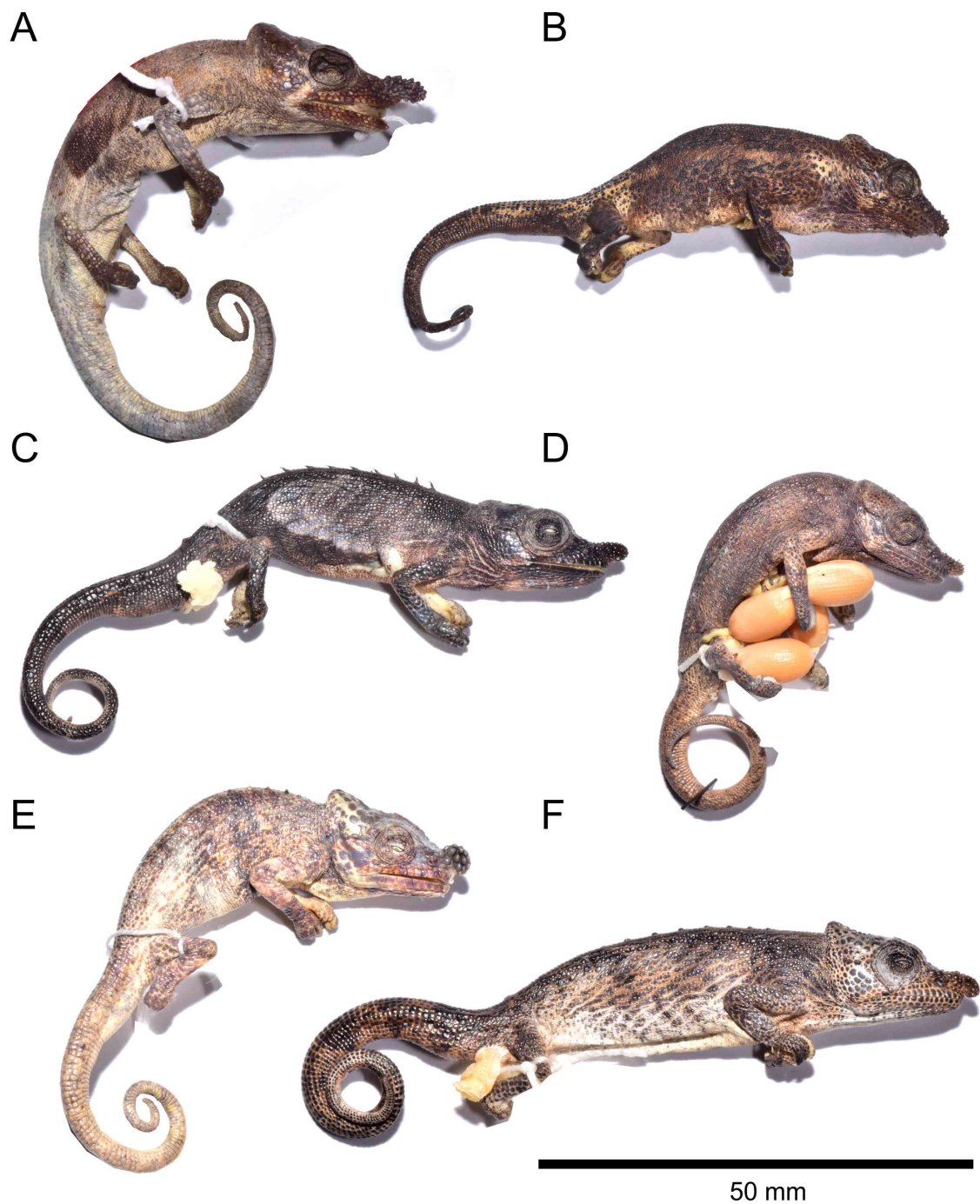
Fig. 3. Preserved type specimens of (**A**) *Calumma nasutum* (lectotype, MNHN 6643C), adult male; (**B**) *C. radamanus* (holotype, SMF 22132), adult male; (**C**) *C. emelinae* sp. nov. (holotype, ZSM 618/2009), adult male; (**D**) *C. tjiasmantoi* sp. nov. (holotype, ZSM 735/2003), adult female; (**E**) *C. fallax* (lectotype, MNHN 1899.317), adult male; (**F**) *C. ratnasariae* sp. nov. (ZSM 35/2016), adult male.
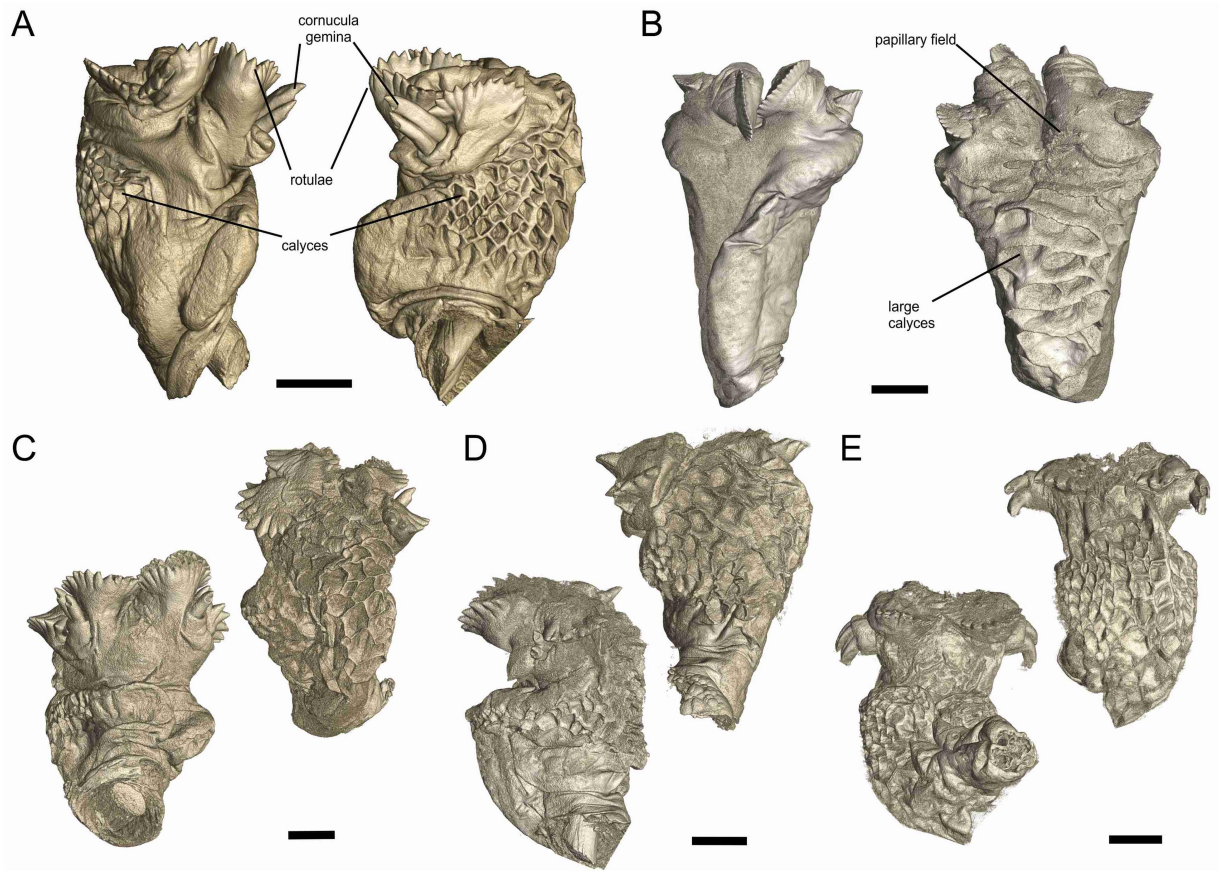
Fig. 4. Micro-CT scans of hemipenes of representative males of the different new or redescribed *Calumma* species (as far as available), each in sulcal (left) and asulcal view (right). (**A**) *C. fallax* (ZSM 694/2003); (**B**) *C. radamanus* (ZSM 443/2005); (**C**) *C. emelinae* sp. nov. (ZSM 618/2009); (**D**) *C. nasutum* (ZSM 924/2003); (**E**) *C. ratnasariae* sp. nov. (ZSM 1724/2010). Scale bar = 1 mm.
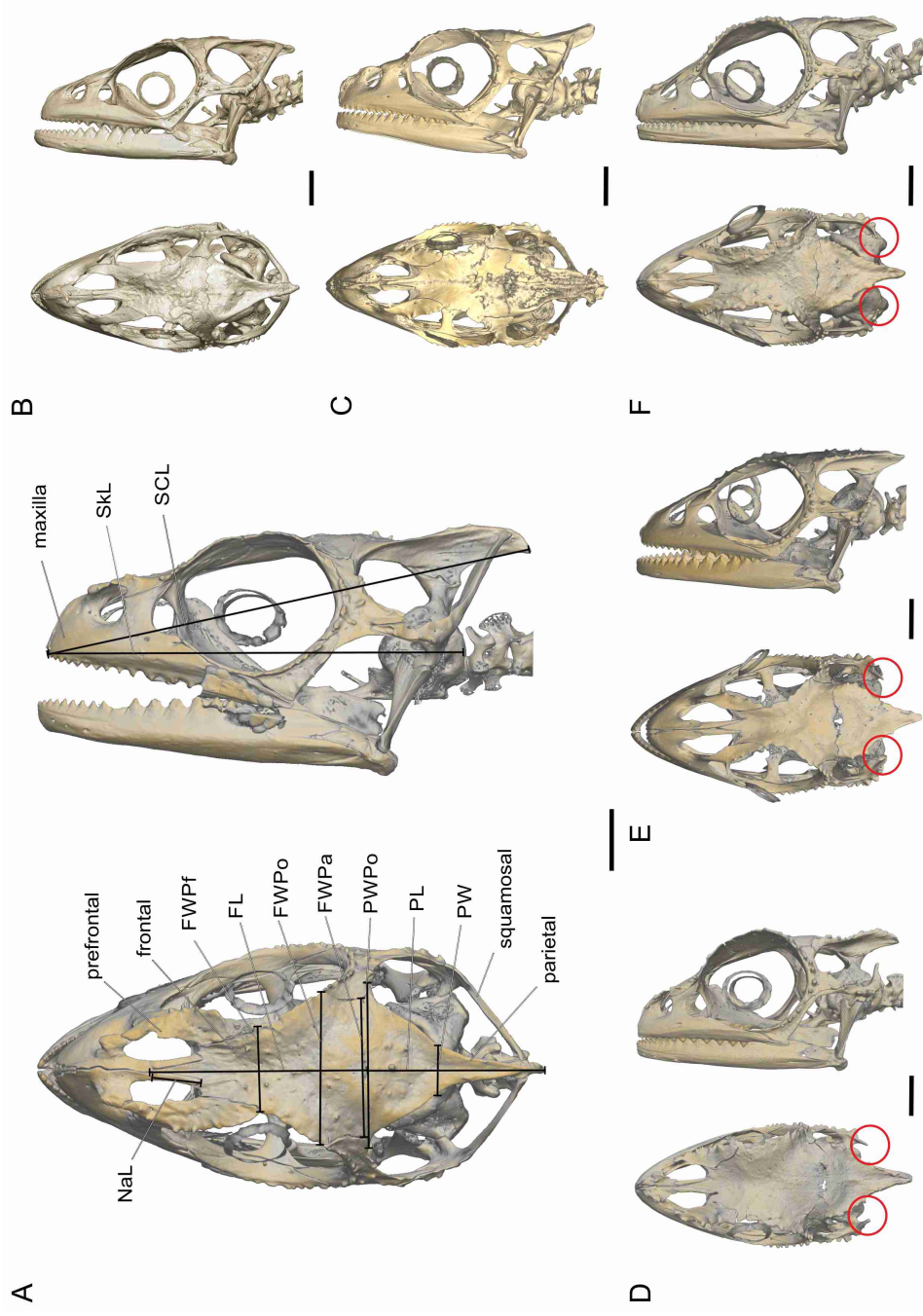
Fig. 5. Micro-computed tomography scans of the skulls of *Calumma nasutum* and *C. radamanus* in dorsal and lateral view. (**A**) *Calumma nasutum* (MNHN 6643C), male lectotype (with scanning artefact at the lower jaw bone); (**B**) *C. nasutum* (MNHN 6643), female paralectotype; (**C**) *C. nasutum* (ZSM 924/2003), male of genetic clade K, assigned to *C. nasutum*; (**D**) *C. radamanus* (SMF 22132), male holotype; (**E**) *C. radamanus* (SMF 26394), female paratype; (**F**) *C. radamanus* (ZSM 475/2010), male of genetic clade GII, assigned to *C. radamanus*. Diagnostic characters are encircled in red. Abbreviations are given in the Material and Methods. Scale bar = 2.0 mm.

Fig. 6. *Calumma nasutum* (clade K) in life from Andasibe region. (**A**, **B**) adult male (not collected) from Mitsinjo/Andasibe in relaxed state, photo: T. Negro/A. Laube; (**C**) adult male (not collected) from Andasibe in stressed colouration, photo: P-S. Gehring; (**D**) juvenile male from Maromizaha Reserve (ZSM 256/2016), slightly stressed; (**E**) juvenile female (not collected) from Maromizaha, in stressed colouration.

Fig. 7. *Calumma nasutum* (clade K) from Sorata, Northern Madagascar. (**A**) juvenile male (FGCZ 3636, UADBA), slightly displaying; (**B**) adult female (not collected), relaxed; (**C**) adult female holotype (ZSM 1699/2012) in stressed colouration.

Fig. 8. Distribution map of six species of the *Calumma nasutum* group in Madagascar. Localities based on collected specimens and/or DNA sequences of Gehring *et al.* (2012) and new sequences shown in Fig. 1.

Fig. 9. *Calumma radamanus* in life. (**A**) adult male (not collected) from Tampolo, Eastern Madagascar, in relaxed state, photo: P-S. Gehring; (**B, C**) juvenile male (ZSM 260/2016) from Masoala, relaxed; (**D**) adult female from Masoala (not collected), relaxed.
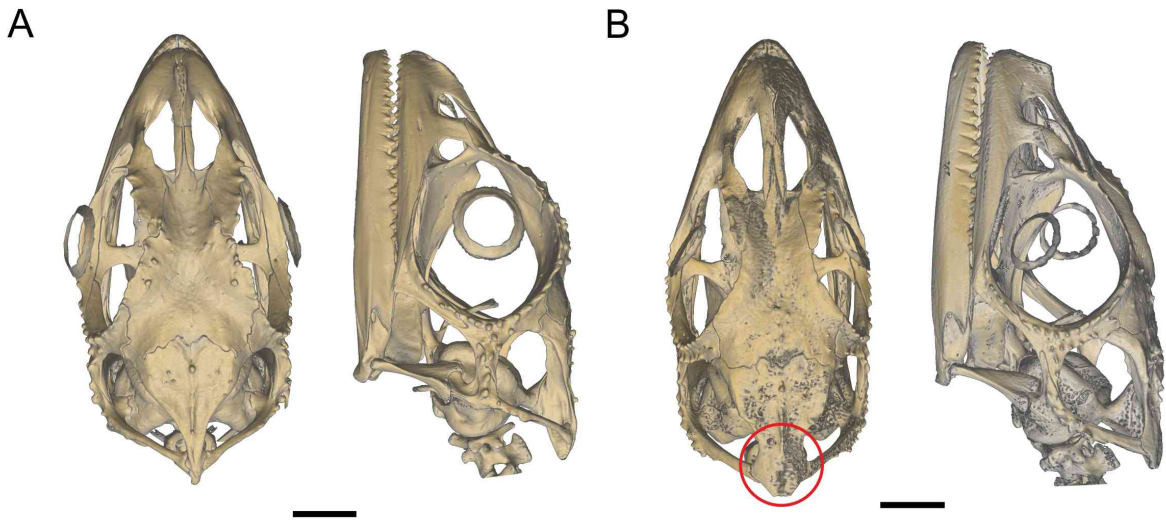
Fig. 10. Micro-computed tomography scans of the skulls of holotypes of species with a closed skull roof in dorsal and lateral view. (**A**) *C. emelinae* sp. nov. (ZSM 618/2009), male holotype; (**B**) *C. tjiasmantoi* sp. nov. (ZSM 735/2003), female holotype. Diagnostic characters are encircled in red. Scale bars: 2.0 mm.

Fig. 11. *Calumma emelinae* sp. nov. in life. (**A**) adult male (not collected) from the type locality in Makira in stress colouration; (**B**) subadult male (not collected) from Mahasoa, in relaxed state; (**C**) adult female (not collected) from Makira, slightly stressed; (**D**) adult female (FGZC 5273, UADBA uncatalogued) from east of Moramanga (Julia Forest) in relaxed state; (**E**) adult female (uncollected) from same location as (D), relaxed.
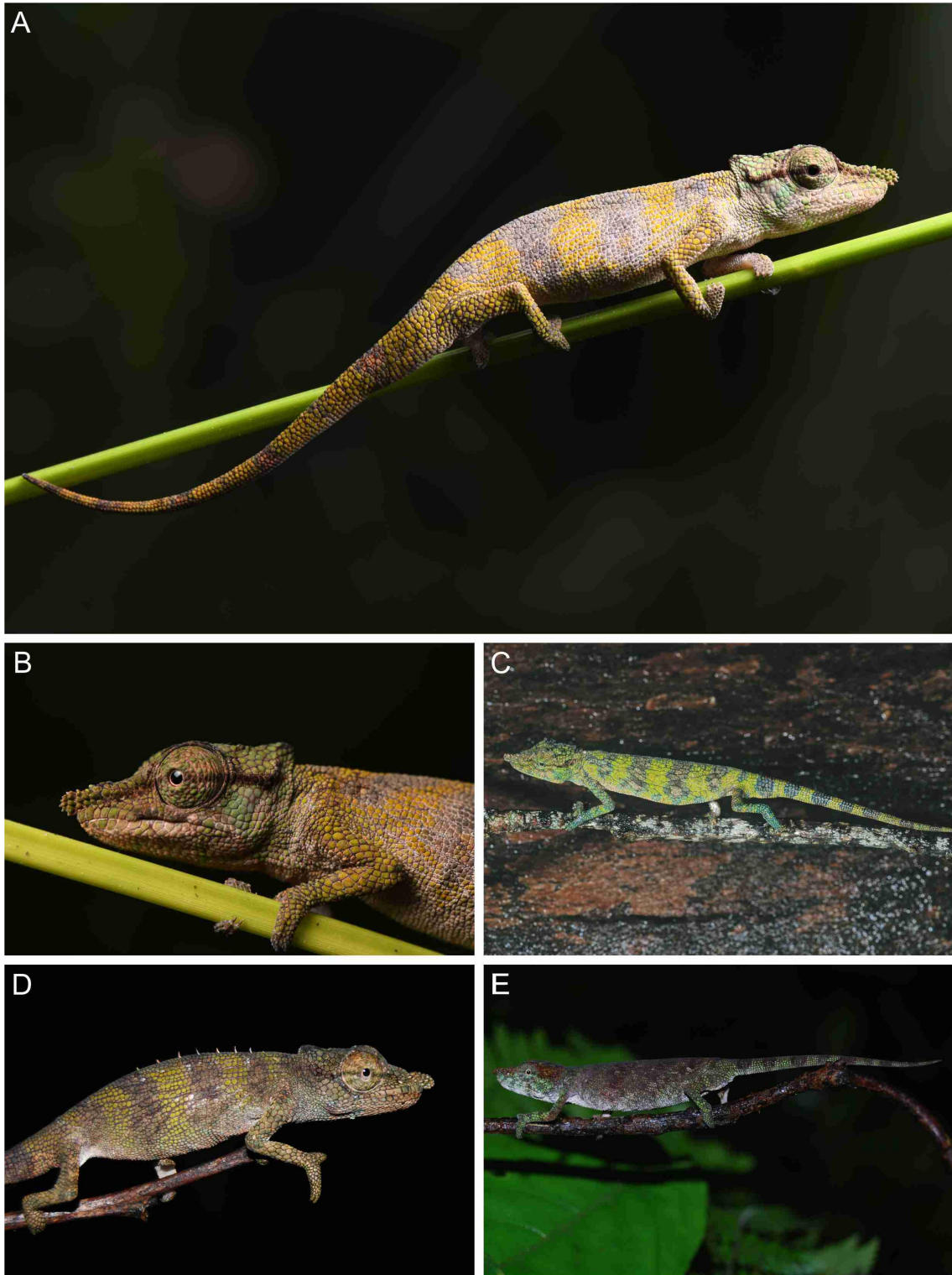
Fig. 12. *Calumma tjiasmantoi* sp. nov. in life. (**A**, **B**) adult male (not collected) from Ranomafana NP in relaxed state, photos: M. Knauf; (**C**) adult male (not collected) from Andohahela (Camp 2 low elevation) in slightly stressed colouration; (**D**) adult male and (**E**) adult female, both from Andreoky, referring to tissue samples PSG_2766, 2768, 2786 in Gehring *et al.* (2012) in relaxed state, photos: P-S. Gehring.
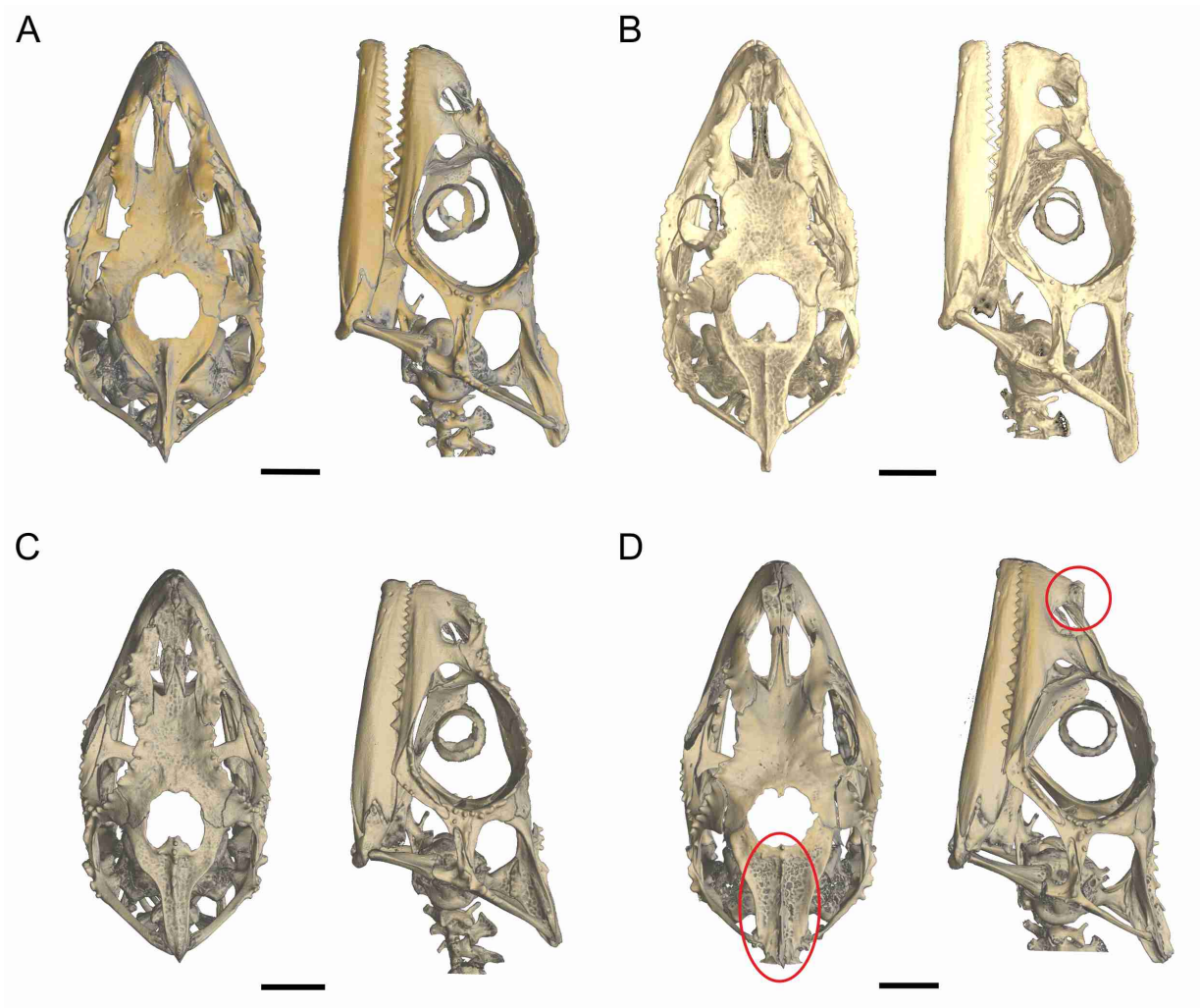
Fig. 13. Micro-computed tomography scans of the skulls of species with a frontoparietal fenestra in dorsal and lateral view. (**A**) *Calumma fallax* (MNHN 1899.317), male lectotype; (**B**) *C. fallax* (MNHN 1840.430), male; (**C**) *C. fallax* (ZSM 286/2016), male of genetic clade H, assigned to *C. fallax*; (**D**) *C. ratnasariae* sp. nov. (ZSM 35/2006), male holotype. Diagnostic characters are encircled in red. Scale bars: 2.0 mm.
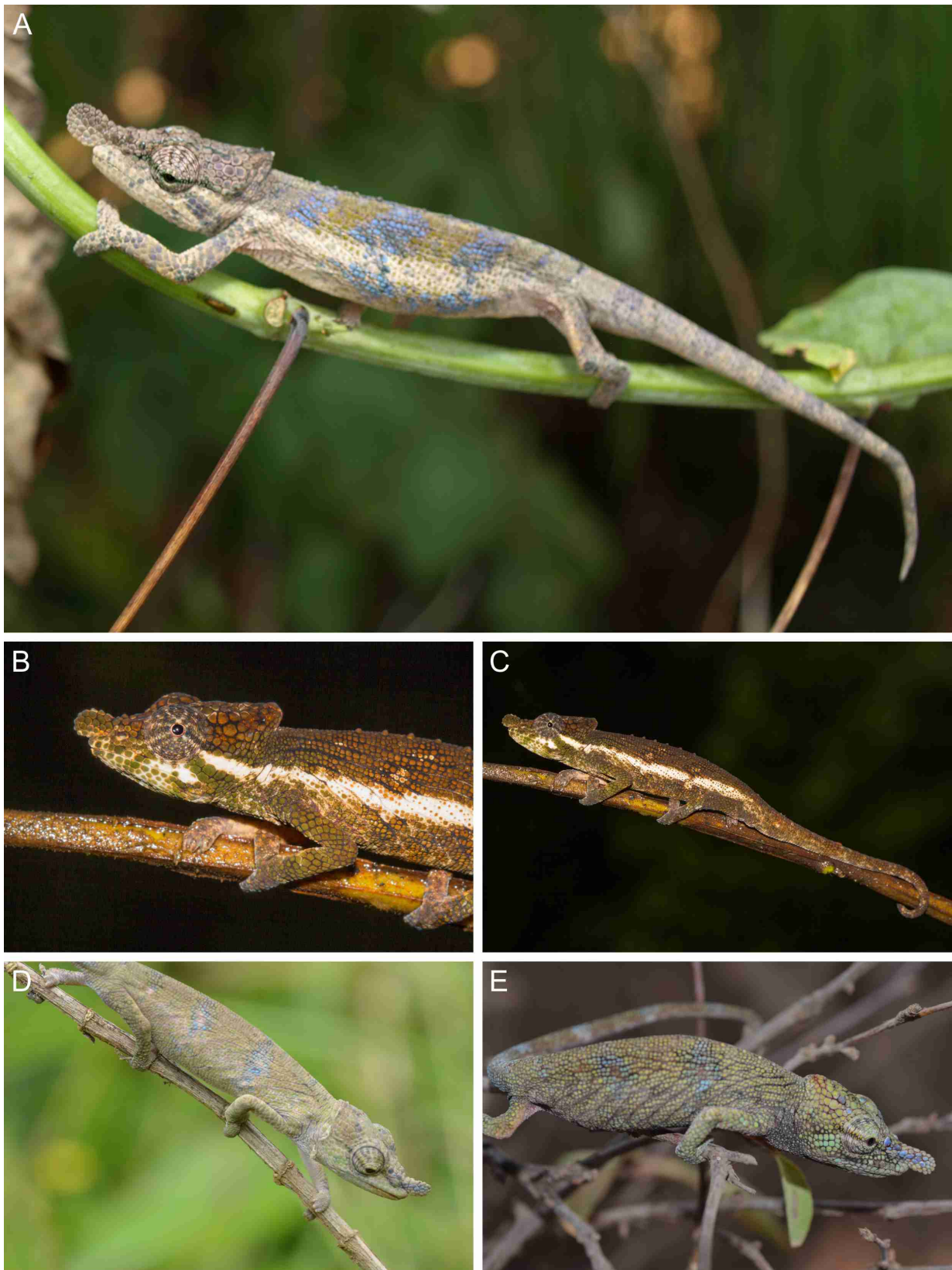
.

Fig. 14. *Calumma fallax* from different locations. (**A**) Adult male (not collected) from Tsinjoarivo in relaxed state; (**B, C**) adult male (not collected) from Ranomafana NP, relaxed, photos: A. Laube/T. Negro; (**D**, **E**) both adult females (ZSM 149/2016 and FGZC 5291, UADBA uncatalogued) from Mandraka, relaxed.
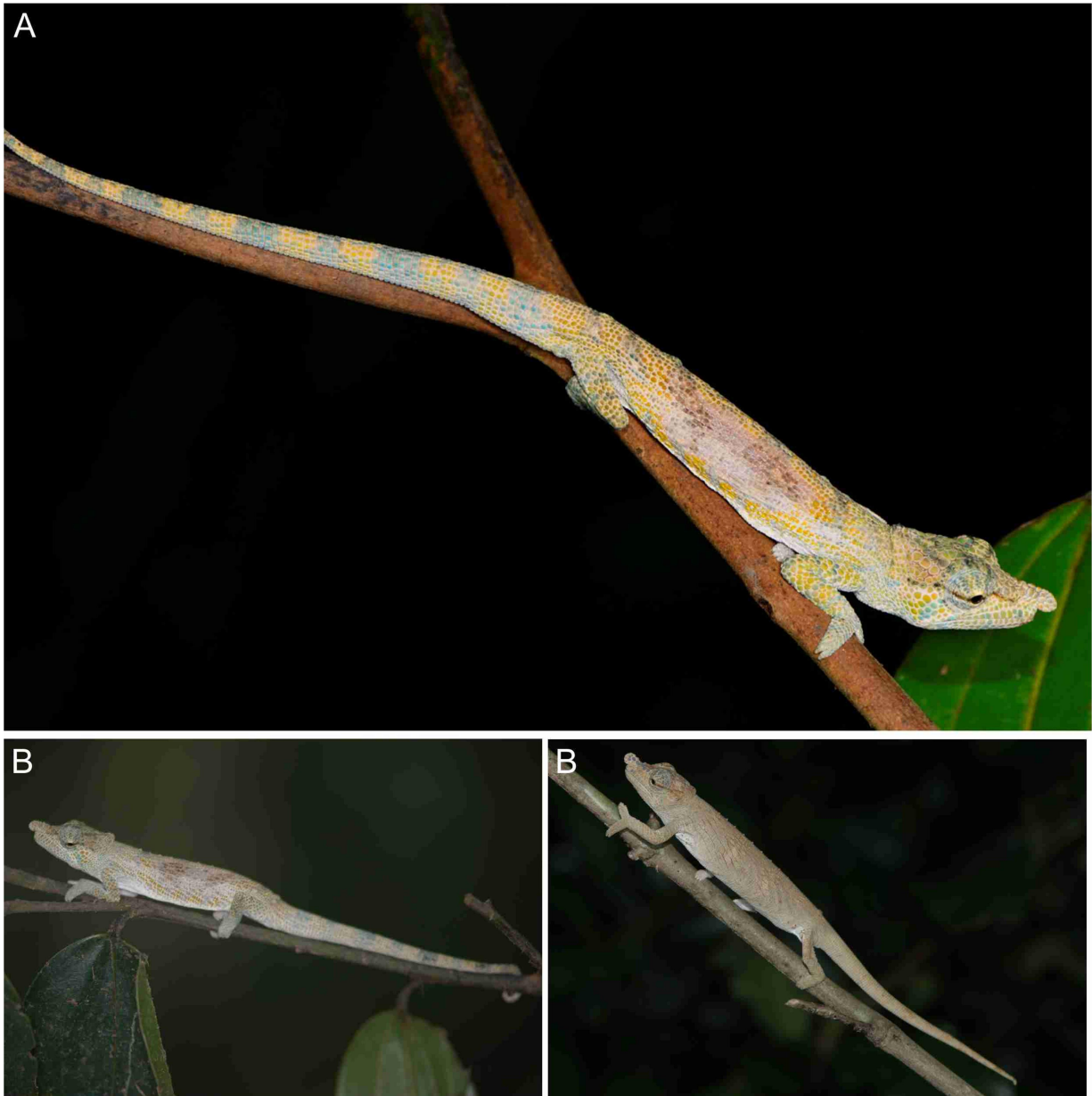
Fig. 15. *Calumma ratnasariae* sp. nov. from Ampotsidy mountains. (**A**, **B**) Adult male holotype (ZSM 35/2016), slightly displaying, and (**C**) adult female (MSZC 0130, UADBA uncatalogued) in relaxed state.

Table 1: Diagnostic characters based on morphology (red numbers indicate diagnostic characters used in the diagnosis): + present; – absent; (+) usually present; +/– absent or present; f, female; m, male; further abbreviations see Material and Methods; all measurements are in millimetres.

species	clade	sex		SVL	TaL	TL	RTaSV	LRA	RRS	RSI	RC	LC	TC	CC	PC	CH	DC	NIL	NSL	UMS	AP	DSCT
				1		1		2	2	3	4	5	6	7	8	9	10	11	11	11	12	13
C. nasutum	**K**	m	N = 4																			
			min	43.7	43.1	89.0	92%	2.2	4.5%	-	+	+	+	(+)	/+	1.5	0	13	12	(s)	(+)	0.9
			max	49.0	51.8	100.8	106%	2.6	5.3%							2.0	12	15	15			1.6
			min–	43.7-	43.1-	89.0-	0.92-	2.2-	0.045-							1.5-	0-	13-	12-			0.9-
			max:	49.0	51.8	100.8	1.06	2.6	0.053							2.0	12	15	15			1.6
			mean:	46.0	46.6	92.6	102%	2.3	5.0%							1.7	5.0	13.7	13.7			1.2
			SD:	2.5	3.7	5.5	6%	0.3	0.4%							0.2	6.0	1.2	1.3			0.3
C. nasutum	**K**	f	N = 4																			
			min	43.0	37.7	80.7	88%	1.2	2.8%	-	+	+	+	(+)	/+	0.7	0	13	14	s	(+)	0.8
			max	49.4	45.7	95.1	97%	1.5	3.2%							1.0		16	15			1.2
			min–	43.0-	37.7-	80.7-95.1	0.88-	1.2-	0.028-							0.7-		13-	14-			0.8-
			max:	49.4	45.7	80.7-95.1	0.97	1.5	0.032							1.0		16	15			1.2
			mean:	46.4	43.3	89.7	93%	1.4	3.0%							0.8		14.8	14.3			1.0
			SD:	2.7	3.8	6.3	4%	0.2	0.2%							0.2		1.3	0.5			0.2
C. radamanus	**GII**	m	N = 4																			
			min	42.6	42.3	84.9	90%	1.4	2.9%	(+)	+	+	(+)	+	-	0.8	0	12	11	s	(-)	0.6
			max	49.2	44.3	93.5	99%	1.7	3.6%							1.5	7	18	15			0.8
			min–	42.6-	42.3-	84.9-93.5	0.9-	1.4-	0.029-							0.8-	0-	12-	11-			0.6-
			max:	49.2	44.3	84.9-93.5	0.9-0.99	1.7	0.036							1.5	7	18	15			0.8
			mean:	46.1	43.2	89.3	94%	1.5	3.3%							1.1	3.3	13.8	13.5			0.8
			SD:	3.0	0.9	4.0	4%	0.2	0.3%							0.4	3.8	2.9	1.9			0.1
C. radamanus	**GII**	f	N = 3																			
			min	43.0	34.0	77.0	79%	0.2	0.5%	+/-	(+)	+	(+)	+	-	0.5	0	13	12	s	-	0.8
			max	49.2	43.7	92.9	89%	1.6	3.4%							0.8	7	15	14			0.9
			min–	43-	34-43.7	77-92.9	0.79-	0.2-	0.005-							0.5-	0-	13-	12-			0.8-
			max:	49.2	34-43.7	77-92.9	0.89	1.6	0.034							0.8	7	15	14			0.9
			mean:	46.4	39.1	85.5	84%	1.0	2.1%							0.6		13.7	12.7			0.8
			SD:	4.7	8.1	24.1	#WERT!	0.6	1.4%							0.4		2.5	2.0			0.1
C. emelinae sp. nov.	**B**	m	N = 3																			
			min	46.6	47.0	93.6	101%	2.3	4.7%	-	+	+	+	+	(+)	0.5	7	14	14	(l)	-	0.7
			max	48.7	54.5	103.2	112%	2.9	6.1%							1.1	10	15	16			0.7

Taxon	Code	Sex	N	Stat																		
C. emelinae sp. nov.	B	f	7	min–max:	46.6-48.7	47-54.5	93.6-103.2	1.01-1.12	2.3-2.9	0.047-0.061	-	(+)	+	+	(-)	0.5-1.1	7-10	14-15	14-16	(I)	-	0.7-0.7
				mean:	47.7	50.7	98.5	106%	2.5	5.2%						0.8	8.7	14.3	14.7			0.7
				SD:	1.1	3.8	4.8	6%	0.3	0.7%						0.3	1.5	0.6	1.2			0.0
C. tjiasmantoi sp. nov.	J	m	1		46.8	48.0	94.8	103%	2.0	4.3%	-	+	+	+	-	1.3	9	16	16	I	(-)	0.6
C. tjiasmantoi sp. nov.	J	f	4	min	43.9	40.2	84.1	92%	1.1	2.4%	-	(+)	+	+	(+)	0.7	0	15	15	I	(-)	0.6
				max	46.1	43.9	90.0	95%	2.1	4.6%						1.2		18	17			0.8
				min–max:	43.9-46.1	40.2-43.9	84.1-90	0.92-0.95	1.1-2.1	0.024-0.046						0.7-1.2		15-18	15-17			0.6-0.8
				mean:	45.2	42.4	87.5	94%	1.6	3.5%						1.0		16.0	15.5			0.7
				SD:	0.9	1.6	2.5	2%	0.4	0.9%						0.2		1.4	1.0			0.1
C. fallax	H	m	7	min	42.9	47.3	90.9	102%	1.8	3.6%	-	+	+	+	-	1.6	6	11	11	I	-	1.1
				max	50.6	57.7	107.3	124%	4.3	8.5%						2.5	11	15	15			1.6
				min–max:	42.9-50.6	47.3-57.7	90.9-107.3	1.02-1.24	1.8-4.3	0.036-0.085						1.6-2.5	6-11	11-15	11-15			1.1-1.6
				mean:	46.7	52.5	99.2	113%	3.1	6.6%						2.0	8.0	12.4	13.1			1.4
				SD:	3.1	3.9	6.3	7%	0.8	1.7%						0.3	2.0	1.6	1.8			0.2
C. fallax	H	f	9	min	40.8	36.5	77.3	89%	1.7	4.2%	-	+	+	+/-	-	0.5	0	10	10	I	-	1.0
				max	50.7	49.1	99.8	104%	3.2	7.6%						1.3	5	14	14			1.8
				min–max:	40.8-50.7	36.5-49.1	77.3-99.8	0.89-1.04	1.7-3.2	0.042-0.076						0.5-1.3	0-5	10-14	10-14			1-1.8
				mean:	46.5	43.8	90.3	94%	2.7	5.9%						0.9	1.0	11.9	12.1			1.3
				SD:	3.4	3.5	6.5	5%	0.5	1.0%						0.3	2.0	1.4	1.2			0.3
C. ratnasariae sp. nov.	I	m	3	min	43.9	53.2	97.1	112%	1.8	3.8%	-	+	+	+	+	1.3	7	11	10	I	-	1.3
				max	52.0	58.7	110.7	121%	2.3	4.8%						1.5	12	14	13			1.5
				min–max:	43.9-52	53.2-58.7	97.1-110.7	1.12-1.21	1.8-2.3	0.038-0.048						1.3-1.5	7-12	11-14	10-13			1.3-1.5

mean:	48.0	55.4	103.4	116%	2.0	4.2%								1.4	8.7	12.7	11.7	1.4
SD:	4.1	2.9	6.9	5%	0.3	0.5%								0.1	2.9	1.5	1.5	0.1

		N = 3																	
C. ratnasariae sp. nov.	f	min	48.7	46.2	95.3	94%	2.1	4.1%	-	+	+	+	+	+	0.7	0	12	11	-
		max	51.5	49.5	101.0	98%	2.2	4.5%							1.0	8	14	12	1.6
		min–	48.7-	46.2-	95.3-101	0.94-	2.1-	0.041-							0.7-	0-	12-	11-	1.2-
		max:	51.5	49.5		0.98	2.2	0.045							1	8	14	12	1.6
		mean:	49.8	47.8	97.5	96%	2.1	4.3%							0.8	4.7	12.7	11.3	1.4
		SD:	1.5	1.7	3.0	2%	0.1	0.2%							0.2	4.2	1.2	0.6	0.2

Table 2: Osteological measurements of the *Calumma nasutum* group. f, female; m, male; further abbreviations see Material and Methods; all measurements are in millimetres.

species	collection no.	sex	FFW	RFFD	NaL	RNaL	FWPf	RFWPf	FWPo	RFWPo	FWPa	RFWPa	PWPo	RPWPo
			14											
C. nasutum	MNHN 6643C	m	-	-	1.6	13.0%	2.4	19.5%	4.9	39.8%	4.2	34.1%	5.0	40.7%
C. nasutum	MNHN 6643B	m	-	-	1.9	15.6%	2.5	20.5%	3.7	30.3%	3.8	31.1%	4.0	32.8%
C. nasutum	ZSM 924/2003	m	-	-	1.8	15.4%	2.8	23.9%	4.3	36.8%	3.6	30.8%	3.5	29.9%
C. nasutum	MNHN 6643	f	-	-	1.9	14.7%	2.5	19.4%	4.1	31.8%	4.0	31.0%	4.3	33.3%
C. nasutum	ZSM 1699/2012	f	-	-	1.9	16.2%	2.4	20.5%	3.8	32.5%	3.6	30.8%	3.7	31.6%
C. emelinae sp. nov.	ZSM 618/2009	m	-	-	1.7	14.5%	3.0	25.6%	4.4	37.6%	3.9	33.3%	4.2	35.9%
C. fallax	MNHN 1899.317	m	2.4	20.0%	1.8	15.0%	2.7	22.5%	4.4	36.7%	3.6	30.0%	3.9	32.5%
C. fallax	MNHN 1890.430	m	2.3	19.0%	1.7	14.0%	3.1	25.6%	4.5	37.2%	3.7	30.6%	3.8	31.4%
C. fallax	ZSM 693/2003	m	2.1	18.6%	2.5	22.1%	2.3	20.4%	4.3	38.1%	3.5	31.0%	3.4	30.1%
C. fallax	ZSM 286/2010	m	2.2	17.3%	1.7	13.4%	3.3	26.0%	4.8	37.8%	4	31.5%	4.2	33.1%
C. ratnasariae sp. nov.	ZSM 35/2016	m	2.5	21.0%	2	16.8%	2.6	21.8%	4.4	37.0%	3.8	31.9%	4.0	33.6%
C. ratnasariae sp. nov.	ZSM 517/2014	m	2.2	18.6%	2	16.9%	2.0	16.9%	4.3	36.4%	3.7	31.4%	4.2	35.6%
C. tjiasmantoi sp. nov.	ZSM 735/2003	f	-	-	2.1	16.9%	2.4	19.4%	4.3	34.7%	3.8	30.6%	4.3	34.7%
C. radamanus	SFM 22132	m	-	-	1.8	15.1%	3.4	28.6%	4.8	40.3%	3.7	31.1%	4.0	33.6%
C. radamanus	ZSM 619/2009	m	-	-	1.6	13.8%	2.7	23.3%	4.9	42.2%	4.0	34.5%	4.1	35.3%
C. radamanus	ZSM 475/2010	m	-	-	2.1	17.8%	3.0	25.4%	4.5	38.1%	4.0	33.9%	3.4	28.8%
C. radamanus complex	ZSM 145/2016	m	-	-	1.6	12.9%	2.6	21.0%	4.5	36.3%	4.1	33.1%	4.6	37.1%
C. radamanus complex	ZSM 451/2016	m	2.0 (j)	-	1.7	16.2%	1.8	17.1%	3.8	36.2%	3.7	35.2%	3.8	36.2%
C. radamanus complex	ZSM 1694/2012	m	-	-	1.3	11.1%	2.4	20.5%	4.5	38.5%	4.0	34.2%	4.6	39.3%
C. radamanus complex	ZSM 1691/2012	m	-	-	1.7	13.5%	3.0	23.8%	4.8	38.1%	4.1	32.5%	4.5	35.7%
C. radamanus complex	ZSM 441/2005	m	-	-	1.9	15.8%	2.2	18.3%	4.0	33.3%	4.0	33.3%	4.3	35.8%

species	collection no.	sex	PSC	PWm	RPWm	PL	RPL	FL	RFL	SCL	RSCL	SkL		
C. radamanus complex	ZSM 88/2015	f	-	-	1.8	15.0%	2.0	16.7%	4.1	34.2%	3.9	32.5%	4.3	35.8%
C. vohibola	ZSM 645/2009	m	-	-	2.0	17.2%	2.2	19.0%	3.9	33.6%	3.5	30.2%	4.0	34.5%
			15	**16**	**16**									
C. nasutum	MNHN 6643C	m	+	1.2	9.8%	5.3	43.1%	6.3	51.2%	15.6	126.8%	12.3		
C. nasutum	MNHN 6643B	m	+	1.4	11.5%	5.4	44.3%	9.6	78.7%	14.5	118.9%	12.2		
C. nasutum	ZSM 924/2003	m	+	1.9	16.2%	4.8	41.0%	9.6	82.1%	13.7	117.1%	11.7		
C. nasutum	MNHN 6643	f	+	1.8	14.0%	5.6	43.4%	7.1	55.0%	15.2	117.8%	12.9		
C. nasutum	ZSM 1699/2012	f	+	2.1	17.9%	4.1	35.0%	6.0	51.3%	13.0	111.1%	11.7		
C. emelinae sp. nov.	ZSM 618/2009	m	+	1.9	16.2%	4.8	41.0%	6.5	55.6%	13.8	117.9%	11.7		
C. fallax	MNHN 1899.317	m	+	0.8	6.7%	4.3	35.8%	5.4	45.0%	14.6	121.7%	12.0		
C. fallax	MNHN 1890.430	m	+	1.9	15.7%	5.2	43.0%	6.1	50.4%	15.2	125.6%	12.1		
C. fallax	ZSM 693/2003	m	- (j)	1.3	11.5%	3.8	33.6%	5.7	50.4%	13.6	120.4%	11.3		
C. fallax	ZSM 286/2010	m	+	1.6	12.6%	4.9	38.6%	5	39.4%	15.8	124.4%	12.7		
C. ratnasariae sp. nov.	ZSM 35/2016	m	+	2.2	18.5%	4.2	35.3%	5.5	46.2%	14.4	121.0%	11.9		
C. ratnasariae sp. nov.	ZSM 517/2014	m	+	2.1	17.8%	3.8	32.2%	5.5	46.6%	13.9	117.8%	11.8		
C.tjiasmantoi sp. nov.	ZSM 735/2003	f	+	2.0	16.1%	4.5	36.3%	6.2	50.0%	14.4	116.1%	12.4		
C. radamanus	SFM 22132	m	-	2.3	19.3%	4.8	40.3%	6.7	56.3%	14.1	118.5%	11.9		
C. radamanus	ZSM 619/2009	m	-	2.6	22.4%	4.7	40.5%	6.5	56.0%	13.8	119.0%	11.6		
C. radamanus	ZSM 475/2010	m	-	1.9	16.1%	4.4	37.3%	6.7	56.8%	13.5	114.4%	11.8		
C. radamanus complex	ZSM 145/2016	m	-	2.8	22.6%	5.0	40.3%	6.8	54.8%	14.8	119.4%	12.4		
C. radamanus complex	ZSM 451/2016	m	-	1.7	16.2%	3.9	37.1%	5.9	56.2%	12.2	116.2%	10.5		
C. radamanus complex	ZSM 1694/2012	m	-	2.8	23.9%	5.5	47.0%	6.8	58.1%	14.8	126.5%	11.7		
C. radamanus complex	ZSM 1691/2012	m	-	2.4	19.0%	5.1	40.5%	6.5	51.6%	15.3	121.4%	12.6		
C. radamanus complex	ZSM 441/2005	m	-	2.2	18.3%	5.3	44.2%	6.1	50.8%	14.8	123.3%	12.0		
C. radamanus complex	ZSM 88/2015	f	-	1.7	14.2%	4.7	39.2%	6.6	55.0%	13.5	112.5%	12.0		
C. vohibola	ZSM 645/2009	m	+	1.6	13.8%	4.6	39.7%	5.6	48.3%	13.6	117.2%	11.6		

Table 3: Mean uncorrected pairwise distances (in percent) between species of the *Calumma nasutum* group for a segment of the ND2 gene. The grey cells show mean distances within species.

	C. boettgeri	C. emelinae sp. nov.	C. fallax	C. gallus	C. gehringi	C. guibei	C. juliae	C. lefona	C. linotum	C. nasutum	C. radamanus	C. ratnasariae sp. nov.	C. roaloko	C. tjiasmantoi sp. nov.	C. uetzi	C. vohibola
.boettgeri	0.2															
C. emelinae sp. nov.	18.5	3.6														
C. fallax	17.5	13.9	7.2													
C. gallus	19.1	17.4	17.3	8.5												
C. gehringi	16.4	13.6	15.1	17.4	6.2											
C. guibei	20.5	15.4	14.8	16.2	14.5	2.7										
C. juliae	11.4	14.6	14.7	16.8	12.8	15.2	0.0									
C. lefona	18.4	15.0	14.8	16.1	14.1	9.1	14.5	0.0								
C. linotum	12.6	13.6	14.8	17.5	15.0	16.7	11.0	14.5	2.1							
C. nasutum	15.8	13.4	14.1	16.3	13.0	14.1	13.3	13.4	13.4	4.5						
C. radamanus	18.8	14.5	14.5	16.0	14.1	14.5	15.7	13.7	15.1	13.5	7.2					
C. ratnasariae sp. nov.	19.1	15.3	13.3	18.1	15.3	15.9	14.7	15.6	15.3	15.0	15.3	6.4				
C. roaloko	17.9	14.2	14.6	17.2	15.3	15.3	13.6	13.9	14.5	14.8	14.7	15.7	0.1			
C. tjiasmantoi sp. nov	16.7	14.6	14.7	16.9	14.6	15.8	14.9	15.9	15.3	14.0	14.5	15.3	16.6	4.7		
uetzi	15.3	12.4	12.8	15.9	12.4	14.7	12.8	13.6	12.2	12.9	12.8	13.3	11.9	13.3	2.4	
vohibola	19.3	12.4	15.4	18.0	14.5	15.8	14.6	15.4	15.5	15.0	15.6	15.2	15.4	14.9	12.1	0.4

Table 4: Diagnostic characters of the *Calumma nasutum* group based on colouration. f, female; m, male; further abbreviations see Material and Methods.

species	sex	colouration of body 17	colouration of rostral appendage 18	colouration of the cheek 19	body patterning 20	stripe crossing the eyes 21
C. nasutum	m	brown, green, yellowish	= body colouration	= body colouration	three to four diffuse dorsoventral blotches of variable colour and a light lateral stripe	indistinct dark stripe
C. nasutum	f	green to beige	= body colouration	= body colouration	four diffuse dark dorsoventral blotches with light spots on the body and a light lateral stripe	indistinct dark stripe
C. radamanus	m	green to beige	turquoise or blue	turquoise or bright green	three blue or violet lateral blotches, crossed by a beige-white stripe	dark stripe
C. radamanus	f	green to beige	turquoise or blue	turquoise or bright green	three blue or violet lateral blotches, crossed by a beige-white stripe	dark stripe
C. emelinae sp. nov.	m	green to beige	= body colouration	bright green	three scattered blotches and white lateral stripe	dark stripe
C. emelinae sp. nov.	f	brown to beige	indistinct green or blue	bright green	no pattern	indistinct dark stripe
C. tjiasmantoi sp. nov.	m	bright green, yellowish	= body colouration	turquoise	five diffuse blotches	indistinct dark stripe
C. tjiasmantoi sp. nov.	f	brown	= body colouration	= body colouration	five diffuse blotches	indistinct dark stripe
C. fallax	m	grey/beige	grey or blue	grey or bright green	three bright blue stripes	indistinct dark stripe
C. fallax	f	grey/beige	grey or blue	grey or bright green	three bright blue stripes	indistinct dark stripe
C. ratnasariae sp. nov.	m	yellow	= body colouration or blue	turquoise	two brown blotches and lateral stripe	brown stripe
C. ratnasariae sp. nov.	f	beige	= body colouration or blue	= body colouration	none	brown stripe

3.1.6 PAPER: No longer single! Description of female *Calumma vatosoa* (Squamata, Chamaeleonidae) including a review of the species and its systematic position

Calumma vatosoa was originally described on the basis of a single male holotype, and the appearance and morphology of the females of the species was unknown at that time (Andreone *et al.*, 2001). Fortunately, we later found female specimens of this species that were mistakenly classified under *C. linotum* but looked similar to *C. vatosoa* in the collection of Senckenberg Museum, Frankfurt am Main, Germany (SMF). Collected in 1933 and fixed using formalin, these specimens could not be studied genetically, and thus species assignment had to be carried out on the basis of morphology alone. In addition to external morphology, micro-CT scans of the skull were analysed. With the help of osteological characters, the females could be assigned to *C. vatosoa* and are now the first known female specimens of this species. Additionally, despite the complete absence of a rostral appendage, *C. vatosoa* was transferred from the *C. furcifer* (Vaillant & Grandidier, 1880) group to the *C. nasutum* group on the basis of statistical analyses of external morphological data.

Prötzel, D, Ruthensteiner, B & Glaw, F (2016): No longer single! Description of female *Calumma vatosoa* (Squamata, Chamaeleonidae) including a review of the species and its systematic position. *Zoosystematics and Evolution 92*, 13–21.

Post-publication comments and errata:

- This assignment of *Calumma peyrierasi* to the *C. nasutum* group was revised again in 3.1.5. Based on distinct sexual dimorphism and a unique morphology in males the species is systematically isolated within the genus.

museum für naturkunde

No longer single! Description of female *Calumma vatosoa* (Squamata, Chamaeleonidae) including a review of the species and its systematic position

David Prötzel[1], Bernhard Ruthensteiner[1], Frank Glaw[1]

1 *Zoologische Staatssammlung München (ZSM-SNSB), Münchhausenstr. 21, 81247 München, Germany*

http://zoobank.org/CFD64DFB-D085-4D1A-9AA9-1916DB6B4043

Corresponding author: *David Prötzel* (david.proetzel@mail.de)

Abstract

Calumma vatosoa is a Malagasy chameleon species that has until now been known only from the male holotype and a photograph of an additional male specimen. In this paper we describe females of the chameleon *Calumma vatosoa* for the first time, as well as the skull osteology of this species. The analysed females were collected many years before the description of *C. vatosoa*, and were originally described as female *C. linotum*. According to external morphology, osteology, and distribution these specimens are assigned to *C. vatosoa*. Furthermore we discuss the species group assignment of *C. vatosoa* and transfer it from the *C. furcifer* group to the *C. nasutum* group. A comparison of the external morphology of species of both groups revealed that *C. vatosoa* has a relatively shorter distance from the anterior margin of the orbit to the snout tip, more heterogeneous scalation at the lower arm, a significantly lower number of supralabial and infralabial scales, and a relatively longer tail than the members of the *C. furcifer* group. These characters are, however, in line with the species of the *C. nasutum* group. In addition the systematic position of *C. peyrierasi* also discussed, based on its morphology.

Introduction

Madagascar is a hotspot of chameleon diversity and endemism (Tolley et al. 2013). Of the currently described 202 chameleon species, 86 species belong to the four Malagasy genera *Brookesia* Gray, 1865, *Calumma* Gray, 1865, *Furcifer* Fitzinger, 1843, and *Palleon* Glaw, Hawlitschek & Ruthensteiner, 2013, and all but two Comorian species of *Furcifer* are endemic to Madagascar (Glaw 2015). Although the Seychelles chameleon, *Archaius tigris* (Kuhl, 1820), was included in the genus *Calumma* until recently, Townsend et al. (2011) demonstrated that it represents a different African lineage and that *Calumma* is endemic to Madagascar. The Malagasy chameleons were relatively intensively studied in the past (Brygoo 1971, 1978), but still many new species are regularly dis-

covered and described (e. g. Raxworthy and Nussbaum 2006, Gehring et al. 2010, Gehring et al. 2011, Glaw et al. 2012), and several species are only known by a single or a few specimens. Within the genus *Calumma*, currently comprising 33 species (Glaw 2015), *C. hafahafa* Raxworthy & Nussbaum, 2006, *C. linotum* (Müller, 1924), *C. peyrierasi* (Brygoo, Blanc & Domergue, 1974), and *C. vatosoa* Andreone, Mattioli, Jesu & Randrianirina, 2001 are such poorly known species. *Calumma linotum* for example was described on the basis of a single male without locality (Müller 1924) and it took more than 90 years to clarify its identity (Prötzel et al. 2015). In the same way, *C. vatosoa* was known only from the male holotype until Lutzmann et al. (2010) made a further record of *C. vatosoa* and presented a photograph of a male individual from near Ampokafo, approximately 50 km southeast of

the type locality (Forêt de Tsararano). So far, no female individual of this species has been recorded. *Calumma vatosoa* is a medium-sized chameleon species and was tentatively assigned to the *C. furcifer* group (sensu Glaw and Vences 1994) due to the absence of occipital lobes, gular and ventral crests and its markedly acute rostral profile, and greenish colouration (Andreone et al. 2001). These authors did not assign it to the *C. nasutum* group (sensu Glaw and Vences 1994), because of the absence of a rostral appendage, absence of a dorsal crest, and presence of axillary pockets. The *C. nasutum* group was recently found to be non-monophyletic (Tolley et al. 2013) and to include *C. peyrierasi*, a species formerly assigned to the *C. furcifer* group. The hemipenis ornamentation of *C. vatosoa* differs from that of all other species of the genus *Calumma* by the coexistence of three pairs of rotulae (Andreone et al. 2001).

In 1931, Bluntschli collected four female chameleons at Col Pierre Radama that were assigned to *Calumma linotum* by Mertens (1933), despite the absence of a rostral appendage and occipital lobes. Mertens (1933) justified this classification due to the absence of a dorsal crest, larger scales at the extremities, the regular gular folds, and the absence of the rostral appendage in the females. As the proper identification of *C. linotum* was recently clarified (Prötzel et al. 2015), we were able to reassign these female specimens to *C. vatosoa*. In this paper we describe for the first time females of *Calumma vatosoa* including the osteology of the species and review its assignment to the *C. furcifer* group. By identifying and reclassifying these individuals, we correct their taxonomic identity and enhance the knowledge about morphology and distribution of this poorly known species.

Material and methods

We studied the male holotype of *Calumma vatosoa* and three females from the Senckenberg Museum at Frankfurt/Main which were labeled as *C. linotum*. Of the four females originally collected (Mertens 1933) only three are still present in the museum collection. In addition, we investigated the external morphology of one adult male and (if available) one female of the species *C. andringitraense* (Brygoo, Blanc & Domergue, 1974), *C. furcifer* (Vaillant & Grandidier, 1880), *C. gastrotaenia* (Boulenger, 1888), *C. glawi* Böhme, 1997, *C. guillaumeti* (Brygoo, Blanc & Domergue, 1974), *C.* cf. *marojezense*, *C. tarzan* Gehring, Pabijan, Ratsoavina, Köhler, Vences & Glaw, 2010, and *C. vencesi* Andreone, Mattioli, Jesu & Randrianirina, 2001 of the *C. furcifer* group, and *C. boettgeri* (Boulenger, 1888), *C. fallax* (Mocquard, 1900), *C. gallus* (Günther, 1877), *C. guibei* (Hillenius, 1959), *C. linotum*, *C. nasutum* (Duméril & Bibron, 1836), and *C. vohibola* Gehring, Ratsoavina, Vences & Glaw, 2011 of the *C. nasutum* group. *Calumma cucullatum* (Gray, 1831) is not considered a part of the *C. furcifer* group in the strict sense (see phylogeny in Tolley et al. 2013). In addition *C.*

peyrierasi was investigated according to its phylogenetic position in the *C. nasutum* group – but it is clearly separated from the other species of the *C. nasutum* group (Tolley et al. 2013). The same specimen, which was analysed genetically in Tolley et al. (2013), was used for morphological measurements together with three more specimens of the same series. The other comparative specimens were chosen randomly, if several specimens were available, as typical representatives of their species. The studied specimens originated from the collections of the Museo Regionale di Scienze Naturali, Torino, Italy (MRSN), Senckenberg Museum, Frankfurt am Main, Germany (SMF), and from the Zoologische Staatssammlung München (ZSM), Germany (see Table 1 for details).

The following characters (Fig. 1) were measured with a digital calliper to the nearest of 0.1 mm or counted using a binocular dissecting microscope: snout-vent length (SVL) from the snout tip (not including the rostral appendage) to the cloaca; tail length (TaL) from the cloaca to the tail tip; total length (TL) as a sum of SVL + TaL; ratio of TaL to SVL (RTaSV); length of rostral appendage (LRA); snout-casque length (SCL), measured from the tip of the snout to the posterior end of the casque; ratio of SCL to SVL (RSCSV); head width (HW); ratio of HW to SVL (RHWSV); distance from the anterior margin of the orbit to the snout tip (DOS); ratio of DOS to SCL (ROSSC); occipital lobes (OL) presence (+) or absence (–); length of lateral crest, starting from the eye horizontally (LC); length of temporal crest that starts upwards from the LC (TC); parietal crest (PC) absence (–) or presence (+); casque height (CH); dorsal crest (DC) absence (–) or presence (+); axillary pits (AP) of the forelimbs presence (+) or absence (–); diameter of largest scale on lower arm (DSA, defined as the area from the elbow to the manus in lateral view); number of scales on lower arm in a line from elbow to manus (NSA); scalation on lower arm (SL), heterogeneous (het) or homogenous (hom); number of supralabial scales (NSL; counted from the first scale next to the rostral to the last scale that borders directly and entirely (with one complete side) to the mouth slit of the upper jaw) on the right side; number of infralabial scales (NIL, analogous to the definition of NSL above, on the right side).

For skeletal morphology, X-ray micro-computed tomography scans (micro-CT scans) of the head of the holotype of *Calumma vatosoa* (MRSN R1628, locality Forêt de Tsararano) and of one presumed female *C. vatosoa* (SMF 26357, from Col Pierre Radama) were prepared. During micro-CT scanning, each specimen was placed in a sealed plastic vessel slightly larger than the specimen itself, with the head oriented upwards, and was stabilised with ethanol-soaked paper. To provide an undisturbed external surface of the head, it was ensured that the paper did not cover this area. Micro-CT scanning was performed with a phoenix nanotom m (GE Measurement & Control, phoenix|x-ray, Wunstorf, Germany) at a voltage of 130 kV and a current of 80 µA for 29 minutes (1800 projections). 3D data sets were processed with VG Studio Max
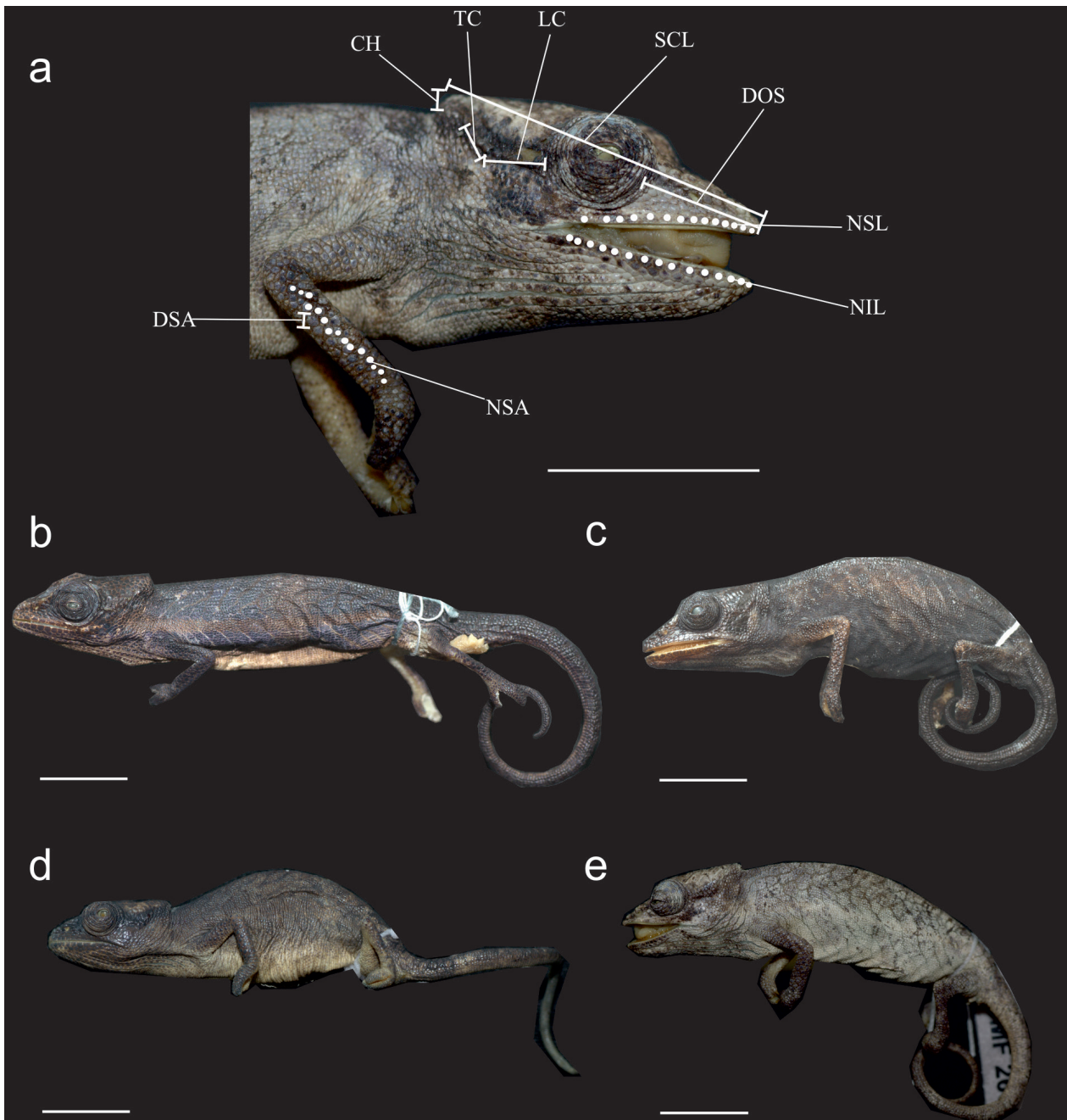
Figure 1. Preserved specimens of *Calumma vatosoa*; (**a**) Landmarks for morphometric measurements and pholidosis, shown in lateral view of the head region and forelegs of a female (SMF 26357, locality Ambatond'Radama); (**b**) male holotype of *C. vatosoa* (MRSN R1628, Forêt de Tsararano) in lateral view; (**c**) female (SMF 26359, Ambatond'Radama) in lateral view; (**d**) female (SMF 26358, Ambatond'Radama) in lateral view; (**e**) female (SMF 26357, Ambatond'Radama) in lateral view. Scale bar = 10 mm. See Materials and Methods for abbreviations.

2.2 software (Visual Graphics GmbH, Heidelberg, Germany); the data were visualised using the Phong volume renderer to show the surface of the skull. Measurements were taken with VG Studio Max 2.2. Osteological terminology follows Rieppel and Crumly (1997). Principal component analyses (PCA) was performed for 11 measurements/ counts (SVL, TaL, LRA, RSCSV, RHWSV, ROSSC, CH, DSA, NSA, NSL and NIL, see above) of all investigated specimens using the statistical analysis software PAST 3.08 (Hammer et al. 2001).

Results

External morphology of females. The three female specimens of *Calumma vatosoa* (SMF 26357, SMF 26358, and SMF 26359) are in a good state of preservation except a slit on the ventral side of the body (Fig. 1); SMF 26357 with mouth open and tip of the tongue between the jaws; SMF 26358 of smaller size and with poorly developed crests – presumably not full-grown; SMF 26359 blackened, presumably due to formalin injection.

Table 1. Morphological measurements of the male holotype and three female *Calumma vatosoa* and *C. peyrierasi* (one male, three females) in comparison with the species of the *C. furcifer* and *C. nasutum* group (represented as one male and one female if possible).

Species	Collection no.	Locality	Sex	SVL	TaL	TL	RTaSV	LRA	SCL	RSCSV	HW	RHWSV	DOS	ROSSC	OL	LC	TC	PC	CH	DC	AP	DSA	NSA	SL	NSL	NIL
C. furcifer group																										
C. andringitraense	ZSM 554/2001	Andringitra	m	45.7	48.4	94.1	1.06	·	16.5	0.36	3.5	0.077	5.5	0.33	·	·	·	·	0.2	·	+	0.3	27	hom	17	20
C. furcifer	ZSM 656/2014	Mahasoa forest	m	58.3	58.6	116.9	1.01	·	21.0	0.36	4.0	0.069	8.3	0.40	·	3.8	·	·	0.0	+	+	0.4	29	hom	21	20
C. furcifer	ZSM 657/2014	Mahasoa forest	f	61.2	54.3	115.5	0.89	·	19.7	0.32	5.1	0.083	8.2	0.42	·	3.6	·	·	0.0	+	+	0.4	25	hom	20	20
C. gastrotaenia	ZSM 1719/2010	Analabe forest	m	65.5	66.0	131.5	1.01	·	23.8	0.36	4.8	0.073	8.5	0.36	·	2.7	·	·	2.2	+	+	0.6	23	hom	17	18
C. gastrotaenia	ZSM 1718/2010	Analabe forest	f	61.7	53.9	115.6	0.87	·	19.7	0.32	5.7	0.092	7.9	0.40	·	·	·	·	0.0	·	+	0.4	22	hom	18	18
C. glawi	ZSM 2042/2008	Ranomafana	m	59.6	64.0	123.6	1.07	·	21.0	0.35	5.3	0.089	8.1	0.39	+	·	·	·	2.4	·	+	0.6	21	hom	16	17
C. guillaumeti	ZSM 1701/2012	Sorata	m	52.8	56.2	109.0	1.06	·	18.7	0.35	3.9	0.074	7.2	0.39	·	·	·	·	0.7	+	+	0.6	24	hom	15	18
C. guillaumeti	ZSM 1702/2012	Sorata	f	57.2	52.9	110.1	0.92	·	18.9	0.33	4.3	0.075	7.5	0.40	·	1.8	·	·	0.0	·	+	0.6	23	hom	15	16
C. cf. marojezense	ZSM 461/2010	Ambodivohangy	m	66.9	65.0	131.9	0.97	·	19.4	0.29	4.6	0.069	7.4	0.38	·	4	·	·	0.0	·	+	0.4	40	hom	17	18
C. tarzan	ZSM 219/2010	Tarzanville	m	72.6	78.0	150.6	1.07	·	22.6	0.31	4.1	0.056	9.3	0.41	·	3.2	·	·	0.6	·	+	0.5	33	hom	18	18
C. tarzan	ZSM 222/2010	Tarzanville	f	67.4	60.0	127.4	0.89	·	20.7	0.31	4.3	0.064	8.6	0.42	·	3.1	·	·	0.6	·	+	0.4	40	hom	20	20
C. vencesi	ZSM 50/2011	F. d'Amboloko-patrika	m	69.3	72.0	141.3	1.04	·	21.9	0.32	4.6	0.066	8.6	0.39	·	5.1	1.5	·	0.6	+	+	0.5	32	hom	18	20
C. nasutum group																										
C. boettgeri	ZSM 444/2000	Nosy Be	m	51.9	55.0	106.9	1.06	2.93	17.0	0.33	3.2	0.062	5.3	0.31	+	3.9	·	·	1.4	+	·	0.4	26	het	12	12
C. boettgeri	ZSM 441/2000	Nosy Be	f	45.5	43.4	88.9	0.95	2.73	15.3	0.34	2.9	0.064	5.0	0.33	+	3.2	·	·	1.4	·	·	0.4	27	het	12	12
C. fallax	ZSM 286/2010	Tsinjoarivo	m	48.8	57.3	106.1	1.17	3.60	16.6	0.34	3.5	0.072	5.2	0.31	·	2.7	2.0	+	1.9	+	·	0.9	11	het	14	15
C. guibei	ZSM 2855/2010	Tsaratanana	m	48.9	61.5	110.4	1.26	3.6	15.6	0.32	3.6	0.074	5.5	0.35	+	2.8	1.1	·	1.0	·	·	0.7	15	het	11	12
C. guibei	ZSM 2856/2010	Tsaratanana	f	45.9	46.5	92.4	1.01	1.3	14.9	0.32	3.1	0.068	4.8	0.32	+	2.6	1.0	·	1.0	·	·	0.6	17	het	12	13
C. gallus	ZSM 321/2000	Vohidrazana	m	45.0	43.7	88.7	0.97	9.7	15.4	0.34	3.1	0.069	4.8	0.31	·	2.9	·	·	1.1	·	+	0.7	16	het	15	14
C. linotum	ZSM 2073/2007	M. d'Ambre	m	59.6	64.8	124.4	0.92	4.50	16.8	0.28	3.1	0.052	5.2	0.31	+	2.3	·	+	1.3	+	+	0.8	16	het	·	12
C. linotum	ZSM 551/2001	Andampy	f	50.6	50.7	101.3	1.00	2.00	15.8	0.31	3.1	0.061	5.0	0.32	+	2.5	·	+	0.8	+	+	0.8	22	het	13	13
C. cf. nasutum	ZSM 924/2003	Andasibe	m	43.7	45.3	89.0	1.04	2.2	13.8	0.32	2.7	0.062	4.6	0.33	·	2.0	0.8	+	1.7	·	·	0.5	14	het	12	13
C. cf. nasutum	SMF 68273	Andasibe	f	46.2	45.8	92.0	0.99	1.8	12.5	0.27	2.8	0.061	4.2	0.34	·	1.5	·	+	1.5	·	·	0.6	15	het	12	12
C. vohibola	ZSM 645/2009	Vohibola	m	46.9	42.1	89.0	0.90	1.1	14.1	0.30	3.1	0.066	4.8	0.34	·	2.6	1.1	·	1.3	+	+	0.9	17	het	15	18
C. vohibola	ZSM 643/2009	Vohibola	f	45.5	40.4	85.9	0.89	0.3	14.2	0.31	2.3	0.051	4.7	0.33	·	2.7	0.7	·	1.3	·	·	0.8	16	het	14	14
C. vatosoa	MRSN R1628	F. de Tsararano	m	57.9	66.6	124.5	1.15	·	18.5	0.32	4.8	0.083	6.4	0.35	·	2.1	3.1	·	1.8	·	+	0.8	15	het	13	14
C. vatosoa	SMF 26357	Col Pierre R.	f	53.8	56.0	109.8	1.04	·	17.3	0.32	4.3	0.080	5.9	0.34	·	3.0	2.4	·	1.0	·	+	0.8	15	het	14	14
C. vatosoa	SMF 26358	Col Pierre R.	f	45.7	51.2	96.9	1.12	·	16.3	0.36	4.7	0.103	5.7	0.35	·	1.5	3.1	·	1.0	·	+	0.9	14	het	14	13
C. vatosoa	SMF 26359	Col Pierre R.	f	47.9	51.4	99.3	1.07	·	16.5	0.34	3.9	0.081	5.4	0.33	·	2.8	2.2	·	0.5	·	+	0.9	20	het	13	13
C. peyrierasi	ZSM 522/2014	Tsaratanana	m	51.1	55.2	106.3	1.08	·	19.9	0.39	4.9	0.096	6.5	0.33	·	3.6	2.4	·	2.5	+	+	0.7	18	hom	12	12
C. peyrierasi	ZSM 1726/2010	Tsaratanana	f	53.2	52.8	106.0	0.99	·	16.2	0.30	4.9	0.093	5.3	0.33	·	3.8	2.1	·	1.4	+	+	0.8	21	hom	12	12
C. peyrierasi	ZSM 17272010	Tsaratanana	f	56.0	54.6	110.6	0.98	·	15.6	0.28	4.9	0.088	5.8	0.37	·	3.5	2.2	·	0.9	+	+	0.7	17	hom	12	14
C. peyrierasi	ZSM 523/2014	Tsaratanana	f	56.4	52.5	108.9	0.93	·	15.2	0.27	4.8	0.085	5.4	0.36	·	3.2	2.1	·	1.2	+	+	0.7	22	hom	13	13

The morphological features of the three female *C. vatosoa* specimens ranged from: SVL 45.7–53.8 mm; tail length 51.2–56.0 mm; tail length 104–112 % of SVL; snout-casque length 16.3–17.3 mm, head width 3.9–4.7 mm; diameter of the orbit 4.7–5.1 mm; number of supralabial and infralabial scales 13 or 14; line of upper labials serrated; distinct rostral ridges that fuse on the anterior snout; no rostral appendage; lateral crest poorly developed and pointing straight posteriorly, fusing to form the poorly developed temporal crest that curves upwards and fading to the highest point of the casque; height of the casque 0.5–1.0 mm; no occipital lobes; no traces of parietal, dorsal, gular, and ventral crest; body laterally compressed with fine homogeneous scalation with the exception of the extremities and head region; legs with enlarged rounded tubercle scales (diameter 0.7–1.0 mm) bordering each other; heterogeneous scalation on the head; upper arm diameter 2.3–2.6 mm; axillary pits evident. Full morphological measurements in comparison to the holotype are provided in Table 1.

Skull osteology of the male holotype (MRSN R1628) (Fig. 2). Strongly developed maxillae extending anteriorly with tubercles at the lateral margin; small nasal bones (length 1.7 mm, width 0.3 mm) paired and meeting anteriorly; anterior tip of the frontal bone not exceeding more than a half of the naris and meeting the maxillae mid-dorsally; naris extending posteriorly up to the frontal bone (apomorphic state of *C. nasutum* according to Rieppel and Crumly 1997) and laterally bordered by the massive prefrontals with distal tubercles; prefrontal not meeting the maxilla; smooth frontal in the shape of a triangle, with a length of 8.4 mm and a width of 5.1 mm at the widest distance; parietal irregularly spotted with a few tubercles and tapering posteriorly from 4.2 mm (largest diameter) to 0.2 mm (smallest diameter); parietal meeting the squamosal and building the casque.

Skull osteology of the female (SMF 26357) (Fig. 2). Smooth maxillae without tubercles; narrow nasal bones (length 1.8 mm, width 0.2 mm) paired and meeting anteriorly; anterior tip of the frontal bone not exceeding more than a half of the naris and meeting the maxillae mid-dorsally; naris extending posteriorly up to the frontal bone and laterally bordered by the massive prefrontals with distal tubercles; prefrontal not meeting the maxilla; smooth frontal in the shape of a triangle with a length of 6.7 mm and a width of 4.9 mm at the widest distance; parietal irregularly spotted with a few tubercles and tapering posteriorly from 4.6 mm (largest diameter) to 0.5 mm (smallest diameter); parietal meeting the squamosal and building the casque.

The skull differs between the sexes in following characters (Fig. 2): The skull of the male holotype is ornamented with more tubercles and appears more robust than the skull of the female. Especially the shape of the maxilla differs with distal tubercles in the male and a smooth surface in the female. Further, the nasals are slightly broader in the male (0.3 mm vs. 0.2 mm in the female) and the

parietal tapers more sharply in the male, to 0.2 mm (vs. 0.5 mm). In conclusion, there is only weak sexual dimorphism in this species.

Colouration in preservative (Fig. 1). The colour of the specimens is faded after storage in alcohol for more than 80 years. The body of the female SMF 26357 is now of beige and bluish grey colour. A black stripe from the snout tip to the casque, crossing the eye, is clearly recognisable (a similar stripe is present in the holotype and on the photograph of the second individual, suggesting that it is characteristic for *C. vatosoa*). The eyelid is covered with light blue and purple spots. A midlateral white stripe runs from the upper lip to the pelvis on either side of the body. The body colour is bluish grey, becoming paler at the throat and venter (lacking a distinct white stripe) and darker at the extremities and the tail. On the legs there are blue tubercle scales, especially on the forearm region. The body is covered with a network of fine black lines. SMF 26358 is homogeneous bluish grey coloured with beige on the belly, the throat, and the inner side of the extremities. The legs bear blue-coloured tubercle scales; no other pattern is visible. The female SMF 26359 is completely coloured black, presumably due to exposure to formalin. Only the inner side of the extremities are of beige in colour. None of the three females shows any traces a yellowish spot on the flanks (which is recognisable on photographs of the living male holotype and the male photographed near Ampokafo). Neither the male holotype nor the three females show any pattern of a beige midventral stripe that is bordered by a white line on each side.

Distribution (Fig. 3). *Calumma vatosoa* is known from a small area of approximately 425 km² (Jenkins et al. 2011) in north-eastern Madagascar. The type locality is Forêt de Tsararano (14°54.8'S, 49°42.6'E, 665 m a.s.l.) between the Anjanaharibe-Sud Massif and the Masoala Peninsula (Andreone et al. 2001). Lutzmann et al. (2010) presented a photograph of one male individual from next to Ampokafo (15°15.4'S, 50°2.5'E, 400 m a.s.l.) which is located 50–60 kilometers south east of the type locality between Maroantsetra and Antalaha. We here add Ambatond'Radama (=Col Pierre Radama, 35–40 km north-east of Maroantsetra, N.E. Madagascar according to Viette (1991); coordinates approximately: 15°17.4'S, 50° 0.2'E) as a third locality of this species. Presumably *C. vatosoa* occurs in the forest among the three known localities.

Systematic position of *Calumma vatosoa*. Morphological measurements and pholidosis of *Calumma vatosoa* revealed substantial differences compared to the species of the *C. furcifer* group (see Table 1 for measurements). *Calumma vatosoa* differs from the species of the *C. furcifer* group in the following characters: heterogeneous scalation on lower arm vs. homogeneous scalation; larger diameter of tubercles on lower arm (DSA, 0.8–0.9 mm vs. 0.3–0.6 mm); lower number of scales in a line on the lower arm (NSA, 14–20 vs. 21–40); lower number of supralabials (NSL, 13–14 vs. 15–21) and infralabials (NIL,
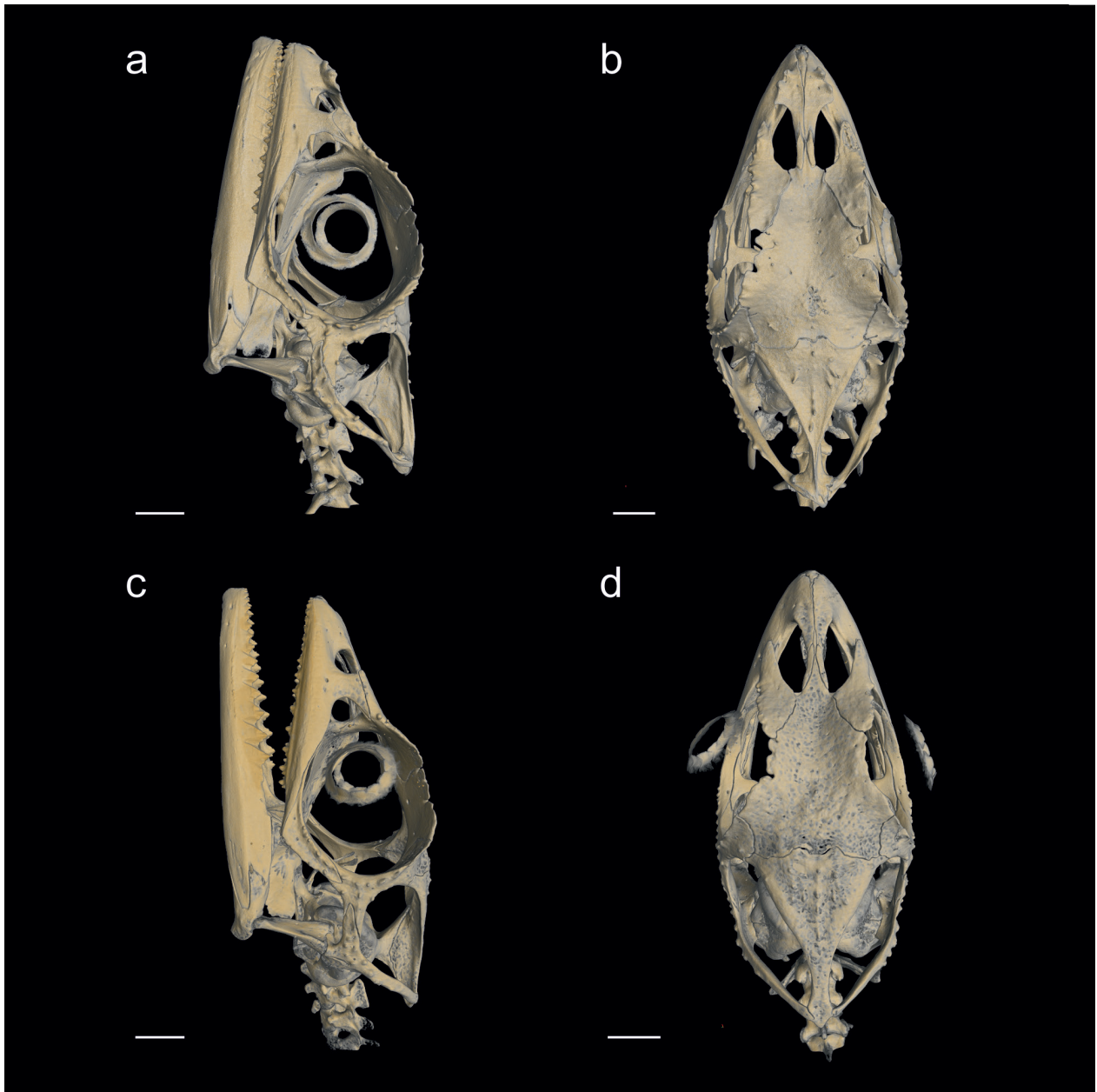
Figure 2. Micro-CT images of skulls of *Calumma vatosoa*; male holotype of *C. vatosoa* (MRSN R1628, Forêt de Tsararano) in (**a**) lateral and (**b**) dorsal view; female (SMF 26357, Ambatond'Radama) in lateral (**c**) and dorsal view (**d**). Scale bar = 2.0 mm.

13–14 vs. 16–20); longer tail relative to SVL, especially in the females (RTaSV, males 115 % vs. 101–107 %, females 104–112 % vs. 87–92 %); shorter distance from the anterior margin of the orbit to the snout tip related to snout-casque length (RSCSV, 0.33–0.35 vs. 0.33–0.42). In terms of colouration all species of the *C. furcifer* group show a distinct pattern of a beige midventral stripe that is bordered by a white line on each side. In *C. vatosoa* the venter is of paler colour than the body but it lacks any striped pattern.

These same measurements in the *Calumma nasutum* group were as follows: distance from the anterior margin of the orbit to the snout tip related to snout-casque length of 0.31–0.35 (RSCSV); heterogeneous scalation at the lower arm, consisting mostly of tubercles of large di-

ameter (DSA, 0.4–0.9 mm); number of scales in a line on the lower arm 11–26 (NSA); 11–15 supralabials (NSL); 12–15 infralabials (NIL; with an exception of the male *C. vohibola* with 18); tail length related to SVL with a maximum of 126 % (RTaSV) in a male *C.* cf. *guibei*. Occipital lobes (OL) and dorsal crests (DC) can occur in both groups (see Table 1). As it is typical for all other species of the *C. nasutum* group, *C. vatosoa* does not show any striped midventral pattern.

Despite the complete absence of a rostral appendage in *Calumma vatosoa*, our data demonstrate that this species is morphologically much more similar to the other species of the *C. nasutum* group than to the species of the *C. furcifer* group (see Table 1) and we, therefore, suggest transferring
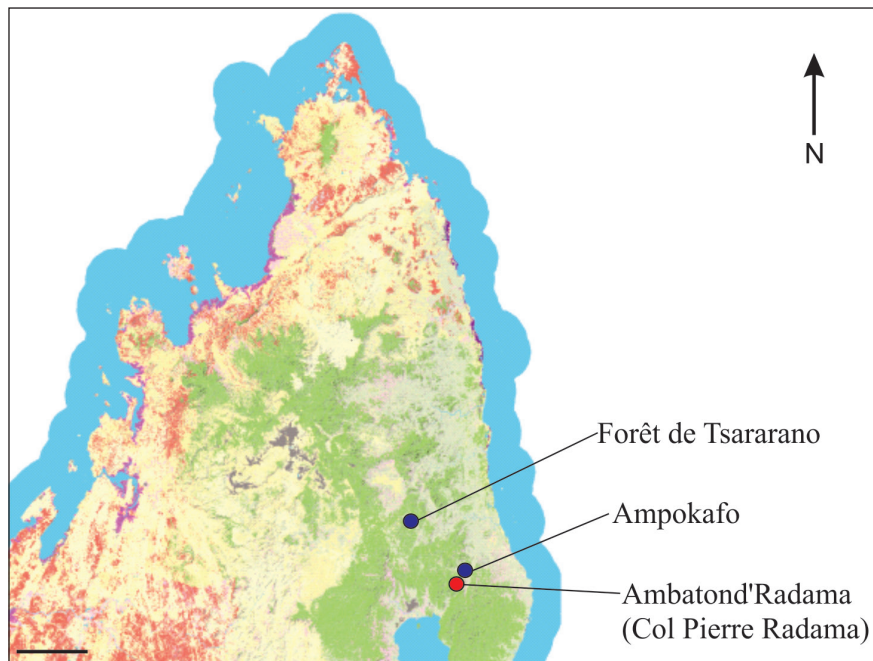
Figure 3. Map of northern Madagascar with previously known localities of *Calumma vatosoa* (purple circles) and the new locality of the females (red circle). Vegetation legend: humid forest (green), wooded grassland-bushland mosaic (beige), plateau grassland-wooded grassland mosaic (light beige), western dry forest (red), mangroves (pink), cultivation (light pink), littoral forest (purple), wetlands (grey). Scale bar = 50 km. Map from www.vegmad.org.
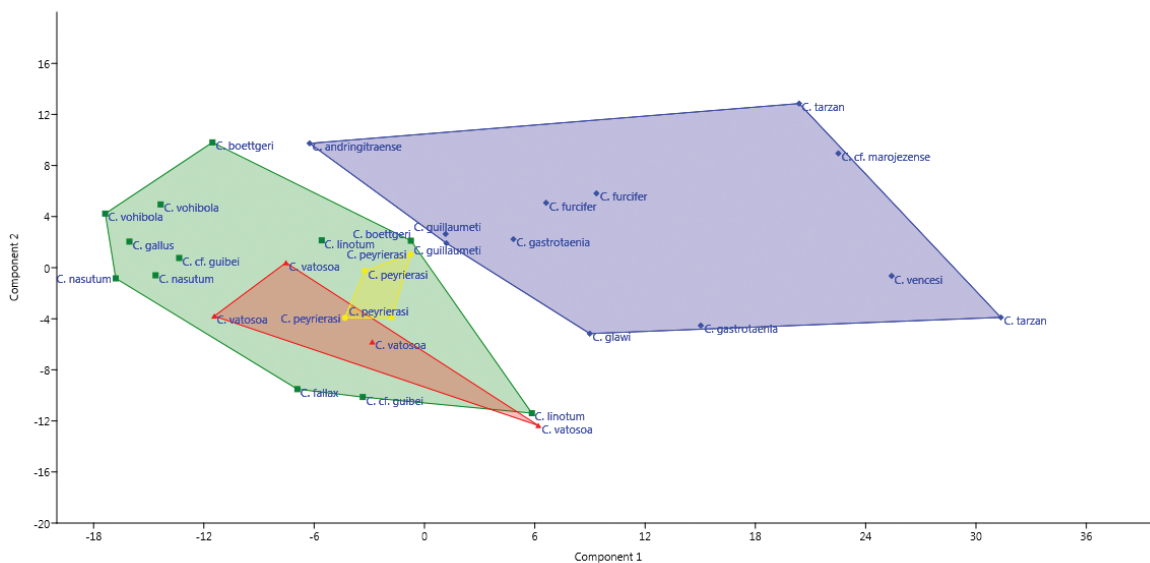
Figure 4. PCA of the species of the *Calumma furcifer* group (n = 12; blue diamonds), the *C. nasutum* group (n = 12; green squares), *C. vatosoa* (n = 4, red triangles) and *C. peyrierasi* (n = 4; yellow dots) based on 11 measurements/counts (SVL, TaL, LRA, RSCSV, RHWSV, ROSSC, CH, DSA, NSA, NSL and NIL of Table 1); Component 1 explains 73.93 % and Component 2 17.49 % of the variance.

it to the *C. nasutum* group. A PCA (Fig. 4, Table 2) clearly separates both groups explaining 73.93 % and 17.49 % of the total variance in PC I and PC II and places *C. vatosoa* within the *C. nasutum* group. Excluding body and tail length, important characters to differentiate between the *C. furcifer* and *C. nasutum* group (NSA, NIL, ROSSC and DSA) are shown in the graphs of Fig. 5, comfirming that, *C. vatosoa* is placed among the species of the *C. nasutum* group.

Systematic position of *Calumma peyrierasi.* As an additional part of this work, the morphological similarity of *C. peyrierasi* to either the *C. nasutum* or *C. furcifer* group was investigated. The following morphological differences from the species of the *C. furcifer* group were identified (see Table 1): larger diameter of tubercles on lower arm (DSA, 0.7–0.8 mm vs. 0.3–0.6 mm); lower number of scales in a line on the lower arm (NSA, 17–22
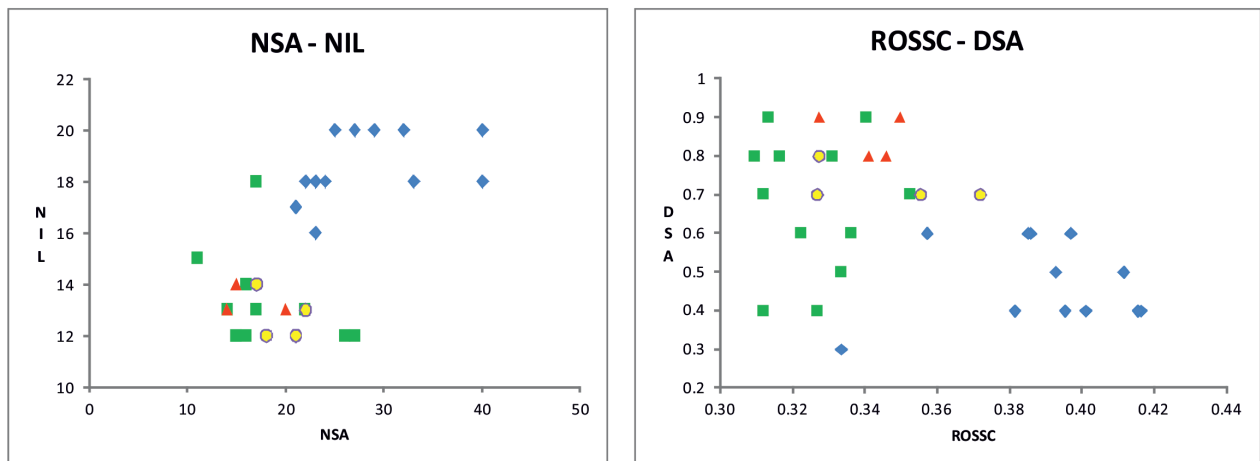
Figure 5. Important characters for the distinction of the *Calumma furcifer* group (n = 12; blue diamonds) and the *C. nasutum* group (n = 12; green squares), including the assignment of *C. vatosoa* (n = 4, red triangles) and *C. peyrierasi* (n = 4; yellow dots). Abbreviations: NSA, number of scales on lower arm in a line from elbow to manus; NIL, number of infralabial scales; DSA, diameter of largest scale on lower arm; ROSSC, ratio of distance from the anterior margin of the orbit to the snout tip and snout-casque length.

Table 2. Factor loadings for PC I–III for the investigated species of *Calumma furcifer* group and *C. nasutum* group (n = 28, Fig. 4)

	PC 1	PC 2	PC 3
SVL	0.6191	0.0197	0.4210
TaL	0.6271	0.5870	0.3080
LRA	0.0623	0.0506	0.1596
RSCSV	0.0001	0.0001	0.0001
RHWSV	0.0001	0.0004	0.0009
ROSSC	0.0019	0.0015	0.0045
CH	0.0155	0.0590	0.0350
DSA	0.0061	0.0171	0.0043
NSA	0.4238	0.7522	0.4997
NSL	0.1388	0.2008	0.4582
NIL	0.1429	0.2062	0.4914
Eigenvalue	161.885	38.306	9.210
%variance	73.928	17.493	4.206

vs. 21–40); lower number of supralabials (NSL, 12–13 vs. 15–21) and infralabials (NIL, 12–14 vs. 16–20). In terms of colouration, all species of the *C. furcifer* group show a distinct pattern of a beige midventral stripe that is bordered by a white line on each side. In *C. peyrierasi* there is only one distinct ventral stripe of white colour.

Compared to the species of the *Calumma nasutum* group the complete absence of a rostral appendage, the homogeneous scalation on the extremities, the predominantly greenish colouration, and the ventral stripe are atypical characters. Nevertheless, *C. peyrierasi* is placed among the species of the *C. nasutum* group in the PCA (Fig. 4) and in the graphs showing the distinctive characters of both groups (Fig. 5).

Discussion

In this work we have enlarged the knowledge of the poorly known chameleon species *Calumma vatosoa* and improved the systematics within the *C. nasutum* group and the *C. furcifer* group. On the basis of external morphology, osteology, and distribution we assign the specimens, which were collected by Bluntschli, to *C. vatosoa* instead of *C. linotum*, and provide the first description of females of this species. Andreone et al. (2001) tentatively assigned *C. vatosoa* to the *C. furcifer* group; however, after comparing the morphology and osteology of the investigated females and the holotype of *C. vatosoa* to all other species of the *C. furcifer* group, we demonstrate that the analysed characters of *C. vatosoa* are more typical of the *C. nasutum* group (Table 1) except for the absence of a rostral appendage and the presence of axillary pits. These characters appear to be variable, because axillary pits occur occasionally within the *C. nasutum* group (Prötzel, unpublished data) and the rostral appendage is strongly reduced in *C. vohibola* (see Table 1) and other members of the *C. nasutum* group (Prötzel, unpublished data). Molecular analyses are necessary to clarify the phylogenetic position of *C. vatosoa* in the *nasutum* group and if the appendage was secondarily reduced as was shown in *Furcifer campani* and *F. lateralis* by the phylogeny in Tolley et al. (2013). In the *C. nasutum* group the rostral appendage is relevant for sexual selection as demonstrated for *C. nasutum* (Parcher 1974), but sexual dimorphism in the length or the shape of the rostral appendage is weak or absent (e.g. in *C. boettgeri* according to Eckhardt et al. 2012). This is true for all members of the *C. nasutum* group with the exception of *C. gallus*. Accordingly the rostral appendage may play an important role in interspecific communication and species recognition as some species respectively candidate species of the *C. nasutum* group live sympatrically (Gehring et al. 2012).

The osteology of the skull of *Calumma vatosoa* is similar to other members of the *C. nasutum* group, e.g. the shape of the nasalia and the frontal (Prötzel, unpublished data) and shows only weak sexual dimorphism. In contrary to Mertens (1933) within the *C. nasutum* group the dorsal crest is not a constant character either, as this character can be present or absent in male *C. boettgeri* (Prötzel et al. 2015). Andreone et al. (2001) described the hemipenis ornamentation of *C. vatosoa* as exclusive within the genus *Calumma* due to their three pairs of rotulae. However, in our study on *C. linotum* (Prötzel et al. 2015) a hemipenis showed, in addition to the two pairs of rotulae that are typical for *C. boettgeri* and *C. linotum*, a third pair of rotulae. Consequently, even the morphology of hemipenes can be variable within a species, and three pairs of rotulae is not a unique character of *C. vatosoa*.

In conclusion, *C. vatosoa* is assigned as a member of the multifaceted *C. nasutum* group. A molecular study of the species would be helpful to confirm this assignment. Similarly, the morphological analyses of *C. peyrierasi* confirm its phylogenetic position in the *C. nasutum* group as revealed by Tolley et al. (2013)

Acknowledgements

References

Andreone F, Mattioli F, Jesu R, Randrianirina JE (2001) Two new chameleons of the genus *Calumma* from north-east Madagascar, with observations on hemipenal morphology in the *Calumma furcifer* group (Reptilia, Squamata, Chamaeleonidae). Herpetological Journal 11: 53–68.

Brygoo ER (1971) Reptiles Sauriens Chamaeleonidae – genre *Chamaeleo*. Faune de Madagascar 33: 1–318.

Brygoo ER (1978) Reptiles Sauriens Chamaeleonidae – genre *Brookesia* et complément pour le genre *Chamaeleo*. Faune de Madagascar 47: 1–173.

Eckhardt FS, Gehring PS, Bartel L, Bellmann J, Beuker J, Hahne D, Korte J, Knittel V, Mensch M, Nagel D, Pohl M, Rostosky C, Vierath V, Wilms V, Zenk J, Vences M (2012) Assessing sexual dimorphism in a species of Malagasy chameleon (*Calumma boettgeri*) with a newly defined set of morphometric and meristic measurements. Herpetology Notes 5: 335–344.

Gehring PS, Pabijan M, Ratsoavina FM, Köhler J, Vences M, Glaw F (2010) A Tarzan yell for conservation: a new chameleon, *Calumma tarzan* sp. n., proposed as a flagship species for the creation of new nature reserves in Madagascar. Salamandra 46(3): 167–179.

Gehring PS, Ratsoavina FM, Vences M, Glaw F (2011) *Calumma vohibola*, a new chameleon species (Squamata: Chamaeleonidae) from the littoral forests of eastern Madagascar. African Journal of Herpetology 60: 130–154. doi: 10.1080/21564574.2011.628412

Gehring PS, Tolley KA, Eckhardt FS, Townsend TM, Ziegler T, Ratsoavina F, Glaw F, Vences M (2012) Hiding deep in the trees: discovery of divergent mitochondrial lineages in Malagasy chameleons of the *Calumma nasutum* group. Ecology and Evolution 2: 1468–1479. doi: 10.1002/ece3.269

Glaw F (2015) Taxonomic checklist of chameleons (Squamata: Chamaeleonidae). Vertebrate Zoology 65(2): 167–246.

Glaw F, Köhler J, Townsend TM, Vences M (2012) Rivaling the world's smallest reptiles: Discovery of miniaturized and microendemic new species of leaf chameleons (*Brookesia*) from northern Madagascar. PLoS ONE 7(2): e31314. doi: 10.1371/journal.pone.0031314

Glaw F, Vences M (1994) A fieldguide to the amphibians and reptiles of Madagascar. Vences & Glaw Verlag, Köln, 480 pp.

Hammer Ø, Harper DAT, Ryan PD (2001) PAST: paleontological statistics software package for education and data analysis. Palaeontologia Electronica 4(1): 9.

Jenkins RKB, Andreone F, Andriamazava A, Anjeriniaina M, Brady L, Glaw F, Griffiths RA, Rabibisoa N, Rakotomalala D, Randrianantoandro JC, Randrianiriana J, Randrianizahana H, Ratsoavina F, Robsomanitrandrasana E (2011) *Calumma vatosoa*. The IUCN Red List of Threatened Species 2011: e.T172928A6943225. [downloaded on 12 November 2015]

Lutzmann N, MacKinnon J, Gehring PS, Wilms TM (2010) A new record of the rarely found Chameleon, *Calumma vatosoa* Andreone, Mattioli, Jesu & Randrianirina 2001. Sauria 32(4): 65–66.

Mertens R (1933) Die Reptilien der Madagaskar-Expedition Prof. Dr. H. Bluntschli's. Senckenbergiana biologica 15: 260–274.

Müller L (1924) Ueber ein neues Chamaeleon aus Madagaskar. Mitteilungen aus dem Zoologischen Museum in Berlin 11: 95–96.

Parcher SR (1974) Observations on the natural histories of six Malagasy Chamaeleontidae. Zeitschrift für Tierpsychologie 34: 500–523. doi: 10.1111/j.1439-0310.1974.tb01818.x

Prötzel D, Ruthensteiner B, Scherz MD, Glaw F (2015) Systematic revision of the Malagasy chameleons *Calumma boettgeri* and *Calumma linotum* (Squamata: Chamaeleonidae). Zootaxa 4048(2): 211–231. doi: 10.11646/zootaxa.4048.2.4

Raxworthy CJ, Nussbaum RA (2006) Six new species of occipital-lobed *Calumma* chameleons (Squamata: Chamaeleonidae) from montane regions of Madagascar, with a new description and revision of *Calumma brevicorne*. Copeia 2006(4): 711–734. doi: 10.1643/0045-8511(2006)6[711:SNSOOC]2.0.CO;2

Rieppel O, Crumly C (1997) Paedomorphosis and skull structure in Malagasy chamaeleons (Reptilia: Chamaeleoninae). Journal of Zoology 243(2): 351–380. doi: 10.1111/j.1469-7998.1997.tb02788.x

Tolley KA, Townsend TM, Vences M (2013) Large-scale phylogeny of chameleons suggests African origins and Eocene diversification. Proceedings of the Royal Society 280(1759): 20130184. doi: 10.1098/rspb.2013.0184

Townsend TM, Tolley KA, Glaw F, Böhme W, Vences M (2011) Eastward from Africa: palaeocurrent-mediated chameleon dispersal to the Seychelles islands. Biology Letters 7(2): 225–228. doi: 10.1098/rsbl.2010.0701

Viette P (1991) Principales localités où des insectes ont été recueillis à Madagascar: Chief field stations where insects were collected in Madagascar. Faune de Madagascar, supplement 2: 1–88.

3.2 Fluorescence in chameleons

3.2.1 PAPER: Widespread bone-based fluorescence in chameleons

Inspired by a photograph taken by Paul Bertner showing a chameleon (*Calumma gastrotaenia*) under UV-light with a few unusual blue spots behind the eye, we checked the preserved specimens of our collection with a standard UV-LED lamp. Surprisingly, the majority of species showed blue patterns on the head or even across the whole body which proved to be fluorescence. We reasoned that this discovery might be of scientific interest as fluorescence has already been reported to function as an intraspecific signal in other organisms (see chapter 2.3) and chameleons are known for their visual communication (see chapter 2.1). Aside from their famous variety in terms of colouration, many chameleons have conspicuous structures on the head which bear aligned tubercles on the skull. These crests have often been used as taxonomic characters (Nečas, 2004; Rieppel & Crumly, 1997), but their biological function has always been unclear. We examined the blue patterns, which appear on the heads of some chameleon species when exposed to UV-light, and found that these patterns result from these skull tubercles. The following chapter shows the histological basis of this phenomenon, the sex/species specificity of fluorescence patterns, and their phylogenetic distribution across the family Chamaeleonidae.

Prötzel, D, Heß, M, Scherz, MD, Schwager, M, van't Padje, A & Glaw, F (2018): Widespread bone-based fluorescence in chameleons. *Scientific Reports 8*, 698.

Post-publication comments:

- This publication received significant media attention (see CV) and is one of the paper with the most online attention within the journal:
    - altmetric score of 643 (accessed on 08.08.2018) meaning that the article is:
    - in the 99th percentile (ranked 525th) of the 330,698 tracked articles of a similar age in all journals
    - in the 99th percentile (ranked 12th) of the 5,642 tracked articles of a similar age in *Scientific Reports*

SCIENTIFIC REP{O}RTS

OPEN

Widespread bone-based fluorescence in chameleons

David Prötzel[1], Martin Heß[2], Mark D. Scherz [1], Martina Schwager[3], Anouk van't Padje[1,4] & Frank Glaw[1]

Fluorescence is widespread in marine organisms but uncommon in terrestrial tetrapods. We here show that many chameleon species have bony tubercles protruding from the skull that are visible through their scales, and fluoresce under UV light. Tubercles arising from bones of the skull displace all dermal layers other than a thin, transparent layer of epidermis, creating a 'window' onto the bone. In the genus *Calumma*, the number of these tubercles is sexually dimorphic in most species, suggesting a signalling role, and also strongly reflects species groups, indicating systematic value of these features. Co-option of the known fluorescent properties of bone has never before been shown, yet it is widespread in the chameleons of Madagascar and some African chameleon genera, particularly in those genera living in forested, humid habitats known to have a higher relative component of ambient UV light. The fluorescence emits with a maximum at around 430 nm in blue colour which contrasts well to the green and brown background reflectance of forest habitats. This discovery opens new avenues in the study of signalling among chameleons and sexual selection factors driving ornamentation.

Fluorescence has been reported from a wide range of organisms such as plants, invertebrates and mainly marine vertebrate species[1–10]. Recently, fluorescence was discovered in the South American tree frog *Boana* (formerly *Hypsiboas*) *punctata*, produced by compounds in lymph and skin glands[11]. Little is known about the function or evolution of fluorescence of organisms[11,12], but conclusions and hypotheses include photo-protection in excessive sunlight[3], UV-light detection, prey-[4] or pollinator-attraction[5], and signalling for mate choice, species recognition, and male-male interaction[2,6,7,9,13]. Proteins, pigments, chitin and lymph/glandular components are known to be the fluorescent agents of these organisms[11,14].

Chameleons often show remarkable colouration[15,16] and have conspicuous bony crests and tubercle pattern on their heads. The shape, size and distribution of these crests are taxonomically informative[17] and sexually dimorphic[18,19], but their purpose has never been established. It is probable that their function is similar to ornamentations used by other taxa for species recognition and intraspecific signalling and communication[19]. We investigated the properties of these tubercles, and here report the first known instance of externally visible bone-based fluorescence in vertebrates. Bone has long been known to fluoresce under UV light[20], a phenomenon that has been used in forensic research[21], but no organism has so far been reported to co-opt this phenomenon for fluorescent signalling. Chameleons are already famed for their exceptional eyes and visual communication[22,23], and now they are among the first known terrestrial squamates that display and likely use fluorescence.

Results and Discussion

Fluorescence of bony tubercles in chameleons. We discovered that the crests and tubercles on the heads of many chameleon species emit blue fluorescence when excited with UV light. Focusing on the genus *Calumma* we investigated the osteological and histological basis of this phenomenon and the sex/species specificity of its patterns, and its phylogenetic distribution across all chameleon genera.

Living and ethanol-preserved *Calumma* chameleons exhibit characteristic tubercle patterns of blue fluorescence on their heads (Fig. 1A). The optimal excitation wavelength is in the UV-A spectrum at 353 nm, inducing an emission spectrum from 360 nm to 500 nm, with a maximum at 433 nm (Fig. 1B) measured from *C. globifer* and *C. crypticum* without notable variation between the species. The fluorescent elements are the centres of raised

[1]Department of Herpetology, Zoologische Staatssammlung München (ZSM-SNSB), Münchhausenstr. 21, 81247, München, Germany. [2]Department Biologie II, Ludwig-Maximilians-Universität München, Großhaderner Straße 2, 82152, Planegg-Martinsried, Germany. [3]Department of Applied Sciences and Mechatronics, Munich University of Applied Sciences, Lothstr. 34, 80335, München, Germany. [4]Department of Ecological Science, Vrije Universiteit Amsterdam, De Boelelaan 1085, 1081 HV, Amsterdam, The Netherlands. Correspondence and requests for materials should be addressed to F.G. (email: frank.glaw@zsm.mwn.de)
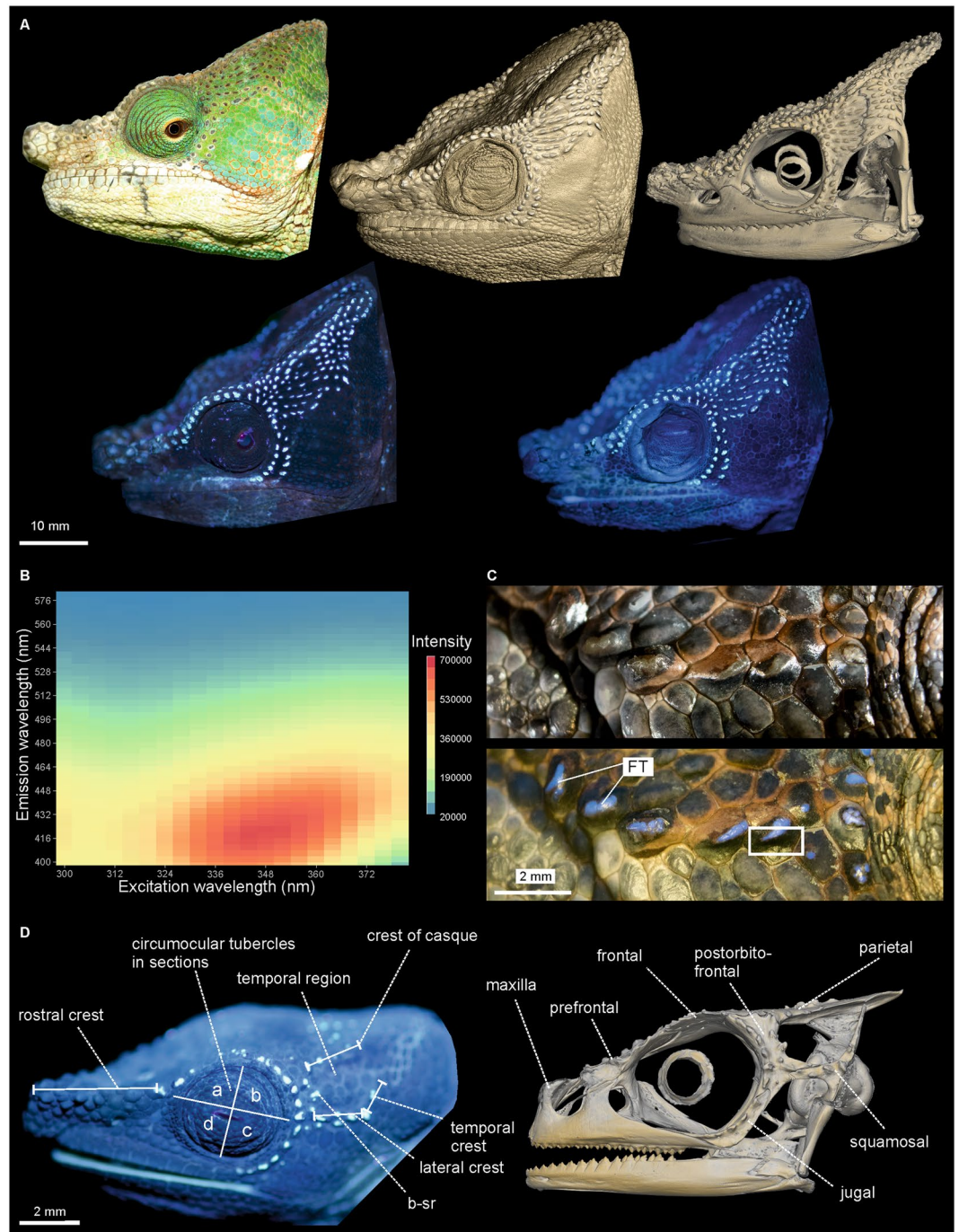
Figure 1. Chameleons of the genus *Calumma* with fluorescent tubercles of bony origin. (**A**) Male *C. globifer* (ZSM 141/2016) showing congruent tubercle/fluorescent patterns (from left to right); top row: alive in the field under sunlight, micro-CT scan of head surface (probable edge artefact in cheek region), micro-CT scan of the skull; bottom row: alive in the field under UV light, ethanol-preserved under UV light. (**B**) Excitation-emission matrix (intensity in arbitrary units) of fluorescent tubercles on right temporal region of *C. globifer* (ZSM 221/2002). (**C**) Fluorescent tubercles (FTs) on temporal region (right body side) of a male *C. crypticum* (ZSM 503/2014) under visible (above) and additional UV light (below); framed area of the skin, including a FT, was histologically sectioned (Fig. 2). (**D**) Distribution of FTs on the head surface (left) and micro-CT scan (right) of the head of *C. guibei* (ZSM 2855/2010) shows the bony origin of the FTs.

scales (Fig. 1C) in most cases. Micro-CT scans reveal these raised scales to be caused by tubercular outgrowths of the underlying bones (Fig. 1A,D, Supplementary Figs S1–4). Histological sections of a fluorescent tubercle (FT, Fig. 2) demonstrate that the top of the bony tubercle is only covered by a thin layer (20–25 µm) of epidermis that functions as a 'window' through which the bone is directly visible (Fig. 2B,D,F, Supplementary Fig. S5A). The
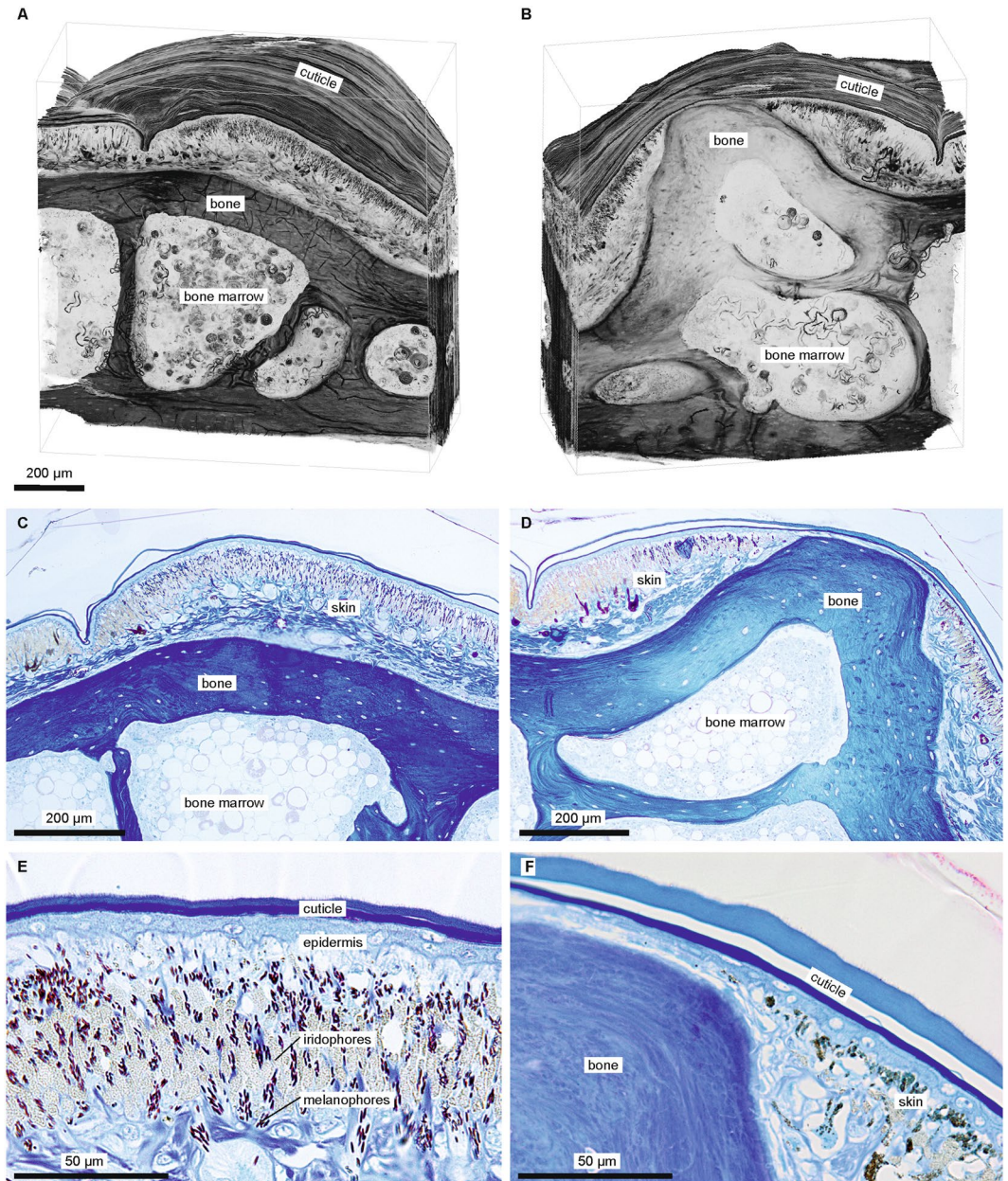
Figure 2. Histological sections of skin of a male *Calumma crypticum* (ZSM 503/2014) from the temporal region (framed in Fig. 1C). (**A,B**) 3D-reconstruction (volume rendering) of 279 histological sections of skin (without tubercle) (**A**) and of tubercle (**B**), i.e. upper margin of frame in Fig. 1C). (**C**) Section of skin and underlying bone in adjacent skin, stained (Richardson). (**D**) Section of FT (centre, stained). (**E**) Detail of skin near FT (stained). (**F**) Detail of FT (stained). For detailed views of the chromatophores, see Supplementary Fig. S5.

bony tubercle displaces the dermis containing melanophores and chromatophores[24], which are present around the protuberance and identical to that of a non-tubercle scale (Fig. 2A,C,E), rendering the layer covering the tubercle thin and transparent. A comparison of fluorescence spectra of a FT with the underlying bone showed that the emission peak of the bone covers the same range and is broadened towards longer wavelengths with a maximum at about 445 nm (Supplementary Fig. S5F,G). This indicates that the FT spectrum is included in that of the bone. Obviously the thin layer of epidermis acts as an optical filter and shifts the fluorescence towards a 'bluer' emission spectrum.

Distribution patterns of FTs. This externally visible bone-based fluorescence is not restricted to *Calumma* but also occurs in at least 8 of the 12 chameleon genera currently recognized (Fig. 3A). We focused on the species specificity and sexual dimorphism of *Calumma*. A quantitative analysis of FTs in 24 of the 34 species[25,26] (126 adult specimens in total) shows that male individuals have on average more tubercles than females in almost all species (Fig. 3B). As we were restricted to using only relatively fresh material, despite having one of the largest
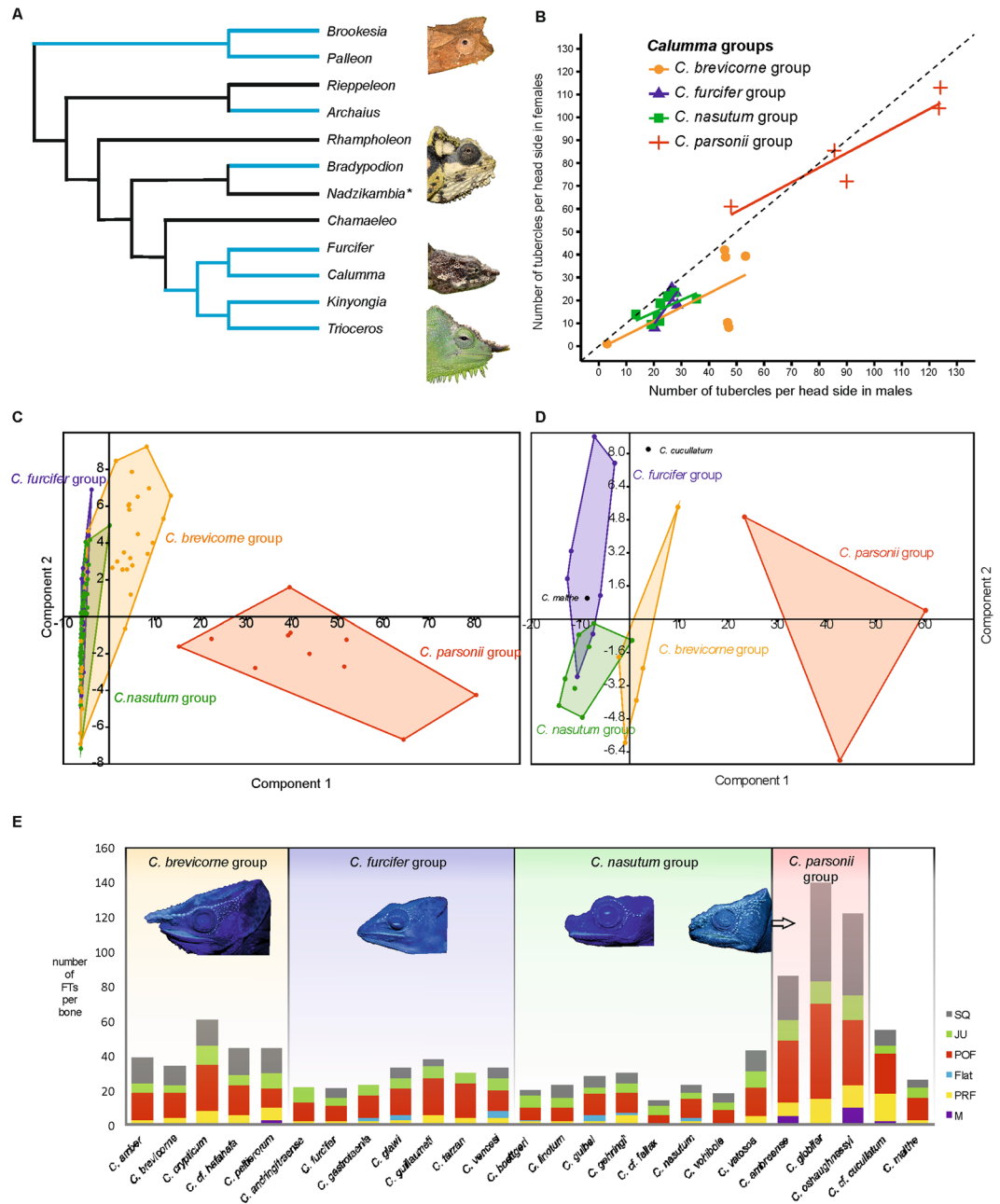
Figure 3. Analysis of distribution of FTs on adult individuals of *Calumma* species groups. (**A**) Schematic chameleon phylogeny of Tolley *et al.*[27] updated with genus *Palleon*, light blue lines indicate genera where fluorescence occurs (* indicates genus where no data was available). (**B**) Mean value of fluorescent tubercles (FTs) per head side and species, males plotted against females of 126 individuals/24 species assigned to four species groups; dashed diagonal line shows 1:1 ratio, samples below it show more tubercles in males than females. (**C,D**) PCA scatter plots assigned to four species groups, factor loadings are given in Supplementary Tables S2, 3; (**C**) Distribution of FTs per head side based on 12 characters (Supplementary Table S4) of 140 individuals/29 species. (**D**) Number of FTs per cranial bone from lateral view of 25 adult males of different *Calumma* species based on 6 characters (Supplementary Table S5). (**E**) Bar charts of number of FTs per cranial bone (M, maxilla; PRF, prefrontal; Flat, frontal seen laterally; POF, postorbitofrontal; JU, jugal; SQ, squamosal; see Fig. 1D) from lateral view of 25 adult males of different *Calumma* species.

collections of *Calumma* specimens outside Madagascar at our disposal, sample sizes per species were low, and the statistical significance of sexual dimorphism is therefore limited; although ANOVA results provide significantly more tubercles in the *C. brevicorne* group, with p = 0.016, and *C. nasutum* group, with p = 0.003 (Supplementary Table S1). The trend appears to be strong across all species (Figs 3B and 4A–D), and we expect that greater sampling will only strengthen it further.
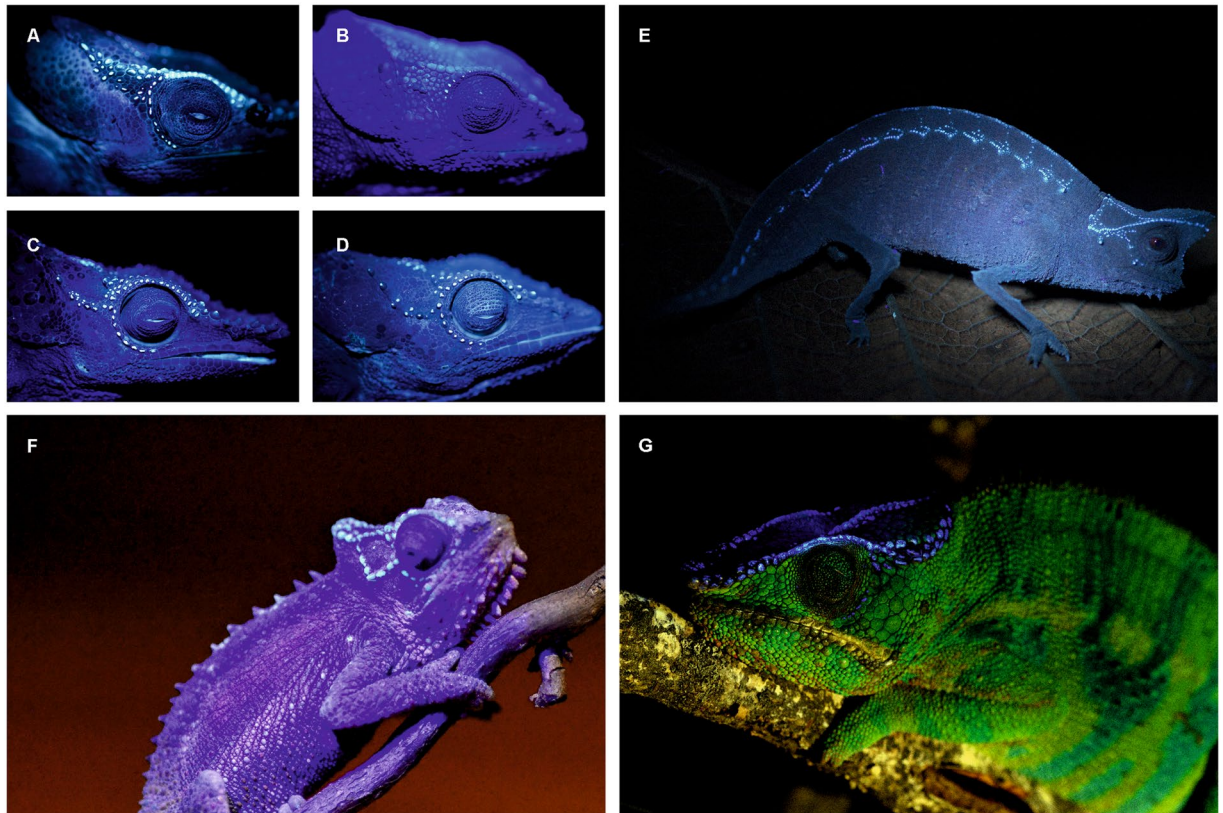
Figure 4. Fluorescent tubercles showing sexual dimorphism under UV light at 365 nm (**A–D**) and fluorescence in further chameleon genera (**E–G**). (**A**) Male *Calumma crypticum* ZSM 32/2016. (**B**) Female *C. crypticum* ZSM 67/2005. (**C**) Male *C. cucullatum* ZSM 655/2014. (**D**) Female *C. cucullatum* ZSM 654/2014. (**E**) *Brookesia superciliaris*, male (only UV light at 365 nm). (**F**) *Bradypodion transvaalense*, male (dim light and additional UV light at 395 nm). (**G**) *Furcifer pardalis*, male (daylight and additional UV light at 365 nm). For details see 'fluorescent photography' in Materials and Methods.

FTs are concentrated around the eye and the temporal region (Supplementary Figs S1–4), which are important areas for colour signalling among chameleons. Their distribution differs however among species, and even more so among species groups (Fig. 3C). A quantitative comparison of the FTs per cranial bone (Fig. 1D) in males of different *Calumma* species is systematically and phylogenetically informative (Fig. 3D,E). Members of the *C. parsonii* group for instance differ clearly from the other species by the presence of a high number of FTs in the temporal region, caused by the broadened postorbitofrontal and squamosal bone which are fused and are densely covered with tubercles (Supplementary Fig. S4). The differences in FT patterns among closely related species are inconsistent, with some sister-species pairs (e.g. *C. brevicorne* and *C. crypticum*[27]) having strongly overlapping values, while others (e.g. *C. tsaratananaense* and *C. hafahafa*) are distinctly different (Supplementary Table S4). FT patterns strongly reflect species groups, and are therefore of significant systematic value at the supraspecific level within *Calumma* (Fig. 3E), but their role within species groups requires further study.

Hypothesis of ecological relevance of fluorescence in chameleons. Phylogenetically, it seems FTs are plesiomorphic to Chamaeleonidae, but are most widespread in *Calumma* being found in almost all known species (Fig. 3A, Supplementary Table S4). In their sister genus *Furcifer*, by contrast, we found only six of 20 studied species to have FTs (Fig. 4G, Supplementary Table S6). *Furcifer* is typically found in more open and dryer habitats in Western Madagascar whereas *Calumma* are usually found in shady, humid forest habitats[28]. Also in *Brookesia*, which are terrestrial and forest dwelling chameleons from Madagascar, bone-based fluorescence even across the whole body is common (Fig. 4E). As shorter (UV, blue) wavelengths are scattered more strongly than longer wavelengths[29] the UV component under the diffuse irradiation in the forest shade is relatively higher compared to the direct irradiation by the sunlight. Consequently, using UV reflections for communication is apparently more common in closed habitats than in open habitats, as has been shown in chameleons of the genus *Bradypodion*[30]. Members of the latter genus also show fluorescence in the head region (Fig. 4F). A function of FTs as UV reflectors could therefore be hypothesised. This can be ruled out however, as these structures do not reflect UV light at 365 or 390 nm (Fig. 1B, Supplementary Fig. S6A) and at least some chameleon lenses are only transmissive above 350 nm[31]. On the other hand, the emission spectrum of FTs with a maximum at 433 nm is deep blue, a colour that is reasonably rare in a tropical forest and appears to be a conspicuous signal against the background reflectance of grey brown leaf litter or green vegetation as shown in Fig. 1 of Andersson *et al.*[32]. The glowing blue of the FTs is near to the maximum absorption of the pigments of the SWS (short-wave-sensitive)

cones with 440–450 nm of the examined chameleons[31]. Additionally, wavelengths of around 433 nm might appear brighter to chameleons as their visual spectrum is shifted towards shorter wavelengths (from about 350 nm to 650 nm) compared to the human visual perception. Assuming that in the shade of a closed forest canopy the relative intensity of the diffuse UV-light is even higher the fluorescent part of the total reflectance might increase considerably. A quantum yield calculation revealed 0.29% of absorbed photons being emitted as fluorescence. This is a typical fluorescence quantum yield for a dye that is immobilised in a matrix (here the bone) and not in a solution (Schwager unpubl.).

Constant fluorescent patterns potentially give chameleons a secondary, stable signalling system that is not influenced by their well-known communication by colour change, and does not compromise their camouflage. Moreover, the systematic relevance of the FTs suggests that they at least correlate with trends in skull evolution, and they may have provided substrate for sexual selection. On this basis, the distribution of FTs could also be used by taxonomists as an additional character to delimitate between taxa. Sexual dichromatism based on fluorescence has been shown in birds[33] which are also highly visual animals. The use of chameleons as model organisms in the understanding of the role of visual ecology and behaviour in sexual selection[34,35] will require some adjustment to account for this newly discovered phenomenon. Important future steps will be behavioural trials as well as the creation of colour visual models (accounting for the spatial acuity of chameleon vision) in order to explore the biological relevance of this phenomenon.

Given the recent discoveries of fluorescence, especially among terrestrial vertebrates[11,36], it is clear that fluorescence evolved by several independent and unique mechanisms. Apparently this tends to occur by the evolution of new mechanisms, rather than implementing features that already have fluorescent properties. Use of such features would be expected to be the most obvious route to fluorescence. We suspect, however, that chameleons are not unique in this regard, and that bone-based fluorescence is in fact widespread among taxa that use bones in their ornamentation, especially other squamates. Fluorescence in terrestrial vertebrates has been underestimated until now, and its role in the evolution of ornamentation remains largely unexplored, but this is a promising avenue for future research.

Materials and Methods

Investigated chameleon specimens. 160 specimens covering 31 species (Supplementary Table S4) of the genus *Calumma* from the collection of the Zoologische Staatssammlung München, Germany (ZSM), the Museo Regionale di Scienze Naturali, Torino, Italy (MRSN), and Senckenberg Museum, Frankfurt am Main, Germany (SMF), were photographed and quantitatively analyzed for the presence and distribution of FTs. Only specimens that were collected in 1998 or later were investigated, due to the decay in their fluorescent ability in preservative[21]. The following species were considered: *C. amber*, *C. brevicorne*, *C. crypticum*, *C. hafahafa*, *C. hilleniusi*, *C. peltier-orum* and *C. tsaratananense* of the *C. brevicorne* group[37]; *C. andringitraense*, *C. furcifer*, *C. gastrotaenia*, *C. glawi*, *C. guillaumeti*, *C. tarzan* and *C. vencesi* of the *C. furcifer* group[38]; *C. boettgeri*, *C. fallax*, *C. gallus*, *C. gehringi*[26], *C. guibei*, *C. linotum*, *C. nasutum*, *C. peyrierasi*, *C. vatosoa*[39] and *C. vohibola* of the (phenetic) *C. nasutum* group[39]; *C. ambreense*, *C. capuroni*, *C. globifer*, *C. oshaughnessyi*, *C. p. parsonii* and *C. p. cristifer* of the *C. parsonii* group[37]; the species *C. cucullatum* and *C. malthe* are phylogenetically isolated[27] and were not assigned to a *Calumma* species group. Additionally 20 species/165 specimens (of the 22 known species) of the genus *Furcifer* from the ZSM collection catalogued in the year 1998 or later were checked for fluorescence (Supplementary Table S6). All other chameleon species of the ZSM were checked and exemplarily one fluorescent specimen per genus (if applicable; no specimens available for *Nadzikambia*) is listed in Supplementary Table S6.

Fluorescent photography. Photographs were taken with a Nikon D5100, using a Tamron SP AF 90 mm f/2.8 Di macro lens. Both living specimens in the field and ethanol-preserved specimens in the laboratory were photographed with standard settings of F/6.3, 0.5 s, and ISO 200. A Tank007-TK-566 flashlight 3 Watt (Tank007 Lighting Inc.), emitting at a maximum of 365 nm, was arranged in a distance of 100 mm from the sample, as the only light source for photography.

Fluorescent photographs of living animals (one each of *Calumma globifer*, *Furcifer pardalis* and *Brookesia superciliaris*) were taken in Madagascar in December 2015/January 2016 and in August 2016. This method was entirely non-invasive and did not disturb the animals.

Detailed photographs of fluorescent tubercles (FTs) were taken using the binocular Olympus SZX12 (Olympus DF Plapo 1XPF objective) and a Sony Nex-5N digital camera (lens replaced by a camera tubus). The investigated specimen was a male *C. crypticum* (ZSM 503/2014, Fig. 1C).

Ultraviolet photography. UV photographs of an ethanol- preserved *Calumma globifer* (ZSM 141/2016, Supplementary Fig. S6) were taken with a modified Canon EOS 750D (internal UV and IR filter removed) and the uncoated, UV light-transmissive lens (Ultra-Achromatic-Takumar 1:4.5/85) with a Baader U-Filter (60 nmHBW/320–380 nm) and a setting of F/4.5, 8/5 s, and ISO 100. The photo lamp DLED4.1-UV365 (40 W, 365 nm with a 366 nm UV pass filter B3) at a 45° angle to the chameleon skin was used as the UV light source.

Fluorescence spectroscopy. Fluorescence excitation-emission spectra were recorded with a Fluorolog (Horiba) fluorimeter (slit width 3 nm). All fluorescence spectra were corrected for the wavelength-dependent output of the Xenon lamp. The intensity of the fluorescence signal shown here represents the detected emission signal divided by the simultaneously measured intensity of the lamp at the same wavelength.

For the comparison of fluorescence spectra of a FT and the underlying bone parts of the skin were removed on the temporal region of a *Calumma crypticum* (ZSM 503/2014) and emission of the externally visible bone was measured (Supplementary Fig. S5F,H).

Quantum yield calculation.   Using the Fluorolog fluorimeter (see above) the following four spectra were recorded with the same spectrometer settings: for the determination of the absorption, two emission spectra of the excitation signal in the range 340–365 nm (max. fluorescence excitation at 353 nm) of an FT region and non-FT region (as background), considering the same irradiation area; and for determination of the fluorescent signal, two emission spectra from 365–680 nm (max. fluorescence emission at 433 nm) of an FT region and non-FT (as background), considering the same irradiation area. The quantum yield is calculated according to

$$\Phi = \frac{N_{emission}}{N_{absorption}}$$

where $N_{emission}$ is the integrated background-subtracted signal of the emission and $N_{absorption}$ is the integrated background-substracted signal of the excitation range.

Analysis of fluorescent pattern.   The occurrence of FTs was assigned to different cranial crests and other parts of the head. The nomenclature of crests follows largely Nečas[40] with some adaptions to the genus *Calumma*, see Fig. 1D. The following characters were analysed: CO, number of FTs on circumocular tubercles in sections (a, b, c, d); RC, number of FTs on the rostral crest (tubercle scales from snout tip to CO, not bordering the eye); b–sr, tubercles that are arranged in a second row behind section 'b'; LC, number of FTs on lateral crest; TC, number of FTs on temporal crest; CC, number of FTs on crest of casque; TR, number of FTs in temporal region; PC, number of FTs on parietal crest; DH, number of FTs on the dorsal head region.

The FTs of 25 adult males of different *Calumma* species were counted per bone of the skull (on the left side and dorsally)—comparing a fluorescent photograph of the head with a micro-CT scan of the skull of the same specimen (Fig. 1D, Supplementary Figs S1–4, and Table S5). FTs of the following bones were counted: M, maxilla; PRF, prefrontal; Flat, FTs that are only laterally seen on frontal; POF, postorbitofrontal; JU, jugal; SQ, squamosal; Pdors, FTs that are seen dorsally on parietal; Fdors, FTs that are seen dorsally on frontal.

For Principal Component Analyses (PCA) the statistical analysis software PAST 3.08[41] was used. A PCA was performed for 12 counts of FTs of the sections that are visible in lateral view (RC, CO-a, CO-b, CO-b-sr, CO-c, CO-c-sr, CO-d, LC, LC-sr, TC, CC, TR) of 140 individuals/29 species assigned to one of the four groups within the genus *Calumma* (Fig. 3C). A second PCA was performed for 6 counts of FTs on bones that are visible in lateral view (M, PRF, Flat, POF, JU, SQ) from 25 specimens and species (Fig. 3D).

ANOVAs were calculated in R v3.0.3[42] based on the total number of FTs per head side (average value of right and left head side) of 133 individuals/25 *Calumma* species (Supplementary Table S1). The residuals of all species groups were checked for normality, and no significant deviations were observed. Due to our unbalanced sampling (variable number of specimens available per species), ANOVAs returned marginally different results depending on whether species or sex was given first in the formula, but this did not have any impact on significance results. Only one species, *C. capuroni*, has considerably more tubercles in females than in males, but the sample size of this species is low (2 specimens).

X-ray micro-CT.   For skeletal morphology, X-ray micro-computed tomography scans (micro-CT scans) of the head (or full body) of 70 specimens were prepared. Methods followed Prötzel *et al.*[43], using diamond or standard target, with the scanner set to 130 kV and 80 μA with a timing of 500 ms, and scans consisting of 1800 projections (i.e. 5 images per degree of rotation) or similar settings. For detailed information, see Supplementary Table S7.

Histology.   A FT from the temporal region (Fig. 1C) of a male *Calumma crypticum* (ZSM 503/2014, stored in 70% ethanol) was dissected with a razorblade. The excised FT was washed in 0.1 M phosphate buffer, stained in buffered 1% Osmium tetroxide (OsO₄) for one hour on ice, dehydrated in a graded acetone series, embedded in epoxy resin[44], serial sectioned in 279 planes à 1.54 μm using a RMC MT-7000 ultramicrotome with a Diatome Histo Jumbo diamond knife, mounted on glass slides, and partly stained with a 1:1 mixture of methylene blue and Azure II for approx. 5 s at 80 °C[45]. Unstained sections (Supplementary Fig. S5A,B) were sealed under coverslips with DPX mounting medium (Agar Scientifics). The glass slides with slice-ribbons were imaged in bright field illumination using an Olympus BX61VS light microscope with UPlanSApo 10 × NA 0.4 objective and CX10 digital camera, and the program VS-ASW FL (Olympus v 2.7) for virtual slide acquisition. Images of single slices were then extracted with OlyVIA software (Olympus v 2.9; 1267 × 2119 px, 24 bit RGB, 0.98 μm/px) for subsequent volume rendering. In addition selected slices were photographed using an Olympus CX 41 light microscope with a DP25 digital camera (objectives: Olympus Plan C 10 × NA 0.25, Olympus UPlanSApo 40 × NA 0.95, and Olympus UPlanSApo 60 × NA 1.2 W); for details see Supplementary Table S8.

Volume rendering.   The colour image stack from OlyVIA was pre-processed in Adobe® Photoshop® CS6 as follows: converted to 8 bit greyscale, brightness and contrast autoscaled, folds in epoxy resin outside the tissue were cropped and replaced by a uniform white background to get a clear view onto the cuticle in 3D renderings (however, some remaining folds inside the tissue cannot be avoided). The stack of greyscale images was imported in Amira 5.6 (FEI), consecutive images were aligned, ROI cropped resulting in a 3D volume of 1011 × 1092 × 297 voxels (voxel size 0.98 × 0.98 × 1.54 μm³), LUT inverted, volume rendering applied, LUT re-inverted, zoomed and rotated in appropriate perspectives to show both sides of the stack with bounding box (Fig. 2A,B), screenshots were saved in JPEG format (8 bit greyscale, 1390 × 1065 px, 1.28 μm/px).

Transmission Electron microscopy.   Subsequent to the semithin section series some ultrathin sections (70 nm) were cut with a diamond knife and mounted on formvar-coated copper slot-grids (Agar Scientific G2500C). The slices were double-stained with 8% uranyl acetate and lead citrate[46] and imaged by using a FEI Morgagni 268 TEM at 80 kV.

References

1. Sparks, J. S. *et al*. The covert world of fish biofluorescence: a phylogenetically widespread and phenotypically variable phenomenon. *PLoS One* **9**, e83259 (2014).
2. Gruber, D. F. *et al*. Biofluorescence in catsharks (Scyliorhinidae): fundamental description and relevance for elasmobranch visual ecology. *Sci. Rep.* **6**, 24751 (2016).
3. Salih, A., Larkum, A., Cox, G., Kühl, M. & Hoegh-Guldberg, O. Fluorescent pigments in corals are photoprotective. *Nature* **408**, 850–853 (2000).
4. Haddock, S. H. & Dunn, C. W. Fluorescent proteins function as a prey attractant: experimental evidence from the hydromedusa *Olindias formosus* and other marine organisms. *Biol. Open* **4**, 1094–1104 (2015).
5. Gandía-Herrero, F., García-Carmona, F. & Escribano, J. Botany: floral fluorescence effect. *Nature* **437**, 334–334 (2005).
6. Mazel, C., Cronin, T., Caldwell, R. & Marshall, N. Fluorescent enhancement of signaling in a mantis shrimp. *Science* **303**, 51–51 (2004).
7. Lim, M. L., Land, M. F. & Li, D. Sex-specific UV and fluorescence signals in jumping spiders. *Science* **315**, 481–481 (2007).
8. Vukusic, P. & Hooper, I. Directionally controlled fluorescence emission in butterflies. *Science* **310**, 1151–1151 (2005).
9. Arnold, K. E., Owens, I. P. & Marshall, N. J. Fluorescent signalling in parrots. *Science* **295**, 92–92 (2002).
10. Gruber, D. F. & Sparks, J. S. First observation of fluorescence in marine turtles. *Am. Mus. Novit.* **3845**, 1–8 (2015).
11. Taboada, C. *et al*. Naturally occurring fluorescence in frogs. *Proc. Natl. Acad. Sci. USA* **114**, 201701053 (2017).
12. Andrews, K., Reed, S. M. & Masta, S. E. Spiders fluoresce variably across many taxa. *Biol. Lett.* **3**, 265–267, https://doi.org/10.1098/rsbl.2007.0016 (2007).
13. Anthes, N., Theobald, J., Gerlach, T., Meadows, M. G. & Michiels, N. K. Diversity and ecological correlates of red fluorescence in marine fishes. *Front. Ecol. Evol.* **4**, 126 (2016).
14. Wucherer, M. F. & Michiels, N. K. A fluorescent chromatophore changes the level of fluorescence in a reef fish. *PLoS One* **7**, e37913 (2012).
15. Stuart-Fox, D. & Moussalli, A. Selection for social signalling drives the evolution of chameleon colour change. *PLoS Biol.* **6**, e25 (2008).
16. Ligon, R. A. & McGraw, K. J. Chameleons communicate with complex colour changes during contests: different body regions convey different information. *Biol. Lett.* **9**, 20130892 (2013).
17. Rieppel, O. & Crumly, C. Paedomorphosis and skull structure in Malagasy chamaeleons (Reptilia: Chamaeleoninae). *J. Zool.* **243**, 351–380 (1997).
18. Karsten, K. B., Andriamandimbiarisoa, L. N., Fox, S. F. & Raxworthy, C. J. Sexual selection on body size and secondary sexual characters in 2 closely related, sympatric chameleons in Madagascar. *Behav. Ecol.* **20**, 1079–1088, https://doi.org/10.1093/beheco/arp100 (2009).
19. Stuart-Fox, D. M., Firth, D., Moussalli, A. & Whiting, M. J. Multiple signals in chameleon contests: designing and analysing animal contests as a tournament. *Anim. Behav.* **71**, 1263–1271 (2006).
20. Bachman, C. H. & Ellis, E. H. Fluorescence of bone. *Nature* **206**, 1328–1331 (1965).
21. Hoke, N. *et al*. Estimating the chance of success of archaeometric analyses of bone: UV-induced bone fluorescence compared to histological screening. *Palaeogeogr. Palaeoclimatol. Palaeoecol.* **310**, 23–31 (2011).
22. Ott, M. & Schaeffel, F. A negatively powered lens in the chameleon. *Nature* **373**, 692–694 (1995).
23. Anderson, C. V. & Higham, T. E. In *The biology of chameleons* (eds Tolley, K. A. & Herrel, A.) Ch. Chameleon anatomy, 7–55 (University of California Press, 2014).
24. Teyssier, J., Saenko, S. V., Van Der Marel, D. & Milinkovitch, M. C. Photonic crystals cause active colour change in chameleons. *Nat. Commun.* **6**, 6368 (2015).
25. Glaw, F. Taxonomic checklist of chameleons (Squamata: Chamaeleonidae). *Vertebr. Zool.* **65**, 167–246 (2015).
26. Prötzel, D., Vences, M., Scherz, M. D., Vieites, D. R. & Glaw, F. Splitting and lumping: an integrative taxonomic assessment of Malagasy chameleons in the *Calumma guibei* complex results in the new species *C. gehringi* sp. nov. *Vertebr. Zool.* **67**, 231–249 (2017).
27. Tolley, K. A., Townsend, T. M. & Vences, M. Large-scale phylogeny of chameleons suggests African origins and Eocene diversification. *Proc. Roy. Soc. Lond. B: Biol. Sci.* **280**, 20130184 (2013).
28. Glaw, F. & Vences, M. *A field guide to the amphibians and reptiles of Madagascar*. 3 edn, (Vences & Glaw Verlag, 2007).
29. Stover, J. C. *Optical scattering: measurement and analysis*. 2 edn, (SPIE optical engineering press, 1995).
30. Stuart-Fox, D., Moussalli, A. & Whiting, M. J. Natural selection on social signals: signal efficacy and the evolution of chameleon display coloration. *Am. Nat.* **170**, 916–930 (2007).
31. Bowmaker, J. K., Loew, E. R. & Ott, M. The cone photoreceptors and visual pigments of chameleons. *J. Comp. Physiol. A* **191**, 925–932 (2005).
32. Andersson, S., Örnburg, J. & Andersson, M. Ultraviolet sexual dimorphism and assortative mating in blue tits. *Proc. Roy. Soc. Lond. B: Biol. Sci.* **265**, 445–450 (1998).
33. Barreira, A., Lagorio, M. G., Lijtmaer, D., Lougheed, S. & Tubaro, P. Fluorescent and ultraviolet sexual dichromatism in the blue-winged parrotlet. *J. Zool.* **288**, 135–142 (2012).
34. Stuart-Fox, D. & Moussalli, A. Camouflage, communication and thermoregulation: lessons from colour changing organisms. *Philos. Trans. Roy. Soc. Lond. B: Biol. Sci.* **364**, 463–470 (2009).
35. Fleishman, L. J., Loew, E. R. & Whiting, M. J. High sensitivity to short wavelengths in a lizard and implications for understanding the evolution of visual systems in lizards. *Proc. Roy. Soc. Lond. B: Biol. Sci.* **278**, 2891–2899 (2011).
36. Taboada, C., Brunetti, A. E., Alexandre, C., Lagorio, M. G. & Faivovich, J. Fluorescent frogs: A herpetological perspective. *S. Am. J. Herpetol.* **12**, 1–13 (2017).
37. Glaw, F. & Vences, M. *A fieldguide to the amphibians and reptiles of Madagascar*. 2 edn, (Vences & Glaw Verlag, 1994).
38. Andreone, F., Mattioli, F., Jesu, R. & Randrianirina, J. E. Two new chameleons of the genus *Calumma* from north-east Madagascar, with observations on hemipenal morphology in the *Calumma furcifer* group (Reptilia, Squamata, Chamaeleonidae). *Herpetol. J.* **11**, 53–68 (2001).
39. Prötzel, D., Ruthensteiner, B. & Glaw, F. No longer single! Description of female *Calumma vatosoa* (Squamata, Chamaeleonidae) including a review of the species and its systematic position. *Zoosyst. Evol.* **92**, 13–21 (2016).
40. Nečas, P. *Chameleons: nature's hidden jewels*. (Edition Chimaira, 2004).
41. Hammer, Ø., Harper, D. & Ryan, P. PAST: Paleontological Statistics Software Package for education and data analysis. *Palaeontol. Electron.* **4**, 9 (2001).
42. R Development Core Team. A language and environment for statistical computing. R Foundation for Statistical Computing (2014).
43. Prötzel, D., Ruthensteiner, B., Scherz, M. D. & Glaw, F. Systematic revision of the Malagasy chameleons *Calumma boettgeri* and *C. linotum* (Squamata: Chamaeleonidae). *Zootaxa* **4048**, 211–231 (2015).
44. Spurr, A. R. A low-viscosity epoxy resin embedding medium for electron microscopy. *J. Ultrastruct. Res.* **26**, 31–43 (1969).
45. Richardson, K., Jarett, L. & Finke, E. Embedding in epoxy resins for ultrathin sectioning in electron microscopy. *Stain Technol.* **35**, 313–323 (1960).
46. Reynolds, E. S. The use of lead citrate at high pH as an electron-opaque stain in electron microscopy. *J. Cell Biol.* **17**, 208 (1963).

Acknowledgements

Author Contributions

D.P., F.G., and M.D.S. conceived the study. All authors collected the primary data. F.G. coordinated the study. D.P., F.G., and M.D.S. developed the methods to visualise the fluorescence. M.H. contributed the histological sections and the microscopy images with help of D.P. M.S. performed the fluorescent spectra analysis. A.vt.P. contributed micro-CT scans. D.P. analysed the data with help from M.D.S. and F.G. D.P., F.G., and M.D.S. wrote the paper with input from the other authors.

Additional Information

Supplementary information accompanies this paper at https://doi.org/10.1038/s41598-017-19070-7.

Competing Interests: The authors declare that they have no competing interests.

Publisher's note: Springer Nature remains neutral with regard to jurisdictional claims in published maps and institutional affiliations.

4 Discussion

"Just as you need a vocabulary before you can speak a language, so it is necessary to have a dictionary of species before you can read the complex book of nature."

Richard Fortey, 2008

4.1 Species diversity of the *Calumma nasutum* group

4.1.1 Species delimitation based on molecular data

Before the beginning of this work, the phenetic *Calumma nasutum* group consisted of seven species (see chapter 2.2.3). With the description of eight new species, the revalidation of one species and the transfer of one additional species to the group, the species number has more than doubled to 16. The newly described species were either discovered on recent expeditions to Madagascar (*Calumma juliae* in 2016; see chapter 3.1.3; *C. roaloko* in 2015, see chapter 3.1.4; and *C. uetzi* in 2012, see chapter 3.1.3) or were proposed as deep mitochondrial lineages in Gehring *et al.* (2012). These authors calculated a total of 27 OTUs for the whole *C. nasutum* group (excluding the *C. gallus* complex, see chapter 2.2.3) and used for that calculation a number of different algorithms (Bayesian net p-distances, SpeciesIdentifier "Cluster" and GMYC model) all based on divergences of an ND2 gene fragment. As the different algorithms resulted in different numbers of OTUs Gehring *et al.* (2012) applied a conservative approach that was supported by two of the three methods (excluding GMYC which produced up to 53 OTUs).

Our integrative taxonomic revision, which is based on the investigation of more than 200 specimens and about 300 genetic samples, resulted in 11 described species out of 27 OTUs (not including the three recently discovered species, and *C. vatosoa* which was transferred to the group later, see chapter 3.1.6). Concluding, less than half of the number of species which were calculated on the basis of mitochondrial lineages alone was actually described. Although the growing number of genetic samples over the last 15 years makes a manual delineation of potential cryptic species difficult and requires specialized algorithms (Hawlitschek *et al.,* 2018; Miralles & Vences, 2013) I do not recommend to rely on species delimitation algorithms alone. The example of the *Calumma nasutum* group fits the general pattern that delimitation algorithms overestimate the number of species and bear a great risk of oversplitting (Leaché *et al.*, 2018). Some algorithms (e.g. GMYC) are apparently better

suited for arthropod taxonomy (Ratnasingham & Herbert, 2013) and appear to oversplit in squamates (Miralles & Vences, 2013).

Besides the algorithms also the molecular dataset must be appropriate for species calculations. With only one molecular marker our dataset is relatively small and, for example, Bayesian species delimitation works more reliable with larger datasets (Yang, 2015). Although the molecular dataset of Gehring *et al.* (2012) was substantially expanded with additional samples and new locations during our work, some locations are still missing or only represented by single specimens (e.g. only one sample each comprises the deep lineage within the *C. radamanus* complex from Nosy Komba (chapter 3.1.5) or *C. lefona* from Andrevorevo (chapter 3.1.3). Finally, clades should ideally form clearly delimited clusters as shown for *C. juliae* or *C. uetzi* (chapter 3.1.3). This is not given in the *C. radamanus complex* where several intermediate lineages occur between the clusters (chapter 3.1.5). Based on our dataset, species delimitation algorithms can be used to detect OTUs but should not be overestimated. For *C. gehringi*, for example, two different OTUs were calculated but all specimens were uniform in terms of external, skull and hemipenial morphology (see chapter 3.1.2) and showed haplotype sharing in CMOS (see below). Consequently, as the ideal molecular dataset barely exists I caution against relying solely on simple DNA-based taxonomy as proposed by Tautz *et al.* (2003). However, calculating OTUs can be used as a first step of an integrative taxonomic approach (see chapter 2.2.1). Therefore, barcoding can be used for reidentification of species though it should not form the basis of species delimitation (Hebert *et al.*, 2003).

In terms of species delimitation it is important to keep in mind that mitochondrial and morphological variations not necessarily need to be linked. Research in anole lizards showed that variations in both are not related and, where the environment changes, great differences in morphology occur without being reflected in the mitochondrial differentiation (Losos, 2009). In chameleons, for example, the genus *Bradypodion* contains morphologically distinct species which differ genetically by only 5% in the ND2 gene or even less in some cases (Branch *et al.*, 2006; Tilbury & Tolley, 2009). That contrasts well to species or the *C. nasutum* group, which are morphologically relatively conserved but differ in ND2 usually more than 10% between sister taxa (e.g. uncorrected pairwise distance of a ND2 fragment of 12.1% between *C. boettgeri* and *C. linotum*, see chapter 3.1.3).

Therefore, as a further line of evidence in species delimitation the absence of haplotype sharing of the nuclear genes is often used (Miralles *et al.*, 2011). The species of the *Calumma nasutum* group, which are clearly differentiated in mitochondrial genes, do not share any haplotypes of the nuclear gene CMOS either; thus there are usually a few mutational steps within a species (e.g. *C. linotum* or *C. gehringi,* see chapter 3.1.3). Samples of species which share the same haplotype are usually from the same location (e.g. *C. juliae* or *C. uetzi*, see chapter 3.1.3). The great diversity of haplotypes within the *C. radamanus* complex underlines the assumption that further (cryptic) species exist within that complex. Recognizing the value of genetic sequences as part of a modern species description, we

deposited sequences (of ND2 and CMOS) from our new species in GenBank for global accessibility.

4.1.2 Micro-CT as an additional tool for integrative taxonomy

In addition to the use of external morphology and molecular data, micro-Computed Tomography (micro-CT) was used and established as a new taxonomic tool in this thesis. Micro-CT scans expose characters of the inner morphology that are otherwise difficult to detect, but are of (potentially) great biological importance. Moreover, the skeleton or inner organs can be analysed without destroying the preserved specimens, which is crucial when examining holotypes (Faulwetter *et al.*, 2013). The skull morphology is often subject to different selective pressures than external characters and proved less variable in many of the species studied here. A comparison of PCA scatterplots of ten external and ten osteological characters indicates that the latter group well to species level in contrast to the highly overlapping external characters (Figure 4). Although, I must state that the number of specimens highly differs in both PCAs due to the limited number of micro-CT scans providing the osteological data. In detail, the shape of the parietal or frontal bone or the extension of the squamosal show less intraspecific variation than, for example, the shape and length of the rostral appendage (e.g. 1.2–4.1 mm in female *Calumma boettgeri*, see chapter 3.1.3) or the presence of a dorsal crest (e.g. present or absent in male *C. linotum*, see chapter 3.1.3). Another diagnostic character of the skull is the frontoparietal fenestra, found in *C. fallax*, *C. lefona, C. gehringi, C. guibei,* and "*C. ratnasariae*" (see chapters 3.1.2, 3.1.3, and 3.1.5). This opening in the skull has already been described in *C. fallax* from Rieppel & Crumly (1997) and interpreted as paedomorphism. We found, however, the ecological correlation that it occurs only in species that live at an elevation of 1000 m above sea level or higher. Dice-CT (Gignac *et al.*, 2016) was used to analyse the soft tissue within the chameleon's head and showed that the cerebrum lies right beneath the frontoparietal fenestra (see chapter 3.1.2) and is apparently not protected by the skull bone. There are other lizards which have a significantly smaller parietal foramen underlying the parietal eye (Eakin, 1973; Evans, 2008). This can be ruled out as there is no such structure visible on the head and the biological function of the frontoparietal fenestra remained unclear.
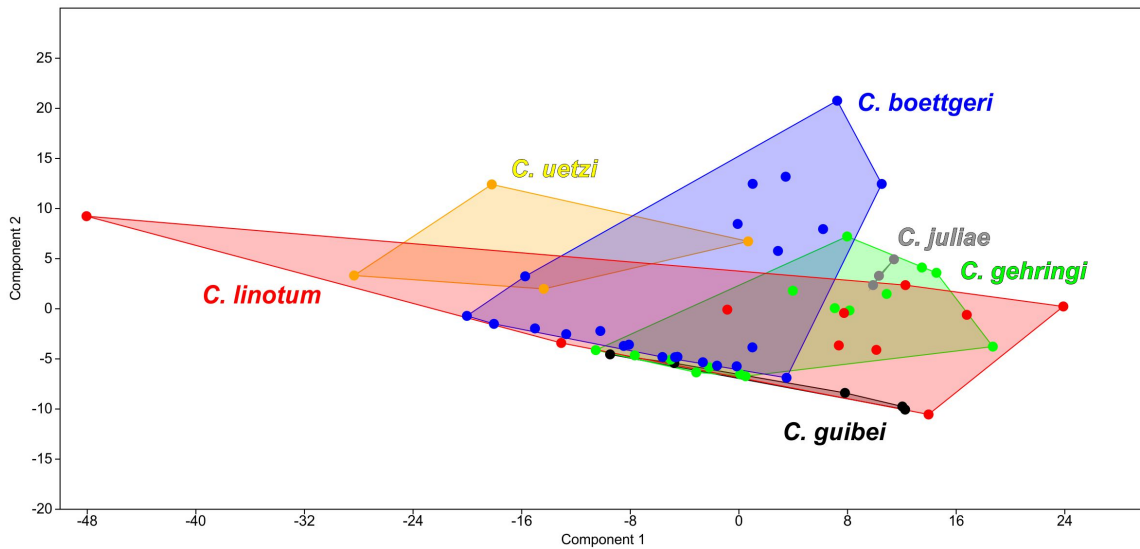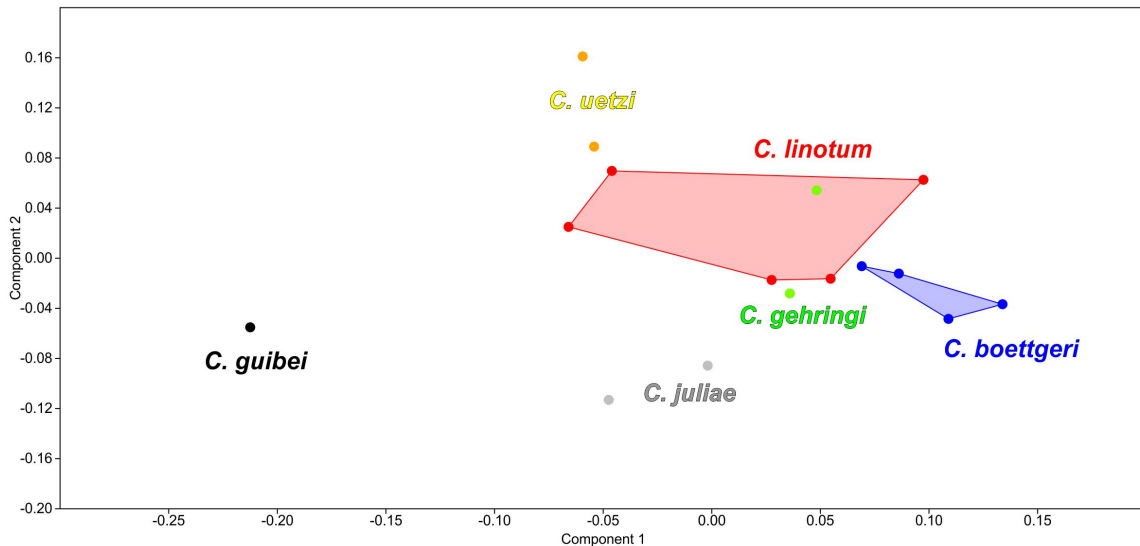
Figure 4: Principal component analysis of six species of the *Calumma boettgeri* complex (A) based on ten characters of external morphology and (B) based on ten osteological characters. The scatterplots indicate that osteological characters are more conservative and appropriate for species delimitation than the highly variable external characters showing a broad overlap between species (see especially *C. boettgeri* and *C. linotum*).

Notes: Characters are meristic or continuous resulting from size-corrected measurements; scatterplot (A): PC 1 explaining 69.0 % and PC 2, 19.4 % of the variance, based on 60 specimens; (B): PC 1 explaining 40.6 % and PC 2, 20.7 % of the variance, based on 17 specimens.

In the context of this dissertation dice-CT scans of chameleon hemipenes were produced for the first time (see chapter 3.1.1). Hemipenis morphology is an important diagnostic character in chameleons (see chapter 2.2.2) as well as in other organisms (E. Arnold, 1986; Branch, 1986). Hemipenes have usually been drawn to illustrate their structure

and ornaments. Drawings, however, are subjective and characters could be interpreted depending on the illustrator's experience. Furthermore, it can be difficult to evaluate whether the hemipenis of the preserved specimen is fully everted or not. For example, drawings of the hemipenes of *Calumma boettgeri* and *C. linotum* in Gehring *et al.* (2012) are completely lacking the cornucula gemina (Figure 5A,C). A dice-CT scan is more detailed (Figure 5B,D) and by changing the threshold of the scan we found that this structure can be almost completely retracted in the hemipenis and thus present but barely visible to external inspection. This ornament, which is reminiscent of paired, small horns (lat., cornucula gemina) has not been mentioned in the literature before (Klaver & Böhme, 1986) and thus we defined it (see chapter 3.1.2). Dice-CT scans enable an objective and detailed view of the outside and inside of a hemipenis, and, additionally, take even less time to produce than traditional illustration methods.
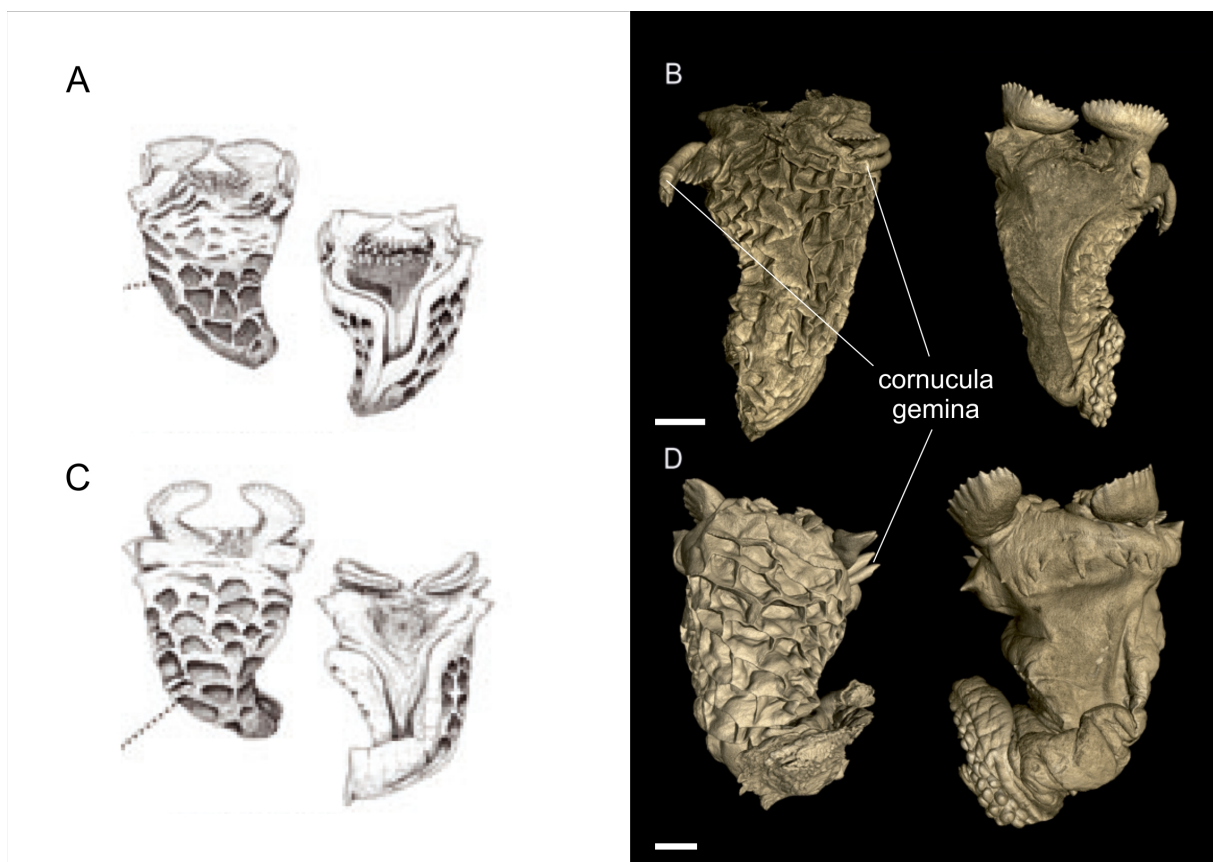
Figure 5. Drawings of hemipenes (A,C) of Gehring *et al.* (2012) and dice-CT scans of hemipenes of the respective species (B,D; see chapter 3.1.1) in asulcal and sulcal view. (A,B) showing hemipenes of *C. boettgeri*; (C,D) showing hemipenes of *C. linotum*. The cornucula gemina (horn-like ornament) are only visible in the dice-CT scans. Scale bar = 1 mm.

Depending on the settings, a micro-CT scan usually consists of 1800–2400 single projections that are processed to 3D data with special software (VG Studio Max 2.2). The resulting 3D file consumes several gigabytes of memory; all scan data generated here used 20–30 GB. Such file sizes are inconvenient and inappropriate as supplementary material. Thus, our scans are provided as either 360°-rotation short clips or as 3D-pdf files, following

Ruthensteiner and Heß (2008). The pdf has the advantage that the 3D object can be individually moved in every angle and even sectioned, combined with a small file size of 20–50 MB. This medium has also recently been proposed for clinical communication and biomedical sciences (Newe & Becker, 2018), also inspired by our paper (Prötzel *et al.,* 2015).

The use of micro-CT significantly enhances the taxonomic methodology at our disposal, and is a critical addition to the comparison of external characters, the genetic sequencing, and the analysis of internal morphology. With micro-CT scans of the skull and dice-CT scans of the hemipenis, we add further methods to the integrative approach of Miralles *et al.* (2011) who used mtDNA, nDNA, and external morphology. Most of the eight chameleon species that are described here were delimited using five separate lines of evidence. However, after using all the different methods it is still the decision of an expert with detailed knowledge of the group to elevate a population to species level or not. From the scientific point of view, the scientific naming of a species can be seen as a hypothesis (Haszprunar, pers. comm.) that is valid until it is revised by another author or new methods enable different delimitation approaches.

4.1.3 The rostral appendage in context with speciation rate

Comprised of 16 species to date and additional OTUs within the *Calumma gallus* and the *C. radamanus* complex (see chapter 3.1.5), the *C. nasutum* group is exceptionally diverse compared to, for example, the *C. furcifer* group which radiated at about the same time (Tolley *et al.,* 2013) and contains only eight described species (Glaw, 2015). Therefore, the *C. nasutum* group appears to have a higher rate of speciation. Recently, Portik *et al.* (2018) showed that diversification within African reed frogs is driven by sexual dichromatism, a relatively rare phenomenon in frogs. Furthermore, Ingram *et al.* (2016) and Losos (2009) showed that signalling structures (dewlaps) in *Anolis* promote speciation by enhancing sexual selection or species recognition. The only anoles completely lacking a dewlap are *A. bartschi* (Cochran, 1928) and *A. vermiculatus* Cocteau, 1837, comprising a very old clade with only these two species (Losos, 2009). Likewise, the *C. furcifer* group is characterised by relatively 'conservative' morphology and its species are usually uniformly green coloured in both sexes. Most species of the *C. nasutum* group, however, have a rostral appendage which is used for species recognition (Parcher, 1974). Additionally, the rostral appendage is of different shape and colour between the sexes in some species, for example in *C. gallus*. *Calumma roaloko* and its sister taxon *C. uetzi* exhibit strong sexual dichromatism of the whole body. Males of both species use conspicuous display coloration that contrasts well with the background of their habitat (see chapter 2.1). Species recognition signals and sexual dichromatism may be promoters of speciation, though this hypothesis remained to be tested in this context. Further, in anoles no cases are known in which sympatric species have identically coloured dewlaps (Losos, 2009)—it might be interesting to see whether this pattern of distinctness applies to the rostral appendages in sympatric species of the *C.*

nasutum complex, as for example "*C. emelinae*", *C. juliae,* and *C. radamanus* living syntopically in Moramanga.

After their taxonomy is clarified the *C. nasutum* group presents an interesting model group for studying speciation mechanisms. A comparison of speciation rates in the whole family Chamaeleonidae is planned in connection with an updated chameleon phylogeny (Scherz *et al.*, unpublished).

4.1.4 Implications for conservation

The newly and re-described chameleon species are potentially endangered, as Madagascar has rapidly lost tropical forests over the last 50 years (Harper *et al.*, 2007) and the deforestation rate still remains high (Grinand *et al.*, 2013). Madagascar's exceptional biodiversity, boasting the exceptional endemism rate of 84 % in land vertebrates (Goodman & Benstead, 2005), is highly threatened and there is the risk that some species will go extinct before their discovery or that they may have already done so (Costello *et al.*, 2013). Like lemurs and birds, chameleons are very popular among both conservationists and tourists and the description of *Calumma tarzan* Gehring, Pabijan, Ratsoavina, Köhler, Vences, Glaw, 2010, and its "Tarzan yell for conservation" (Gehring *et al.*, 2010) received considerable public attention. The species was listed as Critically Endangered on the IUCN Red List (International Union for Conservation of Nature) and its limited habitat was established as a new protected area (Jenkins *et al.*, 2011). Another example of a chameleon being relevant for conservation is *Trioceros narraioca* Nečas, Modry, Slapeta, 2003, from Kenya. Its description led to an expansion of the Mt. Kulal Biosphere Reserve, because this chameleon is the only endemic vertebrate species within a larger area (Nečas, pers. comm.).

A clear taxonomic status is the basis for reasonable conservation efforts for any species. The present revision has specified and restricted the distribution ranges of five chameleon species. *Calumma nasutum,* for example, was thought to occur all over northern and eastern Madagascar and is now restricted to an area between Anosibe An'ala and Andasibe, eastern Madagascar, and an isolated habitat in Sorata, northern Madagascar (Figure 6). Additionally, the nine newly described/revalidated species (Table 1) can now be assessed for future conservation efforts. An IUCN assessment has already been made for *C. boettgeri* and *C. linotum* (Glaw, *et al.,* 2015a, b). For the remaining species IUCN classifications either have been published (see chapter 3.1.3 and 3.1.4) or are suggested in this dissertation (Table 1). Given the limited data available on most of the species, specifically the lack of data on the size of its population or probability of extinction, it can currently only be assessed under criterion B "Geographic range" in the form of either B1 "extent of occurrence" and/or B2 "area of occupancy" of the IUCN Red List Criteria (IUCN, 2012). Based on IUCN classification, conservation efforts must be initiated, for example for *C. juliae* (see chapter 3.1.3) which we consider as "Critically Endangered". Another option is to announce potential flagship species in a press release to attract public attention to

chameleons in general and to their threat due to habitat loss. The effectiveness of this strategy was already evident with the media attention received by the description of the spectacularly-coloured *C. uetzi* (listed as Research Highlight in *Nature*, see chapter 3.1.3). The interview requests which followed gave the opportunity to additionally comment on other chameleon species, which are perhaps less colourful but more threatened.

Table 1. Species of *Calumma* which either were redescribed, revalidated or newly described in this work and their (suggested) IUCN-status.

IUCN criteria: B1, extent of occurrence ("defined as the area contained within the shortest continuous imaginary boundary which can be drawn to encompass all the known, inferred or projected sites of present occurrence of a taxon.", IUCN, 2012); B2, area of occupancy ("defined as the area within its 'extent of occurrence'," …", which is occupied by a taxon, excluding cases of vagrancy." IUCN 2012); a, severely fragmented or number of locations; b, decline observed: (i), in extent of occurrence; (ii), in area of occupancy; (iii) in both or quality of habitat; (iv) in number of locations or subpopulations (IUCN, 2012).

Species	Taxonomic process	Estimated Extent of occurence	Extent of occurrence (IUCN criterion B1)	Assessment under IUCN Red List criterion B	Current IUCN status	Suggested IUCN status
C. boettgeri	redescribed	5900 km^2	< 20000 km^2	B1ab(iii)	Least Concern	*Already updated*
"*C. emelinae*"	in description	200000 km^2	> 20000 km^2	B1ab(iii)c(iv)	–	**Least Concern**
C. fallax	in redescription	15000 km^2	> 20000 km^2	B1ab(iii)c(iv)	Data Deficient	**Least Concern**
C. gehringi	newly described	10000 km^2	< 5000 km^2	B1ab(iii)	–	**Endangered**
C. guibei	redescribed	500 km^2	< 5000 km^2	B1ab(iii)	Near Threatened	**Endangered**
C. juliae	newly described	0.15 km^2	< 100 km^2	B1,2ab(iii)	–	**Critically Endangered** (see 3.1.3)
C. lefona	newly described	–	–	–	–	Data Deficient (see 3.1.3)
C. linotum	redescribed	4700 km^2	< 5000 km^2	B1,2ab(i,ii)	Least Concern	*Already updated*
C. nasutum	in redescription	6000 km^2	< 20000 km^2	B1ab(iii)	Least Concern	**Vulnerable**
C. radamanus	in revalidation	75000 km^2	> 20000 km2	B1ab(iii)c(iv)	–	**Least Concern**
"*C. ratnasariae*"	in description	2500 km^2	< 5000 km^2	B1ab(iii)	–	**Endangered**
C. roaloko	in description	300 km^2	< 5000 km^2	B1ab(iii)	–	**Endangered** (see 3.1.4)
"*C. tjiasmantoi*"	in description	20000 km^2	> 20000 km^2	B1ab(iii)	–	**Least Concern**
C. uetzi	newly described	2500 km^2	< 5000 km^2	B1ab(iii)	–	**Endangered** (see 3.1.3)
C. vatosoa	redescribed/ added to the group	2000 km^2	< 5000 km^2	B1ab(iii)	Data Deficient	**Endangered**
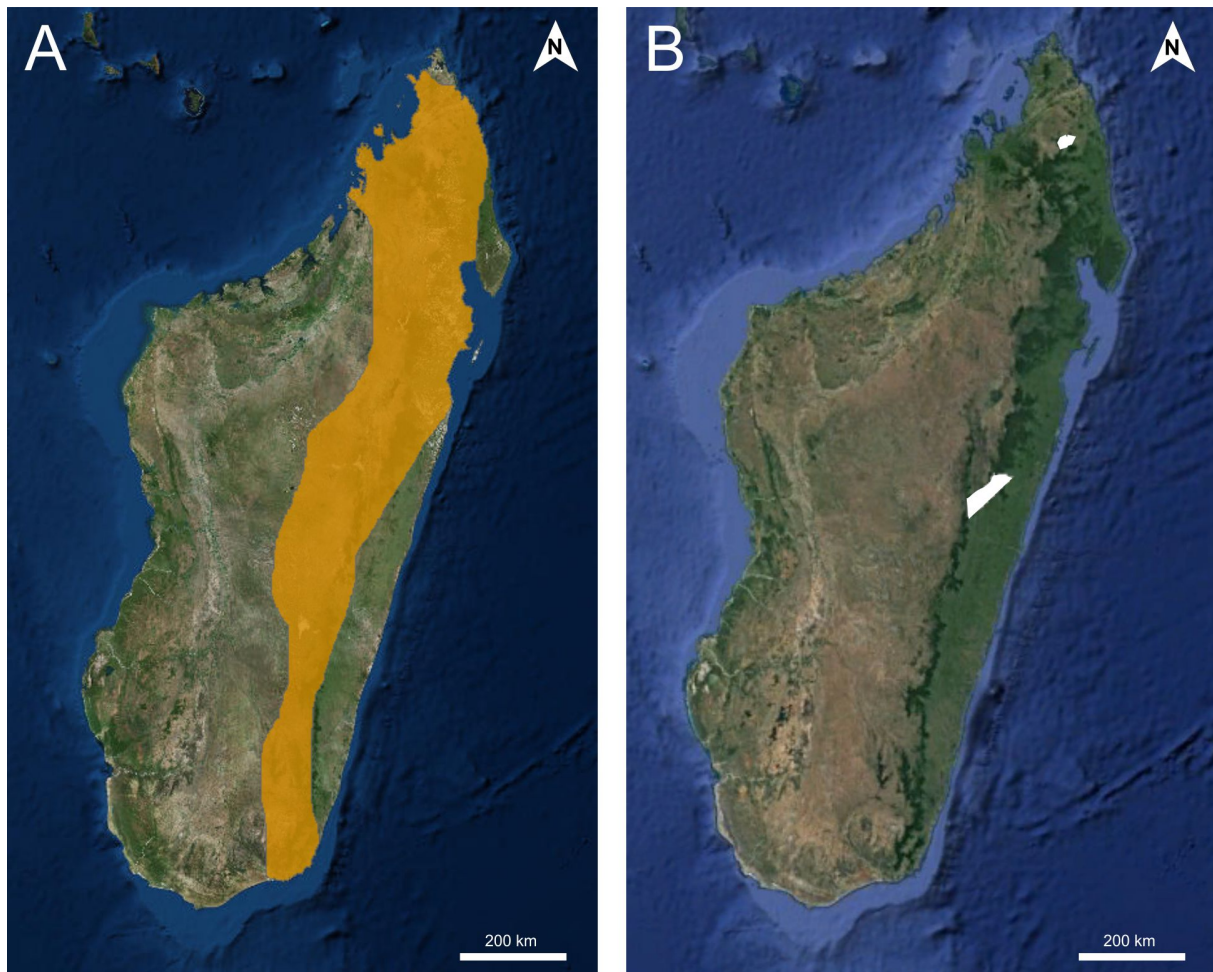
Figure 6: (A) Distribution of *Calumma nasutum* all across Madagascar before the redescription according to the IUCN (area marked in orange, Jenkins *et al.*, 2011); **(B)** the recent disjunctive distribution in eastern and northern Madagascar (area marked in white). Imagery from Google Earth.

4.2 Fluorescence in squamates – a newly-discovered communication system?

4.2.1 Potential biological function of fluorescence in chameleons

The images of chameleons with fluorescent pattern look impressive and suggest a signalling function within these visually communicating animals (see chapter 2.1). However, all photographs of fluorescent chameleons were taken under artificial illumination and humans cannot see the fluorescence under natural conditions, not even in a living chameleon in a Madagascan rainforest. Thus, the biological function of fluorescence has not been fully understood yet. Nevertheless, I suggest that chameleons can perceive fluorescence under natural light conditions and that they use the fluorescent patterns as a constant signal for species recognition in addition to their communication via colour change based on following points (see also chapter 3.2.1): (1) chameleons have a UV cone in their

retina and their visual spectrum is shifted towards shorter wavelengths (from about 350 nm to 650 nm, Bowmaker *et al.,* 2005) compared to the visual spectrum of humans. Consequently, the fluorescent tubercles (FTs) that emit light in the blue range with a maximum of 433 nm might appear brighter to them than they do to human perception (see chapter 2.3), analogous to 550 nm photons which appear ten times brighter to a human eye than the same amount of 440 nm photons (Johnsen *et al*., 2012). (2) Genera that inhabit dense forest habitats have fluorescent patterns in almost all species (e.g. *Calumma* and *Brookesia;* the latter, moreover, have very limited colour change abilities, see chapter 2.1, and could be using fluorescent signals instead). As the UV-A component at about 350 nm is relatively higher under the diffuse irradiation found in forest shade compared to direct irradiation by sunlight (Stover, 2012) there is relatively strong excitation combined with weak background reflections. (3) Blue is relatively rare in tropical forests and is used as a conspicuous signal against the green or brown background reflectance (Andersson & Andersson, 1998). (4) Species groups and even single species—at least in *Calumma*—can be distinguished based on the distribution of FTs on the body. Fluorescent tubercle density and distribution also exhibits strong sexual dimorphism, with males generally having more FTs than females.

Nevertheless, further studies are necessary to support the hypothesis that FTs play an important role in visual communication and/or species recognition. Visual modelling could provide key evidence about the visual spectrum of chameleons and their perception of fluorescent patterns. Additionally, neurological investigation of the optic nerve could measure excitation signals while the chameleon perceives florescent signals given off by the tubercles. Also, behavioural experiments with or without UV-light illumination, or blocking the FTs from UV-light by applying sunblock, following K. Arnold *et al.* (2002), might reveal new insights.

Captured by the descriptive and innovative illustrations, the phenomenon of fluorescence in chameleons received impressive media attention. We thus had the great opportunity to arouse interest in chameleons or zoological collections and zoological science in general via popular science magazines, youth magazines or as part of TV productions. Inspired by our study, a few additional observations of new (putative) fluorescent terrestrial vertebrates have already followed (Deschepper *et al.*, 2018; Sloggett, 2018).

4.2.2 Fluorescent geckos – an outlook for future projects

Additionally to the chameleons, we discovered fluorescence in another squamate, the web-footed gecko *Pachydactylus rangei* (Prötzel, unpubl. data). This species inhabits the Namib, a desert in Namibia, and lives in open and sandy habitats. Under UV-light the usually beige skin (Figure 7A,B) shows strong yellow fluorescence around the eyes and along a lateral stripe in both sexes (Figure 7C,D). From ventral and dorsal view the fluorescence is only barely visible (Figure 7D). The maximum emission of the fluorescence is at a

wavelength of 550 nm in the yellow spectrum and the excitation maximum at 470 nm in the blue spectrum (Figure 8).
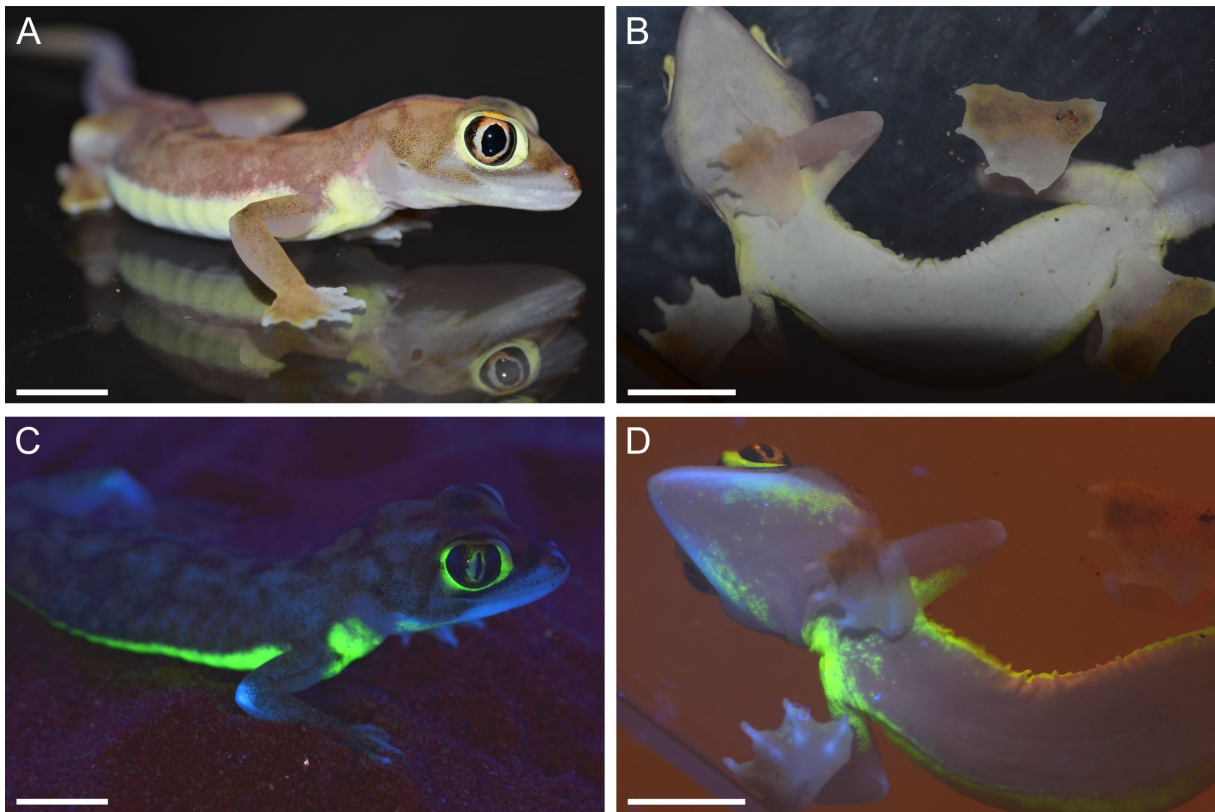
Figure 7. Male web-footed gecko (*Pachydactylus rangei*) under visible light in lateral view (A) and ventral view (B). The same specimen under UV-light with a maximum emission at 365 nm in lateral view (C) and ventral view (D) showing yellow fluorescence around the eyes and along a ventral-lateral stripe. Scale bar = 1 cm.
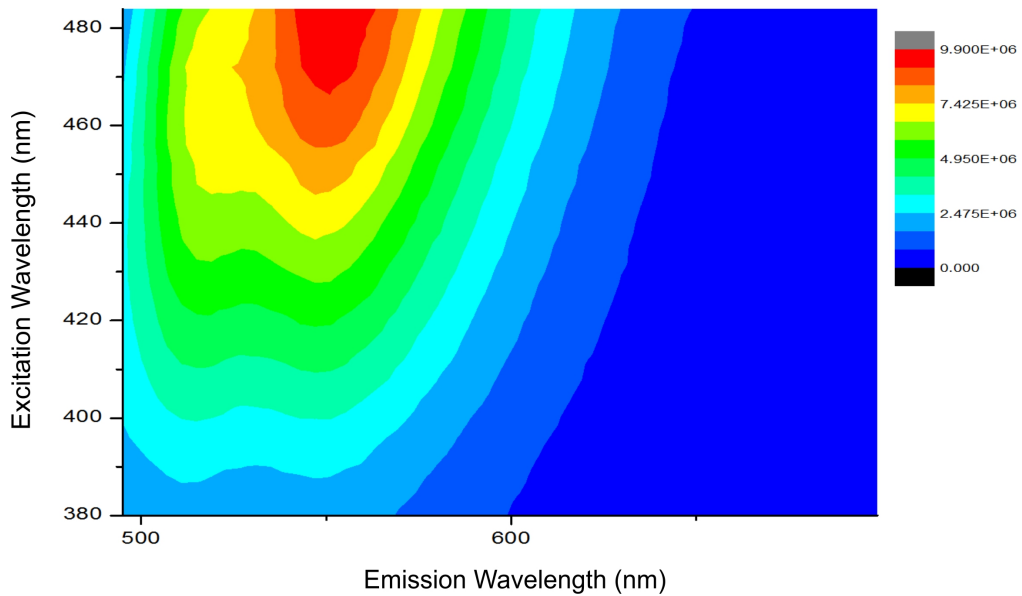
Figure 8. Excitation-emission matrix (intensity in arbitrary units) of fluorescence from the lateral stripe of *Pachdactylus rangei* with a maximum emission of the fluorescence at 550 nm (yellow) and an excitation maximum at 470 nm (blue).

In a future project the following hypotheses could be tested: (1) the excitation maximum of the fluorescence in the blue range correlates with the spectrum of the moonlight. (2) The yellow light, emitted by the fluorescence, appears particularly bright in the gecko's visual spectrum. (3) The fluorescent area that is well seen from the gecko's perspective is used for intraspecific communication and helps them to find each other in their extensive desert habitat. Geckos approach each other not only for social needs but also for water absorption using their conspecifics as condensation nuclei for the nocturnal fog (Prötzel, 2014). (4) The fluorescence is produced by an unknown mechanism, different from the bone-based mechanism in the chameleons and possibly unique among squamates or even terrestrial vertebrates. Possibly, either guanine crystals in the dermis of the gecko cause the fluorescence as has been shown for reef fish (Michiels *et al.*, 2008; see chapter 3.2.1 and the supplementary material for the layer of guanine crystals in histological sections of squamate skin). Alternatively, the gecko could have a yellow fluorescent protein, cf. Nagai *et al.* (2002), embedded in the fluorescent parts of the skin. Although, the first fluorescent protein in vertebrates has already been described for the eel *Anguilla japonica* Temminck & Schlegel, 1846 (Kumagai *et al.*, 2013), this potential protein would presumably be of a different molecular structure and might be used for new fields of applications.

Although warmth, vision, and photosynthesis depend directly on it, light is still relatively understudied by biologists. One reason might be that biologists receive only little training in the physics of light and that physicists lack the knowledge or the interest in biological examples (Johnsen, 2012). Thus, the phenomenon of fluorescence in squamates is still a relatively unexplored field in the realm of research and has the potential to be of great interest, well beyond the field of herpetology.

5 References

Anderson, CV (2016): Off like a shot: Scaling of ballistic tongue projection reveals extremely high performance in small chameleons. *Scientific Reports, 6*, 18625, 1–9.

Anderson, CV & Deban, SM (2010): Ballistic tongue projection in chameleons maintains high performance at low temperature. *Proceedings of the National Academy of Sciences, 107*, 5495–5499.

Anderson, CV & Higham, TE (2014): Chameleon Anatomy. *In:* KA Tolley & A Herrel (Eds), *The Biology of Chameleons*. University of California Press, Berkeley, pp. 7–55.

Andersson, S & Andersson, M (1998): Ultraviolet sexual dimorphism and assortative mating in blue tits. *Proceedings of the Royal Society of London B: Biological Sciences, 265*, 445–450.

Andreone, F, Mattioli, F, Jesu, R & Randrianirina, JE (2001): Two new chameleons of the genus *Calumma* from north-east Madagascar, with observations on hemipenal morphology in the *Calumma furcifer* group (Reptilia, Squamata, Chamaeleonidae). *Journal of Herpetology, 11*, 53–68.

Andrews, K, Reed, SM & Masta, SE (2007): Spiders fluoresce variably across many taxa. *Biology Letters, 3*, 265–267.

Arnold, E (1986): Why copulatory organs provide so many useful taxonomic characters: The origin and maintenance of hemipenial differences in lacertid lizards (Reptilia: Lacertidae). *Biological Journal of the Linnean Society, 29*, 263–281.

Arnold, K, Owens, IP & Marshall, NJ (2002): Fluorescent signalling in parrots. *Science, 295*, 92.

Arun, KHS, Kaul, CL & Ramarao, P (2005): Green fluorescent proteins in receptor research: An emerging tool for drug discovery. *Journal of Pharmacological and Toxicological Methods, 51*, 1–23.

Balme, DM (1975): Aristotle's use of differentiae in zoology. *Articles on Aristotle, 1*, 183–193.

Bowmaker, JK, Loew, ER & Ott, M (2005): The cone photoreceptors and visual pigments of chameleons. *Journal of Comparative Physiology A, 191*, 925–932.

Branch, W (1986): Hemipenial morphology of African snakes: A taxonomic review. Part 1. Scolecophidia and Boidae. *Journal of Herpetology*, 285–299.

Branch, W, Tolley, KA & Tilbury, CR (2006): A new Dwarf Chameleon (Sauria: *Bradypodion* Fitzinger, 1843) from the Cape Fold Mountains, South Africa. *African Journal of Herpetology, 55*, 123–141.

Brygoo, ER, Blanc, CP & Domergue, CA (1970): Notes sur les chamaeleo de Madagascar. – VI. *C. gastrotaenia marojezensis* n. subsp. d'un massif montagneux du nord-est. *Annales Université Madagascar (Sciences), 7*, 273–278.

Brygoo, ER, Blanc, CP & Domergue, CA (1973): Notes sur les chamaeleo de Madagascar. – XI. Un nouveau Caméléon de l'Ankaratra: *C. brevicornis hilleniusi* n. subsp. *Bulletin de la Societé zoologique de France, 98*, 113–120.

Brygoo, ER & Domergue, CA (1971): Notes sur les *Brookesia* (Caméléonidés) de Madagascar. Description d'une espèce nouvelle, *B. antoetrae* n. sp., et des hémipénis de *B. stumpffi* et *B. ebenaui*. Remarques sur la répartition de *B. stumpffi. Bulletin du Muséum National d'Histoire Naturelle, 42*, 830–838.

Cope, ED (1896): On the hemipenes of the Sauria. *Proceedings of the Academy of Natural Sciences of Philadelphia, 48*, 461–467.

Costello, MJ, May, RM & Stork, NE (2013): Can we name Earth's species before they go extinct? *Science, 339*, 413–416.

Cuadrado, M (1998): The use of yellow spot colors as a sexual receptivity signal in females of *Chamaeleo chamaeleon. Herpetologica, 54*, 395–402.

Cuvier, G (1824): *Recherches sur les ossements fossiles, de quadrupèdes, où l'on rétablit les caractères du plusieurs espèces d'animaux que les révolutions du globe paroissent avoir détruites, 2e édition.* (Vol. 5). Paris: Dufour & d'Ocagne, pp. 269.

Cuvier, G (1829): Le règne animal. pp. 60.

Darwin, C (1859): *On the origin of species by means of natural selection, or the preservation of favoured races in the struggle for life.* London: John Murray, pp. 491.

Dayrat, B (2005): Towards integrative taxonomy. *Biological Journal of the Linnean Society, 85*, 407–415.

De Queiroz, K (2005): Ernst Mayr and the modern concept of species. *Proceedings of the National Academy of Sciences, 102*, 6600–6607.

De Queiroz, K (2007): Species concepts and species delimitation. *Systematic Biology, 56*, 879–886.

Deschepper, P, Jonckheere, B & Matthys, J (in press): A light in the dark: The discovery of another fluorescent frog in the Costa Rican rainforests. *Wilderness & environmental medicine.*

Dobzhansky, T (1937): *Genetics and the Origin of Species* (Vol. 11): Columbia University Press, pp. 364.

Dollion, AY, Cornette, R, Tolley, KA, Boistel, R, Euriat, A, Boller, E, Fernandez, V, Stynder, D & Herrel, A (2015): Morphometric analysis of chameleon fossil fragments from the Early Pliocene of South Africa: a new piece of the chamaeleonid history. *The Science of Nature, 102*, 1–14.

Dollion, AY, Measey, GJ, Cornette, R, Carne, L, Tolley, KA, da Silva, JM, Boistel, R, Fabre, AC & Herrel, A (2017): Does diet drive the evolution of head shape and bite force in chameleons of the genus *Bradypodion*? *Functional Ecology, 31*, 671–684.

Drummond, AJ & Rambaut, A (2007): BEAST: Bayesian evolutionary analysis by sampling trees. *BMC Evolutionary Biology, 7*, 1–8.

Duméril, A & Bibron, G (1836): Erpétologie Générale ou Histoire Naturelle Complete des Reptiles. *In*. Librairie encyclopédique de Roret, Paris, pp. 517.

Eakin, RM (1973): *The Third Eye.* Berkely and Los Angeles: University of California Press, pp. 157.

Evans, S (2008): The skull of lizards and tuatara. *Biology of the Reptilia, 20*, 1–347.

Ellis-Quinn, BA & Simony, CA (1991): Lizard homing behavior: the role of the parietal eye during displacement and radio-tracking, and time-compensated celestial orientation in the lizard *Sceloporus jarrovi. Behavioral Ecology and Sociobiology, 28*, 397–407.

Fasel, A, Muller, P-A, Suppan, P & Vauthey, E (1997): Photoluminescence of the African scorpion "Pandinus imperator". *Journal of Photochemistry and Photobiology B: Biology, 39*, 96–98.

Faulwetter, S, Vasileiadou, A, Kouratoras, M, Dailianis, T & Arvanitidis, C (2013): Micro-computed tomography: Introducing new dimensions to taxonomy. *ZooKeys, 263*, 1–45.

Flashar, H (2015): *Aristoteles: Lehrer des Abendlandes.* München: C.H.Beck, pp. 416.

Gandía-Herrero, F, García-Carmona, F & Escribano, J (2005): Botany: floral fluorescence effect. *Nature, 437*, 334–334.

Gehring, P-S, Pabijan, M, Ratsoavina, FM, Köhler, J, Vences, M & Glaw, F (2010): A Tarzan yell for conservation: a new chameleon, *Calumma tarzan* sp. n., proposed as a flagship species for the creation of new nature reserves in Madagascar. *Salamandra, 46*, 167–179.

Gehring, P-S, Ratsoavina, FM, Vences, M & Glaw, F (2011): *Calumma vohibola*, a new chameleon species (Squamata: Chamaeleonidae) from the littoral forests of eastern Madagascar. *African Journal of Herpetology, 60*, 130–154.

Gehring, P-S, Tolley, KA, Eckhardt, FS, Townsend, TM, Ziegler, T, Ratsoavina, F, Glaw, F & Vences, M (2012): Hiding deep in the trees: discovery of divergent mitochondrial lineages in Malagasy chameleons of the *Calumma nasutum* group. *Ecology and Evolution, 2*, 1468–1479.

GenBank https://www.ncbi.nlm.nih.gov/. Accessed 2018-08-15.

Gerlach, T, Sprenger, D & Michiels, NK (2014): Fairy wrasses perceive and respond to their deep red fluorescent coloration. *Proceedings of the Royal Society of London B: Biological Science, 281*, 20140787, 1–7.

Gignac, PM, Kley, NJ, Clarke, JA, Colbert, MW, Morhardt, AC, Cerio, D, Cost, IN, Cox, PG, Daza, JD & Early, CM (2016): Diffusible iodine based contrast enhanced computed tomography (diceCT): An emerging tool for rapid, high resolution, 3D imaging of metazoan soft tissues. *Journal of Anatomy, 228*, 889–909.

Glaw, F (2015): Taxonomic checklist of chameleons (Squamata: Chamaeleonidae). *Vertebrate Zoology, 65*, 167–246.

Glaw, F, Jenkins, R, Prötzel, D & Tolley, K (2015a): *Calumma boettgeri. The IUCN Red List of Threatened Species*, e.T176301A82125738.

Glaw, F, Köhler, J, Townsend, TM & Vences, M (2012): Rivaling the world's smallest reptiles: Discovery of miniaturized and microendemic new species of leaf chameleons (*Brookesia*) from northern Madagascar. *PLoS One, 7*, e31314, 1–24.

Glaw, F, Prötzel, D & Jenkins, R (2015b): *Calumma linotum. The IUCN Red List of Threatened Species*, e.T75976541A75976544.

Glaw, F & Vences, M (2007): *A field guide to the amphibians and reptiles of Madagascar* (3th ed.). Cologne: Vences & Glaw Verlag, pp. 496.

Goodman, SM & Benstead, JP (2005): Updated estimates of biotic diversity and endemism for Madagascar. *Oryx, 39*, 73–77.

Grbic, D, Saenko, SV, Randriamoria, TM, Debry, A, Raselimanana, AP & Milinkovitch, MC (2015): Phylogeography and support vector machine classification of colour variation in panther chameleons. *Molecular Ecology, 24*, 3455–3466.

Grinand, C, Rakotomalala, F, Gond, V, Vaudry, R, Bernoux, M & Vieilledent, G (2013): Estimating deforestation in tropical humid and dry forests in Madagascar from 2000 to 2010 using multi-date Landsat satellite images and the random forests classifier. *Remote Sensing of Environment, 139*, 68–80.

Gruber, DF, Loew, ER, Deheyn, DD, Akkaynak, D, Gaffney, JP, Smith, WL, Davis, MP, Stern, JH, Pieribone, VA & Sparks, JS (2016): Biofluorescence in catsharks (Scyliorhinidae): Fundamental description and relevance for elasmobranch visual ecology. *Scientific Reports, 6*, 24751, 1–16.

Gruber, DF & Sparks, JS (2015): First Observation of fluorescence in marine turtles. *American Museum Novitates, 3845*, 1–8.

Haddock, SH & Dunn, CW (2015): Fluorescent proteins function as a prey attractant: Experimental evidence from the hydromedusa *Olindias formosus* and other marine organisms. *Biology Open, 4*, 1094–1104.

Haddock, SH, Dunn, CW, Pugh, PR & Schnitzler, CE (2005): Bioluminescent and red-fluorescent lures in a deep-sea siphonophore. *Science, 309*, 263–263.

Haddock, SH, Moline, MA & Case, JF (2010): Bioluminescence in the sea. *Annual Review of Marine Science, 2*, 443–493.

Harper, GJ, Steininger, MK, Tucker, CJ, Juhn, D & Hawkins, F (2007): Fifty years of deforestation and forest fragmentation in Madagascar. *Environmental Conservation, 34*, 325–333.

Hawlitschek, O, Scherz, MD, Ruthensteiner, B, Crottini, A & Glaw, F (2018): Computational molecular species delimitation and taxonomic revision of the gecko genus *Ebenavia* Boettger, 1878. *The Science of Nature, 105*, 1–21.

Hebert, PD, Cywinska, A & Ball, SL (2003): Biological identifications through DNA barcodes. *Proceedings of the Royal Society of London B: Biological Sciences, 270*, 313–321.

Hebrard, J, Reilly, S & Guppy, M (1982): Thermal ecology of *Chamaeleo hoehnelii* and *Mobuya varia* in the Aberdare Mountains: Constraints of heterothermy in an alpine habitat. *Journal of the East Africa Natural History Society and National Museum, 176*, 1–6.

Hennig, W (1950): *Gründzuge einer Theorie der phylogenetischen Systematik*. Berlin: Deutscher Zentralverlag, pp. 370.

Hennig, W (1965): Phylogenetic systematics. *Annual Review of Entomology, 10*, 97–116.

Hillenius, D (1959): The differentiation within the genus *Chamaeleo* Laurenti, 1768. *Beaufortia, 8*, 1–92.

Hughes, DF, Kusamba, C, Behangana, M & Greenbaum, E (2017): Integrative taxonomy of the Central African forest chameleon, *Kinyongia adolfifriderici* (Sauria: Chamaeleonidae), reveals underestimated species diversity in the Albertine Rift. *Zoological Journal of the Linnean Society, 181*, 400–438.

ICZN (1999): International code of zoological nomenclature, 4th ed. Natural History Museum, London, UK.

Ingram, T, Harrison, A, Mahler, DL, del Rosario Castañeda, M, Glor, RE, Herrel, A, Stuart, YE & Losos, JB (2016): Comparative tests of the role of dewlap size in Anolis lizard speciation. *Proceedings of the Royal Society of London B: Biological Sciences, 283*, 20162199, 1–9.

IUCN (2012): *IUCN red list categories and criteria: version 3.1*. Gland, Switzerland and Cambridge, UK: IUCN.

Jenkins, RKB, Andreone, F, Andriamazava, A, Anjeriniaina, M, Brady, L, Glaw, F, Griffiths, RA, Rabibisoa, N, Rakotomalala, D, Randrianantoandro, JC, Randrianiriana, J, Randrianizahana, H, Ratsoavina, F & Robsomanitrandrasana, E (2011): *Calumma nasutum*. The IUCN Red List of Threatened Species, e.T172861A6931331.

Jenkins, RKB, Andreone, F, Andriamazava, A, Anjeriniaina, M, Brady, L, Glaw, F, Griffiths, RA, Rabibisoa, N, Rakotomalala, D, Randrianantoandro, JC, Randrianiriana, J, Randrianizahana, H, Ratsoavina, F & Robsomanitrandrasana, E (2011): *Calumma tarzan*. *The IUCN Red List of Threatened Species*, e.T193482A8862229.

Johnsen, S (2012): *The Optics of Life: A Biologist's Guide to Light in Nature*. New Jersey, Oxfordshire: Princeton University Press, pp. 336.

Karsten, KB, Andriamandimbiarisoa, LN, Fox, SF & Raxworthy, CJ (2009): Sexual selection on body size and secondary sexual characters in two closely related, sympatric chameleons in Madagascar. *Behavioral Ecology, 20*, 1079–1088.

Keren-Rotem, T, Levy, N, Wolf, L, Bouskila, A & Geffen, E (2016): Male preference for sexual signalling over crypsis is associated with alternative mating tactics. *Animal Behaviour, 117*, 43–49.

Klaver, C & Böhme, W (1986): Phylogeny and classification of the Chamaeleonidae (Sauria) with special reference to hemipenis morphology. *Bonner Zoologische Monographien, 22*, 1–64.

Kloock, CT (2008): A comparison of fluorescence in two sympatric scorpion species. *Journal of Photochemistry and Photobiology B: Biology, 91*, 132–136.

Kloock, CT, Kubli, A & Reynolds, R (2010): Ultraviolet light detection: A function of scorpion fluorescence. *Journal of Arachnology, 38*, 441–445.

Kumagai, A, Ando, R, Miyatake, H, Greimel, P, Kobayashi, T, Hirabayashi, Y, Shimogori, T & Miyawaki, A (2013): A bilirubin-inducible fluorescent protein from eel muscle. *Cell, 153*, 1602–1611.

Leaché, AD, Zhu, T, Rannala, B & Yang, Z (2018): The spectre of too many species. *Systematic Biology*, syy051.

Lim, ML, Land, MF & Li, D (2007): Sex-specific UV and fluorescence signals in jumping spiders. *Science, 315*, 481–481.

Linnaeus, C (1758): *Systema Naturae per Regna Tria Naturae: Secundum Classes, Ordines, Genera, Species, cum Characteribus, Differentiis, Synonymis, Locis* (Vol. 10). Holmiae (Laurentii Salvii). pp. 824.

Losos, JB (2009): *Lizards in an Evolutionary Tree* (Vol. 10). Berkeley: University of California Press, pp. 509.

Maitland, D & Hart, A (2008): A Fluorescent Vertebrate: the Iberian Worm-lizard Blanus cinereus (Amphisbaenidae). *Herpetological Review, 39*, 50–51.

Mayden, RL (1997): A hierarchy of species concepts: The denouement in the saga of the species problem. *In:* Claridge, MF, Dawah, HA & Wilson, MR (Eds): *Species: The Units of Diversity*. Chapman & Hall, London, UK, pp. 381–423.

Mayr, E (1942): *Systematics and the Origin of Species from the Viewpoint of a Zoologist*. New York, USA: Columbia University Press, NY, USA. pp. 334.

Mayr, E (1982): *The Growth of Biological Thought: Diversity, Evolution, and Inheritance*. Cambridge, USA; London, UK: The Belknap Press of Harvard University, pp. 974.

Mazel, C, Cronin, T, Caldwell, R & Marshall, N (2004): Fluorescent enhancement of signaling in a mantis shrimp. *Science, 303*, 51.

Meier, R, Shiyang, K, Vaidya, G & Ng, PK (2006): DNA barcoding and taxonomy in Diptera: A tale of high intraspecific variability and low identification success. *Systematic Biology, 55*, 715–728.

Michiels, NK, Anthes, N, Hart, NS, Herler, J, Meixner, AJ, Schleifenbaum, F, Schulte, G, Siebeck, UE, Sprenger, D & Wucherer, MF (2008): Red fluorescence in reef fish: a novel signalling mechanism? *BMC Ecology, 8*, 1–14.

Miralles, A, Vasconcelos, R, Perera, A, Harris, DJ & Carranza, S (2011): An integrative taxonomic revision of the Cape Verdean skinks (Squamata, Scincidae). *Zoologica Scripta, 40*, 16–44.

Miralles, A & Vences, M (2013): New metrics for comparison of taxonomies reveal striking discrepancies among species delimitation methods in *Madascincus* lizards. *PLoS One, 8*, e68242, 1–20.

Müller, L (1924): Ueber ein neues Chamaeleon aus Madagaskar. *Mitteilungen aus dem Zoologischen Museum in Berlin, 11*, 95–96.

Nagai, T, Ibata, K, Park, ES, Kubota, M, Mikoshiba, K & Miyawaki, A (2002): A variant of yellow fluorescent protein with fast and efficient maturation for cell-biological applications. *Nature Biotechnology, 20*, 87–90.

Nečas, P (2004): *Chameleons: Nature's Hidden Jewels*. Frankfurt am Main: Edition Chimaira, pp. 380.

Newe, A & Becker, L (2018): Three-Dimensional Portable Document Format (3D PDF) in Clinical Communication and Biomedical Sciences: Systematic Review of Applications, Tools, and Protocols. *JMIR Medical Informatics, 6*, e10295, 1–22.

Ott, M (2001): Chameleons have independent eye movements but synchronise both eyes during saccadic prey tracking. *Experimental Brain Research, 139*, 173–179.

Ott, M & Schaeffel, F (1995): A negatively powered lens in the chameleon. *Nature, 373*, 692–694.

Ott, M, Schaeffel, F & Kirmse, W (1998): Binocular vision and accommodation in prey-catching chameleons. *Journal of Comparative Physiology A, 182*, 319–330.

Padial, JM, Castroviejo-Fisher, S, Köhler, J, Vilà, C, Chaparro, JC & De la Riva, I (2009): Deciphering the products of evolution at the species level: the need for an integrative taxonomy. *Zoologica Scripta, 38*, 431–447.

Padial, JM, Miralles, A, De la Riva, I & Vences, M (2010): The integrative future of taxonomy. *Frontiers in Zoology, 7*, 1–14.

Parcher, SR (1974): Observations on the natural histories of six Malagasy Chamaeleontidae. *Zeitschrift für Tierpsychologie, 34*, 500–523.

Pook, C & Wild, C (1997): The phylogeny of the *Chamaeleo (Trioceros) cristatus* species group from Cameroon inferred from direct sequencing of the mitochondrial 12S ribosomal RNA gene: Evolutionary and paleobiogeographic implications. *Herpetologia Bonnensis. Bonn, Germany: Societas Europaea Herpetologica*, 297–306.

Portik, DM, Bell, RC, Blackburn, DC, Bauer, AM, Barratt, CD, Branch, WR, Burger, M, Channing, A, Colston, TJ, Conradie, W, Dehling, JM, Drewes, RC, Ernst, R, Greenbaum, E, Gvoždík, V, Harvey, J, Hillers, A, Hirschfeld, M, Jongsma, G, Kielgast, J, Kouete, MT,

Lawson, LP, Leaché, AD, Loader, SP, Lötters, S, van der Meijden, A, Menegon, M, Müller, S, Nagy, ZT, Ofori-Boateng, C, Ohler, A, Papenfuss, TJ, Rößler, D, Sinsch, U, Rödel, M-O, Veith, M, Vindum, J, Zassi-Boulou, A-G & McGuire, JA (2018): Sexual dichromatism drives diversification within a major radiation of African amphibians. *bioRxiv*.

Prötzel, D (2014): Der Palmatogecko – ein sozialer Gecko? *Reptilia, 107*, 4–5.

Prötzel, D, Lambert, SM, Andrianasolo, GT, Hutter, CR, Cobb, KA, Scherz, MD, Glaw, F (2018a):The smallest 'true chameleon' from Madagascar: A new, distinctly colored species of the Calumma boettgeri complex (Squamata: Chamaeleonidae). Zoosystematics and Evolution *94*, 409–423.

Prötzel, D, Ruthensteiner, B, Scherz, MD, Glaw, F (2015): Systematic revision of the Malagasy chameleons *Calumma boettgeri* and *Calumma linotum* (Squamata: Chamaeleonidae). *Zootaxa 4048*, 211–231.

Prötzel, D, Vences, M, Hawlitschek, O, Scherz, MD, Ratsoavina, FM & Glaw, F (2018b): Endangered beauties: Micro-CT cranial osteology, molecular genetics and external morphology reveal three new species of chameleons in the *Calumma boettgeri* complex (Squamata: Chamaeleonidae). *Zoological Journal of the Linnean Society*, *184*, 471–498.

Prötzel, D, Vences, M, Scherz, MD, Vieites, DR & Glaw, F (2017): Splitting and lumping: An integrative taxonomic assessment of Malagasy chameleons in the *Calumma guibei* complex results in the new species *C. gehringi* sp. nov. *Vertebrate Zoology, 67*, 231–249.

Ratnasingham, S & Hebert, PDN (2013): A DNA-based registry for all animal species: The Barcode Index Number (BIN) System. *PLoS One, 8*, e66213, 1–16.

Raxworthy, CJ, Forstner, MRJ & Nussbaum, RA (2002): Chameleon radiation by oceanic dispersal. *Nature, 415*, 784–787.

Raxworthy, CJ, Pearson, RG, Rabibisoa, N, Rakotondrazafy, AM, Ramanamanjato, JB, Raselimanana, AP, Wu, S, Nussbaum, RA & Stone, DA (2008): Extinction vulnerability of tropical montane endemism from warming and upslope displacement: a preliminary appraisal for the highest massif in Madagascar. *Global Change Biology, 14* , 1703–1720.

Reilly, SM (1982): Ecological notes on *Chamaeleo schubotzi* from Mount Kenya. *The Journal of the Herpetological Association of Africa, 28*, 1–3.

Rieppel, O (1981): The skull and jaw adductor musculature in chamaeleons. *Revue Suisse de Zoologie, 88*, 433–445.

Rieppel, O & Crumly, C (1997): Paedomorphosis and skull structure in Malagasy chamaeleons (Reptilia: Chamaeleoninae). *Journal of Zoology, 243*, 351–380.

Ruthensteiner, B & Heß, M (2008): Embedding 3D models of biological specimens in PDF publications. *Microscopy Research and Technique, 71*, 778–786.

Salih, A, Larkum, A, Cox, G, Kühl, M & Hoegh-Guldberg, O (2000): Fluorescent pigments in corals are photoprotective. *Nature, 408*, 850–853.

Sándor, PS, Frens, MA & Henn, V (2001): Chameleon eye position obeys Listing's law. *Vision research, 41*, 2245–2251.

Schlick-Steiner, BC, Steiner, FM, Seifert, B, Stauffer, C, Christian, E & Crozier, RH (2010): Integrative taxonomy: A multisource approach to exploring biodiversity. *Annual Review of Entomology, 55*, 421–438.

Sloggett, JJ (2018): Field observations of putative bone-based fluorescence in a gecko. *Current Zoology, 64*, 319–320.

Sparks, JS, Schelly, RC, Smith, WL, Davis, MP, Tchernov, D, Pieribone, VA & Gruber, DF (2014): The covert world of fish biofluorescence: A phylogenetically widespread and phenotypically variable phenomenon. *PLoS One, 9*, e83259, 1–9.

Srinivasan, MV (1999): When one eye is better than two. *Nature, 399*, 305–307.

Stover, JC (2012): *Optical Scattering: Measurement and Analysis* (Vol. 2). Bellingham: SPIE Optical Engineering Press, pp. 330.

Stuart-Fox, D (2014): Chameleon behavior and color change. *In:* KA Tolley & A Herrel (Eds), *The Biology of Chameleons*. University of California Press, Berkeley, pp. 115–130.

Stuart-Fox, D, Firth, D, Moussalli, A & Whiting, MJ (2006): Multiple signals in chameleon contests: Designing and analysing animal contests as a tournament. *Animal Behaviour, 71*, 1263–1271.

Stuart-Fox, D & Moussalli, A (2008): Selection for social signalling drives the evolution of chameleon colour change. *Plos Biology, 6*, 22–29.

Stuart-Fox, D & Moussalli, A (2009): Camouflage, communication and thermoregulation: Lessons from colour changing organisms. *Philosophical Transactions of the Royal Society of London B: Biological Sciences, 364*, 463–470.

Stuart-Fox, D, Moussalli, A & Whiting, MJ (2007): Natural selection on social signals: Signal efficacy and the evolution of chameleon display coloration. *The American Naturalist, 170*, 916–930.

Taboada, C, Brunetti, AE, Alexandre, C, Lagorio, MG & Faivovich, J (2017a): Fluorescent frogs: A herpetological perspective. *South American Journal of Herpetology, 12*, 1–13.

Taboada, C, Brunetti, AE, Pedron, FN, Neto, FC, Estrin, DA, Bari, SE, Chemes, LB, Lopes, NP, Lagorio, MG & Faivovich, J (2017b): Naturally occurring fluorescence in frogs. *Proceedings of the National Academy of Sciences, 114*, 201701053, 1–6.

Tautz, D, Arctander, P, Minelli, A, Thomas, RH & Vogler, AP (2003): A plea for DNA taxonomy. *Trends in Ecology & Evolution, 18*, 70–74.

Teyssier, J, Saenko, SV, van der Marel, D & Milinkovitch, MC (2015): Photonic crystals cause active colour change in chameleons. *Nature Communications, 6*, 6368, 1–7.

Tilbury, C (2014): Overview of the systematics of the Chamaeleonidae. *In:* KA Tolley & A Herrel (Eds), *The Biology of Chameleons*. University of California Press, Berkeley, pp. 151–174.

Tilbury, C (2018): *Chameleons of Africa: An atlas: Including the chameleons of Europe, the Middle East and Asia* (Vol. 2). Frankfurt am Main: Edition Chimaira, pp. 643.

Tilbury, C & Tolley, KA (2009): A new species of dwarf chameleon (Sauria; Chamaeleonidae, *Bradypodion* Fitzinger) from KwaZulu Natal South Africa with notes on recent climatic shifts and their influence on speciation in the genus. *Zootaxa, 2226*, 43–57.

Tolley, K & Herrel, A (2014): Biology of the chameleons. *In:* KA Tolley & A Herrel (Eds), *The Biology of Chameleons*. University of California Press, Berkeley, pp. 1–5.

Tolley, K & Menegon, M (2014): Evolution and biogeography of chameleons. *In:* KA Tolley & A Herrel (Eds), *The Biology of Chameleons*. University of California Press, Berkeley, pp. 131–150.

Tolley, K, Townsend, TM & Vences, M (2013): Large-scale phylogeny of chameleons suggests African origins and Eocene diversification. *Proceedings of the Royal Society of London B: Biological Sciences, 280*, 20130184, 1–8.

Townsend, T & Larson, A (2002): Molecular phylogenetics and mitochondrial genomic evolution in the Chamaeleonidae (Reptilia, Squamata). *Molecular Phylogenetics and Evolution, 23*, 22–36.

Townsend, TM, Vieites, DR, Glaw, F & Vences, M (2009): Testing species-level diversification hypotheses in Madagascar: The case of microendemic *Brookesia* leaf chameleons. *Systematic Bology, 58*, 641–656.

Uetz, P, Hallermann, J & Hosek, J (2018): The Reptile Database. http://reptile-database.reptarium.cz. Accessed: 2018–10-05.

Vasconcelos, R, Perera, A, Geniez, P, Harris, DJ & Carranza, S (2012): An integrative taxonomic revision of the *Tarentola* geckos (Squamata, Phyllodactylidae) of the Cape Verde Islands. *Zoological Journal of the Linnean Society, 164*, 328–360.

Vukusic, P & Hooper, I (2005): Directionally controlled fluorescence emission in butterflies. *Science, 310*, 1151–1151.

Wucherer, MF & Michiels, NK (2012): A fluorescent chromatophore changes the level of fluorescence in a reef fish. *PLoS One, 7*, e37913, 1–7.

Yang, Z (2015): The BPP program for species tree estimation and species delimitation. *Current Zoology*, *61*, 854–865.

Yovanovich, CA, Koskela, SM, Nevala, N, Kondrashev, SL, Kelber, A & Donner, K (2017): The dual rod system of amphibians supports colour discrimination at the absolute visual threshold. *Philosophical Transactions of the Royal Society B: Biological Science, 372*, 20160066, 1–10.

6 Acknowledgments